UNCLASSIFIED

AD NUMBER AD907739 **NEW LIMITATION CHANGE** TO Approved for public release, distribution unlimited **FROM** Distribution authorized to U.S. Gov't. agencies only; [Test and evaluation; Feb 1973. Other requests shall be referred to Air Force Weapons Laboratory [AFWL/DYX], Kirtland AFB, NM, 87117. **AUTHORITY** ST-A AFWL ltr, 20 aug 1973

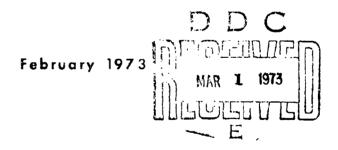


REVIEW OF DIELECTRICS AND SWITCHING

A. S. Denholm et al.

Energy Sciences, Inc.





AIR FORCE WEAPONS LABORATORY
Air Force Systems Command
Kirtland Air Force Base
New Mexico

Distribution limited to US Government agencies only because test and evaluation information is discussed in the report (Feb 73). Other requests for this document must be referred to AFWL (DYX), Kirtland AFB, NM, 87117.

AIR FORCE WEAPONS LABORATORY
Air Force Systems Command
Kirtland Air Force Base
New Mexico 87117

When US Government drawings, specifications, or other data are used for any purpose other than a definitely related Government procurement operation, the Government thereby incurs no responsibility nor any obligation whatsoever, and the fact that the Government may have formulated, furnished, or in any way supplied the said drawings, specifications, or other data, is not to be regarded by implication or otherwise, as in any manner licensing the holder or any other person or corporation, or conveying any rights or permission to manufacture, use, or sell any patented invention that may in any way be related thereto.

DO NOT RETURN THIS COPY. RETAIN OR DESTROY.

REVIEW OF DIELECTRICS AND SWITCHING

A. S. Denholm et al. Energy Sciences, Inc.

TECHNICAL REPORT NO. AFWL-TR-72-88

Distribution limited to US Government agencies only because test and evaluation information is discussed in the report (Feb 73). Other requests for this document must be referred to AFWL (DYX), Kirtland AFB, NM, 87117.

I-OREWORD

This report was prepared by Energy Sciences, Inc., Burlington, Massachusetts, under Contract F29601-71-C-0034. The research was performed under Program Elements 61101F and 62601F, Project 8809, Subtask 006.

Inclusive dates of research were February 1971 through December 1972. The report was submitted 13 December by the Air Force Weapons Laboratory Project Officer, Captain William E. Schwinkendorf (DYX). The former project officer was Ronald R. Rogers.

In addition to the author listed on the cover, the following also are coauthors: J. J. Moriarty, W. R. Bell, J. R. Uglum, G. K. Simcox, J. Hipple, and S. V. Nablo. The principal investigator was Dr. A. Stuart Denholm. The project engineer was Dr. Arthur H. Guenther (AFWL).

This technical report has been reviewed and is approved.

William & Shurkender & WILLIAM E. SCHWINKENDORF

Captain, USAF Project Officer

DARRELL R. JAMES Captain, USAF

Chief, Scientific Support Branch

JOHN L. LEROHL Colonel, USAF

Chief, Technology Division

ABSTRACT

Systems to generate high power levels frequently operate at high voltage, and their design requires special knowledge of dielectric and switching technology. The treatment of these technologies in this report starts with a discussion of electric field analysis then covers insulation and switching in the four dielectric media; namely gas, liquid, solid and vacuum. An extensive search of the literature produced a listing of relevant books, reports and papers and the establishment of a punched card classification and retrieval system specially designed for the subject area.

(Distribution Limitation Statement B)

CONTENTS

Section				Page		
1	INTR	ODUCTI	ODUCTION			
2	ELEC	CTRIC F	TELD DETERMINATION	5		
	2,1	Basic C	Concepts of Electrostatics	5		
	2.2	Field E Geomet	chancement Factors for Several Useful cries	6		
		2.2.1	Concentric Spheres	8		
		2.2.2	Concentric Cylinders	9		
		2,3,3	Sphere Above Infinite Plane	12		
		2.2.4	Cylinder Above Infinite Plane	12		
		2.2.5	Cylinder Passing Through a Radiused Hole	15		
		2.2.6	Crossed Unequal Cylinders	15		
		2.2.7	Rogowski (Bruce) Profiles	17		
	2.3		and Digital Techniques, with Applications od Dielectric Problems	17		
3	DIEL	ECTRIC	S IN GENERAL	25		
	3.1	Field S	trength	27		
	3.2	Field E	imission	28		
	3.3	Field I	Polarity Effects	29		
	3.4	Total V	Oltage Effect	30		
	3.5	Area E	Treet	30		
	3.6	Purity	and Homogeneity	33		
	3.7		ode Materials, Surface Condition and ric Coatings	33		
	3,8	Freque	ency Effect	34		
	3.9	Statisti	ical and Formative Time Lags	35		
	3.10	Tracki	ng and Flashover	36		
4	GAS	DIELEC	CTRIC	40		
	4.1	Genera	al Discussion	40		

Section				Page
	4.2	de Prop	perties	50
		4.2.1	Air (Uniform Field)	50
		4.2.2	Air (Nonuniform Field)	51
		4.2.3	SF ₆ (Uniform Field)	61
		4.2.4	SF ₆ (Nonuniform Field)	73
	4.3	ac Prop	perties	78
		4.3.1	Air (Uniform Field)	78
		4.3.2	Air (Nonuniform Field)	87
		4.3.3	Sulfur Hexafluoride (Unitorm Field)	90
		4.3.4	Sulfur Hexafluoride (Nonuniform Field)	97
	4.4	Impulse	e Properties	106
		4.4.1	General	196
		4.4.2	Air (Uniform Field)	108
		4.4.3	Air (Nonuniform Field)	110
		4.4.4	SF ₆ (Uniform Field)	118
		4.4.5	SF (Nonuniform Field)	121
	4.5	Freons	(dc/ac and Uniform Field)	129
		4.5.1	Freon-116 and C-318	129
		4.5.2	Freon 12	135
	4.6	Flasho	ver of Solid Dielectries in Gas	148
	4.7		ment Supported Design Studies (Gas	
		Dielect		159
	4.8		Considerations	172
		4.8.1	Dielectric Performance	172
		4.8.2	Chemical Stability and Toxicity	184
		4.8.3	Physical Considerations	187

Section					Page
5	LIQUID DIELECTRICS				
	5.1	The Att		Applications of Liquid	194
	5.2	Properties of Liquid Dielectrics			196
		5.2.1	General I	Properties of Liquids	196
		5.2.2	Particula	r Properties of Certain Liquids	199
			5.2.2.1	Mineral Oil	199
			5.2.2.2	Askarels	202
			5.2.2.3	Polybutenes	202
			5.2.2.4	Fluorocarbons	205
			5.2.2.5	Silicone Oils	205
			5.2.2.6	Castor Oil	209
			5.2.2.7	Research Liquids	209
	5.3	Factors Influencing the Properties of Liquids		g the Properties of Liquids	210
		5.3.1	Environm	iental Factors	210
			5.3.1.1	Electrode/Area Dielectric Volume	210
			5.3.1.2	Temperature	212
			5.3.1.3	Pressure	214
		5.3.2	Electrica	1 Stress-Time Effects	217
	5.4	Dielect	ric Perfor	nance	21 9
		5.4.1		d Stress and Associated Impulse ental Data	221
			5.4.1.1	ac StressingExperimental Data	222
			5.4.1.2	Impulsive StressesRelevant to Equipment Testing	245
			5.4.1.3	Experimental Results	245
		5.4.2	Impulsive Equipmen	e StressesLow Duty Cycle nt	257

Section					Page
			5.4.2.1	AWRE Techniques and Programs	25 8
			5.4.2.2	Streamer Propagation and Time Dependence	260
			5, 4, 2, 3	Figures of Merit for Various Liquids	264
			5.4.2.4	AWRE Data and Stress Re- lationships	268
			5.4.2.5	Summary of AWRE Programs	276
:			5.4.2.6	US Experimental Data for Large Areas	278
			5.4.2.7	Repetitive Pulsing	286
			5.4.2.8	Liquid Performance Under Pressurization	2 90
	5.5	Theory	of Breakdo	nwn	293
6	SOLI	ID DIELE	CTRIC		298
	6.1	Introduction			
	6.2	2 Breakdown Mechanisms			
		6.2.1	Intrinsic	Breakdown	303
		6.2.2	Electron	eehanical Breakdown	304
		6.2.3	Tracking	or Surface Breakdown	308
		6.2.4	Partial E	Discharges	309
		6.2.5	Thermal	Instability	313
		6.2.6	Electroel	hemical Deterioration	314
i	6.3	Factors	Λ ffecting	the Breakdown Voltage of Solids	316
v		6.3.1	Time at	Stress	316
•		6.3.2	Insulatio	n Thickness	321
		6.3.3	Electrod	e Area and Stressed Volume	324

Section				Page
		6.3.4	Environment	332
		6.3.5	Waveform	335
			6.3.5.1 Direct Voltage	337
			6.3.5.2 Power Frequency	337
			6.3.5.3 Pulse	337
		6.3.6	Nonuniform Field	340
	6.4	Conclus	ions	340
7	VAC	UUM DIE	LECTRIC	348
	7.1	General	Discussion	348
	7.2	Continue	ous Stressing	361
		7.2.1	Breakdown Across Unbridged Gaps with Continuous Voltage	361
		7.2.2	Flashover Across Dielectries with Continuous Voltage	379
	7.3	Alternat	ting Stressing	382
	7.4	Pulsed	Stressing	390
		7.4.1	Pulsed Breakdown of Unbridged Gaps	390
		7.4.2	Pulsed Flashover Across Dielectrics	397
	7.5	Design	Considerations	401
8	SWIT	rches in	GENERAL	417
	8.1	Comme	rcial Switch Tubes	418
	8.2	Solid Sta	ate Switches	420
	8.3	Vacuum	Interruption Devices	423
	8.4	Switche	s for Inductive Storage Systems	423
	8.5	Dischar	ge Gap Switching	425
		8, 5, 1	Delay and Jitter	425
		8.5.2	Risetime Considerations ,	426
		Ω 5 3	Lifetime English and Deignization	490

Section					Page
9	GAS S	SWITCH	ES		431
	9.1	Overvol	ited Switch		431
		9.1.1	The Rope	Switch	432
		9.1.2	Nonunifor	m Geometry	432
		9.1.3	Repetitive	e Operation and Fast Restriking	434
			9,1,3,1	Dielectric Recovery of the Spark Gap	435
			9.1.3.2	Electrode Erosion	437
	9.2	Three-	ر Electrode S	Switch	439
		9.2.1	The Field	I-Distortion Switch	439
		9.2.2	The Trig	atron	443
	9.3	Photon	Initiated Sv	viteh	446
	9,4	Electro	n Beam Ini	tiated Switch	456
	9.5	Design	Considerat	ions	457
10	LIQUID SWITCHES				
	10.1	Overvo	lted Switch		465
	10.2	Three-	Electrode :	Switch	466
	10.3	Laser I	Initiated Sw	itch	467
	10.4	Design	Considerat	ions	468
11	SOLI	D SWIT	ЯES		472
	11.1	Overvo	lted Switch		472
	11.2	Multi-!	Hectrode S	witches	474
	11.3	Laser :	Initiated Sw	ritches	477
	11.4	Design	Considerat	ions	477
12	VAC	JUM SW	ITCHES		480
	12.1	Spark-	Initiated Va	cuum Gap	482
	12.2	Plasm:	Injection		488

Section		Page
	12.3 Laser-Triggered Switch	490
	12.4 Design Considerations	491
13	GENERAL DESIGN CONSIDERATIONS	494

ILLUSTRATIONS

Figure		l'age
2.1	Maximum field strength E with a potential difference U between the electrodes, for different electrode configurations.	7
2.2	Field enhancement factors for concentric spheres.	10
2.3	Field enhancement factors for concentric cylinders.	11
2.4	Field enhancement factors for sphere-plane geometry.	13
2.5	Field enhancement factors for cylinder-plane geometry.	14
2.6	Field enhancement factors for cylinder passing through radiused hole.	16
2.7	Curve for constructing Rogowski profiles.	18
3.1	Voltage breakdown distributions for partial and multiple areas of an elemental area (n = 1) when the distribution for the elemental area has an average value of ten units and a standard deviation of one unit.	32
4.1	Typical breakdown voltage curves for different gases between parallel plate electrodes.	42
4.2	Breakdown voltage gradient in air at 1 atm - as a func- tion of gap length between parallel plates.	44
4.3	Representation of the distribution of electrons and positive ions in an electron avalanche.	45
4.4	Transition from an electron avalanche to a streamer and the subsequent growth of a streamer across the gap.	45
4.5	Breakdown voltages for plane electrodes in air at various constant spacings.	52
4.6	Breakdown voltage gradients for several gases at high pressures for uniform fields between stainless-steel electrodes and between aluminum electrodes.	53
4.7	Variation of de breakdown voltage of air and of Freon-12 with electrode separation at several absolute pressures in pounds per square inch. Uniform field.	54

Figure		Page
4.8	The effect of spark conditioning on the electric strength of compressed nitrogen, using parallel plane oxidized copper electrodes of 2-5 cm diameter at a spacing of 1 mm.	55
4.9	Breakdown voltage curves in air at 751 mm Hg between coaxial cylinders as a function of the radius of the inner cylinder. The radius of the outer cylinder is constant at 5 cm.	57
4,10	Breakdown voltage curves for coaxial cylinders in compressed air.	58
4.11	Breakdown voltage curves in air, at various gauge pressures in atm, between a sphere of 5 mm diameter and a plane.	59
4.12	Breakdown voltage curves in compressed air, at different gauge pressures, between a 5 cm diameter sphere and a plane.	60
4.13	de breakdown voltage curves for air between a 30° conical point and a plane.	62
4.14	de breakdown voltage curves for air between a hemispherically-ended rod, of 0.4 cm diameter, and a plane.	63
4.15	dc breakdown voltage curves in air at atmospheric pressure for various combinations of point and sphere electrodes. The sphere diameter is 5 cm.	63
4.16	Voltage and current characteristics for a 0.25 inch and 0.5 inch gaps in air between a negative point and a plane.	64
4.17	Voltage characteristics for a positive point-plane gap in compressed air, nitrogen, Freon, and sulfur hexafluoride.	64
4.18	Breakdown voltage curves in compressed air between two points.	65
4.19	Paschen curve for sulfur hexafluoride.	67
4.20	Dielectric strength of SF ₆ mixed with nitrogen (upper curves) and air (lower curves).	69
4.21	de breakdown versus gap length in SF ₆ -N ₂ mixtures (15 cm diameter uniform field electrodes).	70

Figure		Page
4.22	de breakdown versus SF guniform field1em gap (15 cm diameter uniform field electrodes and procelain insulator).	71
4.23	Preliminary dc breakdown characteristics for ${\rm SF_6}$, ${\rm N_2}$, and ${\rm CO_2}$ gas mixtures between concentric cylinder electrodes with a gap spacing of 58.5 cm.	72
4.24	de voltage breakdown versus gap spacing for 12 inch diameter brass parallel plane electrodes.	74
4,25	de voltage breakdown versus gauge pressure of ${ m SF_6}$ for 12 inch diameter brass parallel plane electrodes at gap spacings of 0.25, 0.5, 1.0, and 1.5 inch.	75
4.26	Sparking voltage in concentric cylindrical system as a function of gas pressure - various coatings on inner conductor (11.5 cm diameter) aluminum outer conductor (25 cm diameter).	76
4.27	The comparative dielectric strength of sulfur hexafluoride has tested under de and ac voltage at room temperature and pressure.	77
4.28	Breakdown voltage for sulfur bexaffuoride between coaxial cylinders.	79
4.29	The ratio of the corona and breakdown voltages for air and ${\rm SF}_6$ as a function of the testing conditions in a non-uniform field.	80
4.30	Dielectric strength as a function of gas pressure for de and 60 cps ac voltage.	81
4.31	The effect of pressure on the dielectric strength of sulfur hex (fluoride gas in a nonuniform (de) electrical field for selected gap distances.	82
4.32	The corona breakdown relation for sulfur hexafluoride as affected by pressure.	N. 83
4.33	Breakdown voltage in air at atmospheric pressure as a function of gap length between plates and between points for frequencies of 50 c/s, 0.5 Me/s and 1.9 Me/s.	85
4.34	Breakdown voltage as a function of gap length between plates in compressed air for dc and 1.05 x $10^5~{\rm c/s}$ voltages.	85

Figure		Page
4.35	Breakdown voltage curves in nitrogen as a function of gap length between spheres of 2.0 cm diameter.	86
4.36	Variation of breakdown voltage with gap length between plates in air at different frequencies.	86
4.37	Variation of breakdown voltage with gap length between plates in air at 200 Mc/s for different gas pressures.	88
4.38	Variation of breakdown voltage with pressure for coaxial line spark-gap.	88
4.39	Breakdown voltage and corona onset voltage curves for sphere-plane gaps.	91
4.40	60 c/s and impulse breakdown voltage curves between 0.5 in. square-cut rods in compressed nitrogen.	92
4.41	60-cycle relative strength of sulfur hexafluoride to dry air as a function of configuration and spacing of the electrodes. Gases at 25°C and at atmospheric pressure.	93
4.42	Breakdown voltage between 5 cm diameter spheres for sulfur hexafluoride.	94
4.43	60-cycle breakdown voltages of ${\rm SF}_6$ as a function of pressure. (Gas at room temperature.)	95
4.44	60-cycle breakdown voltages of ${\rm SF}_6$ at 100° C as a function of pressure.	98
4.45	Effect of air on dielectric strength of SF6.	98
4.46	Critical breakdown voltage between 43 cm diameter Rogowski profiled electrodes as function of p x d (corrected to 20° C).	99
4.47	ac breakdown voltages of sphere-sphere gap as a function of sphere radius.	101
4.48	ac breakdown voltage for gap A.	101
4.49	ac breakdown or corona inception voltage for gap B.	102
4.50	ac breakdown or corona inception voltage for gap C.	102
4.51	Field uniformity factor of sphere-sphere and rod-rod gaps.	103

Figure		Page
4.52	Breakdown voltage curves for various gases between a hemispherically-ended rod, of 0.1 inch diameter, and a sphere of 1.0 inch diameter. The gas pressure is 1 atm.	103
4.53	Breakdown voltage curves for SF ₆ at various pressures as a function of the spacing between a hemisphericallyended rod of 0.1 inch diameter and a sphere of 1.0 inch diameter.	104
4.54	Breakdown voltage characteristics with point-sphere electrodes for ${\rm SF}_6$.	104
4.55	ac spark-over and corona onset voltages of sulfur hexafluoride for indicated gaps between 1/16 inch hemisphere point and 6 inch diameter plane in 12 inch diameter steel tank as a function of pressure.	105
4.56	Breakdown voltage, nonuniform field, 1/4 inch rod.	105
4.57	Influence of the nature of the electrode surfaces on the time-lag distribution curves for a gap of 1.1 mm between 5 cm diameter spheres.	107
4.58	Summary of formative-time measurements in sine gases.	109
4.59	Positive and negative impulse voltage characteristics of rod-to-plane gap.	111
4.60	Time-lag curves of standard rod gaps (1/50 microsecond wave).	112
4.61	Time-lag curves of suspension strings of insulators, 10 inch diameter by 5 inch spacing, without areing fittings (1/50 microsecond wave).	113
4.62	Impulse volt-time characteristics of parallel conductorconductor gaps (at 760 mm Hg, 20° C, not corrected for humidity conditions (with negative impulse).	114
4.63	Impulse volt-time characteristics of parallel conductor conductor gaps (at 760 mm Hg, 20° C, not corrected for humidity conditions (with positive impulse)).	115
4.64	Negative impulse breakdown versus pressure. Uniform	119

Figure		Page
4.65	Time and voltage dependence of breakdown under impulse conditions for uniform field stainless steel in 150 psig, $10\%~{\rm SF}_6$, $40\%~{\rm N}_2$, $50\%~{\rm Ar}$ gas mixture - 0.58 cm gap.	122
4.66	The dielectric strength-temperature relation for sulfur hexafluoride tested at atmospheric pressure.	123
4.67	The dielectric strength-gap distance relation for sulfur hexafluoride gas as a function of the electrode configuration measured at atmospheric pressure.	125
4.68	Showing the decrease in the voltage gradient at break- down which accompanies the increase in the test gap for different electrode configurations for sulfur hexafluoride when tested by impulse voltage at atmospheric pressure.	126
4.69	Critical breakdown gradient $E_{\rm crit}$ between coaxial cylinder electrodes as a function of pressure (corrected to 20° C).	127
4.70	50% breakdown voltage for point to plane geometry.	128
4.71	Comparing the impulse dielectric strength of fluorinated hydrocarbon gases.	131
4.72	The dielectric strength of the fluorinated hydrocarbon gases as affected by pressure, tested under nonuniform field conditions.	132
4.73	The effect of gas pressure on the breakdown of dichlor-odifluoromethane (Freon 12).	132
4.74	Breakdown voltages versus pressure.	133
4.75	Comparison of breakdown voltage as a function of pressure for Freon 116/N ₂ O (90/10 by wt) and $\rm SF_6$ in a section of coaxial gas-filled transmission line. Inner conductor diameter-3 inches, outer conductor diameter-6 inches	134
4.76	Breakdown voltages measured in a Seavy cell, ASTM D-2477-66T.	134
4.77	Breakdown voltage with ${\rm SF_6}$, Freon 116, and Freon 116/N ₂ O (90/10 by wt) in a uniform field as a function of pressure in a steel tube, 36 inches long and with an ID of 20 inches.	1 3 6

Figure		Page
4.78	Corona inception and breakdown voltages versus pressure. Gap spacing 0.1 inch.	136
4.79	Corona inception and breakdown voltages versus pressure. Gap spacing 1.0 inch.	137
4.80	Corona inception and breakdown voltages versus pressure. Gap spacing 0.1 inch.	138
4.81	Corona inception and breakdown voltages versus pressure. Gap spacing 1.0 inch.	138
4.82	Corona inception voltages versus pressure.	139
4.83	Paschen curve for Freon 12.	139
4.84	60 cycle dielectric strength of Freon 12, tested between two 1 inch diameter spheres spaced 1/4 inch.	140
4.85	Impulse dielectric strength of Freon 12, tested between two 1 inch diameter spheres spaced 1/4 inch.	140
4.86	Breakdown voltage between 5 cm diameter spheres for Freon 12 as a function of pressure.	141
4.87	Sparking voltages in mixtures of Freon 12 and nitrogen.	143
4.88	Breakdown voltage for difluorodichloromethane between coaxial cylinders.	144
4.89	60 cycle dielectric strength of Freon 12, tested between tungsten rod and 1 inch diameter sphere spaced 1 inch.	145
4.90	Impulse dielectric strength of Freon 12.	145
4.91	60 cycle and impulse breakdown between 1/2 inch square rod gaps in $\text{CC1}_2\text{F}_2$.	146
4.92	Breakdown voltage with difluorodichloromethane and non-irradiated point-sphere electrodes.	147
4.93	The flashover of porcelain insulators as affected by the surrounding gas and its moisture content.	149
4.94	Representation of dielectric/metal interface.	151
4.95	Effect of cohesion in case of coaxial electrode.	152
4.96	dc breakdown versus pressure across 1 cm porcelain insulator in mixtures of SF $_6$ with ${ m N}_2$.	153

Figure		Page
4.97	Effect of crease length extension on spacer characteristics.	156
4.98	Concept of internal shielding.	157
4.99	The effect of the shielding electrode.	158
4.100	Effect on breakdown voltage of adding $\rm N_2$ to fixed pressure of $\rm SF_{6}.$	161
4.101	Surface flashover data for Permali material.	166
4.102	Breakdown voltage vs gap for test electrodes in air and ${\rm SF}_6.$	169
4.103	Test results of negative polarity on electrodes.	171
4.104	Sphere/sphere, air, 1 atmosphere.	17 5
4,105	Sphere/plane, air, 1 atmosphere $r + g = 80 \text{ mm}$.	176
4.106	Concentric and occentric cylinders, air, 1 atmosphere, $R = 63.5 \ \mathrm{mm}$.	176
4.107	Conductor and earthed metal plate, air, 1 atmosphere, $R=140~\mathrm{mm}$.	177
4.108	Concentric sphere/hemisphere, air, R = 38.1 mm.	177
4.109	Concentric sphere/hemisphere, SF ₆ , 1 atmosphere, R = 38.1 mm.	178
4.110	Eccentric sphere/hemisphere, SF_6 , 3 atmospheres, r = 15 mm, R = 38.1 mm.	178
4.111	Effect of electrode area on the maximum gradient in compressed gas insulation.	179
4.112	Negative inner conductor, ${ m SF}_{6}.$	181
4.113	Positive inner conductor, SF6.	181
5, 1	The electrode area effect on the dielectric strength of transformer oil.	213
5.2	The effect of temperature on the breakdown voltage of transformer oil.	213
5.3	Temperature dependence of the electric strength of n-alkanes.	213

Figure		Page
5.4	The effect of temperature on the dissipation factor of a typical European transformer oil over a range of frequency (cps).	215
5.5	The power factor of pentachlor diphenyl (1476 Pyranol) tested under 3 kV (30 vpm) at 60 cycles.	215
5. 6	The effect of frequency on the power factor of SF96(40) silicone liquid at selected temperatures of test.	216
5.7	The dielectric constant of pentachlor diphenyl tested at frequencies in the range from 500 to 3000 cycles per second.	216
5.8	The breakdown voltage of transformer oil as affected by the absolute pressure.	218
5.9	The effect of high values of air pressure on the break-down voltage of mineral oil.	218
5.10	Breakdown strength of liquids as a function of applied pulse length.	220
5.11	The devoltage strength of transformer oil as affected by electrode polarity in nonuniform fields, including the effect of oil treatment.	223
5.12	Breakdown distribution and area effect.	229
5.13	Breakdown voltage distributions of transformer oil for electrodes of four different areas.	230
5.14	Minima-of-groups area effect. Breakdown voltage distributions of transformer oil for minima of successive groups of ten for data of Figure 5.13.	230
5. 15	Minima-of-groups area effect. Comparison of the distribution of individual breakdown voltages for electrode pair 1 with those of minima of successive groups of 10 and 100 breakdown voltages.	231
5.16	Breakdown probability density for circulating limit subjected to 20s step-by-step test.	233
5.17	Conditions of the oil dielectric test bed.	235
5. ±3	Cumulative distribution of all results.	238
5.19	Breakdown strengths under various conditions.	239

Figure		Page
5.20	Sectioned view of large electrode system.	241
5.21	Variation of electric strength with moisture content (supply-frequency voltages) at 22° C.	242
5.22	Influence of time between discharges (supply-frequency voltages).	242
5.2 3	Cumulative probability for stationary and circulating- oil samples.	243
5.24	Effect of nature of gas in solution (supply-frequency voltages).	244
5.25	Deviation of normal-probability area effect from the experimental and theoretical values.	246
5.26	Impulse wave shapes.	247
5.27	Variation of breakdown voltage with gap setting.	2 49
5, 28	The conditioning effect,	25 0
5.29	Ogive curves for first-impulse testing technique.	252
5.30	Volume effects.	253
5.31	Plate area versus mean breakdown field strength.	255
5.32	Pulse length versus mean breakdown field strength.	256
5.33	Oil streamer velocities.	265
5.34	Glycerine streamer velocities.	266
5.35	Water streamer velocities.	267
5.36	The effect of electrode area upon the impulsive break-down strength of transformer oil.	271
5.37	The effect of electrode area upon the impulsive break-down strength of ethylene glycol.	272
5.38	Area effect for deionized water.	274
5.39	Impulse breakdown of deionized water.	275
5.40	Russian data for small ball gaps.	277
5. 41	Variability of waveshape for constant risetime.	281

Figure		Page
5.42	Breakdown strength of oil with aluminum electrodes constant breakdown phase.	282
5.43	Breakdown strength of oil with a steel positive electrode.	283
5.44	Facility 1 - time dependence of large area oil break-down.	2 84
5.45	Breakdown stress as a function of pulse repetition rate for Gulfcrest 62.	288
5,46	Strength of Freons under repetitive pulses.	289
5.47	Strength of Freons under repetitive pulses.	2 91
5.48	Pressure effect in oil.	292
6.1	Electrical breakdown of some polymeric materials.	307
6.2	Various locations for partial discharges.	310
6.3 6.4	Equivalent circuit and typical voltage waveform of a void. Life data for plastics with internal discharges.	31 2 319
6.5	Life/stress for polystyrene (uniform field).	3 2 0
6. 6	Life of PTFE with and without corona.	322
6.7	Breakdown voltage versus insulation thickness for polyethylene cable (27) (two layers extruded in tandem).	323
6.8	Breakdown voltage U in kV of epoxy resin moldings versus wall thickness S in mm.	325
6.9	Relation between the distribution functions of a model and of an object n times larger.	327
6.10	Effect of increasing volume and standard deviation on mean breakdown strength.	3 2 8
6.11	Volume effect: electrical breakdown in plastics.	330
6.12	Electric strength of the three encapsulating materials relating to test area.	331
6,13	Variation of the dielectric strength of styroflex, teflon, mica, lucite, polystyrene, and bulk teflon, with the voltage risetime, uniform field.	339

Figure		Page
6.14	Average life in shots versus stress in kV/mil and voltage in kV for polyester film.	341
7.1	Theoretical anode and cathode dominated regions of field emission initiated breakdown.	352
7.2	Microdischargevoltage and current for steel electrodes, 1 mm gap, 22 kV.	355
7.3	Schematic representation of selective ion bombardment of a one micron (10^{-4} cm) projection.	357
7.4	Vacuum-breakdown voltages and insulation strength.	362
7.5	Voltage insulated vs gap for 303 & 304 stainless steel electrodes.	363
7.6	Insulation strength as a function of electrode surface finish.	366
7.7	Insulation of continuous voltage and threshold for microdischarges and breakdown.	367
7.8	Voltage in vacuum between titanium electrodes as a function of the gap.	369
7.9	Electrode area effect.	371
7.10	Effect of electrode areas (cathode, SS and anode SS).	372
7.11	Effect of electrode areas (cathode oxidized aluminum, and anode SS).	372
7.12	Typical bare and coated cathode performance in non-uniform field.	3 74
7.13	Log U- log d plot.	377
7.14	Voltage holdoff properties of some tubes.	378
7.15	Insulation strengths over ${\rm Al}_2{\rm O}_3$ surfaces in vacuum.	380
7.16	de flashover of glass insulators of various shapes.	383
7.17	Effect of shielding negative junction with re-entrant sphere flashover voltage of standoff insulation.	384
7.18	Maximum breakdown stresses and insulation strength, steel.	385

Figure		Page
7.19	Ratio of vacuum breakdown voltage at 21.5 MHz to 60 Hz.	388
7.20	Oscillograms showing three types of breakdown.	392
7.21	Discharge probability P.	394
7.22	Development of gap luminosity in nanosecond breakdown of vacuum gaps.	396
7.23	Comparison of dc, ac and 1.2/50 µsec.	398
7.24	Effect of surge front duration on FO voltages.	398
7.25	The flashover strength of glass and lexan as a function of geometry.	400
7.26	Flashover voltage for some dielectrics.	400
7.27	Flashover strength versus gap distance for lucite.	402
7.28	Flashover voltage versus angle θ for some insulators.	402
7.29	Flashover voltage versus angle θ for 7740 glass and crosslinked styrene.	403
7.30	Flashover voltage versus angle θ for lucite.	403
7.31	Pressure effect for various electrode systems.	409
8.1	Single-stage inductive storage system.	424
9.1	Risetime of thin-cone gap.	433
9.2	Arc recovery strength in ${ m N}_2^{}$ at 1 atmosphere.	436
9.3	Field distortion switch.	440
9.4	Swinging cascade breakdown mode for 3-electrode switch.	441
9.5	Trigatron.	444
9.6	Schematic diagram of the laser-triggered switching apparatus.	450
9.7	Delay versus laser power from 0.028 to 11 MW.	452
9.8	Jitter versus laser power.	452
0 0	Frequency of delay occurrence	455

Figure	•	Page
11.1	Self-break curve for polyethylene switches.	473
11.2	Mechanical triggering method.	475
12.1	Recovery strength for vacuum and gas; 1600 amperes, 6.35 mm gap, gas pressure 1 atmosphere.	481
12.2	Dependence of the spontaneous breakdown voltage(U_s) of a partitionless spark gap on the initial pressure (p_0) for various interelectrode spacings.	483
12.3	Design of sectioned spark gap.	484
12.4	The effect of pressure and voltage on triggering delay.	486
12.5	The delay (t_d - $f(V)$) in the firing of an unpartitioned spark gap ($d=35$ mm) as a function of V_0 , the initial voltage applied to it, with triggering from the cathode (continuous curves) and from the anode (dashed curves); the trigger pulse amplitudes were -10, -30, and \pm 40 kV.	487
12.6	Variation of the time lag of the discharge with the voltage for negative (4) and positive (2) polarities of the high voltage electrode.	489
13.1	Generalized concept - pulse power system.	496

TABLES

Table		Page
4.1	Values of relative electric strengths.	48
4.2	Typical properties of gases at 760 mm Hg.	49
4.3	Breakdown voltage between 5 cm diameter spheres in ${ m SF}_6$.	68
4.4	Onset voltage at several frequencies for visual corona on wires coaxially within a 5 cm diameter cylinder.	89
4.5	Minimum breakdown voltages in kV for 60 Hz and impulse voltages applied to gaps between 1/2 inch square rods in air.	91
4.6	Effect of frequency on breakdown in SF 6.	98
4.7	Positive and negative impulse breakdown voltages of point-plane gaps, rod gaps, and wire-plane gaps in air at 20° C, 760 mm Hg, and absolute humidity 11 gm/m ³ , 1.5/40 microsecond impulse wave.	111
4.8	Values of $k = Ft^{1/6}d^{1/10}$ for positive point or small sphere.	117
4.9	Values for kfor negative point and small sphere	117
4.10	dc breakdown voltage (kV) of ${ m SF}_6$ in uniform field gap.	120
4.11	Strength of Freon vapors at their boiling point.	131
4.12	Mean spacer efficiencies for the flashover of cylindrical insulators in a uniform field in ${ m SF}_6$.	154
4.13	Dielectric design studies (gas).	160
4,14	Maximum de stresses in FX machinescoaxial line geometryand operating stresses in emp systems.	163
4.15	Flashover data for epoxy materials.	165
4.16	de puncture strengths and flashover of machined plastics tested in high pressure gas.	167
4.17	Enhanced field stress for breakdown or flashover-cylinders to ground plane in air (kV/cm)	170
4.18	Properties of several insulating gases.	173

TABLES (Continued)

Table		Page
4.19	Larger area studies with SF 6.	183
4.20	Resistance to attack by SF (decomposed).	186
5.1	Typical properties of liquids.	200
5.2	Comparison of oil testing techniques and requirements for the dielectric strength of transformer oil.	201
5.3	The characteristics of General Electric Company pyranols.	203
5.4	Polybutenesproperties, thermal aging and mixtures.	204
5,5	Typical properties of liquids.	2 06
5. 6	General properties of fluorinated liquids.	207
5.7	The physical properties of selected silicone fluids manufactured by the General Electric Company.	2 08
5.8	Test conditions and breakdown data.	225
5.9	Statistical values for breakdown voltage distributions.	227
5.10	Breakdown values obtained under varying electrode conditions.	236
5.11	Test results for oil of varying quality with and without motion.	2 38
5.12	Distribution indices for stationary and circulating oil.	244
5.13	Dependence of electric strength on testing technique.	249
5.14	Electrode gap and area effects for power-frequency and surge voltages.	252
5.15	Streamer velocities.	261
5.16	Figures of merit.	269
5.17	Streamer velocities.	279
5.18	Breakdown voltage ($v_{\rm B}$) for various transformer oils in different initial states.	287
5.19	Physical properties of the Freons.	291
6.1	Typical working stresses in practice.	299

TABLES (Continued)

<u>Table</u>		Page
6.2	Properties of interest for insulating materials.	300
6.3	Breakdown processes in solids.	302
6.4	Electric strengths of various polymeric organic materials measured at or near ambient temperature.	305
6.5	Intrinsic strengths of organic polymeric materials.	306
6.6	Maximum thermal voltages.	315
6.7	Factors affecting the breakdown voltage of solids.	317
6.8	Dose of high energy radiation to produce measurable changes in properties.	334
6.9	Frequency "constant" (Hz).	336
6.10	Properties of some solid dielectrics in common use.	343
7.1	Factors and effects in vacuum insulation.	358
7.2	Insulation strengths obtained using buff polished high strength alloy electrodes.	365
7.3	Insulation strengths obtained using metallographically polished allotropic transformation type alloys.	365
7.4	Vacuum breakdown voltage V in kV for a bushing at ambient pressure p torr, utilizing voltage biased grids.	370
7.5	Typical bare and coated cathode performance in uniform field at 1 mm gap.	375
7.6	60 Hz breakdown voltages.	386
7.7	Vacuum breakdown in a titania-loaded cavity.	389
7.8	Relative contamination caused by vacuum materials.	405
7.9	Outgassing rate for various polymers.	406
8.1	Characteristics of Soviet thyratrons.	421
8.2	Some commercial switching devices.	422
9.1	Properties of copper-tungsten composites.	438
9,2	Electrode polarity and trigatron characteristics.	445
9.3	LTS operation and power related laser parameters.	453

TABLES (Continued)

<u> Table</u>		Page
13.1	Energy densities in dielectrics.	499
13.2	Active volume of dielectrics for 100 kJ.	500
13.3	Active volume of dielectric for 100 kJ (after J.C. Martin).	500

SECTION 1

INTRODUCTION

The need to simulate, without fusion, the radiation phenomena produced by nuclear devices has led to the development over the last decade of new technology which is broadly applicable. In most cases simulation has required the production of very high power transients, generated usually by the delivery of energy stored electrostatically through a suitable switching system. As a consequence of these activities significant advances have been made in high voltage technology, specifically in the engineering of dielectrics and high power closing switches—the subject of this volume.

The prime purpose of this text is to provide a condensation of the extensive but scattered information on dielectries and switching to facilitate high voltage design. All available sources of information have been used including government reports, some of which cover large development programs on high voltage equipment. In such reports the information on dielectrics is sometimes significant but not prominently advertised. In general the objective is to provide a design handbook; theoretical treatment is minimized but with appropriate references for further study.

Dielectrics are used in high voltage systems not only as insulation but as energy storage media, the commonest storage device—being the capacitor, usually with paper dielectric. In general, dielectric quality can be represented by the maximum electric field (Em) supportable in a particular set of circumstances. The choice of a suitable insulant would seem then to be simply a matter of choosing the most economic medium which would support the stress. The choice of a dielectric for energy storage would similarly be related to the energy density required (1/2 ϵ_r $\epsilon_0 \frac{E_r^2}{m}$). These statements

are true, but the judgment is not simple, primarily because the maximum electric field which can be supported is determined to varying degrees by the particular circumstances, as we will see as the text progresses. As an example, the maximum field is determined not only by the size of the system to be insulated, but also by the time during which the stress is sustained. Relatively high stresses can be supported for short times, for example in liquids. This fact is used in pulse power systems where large energies have to be delivered quickly, by using intermediate energy storage elements, or power concentrators. These concentrators are pulse charged and hold their energy only briefly before delivery to the load or transmission system.

High-power transmission systems, or lines, obviously have to be carefully insulated. In selecting a dielectric for a line, it should be remembered that for energy flow the figure of merit is proportional to $\sqrt{\varepsilon_r} E_m^2$ and not to $\varepsilon_r E_m^2$ as it is for energy storage, so that with all circumstances being equal (area, stress duration, etc.) it is not necessarily the case that the best storage medium is also the best transmission medium. This difference can be attributed to the dependence of the propagation velocity on the dielectric constant of the medium.

The desire for high-energy density in energy storage or transmission systems is usually based on the need for compactness, mobility perhaps, and overall economy. However, in some cases the energy density achievable determines technical feasibility. This will become obvious from the following considerations, where for simplicity the example taken is a coaxial energy storage system, which is a fairly common situation. The system delivers its energy in a pulse, through a switch, to a resistive load at one end. The switch initially will be considered perfect; that is, either completely insulating or completely conducting. The radial dimensions of the energy storage system and the switch geometry introduce an effective inductance thus degrading pulse risetime and fall time, but this will be neglected and the system is assumed to be a "long" transmission line with a characteristic impedance Z and a dielectric constant e.

The objective of the design is to develop a specific power in the load in the form of a square pulse of given duration (τ). The line is designed to match the load, the condition for 100% efficiency, i.e., stored energy in the line equals energy delivered to the load. From simple transmission line considerations, the line length must equal $\tau/6.6 \sqrt{\epsilon_r}$ meters where τ is the pulse duration in nanoseconds. Obviously the energy density in the transmission line must be sufficient to allow the pulse energy to be stored in this length, and if this energy density cannot be achieved by suitable combination of dielectric, geometry and charging time then this direct approach is not possible.

As already noted the radial dimensions of the line have been neglected for simplicity, but this omission does not detract from the argument that it is physically impossible, from basic considerations of propagation velocity, to deliver energy stored at one point to another point where switching is initiated in less than 6.6 \mathcal{L} $\sqrt{\epsilon_r}$ nanoseconds, where \mathcal{L} is the distance between the points in meters.

Where it is impractical to store sufficient energy within the required distance from the output switch, recourse can be taken to multiple energy stores, each with its own output switch. The pulses generated by each store are carried by transmission lines to the load. Obviously the dielectric design around the load to carry the combined power is yet another problem hopefully made tractible by the shortness of the pulse duration. Such a technique obviously requires advanced switch synchronization technology, but as will be seen later it is now possible to close high-power switches spaced far apart within a one nanosecond window.

Consider now the situation where the output switch is imperfect. The switch is often an electrical discharge (or breakdown) device such as a high pressure gas spark gap. Various ways of initiating the discharge are available depending on the nature of the device; for example, lasers or field intensification trigger electrodes may be used.

The operation of the switch can be roughly separated into three phases. In the final phase the voltage drop across the switch is usually negligible compared to the other circuit voltages--perfect conduction can generally be assumed. Although there are almost certainly minor variations occuring during this phase, for example, in the "arc" drop, it is reasonable to call this 'he "stable" phase because these changes are usually not significant to the performance of systems.

The two earlier phases, which tend to blend together, exist during the growth towards the final "stable" stage. The first of these is the resistive phase. This occurs at the start of the discharge and involves the growth of conduction processes. In this phase energy is being absorbed by the switch to appear mostly as heat in the electrodes and switch medium.

The second phase, called the inductive phase, in general, exists once the conduction processes are adequately established, and as the name suggests is related to the geometrical inductance of the discharge channel, or channels, and the return path. The voltage drop across the switch in this phase is related to the rate of change of current through the inductance, and the energy being absorbed is stored in the magnetic field.

The risetime associated with the inductive phase, for example in the case of the transmission line with matched load discussed earlier, is given by 1.1 L $_{\rm S}/{\rm Z}_{\rm O}$ where L $_{\rm S}$ is the switch inductance. A pessimistic estimate for total risetime is the sum of the resistive and inductive phase durations. A better approximation seems to be the root mean square value as used in the risetime summation of series pulse amplifiers. In many cases, of course, one phase dominates.

These switch characteristics can be critical factors in the design of high-power pulse systems and are treated at length in later sections along with other important features such as electrode erosion, shock generation and recovery time.

SECTION 2

ELECTRIC FIELD DETERMINATION

2.1 Basic Concepts of Electrostatics

It is appropriate, in a review text on dielectrics, to emphasize the importance of proper grading of electrical fields. Since failure, or breakdown, of a dielectric is dependent on the maximum electrical stress in the dielectric, the designer must ensure that all grading be as uniform as possible in order to utilize the dielectrics most efficiently and economically.

A field is a region of space, empty or occupied by some solid, liquid, or gaseous medium, in which certain physical states, occur. The region contains an electric field if it is concerned with a manifestation of stored electrical energy--i.e., if an electric charge placed in the region moves under the influence of electrical forces. In electrostatics, the field is most conveniently described in terms of a scalar potential function--V (x,y,z)--which satisfies Poisson's equation $\sqrt{2}V = -\rho/\epsilon_0$. The electric field intensity is the gradient of the potential function $\vec{E} = -\vec{\nabla} V$ and is a vector quantity. When there is no free charge in the field region, which is the case usually encountered in practice, then one deals with Laplace's equation $|\nabla|^2 V = 0$ or $|\vec{\nabla} \cdot \vec{E}| = 0$. Rationalized MKS units will be used throughout.

When dealing with Laplace's equation, the solution is determined by the boundary conditions which are imposed externally. Normally, boundary conditions consist of conducting equipotential surfaces on which fixed voltages are applied, and formally it is possible to show that a specification of the boundary conditions is sufficient, and necessary, to uniquely determine the potential distribution within the region.

There are many mathematical techniques available for solving Laplace's equation in one-, two-, or three-dimensional geometries. The method of images, Green's functions, separation of variables and conformal mappings are but a few. There are many texts available which outline one

or more of the formal methods available, and rather than present a sketchy review when several comprehensive treatments exist the reader is referred to the literature; for example, the books by Morse and Feshbach⁽¹⁾ and Vitkovich⁽²⁾ are excellent.

The remaining parts of this section are devoted to:

- (a) Presentation of field enhancement factors for some commonly used electrode configurations.
- (b) Discussion of analog and digital techniques available for the solution of potential distributions in complicated geometries. This leads to consideration of mixed dielectrics, since these techniques are particularly useful for analyzing the mixed dielectric situations.

2.2 Field Enhancement Factors for Several Useful Geometries

The designer of high-voltage systems is confronted with the proble n of minimizing electric field enhancements which inevitably arise in a mechanically and fiscally sound design. Real life electrode configurations are rarely amenable to analytic scrutiny, and aside from computer analysis of the system (which is discussed later) one usually has to approximate various parts of the design in terms of geometries for which solutions exist. In this way, however, it is often possible to estimate within 20%, using known breakdown data, whether that portion of the system is liable to cause breakdown problems.

The number of possible analytic solutions for two dimensional electrode configurations, and three dimensional configurations having one symmetry axis, is extremely large. Figure 2.1 gives a summary table of several simple geometries. (3) The formulas for maximum stress are only approximate, and apply for large electrode separations. For more detailed information on solutions in two dimensions using analytic functions and conformal mapping, the book by Bewley (4) is recommended. For an analysis

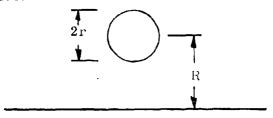
Configuration		Formula for E	Example
Two parallel plane plates		U- ā	U = 100 kV, a = 2 cm, E = 50 kV/cm.
Two concentric	9	Ur+a ar	U = 150 kV, r = 3 cm, a = 2 cm, $E = 125 kV/cm.$
Sphere and plane plane	23.4.	0.9 U r+a	U = 200 kV, r = 5 cm, a = 8 cm, E = 58.5 kV/cm.
Two spheres at a distance a from each other	3.0	0.9 U r-! a/2	U = 200 kV, r = 5 cm, a = 12 cm, E = 33 kV/cm.
Two coaxial cylinders	i 🕢	2.3 r lg r + a	U = 100 kV, r = 5 cm, a = 7 cm, $E = 22.9 kV/cm.$
Cylinder parallel to plane plate	27/2	0.9 U 2.3 r lg r + a	U - 200 kV, r == 5 cm, a == 10 cm, E == 32.8 kV/cm.
Two parallel cylinders		$ \begin{array}{c c} U/2 \\ 2.3 & r \lg \frac{r+a/2}{r} \end{array} $	U == 150 kV, r == 6 cm, a == 20 cm, E == 11.5 kV/cm.
Two perpendicular cylinders	27/1 27	$ \begin{array}{c c} 0.9 & U/2 \\ 2.3 & r & \text{lg} & r + a/2 \\ \end{array} $	U = 200 kV, r = 10 cm, a = 10 cm, $E = 22.2 kV/cm.$
Hemisphere on one of two paral- lel plane plates	21.	3[/ ; (a ≫ r)	$U \approx 100$ kV, $a = 10$ cm, $E \approx 30$ kV/cm.
Semicylinder on one of two paral- lel plane plates	ar ()	$\frac{2U}{a}$; $(a \gg r)$	U = 200 kV, a = 12 cm, E = 33.3 kV/cm.
Two dielectries between plane plates $(a_1 > a_2)$		$U \varepsilon_1$ $a_1 \varepsilon_2 + a_2 \varepsilon_1$	$U = 200 \text{ kV}, \epsilon_1 = 2, \epsilon_2 = 4, a_1 = 6 \text{ cm}, a_2 = 5 \text{ cm}.$ $E = 11.8 \text{ kV/cm}.$

Figure 2.1 Maximum field strength E with a potential difference U between the electrodes, for different electrode configurations.

of analytic solutions in some of the 27 separable coordinate systems, the book by Moon and Spencer (5) is very useful.

For a general two electrode configuration, a field enhancement factor--f₁--can be defined as the maximum electric field strength divided by the average electric field strength. The maximum field may occur on either electrode, and normally arises on that portion of an electrode surface which has the smallest radius of curvature. The average electric field is defined as the potential difference between the two electrodes divided by the minimum separation between them. This field enhancement factor is thus a measure of how much worse the peak field strength is than that for parallel plate geometry. Another field factor--f₂--can be derived from f₁ by multiplying it by the ratio of the maximum system dimension to the minimum electrode separation. This factor is useful since it normalizes everything to the overall system size, and as will be evident below, this factor always has a minimum value. At the minimum one has a situation in which the maximum stress occuring in the system has as low a value as is physically possible (this, of course, being for a fixed geometrical configuration, voltage, and total system size).

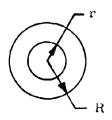
The geometries considered in this section mainly consist of spherical, or cylindrical, electrodes above ground planes. Thus, the figure shown below is representative:



We will use a dimensionless geometrical parameter p = R/r to characterize such a system. This parameter will be used almost exclusively in the following treatment. Also, using this notation we have $f_2 = f_1 \times (p/p-1)$.

2.2.1 Concentric Spheres

This system is shown below:



The average electric field is $E_{ave} = V_o/(R-r)$. We define $f_1 = E_{max}/E_{ave}$, and it is easy to show that $f_1 = p$, and thus $f_2 = p^2/(p-1)$. Figure 2.2 graphically shows the two factors. Notice the two limits which are approached:

(a) $p \to 1$, $f_1 \to 1$

This simply states that for small radial separations, the field looks like that of two parallel plates.

(b) $p = 2, f_2 = minimum$

This is a statement of the fact that for a given voltage and outer sphere, the minimum electrical stress on the inner sphere occurs when it has one half the radius of the outer sphere.

2.2.2 Concentric Cylinders

This geometry is characterized by the same figure as that for concentric spheres (see schematic of previous section). The enhancement factors f_1 and f_2 were defined previously, and are expressed as $f_1 = (p-1)/\ln p$ and $f_2 = p/\ln p$.

Figure 2.3 shows the behavior of these two functions. Again, $f_1 \to 1$ as $p \to 1$, i.e., a parallel plate situation is approached. In the present case, no end effects are considered. The cylinders are taken to be infinite in extent.

In practice, it is often required to achieve the minimum stress for concentric cylinders. This is easily seen from the graph of f_2 to be satisfied for p = e = 2.718----.

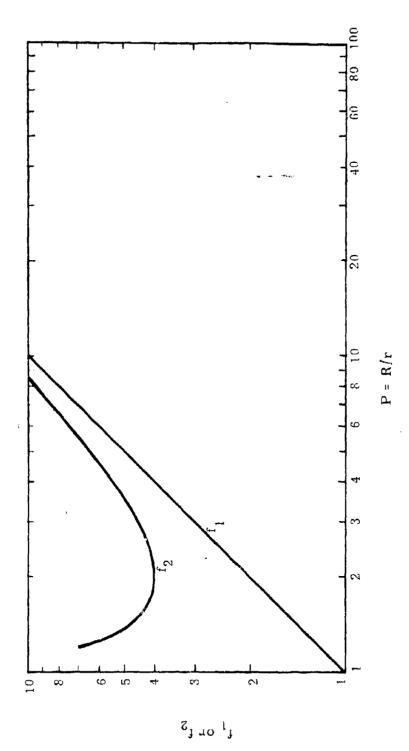


Figure 2.2 Field Enhancement Factors for Concentric Spheres

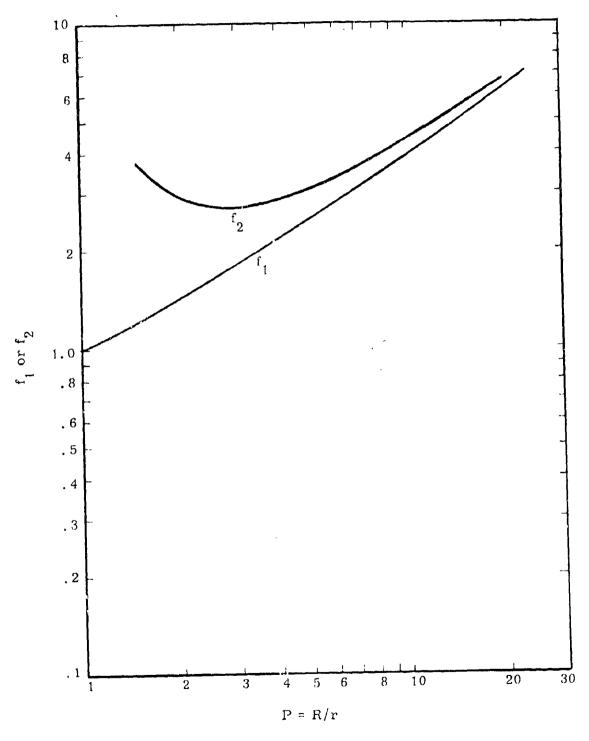
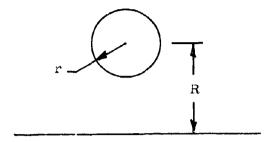


Figure 2.3 Field Enhancement Factors for Concentric Cylinders

2.2.3 Sphere Above Infinite Plane

This geometry is characterized in the sketch below:



The exact analytic solution can be carried out using bi-spherical coordinates (see reference 6), and is quite cumbersome. Figure 2.4 shows the results obtained for f_1 and f_2 .

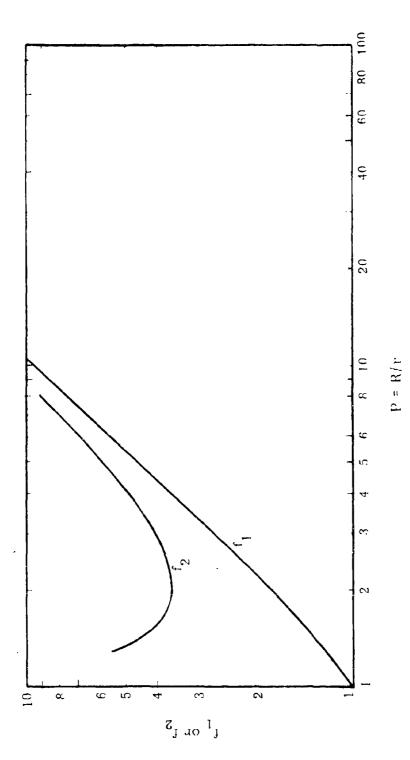
An approximate equation, useful when tables or graphs are not available, can be derived by placing a point charge at the center of the sphere. Using the method of images, and choosing the charges in such a way as to get the right potential at the point of the spherical surface closest to the ground plane, one obtains $f_1 = p(p-1)/p-1/2$, $f_2 = p^2/(p-1/2)$. These formula are good to a few percent for $p \ge 4$.

The above formulas and curves apply also to two equal spheres separated by a distance 2 (R-r), with a potential difference of 2 $_{
m O}^{
m V}$ between them.

2.2.4 Cylinder Above Infinite Plane

The figure characterizing this geometry is the same as in the previous subsection. Using bi-cylindrical coordinates an exact formula can be derived. Again, the result is cumbersome. Figure 2.5 shows how the two field enhancement factors depend on the dimensionless geometrical factor.

The method of images can again be used to obtain approximate equations. They are $f_1 = (p-1)/\ln{(2p-1)}$, $f_2 = p/\ln{(2p-1)}$. Note that the graphs can also be used to calculate the maximum stress of two equal cylinders separated by 2 (R-r) at a potential difference of 2 V_0 .



Field Enhancement Factors for Sphere-Plane Geometry Figure 2.4

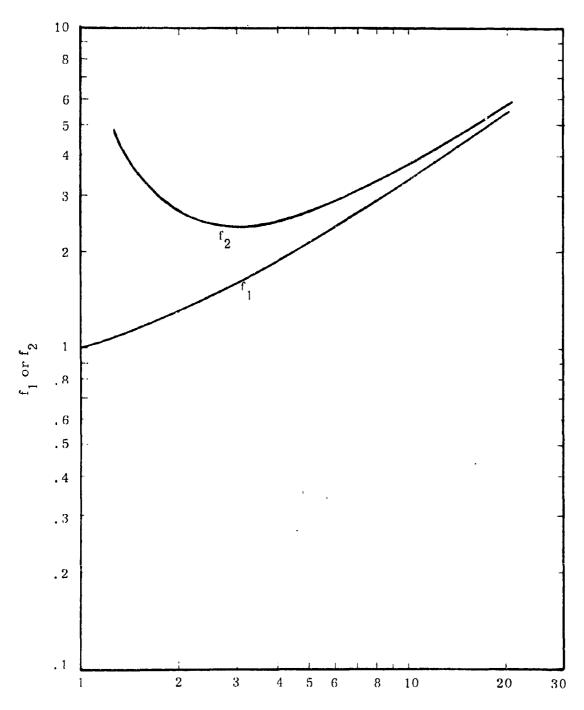
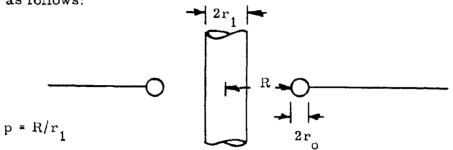


Figure 2.5 Field Enhancement Factors for Cylinder-Plane Geometry

2.2.5 Cylinder Passing Through a Radiused Hole

Ryan and Walley (7) have analyzed the field enhancement associated with a cylindrical conductor passing through a radiused hole in a plate. The geometry is as follows:



They use oblate-spheroidal coordinates, with rotational hyperboloid equipotentials, to approximate this configuration. The minimum field enhancement, for which breakdown is equally likely to occur from either electrode, is satisfied when $r_0 = r_1/p$. For this optimum value of r_0 , which in practice can be somewhat larger and not change the results significantly, the behavior of r_0 and r_0 is shown in Figure 2.6 as a function of r_0 . The comparison with experiment is good to within 5% (see reference 7).

For a given value of R, it is possible to show that there is an optimum value of r_1 by looking at the behavior of f_2 . It is clear that $P_{\text{opt}} = 3 \text{ or } r_1 = 0.33 \text{ R}$, $r_0 = 0.11 \text{ R}$. It should be noted that Ryan and Walley⁽⁷⁾ report a much better agreement between theory and experiment using these results than by approximating the geometry by two crossed cylinders.

2.2.6 Crossed Unequal Cylinders

This problem is treated in detail in an article by Harper and O'Dwyer. (8) The results are difficult to present in a useful way, and it is recommended that the original article be consulted. For crossed equal cylinders, when the spacing is large compared to their radii, the formula for parallel cylinders can be used.

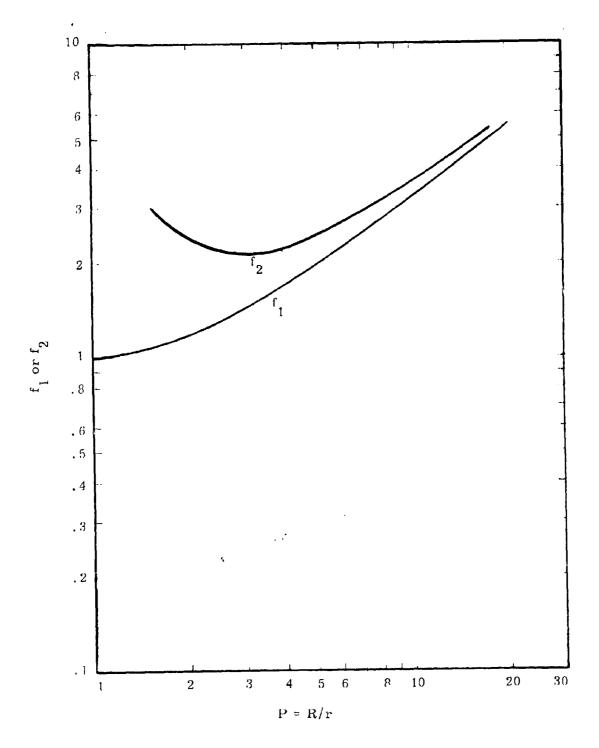


Figure 2.6 Field Enhancement Factors for Cylinder Passing Through Radiused Hole

2.2.7 Rogowski (Bruce) Profiles

In many experimental situations, it is desired to produce a parallel disk configuration in which the field strength is nowhere greater than in the center of the electrode system. Cobine (9) gives a review of the original analysis performed by Rogowski. A Bruce profile system (10) is slightly easier to fabricate, but in practice there is no difference in their electrical properties.

Rather than describe the analysis for the Rogowski contour, only the results will be given. As shown in Figure 2.7, suppose that one desires a gap spacing (to an infinite ground plane) of distance a, and a flat region which extends to a diameter D_0 . Let h_0 be the acceptable deviation from the flat one would allow at the diameter D_0 (typically $h_0/a \approx 10^{-2} \, \text{to} \, 10^{-3}$). This, utilizing the curve shown, defines a value of d_0 . Then for any value of diameter D_0 define $d = (D-D_0) + d_0$. Then from the curve one can determine h and in this way produce the whole contour. In practice, the profile is terminated with a radiused edge in the low field region.

2.3 Analog and Digital Techniques, with Applications to Mixed Dielectric Problems

As was mentioned previously, real life high-voltage systems rarely take a form which is amenable to analytic solution. In order to study real configurations, use is normally made of either analog techniques or digital computer programs. Analog methods rely on the fact that Laplace's equation occurs in many other physical situations—e.g., steady-state heat flow, mechanical stress distributions, gravitational fields, ohmic current conduction, hydromechanics, etc.—and that by solving experimentally for one problem one, in fact, solves Laplace's equation for many other situations (in particular, the field distribution problem in electrostatics).

The most commonly used analog methods -- Teledeltos paper and electrolytic tanks -- rely on electrical conduction to establish the equipotential surfaces and field lines, and are only useful for configurations which

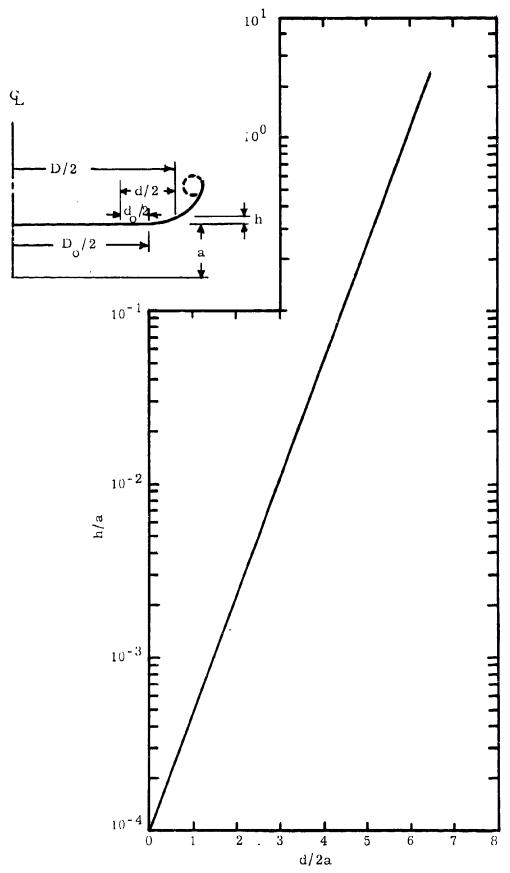


Figure 2.7 Curve for Constructing Rogowski Profiles -18-

have one symmetry axis (x-y symmetry for Teledeltos paper, and either x-y or cylindrical symmetry for electrolytic planar or wedge tanks). The conductivity of the analog medium is constant in space and time, and because of this one can look at the following Maxwell equations:

$$\vec{r} \cdot \vec{E} = \frac{\rho}{\epsilon_0 \epsilon_r} \tag{1}$$

$$\frac{\vec{n} \cdot \vec{n}}{\vec{n} \cdot \vec{j}} + \vec{\nabla} \cdot \vec{j} = 0$$
 (2)

$$\vec{j} = \sigma \vec{E} \tag{3}$$

Combining these, we obtain

$$\vec{r} \cdot \left(\frac{o \cdot \mathbf{E}}{o \cdot \mathbf{t}} + \frac{o}{e_0 \cdot e_r} \cdot \vec{\mathbf{E}} \right) = 0 \tag{4}$$

Aside from an initial turn-on transient, one can consider a situation in which the externally imposed stress (or really, imposed potential on the boundaries) is either dc or ac.

Typically

$$\frac{\sigma}{\epsilon_0} \approx 10^6 - 10^8 \text{ cps} \tag{5}$$

and for a 1 kHz applied potential,

$$\frac{\delta}{2} \approx 10^3 \text{ cps}$$
 (6)

Thus, the time derivative term is negligible and we can write

$$\vec{\nabla} \cdot \vec{E} = -\nabla^2 V = 0 \tag{7}$$

or, in other words, the field distribution within a conducting media is exactly the same as in a non-conducting case-- this, of course, being for the same electrode geometry.

To see how a wedge tank simulates a cylindrically symmetric geometry, consider a tank whose bottom is slightly tilted (5° to 10°) from the horizontal. Taking the Z-axis along the "shoreline" (the intersection of the free surface of the conducting media and the bottom of the tank), we can look at the conductivity variation within the conducting media in the direction normal to the Z-axis. In any plane parallel to the Z-axis the area of conducting media is proportional to the distance from that axis, and thus

σ ~ **x**

Thus, from the equation

$$\vec{\nabla}$$
 ($\sigma \vec{E}$)

we get

$$\frac{1}{x} \frac{\delta}{\delta x} \left(x \frac{\delta V}{\delta x} \right) + \frac{\delta^2 V}{\delta y^2} = 0 \tag{8}$$

which is precisely Laplace's equation for a cylindrically symmetric geometry.

While use of a conducting analog may seem completely straightforward, there are many experimental subtleties to be considered. Rather than list them all, which would require a rather long document, the excellent reviews in reference (2) are recommended. These articles also describe how mixed dielectric mediums can be modelled using the conduction analog.

Other analogs which have been used are resistor networks and rubber membranes. While not as flexible as the conduction analog, they have historically been quite useful and are capable of giving very precise field determinations. However, it is probably fair to say that with the advent of modern high speed, large memory computing systems the digital computation technique has come into its own as a fast, extremely flexible and accurate means of determining field distributions.

The essence of the digital computation method is the replacement of the continuum of real space by a mesh of discrete points, and the rewriting of Laplace's equation in finite difference form. While an excellent review of numerical techniques is contained in reference (2), we will consider a few details here. First, one should consider the type of mesh to be used. While many regular "star" configurations are possible, the most convenient one to use is the rectangular mesh, or more specifically a square mesh. Since computer memory size largely restricts the use of numerical techniques to two dimensional problems (x-y or cylindrical symmetry), the square mesh simply means that the spatial increments used are the same physical size in both dimensions. Laplace's equation can be recast in finite difference form by using a Taylor series expansion:

$$V(x + \Delta s, y) = V(x, y) + \frac{\delta V}{\delta x} \Delta s + \frac{1}{2} + \frac{\delta^2 V}{\delta x^2} \Delta s^2 + \dots$$
 (9)

and

$$V(x, y + \Delta s) = V(x,y) + \frac{\delta V}{\delta y} \Delta s + \frac{1}{2} \frac{\delta^2 V}{\delta y^2} \Delta s^2 + \cdots$$
 (10)

Noting that

$$\frac{2^{2}V}{3x^{2}} = \frac{V(x + \Delta s, y) - 2V(x, y) + V(x - \Delta s, y)}{\Delta s^{2}}$$
(11)

and

$$\frac{\delta^2 V}{\delta y^2} = \frac{V(x, y + \Delta s) - 2V(x, y) + V(x, y - \Delta s)}{\Delta s^2}$$
(12)

then the equation

$$\frac{\delta^2 V}{\delta x^2} + \frac{\delta^2 V}{\delta y^2} = 0$$

can be re-written as

$$V(x,y) = \frac{V(x + As,y) + V(x - As,y) + V(x,y + As) + V(x,y - As)}{4}$$
(13)

In practice, the problem is set up so that boundary conditions (electrode surfaces and potentials) are part of the program input. The finite difference equation given above is cycled through iteratively until the program has converged to the solution. "Acceleration" factors (see reference (2)) are often used to speed up the rate of convergence, and for not too complicated geometries 5 or 6 cycles are all that is required to obtain a solution accurate to a few percent.

Dr. Jack Boers, at the Sandia Corporation in Albuquerque, has written a general program for numerically solving Laplace's equation and a description of it can be found in reference (11). Mr. John Shipman of the Naval Research Laboratory has taken this program and modified it somewhat. The programs of Dr. Boers and Mr. Shipman both handle mixed dielectric

problems, and it is this feature which makes them extremely useful. While the solution of Laplace's equation for a single dielectric media is difficult enough, mixed dielectrics present a much harder problem. In this case, one really has to solve the equation.

$$\overrightarrow{\nabla}$$
. $\overrightarrow{D} = 0$

where

$$\vec{D} = \epsilon_0 \epsilon_r \vec{E}$$

with the added requirements that the normal components of D and the tangential components of E be continuous at the interface between two dielectrics. The programs which are available do this automatically.

An optical analog which is often used in dealing with dielectric interfaces is the Brewster angle. In optics, if a wave of the proper polarity strikes an interface at an angle to the normal exceeding the Brewster angle, the wave will be completely reflected and no energy transmitted across the interface. However, in pulse power systems the wavelengths of interest are normally large compared to the transverse dimensions of dielectric inserts, and the phenomena of "evanescent" waves assures that energy will in fact flow through the interface. The Brewster angle analog is probably most important in terms of grading considerations. This comes about because one dielectric media may dominate the problem, and large changes in slope occur in the field lines at an interface. This change in slope can lead to a bunching of the field lines in certain regions and thus produce a very nonuniform grading. In such cases, interaction between the designer and computer program can usually lead to a nearly optimum design.

SECTION 2

REFERENCES

- (1) Morse, P.M. and Feshbach, H., "Methods of Theoretical Physics, Vols. I and II," McGraw-Hill, N.Y. (1953).
- (2) Vitkovitch, D., editor, "Field Analysis: Experimental and Computational Methods" Van Nostrand, Princeton (1966).
- (3) Bowers, A. and Cath, P.G., "The Maximum Electric Field Strength for Several Simple Electrode Configurations," Philips Tech. Rev., 6, 270 (1941).
- (4) Bewley, L.V., "Two-Dimensional Fields in Electrical Engineering,"
 Dover Publications, N.Y. (1963).
- (5) Moon, P. and Spencer, D. E., "Field Theory for Engineers," Van Nostrand, Princeton (1961).
- (6) Ryan, H. McL. and Walley, C.A., "Field Auxiliary Factors for Simple Electrode Geometries," Proc. IEE, 114, #10, pp. 1529-1536 (Oct. 1967).
- (7) Ryan, H. McL. and Walley, C.A., "Sparking Voltage of a Conductor Passing Through an Earthed Plate," Proc. IEE, 114, #1, pp. 172-178 (Jan. 1967).
- (8) Harper, P.G. and O'Dwyer, J.J., "Electric Field Strength Between Crossed and Parallel Circular Cylinders," Proc. IEE, 104C, pp. 439-440 (1957).
- (9) Cobine, J.D., "Gaseous Conductors: Theory and Engineering Applications," Dover Publications, N.Y. (1958).
- (10) Bruce, F. M., "Calibration of Uniform-Field Spark Gaps for High Voltage Measurement at Power Frequencies," IEE, 94, (Pt. 11), 138 (1947).
- (11) Boers, J.E., "FFEARS--A Digital Computer Program for the Simulation of Laplace's Equation Including Dielectric Interfaces and Small Ungrounded Electrodes," SC-RR-71-0377, Sandia Laboratories, Albuquerque, N.M., July 1971.

SECTION 3

DIELECTRICS IN GENERAL

The science of dielectrics can be said to start with Otto von Guericke who developed the first electrostatic machine in 1660 and shortly thereafter made the first insulated lines. About a hundred years later Benjamin Franklin pioneered experiments with really high voltages, although it must be admitted that some of his experimental equipment had been around for some time. By the early 1800s underground and submarine cables had been demonstrated. It was not, however, until the last quarter of the 19th century with the invention by Edison of the electric light and the subsequent growth of power generation and distribution that research and development in dielectric technology was supported by significant economic resources. From then until the late 1920s when the special demands of nuclear physics started, dielectric technology was associated almost solely with the needs of generation and distribution. The 1940s saw the beginning of high-power radar systems leading to modulators and tubes operating at voltages as high as 300 kV, and the early 1960s saw the first developments in high-power pulses for the simulation of nuclear weapons effects, with voltages now as high as 15 million volts.

There are several excellent review articles and books on dielectrics which provide good introductions to the subject, and many literature references for more detailed study. These tend, however, to be more relevant to industrial applications, for example to the power industry, than to the pulse power needs of the Department of Defence. Some of these articles and books cover dielectrics in general, but more often they are restricted to a particular dielectric medium such as gas or liquid. One of the broader treatments is in the book by Clark which provides an excellent and comprehensive review of solids, liquids and gases. His text is directed towards the needs of the industrial designer. For example, ionization and aging, critical

to reliability and longevity, are treated at length. These factors are not necessarily as important for some pulse power purposes, in testing equipment for example, where feasibility and cost for a shorter term need may be more important. The reference includes a long list of visual, mechanical, chemical and electrical properties which can be important in the selection of solid dielectrics. Chemical and mechanical properties become particularly important where longevity is required. A comprehensive glossary of terms used in dielectric technology is also included.

Probably the most valuable book on liquid dielectrics is that by Adamczewski. Fortunately an updated (1969) English translation of the original Polish work is available. (2) Most of the important factors in design using liquid dielectries are discussed. Although the information tends to be more theoretical than practical, there is much of real value to the practitioner. One of the unexpected but valuable features is a lengthy discussion of the effect of ionizing radiation on liquids. The book concludes with a useful tabulation of the various theories of liquid breakdown together with the basic assumptions and supporting experimental data. Kok (3) has written a much smaller, less comprehensive but nevertheless useful book on liquids, basing his approach on the several impurity effects (colloids, particles, floculation, bubbles, acidity, etc.) which in practice determine the strength of liquid dielectric systems. The chapters covering formative time lag and the effect of gap spacing are particularly relevent to pulse power applications.

There are many books on solid dielectrics, most of these tending to emphasize the theoretical aspects of breakdown, polarization, etc. One of the most useful from a practical point of view is that by Whitehead. (4) His text discusses the various factors which influence breakdown and relates them to the theories, and treats the subjects of internal discharges with their importance to lifetime; and external discharges, including temporal effects. The concluding chapter on working stresses in various solids is particularly relevant. Another volume containing much practical information on solid dielectrics

is that edited by von Hippel. (5) Some 22 contributors, most of them writing on solids, cover the field from rubber and plastics to ceramics, including piezoelectrics. The book concludes with a table of dielectric materials which summarizes the measurements of the Laboratory for Insulation Research (MIT) on the complex permittivity and permeability of more than 600 dielectrics for a frequency range of 10^2 to 2.5 x 10^{10} cycles per second, and for temperatures up to 500° C.

Meek and Craggs⁽⁶⁾ have written one of the most definitive texts on breakdown in gases. Dielectric strengths for high pressure gases, including electronegative types are given and there is an excellent treatment of irradiation and time lags. High frequency breakdown is discussed at some length, as is the formation and expansion of spark channels, an important consideration in switching. This book together with the review article by Trump in reference (E^{*} rovers very effectively the field of gaseous dielectrics.

The only bo- on electrical breakdown in vacuum is that by Sliv-kov, (7) which in see instated, although there are several excellent review articles. (8, 9, 10) Hawley and Maitland have published an indexed bibliography on vacuum as an insulator. (11)

Many factors influence dielectric performance, and although these will be discussed in detail later it is useful to treat them briefly at this point. The factors include field strength, field polarity, total voltage, electrode area and dielectric volume, purity and homogeneity, electrode material and surface condition, electrode coating, pulse duration and frequency.

3.1 Field Strength

The parameter normally used to characterize the "quality" of a dielectric is the maximum electric field which it will withstand. Since this can vary quite significantly when the factors just listed are changed the strength is obviously not necessarily constant for a given dielectric. However,

most of the processes which lead to breakdown are stress dependent, for example Townsend's ionization coefficient (α), or field emission from surfaces, and in almost all practical situations, all else being equal, breakdown develops at constant field strength. Probably the best known value of maximum field strength is that for air at atmospheric pressure and temperature which breaks down at roughly 30 kV/cm, whether geometry generates a uniform field (breakdown) or a moderately nonuniform field (breakdown or corona). For highly nonuniform fields the stress for corona onset in air can be significantly higher than 30 kV/cm.

At this point it is useful to discuss the phenomenon of field emission because of its relevance to several of the important processes in dielectric breakdown.

3.2 Field Emission

Electrons can be extracted from cold metal surfaces by the application of high electric fields, a process contributing to the failure of many dielectrics at high stresses. Fowler and Nordheim using quantum mechanics theory and a one dimensional surface potential barrier model obtained an expression for the electron emission current density $J(O^OK)$, which can be simplified to a good approximation to the expression

$$J_{\text{of}} = AE^2 \exp \left(16.42 \times 10^7 - \frac{3/2}{\phi}\right) \exp \left(-\frac{2}{10}\right)$$
 (1)

where E is in V/cm and the emitter work function φ is in electron volts. The factor "A" depends on the work function and is equal to 3.5 x 10^{-5} amp/V² for tungsten (φ = 4.5 ev). Adamcewski⁽²⁾ discusses the situation where emission is into a medium of dielectric constant ε greater than one, as with a liquid. The presence of the medium reduces the work function of an electron passing from the metal to the liquid by the value $\varepsilon \Delta \varphi$ where

Theoretically, fields of the order 10 V/cm are required to give measurable field emission, but in practice emission can be detected and produces electrical breakdown at levels two orders of magnitude below this because of field intensifying micro projections on cathode surfaces. In vacuum experiments intensifications at least as high as 150 have been measured. (13) Where field emission conduction is occurring, a plot of the logarithm of current divided by the voltage squared against the reciprocal of the voltage yields a straight line, as would be expected from the above Fowler and Nordheim expression. In general, on a large area surface several sites would be emitting, and Tomaschke et al. (13) have shown that the combined currents from a group of emitting points produce a linear Fowler Nordheim plot.

3.3 Field Polarity Effects

Where nonuniform geometries exist, which is the more usual situation, the dielectric strength of the system can be significantly influenced by the polarity of the most intense field region, which of course normally determines the voltage breakdown value. The clearest situation is with vacuum dielectric because in that medium field emission is usually a dominating process (ion emission does not occur until fields are two orders of magnitude higher). Consequently, when the high field region is negative vacuum insulation strength is much less than when it is positive. On the other hand the reverse tends to be true for gases and liquids, probably because of space charge effects at the negative electrode modifying the electric field values when the intense field is negative. As an example, the direct breakdown voltage of a negative point to plane in air can be twice that for a positive point. With liquids the polarity effect in general is not so evident, although negative fields required for breakdown tend to be stronger than positive fields. The difference is very marked with fast pulses when negative strength can be better than twice the positive.

3.4 Total Voltage Effect

This term is applied to the condition where the maximum electric field which can be withstood falls as the dielectric spacing is increased. Some dielectrics are much poorer in this regard than others, the worst case being vacuum. With vacuum it becomes increasingly difficult to hold direct voltage as the value required exceeds about 100 kV. Above this voltage region breakdown processes related to the higher energies achieved by particles in this medium determine voltage performance. This effect is experienced also with high-pressure gases, but for different reasons, and is most evident where field strengths are high in the first instance, that is at high pressure. Where the breakdown strength is low to begin with, for example in air at atmospheric pressure, there is essentially no total voltage effect if uniform field conditions can be maintained.

3.5 Area Effect

One of the unfortunate facts of high-voltage design is the increasing probability of failure at a given stress level as size increases. Admittedly with larger equipment there are opportunities for introducing, for example, new sources of contamination or field concentrations, but even without such effects, using the same insulating medium with its basic variability, a reduction in strength must be expected from statistical considerations. This is essentially a "weak link" phenomenon and Gumbel (14) has expanded at length on the theoretical foundation of extreme value statistics which predicts this effect.

Using the results of this theory, it is possible to predict from data on small area samples the performance to be expected with much larger areas. This, of course, will be the maximum performance to be expected, since increase in scale may involve new limiting factors not associated with the basic variability of the dielectric.

A number of tests on small samples will give breakdown voltage values which are distributed about a mean, and usually the distribution is roughly normal. The probability of breakdown at any voltage is the ratio of the number failing at that value to the total number tested, and when the insulation variability is high, the standard deviation is high. Hill and Schmidt (15) give typical percentage standard deviations: air 1-2%, oil 4-8%, paper 6-15%, laminated mica 10-40%. It will be seen later in Section 6 that this indicates that the area effect for air will be small, and for mica large.

A convenient way to study normal distributions is to use a special graph paper (probability paper) so designed that a straight line is obtained when a normal population is graphed, i.e., cumulative percentage up to and including a value is plotted against the value. On such paper, which is commercially available, the average value is that where the line intercepts the 50% cumulative percentage line, and the standard deviation is the difference between this average value and where the line intercepts the 16 or 84 cumulative percentage coordinate.

For the usual continuous distribution the cumulative probability of breakdown for "n" areas in parallel is related to that for one area by the expression

$$\operatorname{cum} \operatorname{Pbd}_{n} = 1 - (1 - \operatorname{cum} p)^{n} \tag{3}$$

where cum Pbd_n is the cumulative probability of breakdown at R volts for n areas in parallel and cum p is the cumulative probability of breakdown at R volts for 1 area. To put some numbers in this expression, if the cumulative probability of breakdown at a specific voltage with a small area is 1%, and the area is increased by two orders of magnitude, the probability becomes 64%, and if by three orders of magnitude it becomes greater than 99.99%! Hill and Schmidt (15) have constructed Figure 3.1 for a standard deviation of 10% of the average. These authors also discuss briefly the situation where

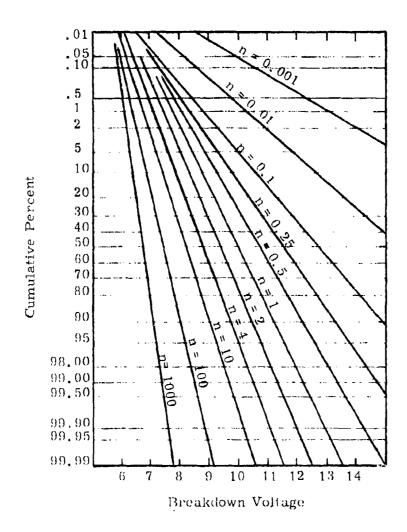


Figure 3.1 Voltage breakdown distributions for partial and multiple areas of an elemental area (n = 1) when the distribution for the elemental area has an average value of ten units and a standard deviation of one unit.

the distribution of values from small sample tests is found to be discontinuous. Although the preceding discussion has been using the term "area" effect, it could just as well be "volume" effect; the pertinent parameter presumably being determined by whether the "weak link" is associated with a surface or a volume.

3.6 Purity and Homogeneity

In practice the presence of a "weak" region in the volume of a dielectric is the most usual cause of breakdown. This can take the form of an impurity, an element of foreign substance that has a lower strength or dielectric constant, the lower dielectric constant causing higher stressing than in the main body of the material because of flux continuity (D = e E = constant). Examples of this are cavities in a solid or bubbles in a liquid,

th cases strength and dielectric constant would be lower than in the tric. Discharges initiated in such regions often trigger collapse of the dielectric system. In the case of cavities in a solid, continual ionization may lead to slow erosion of the dielectric producing breakdown after a long time under stress rather than an immediate catastrophic failure.

Other forms of weakening impurity include metal particles which initiate breakdown by field intensification, and non-metallic particles which, for example, can form bridges in liquids (flocculation) to channel a discharge. In the case of the vacuum dielectric, contamination of the metal surfaces on which field lines terminate adversely affects performance, not only because of field emission with its dependence on surface work function and microprotrusions, but also because of other processes such as secondary emission and the evaporation of surfaces.

3.7 Electrode Materials, Surface Condition and Dielectric Coatings

The earlier discussion on field emission suggests that the work function of electrode material and its roughness should be important to the

performance of dielectrics. This has been confirmed where the medium can support an electric field sufficiently high to develop emission. The performance of the vacuum dielectric is of course very dependent on electrode material, even different stainless steels perform differently. For gases at lower pressures, electrode material is not a significant factor because the field strength remains low; but at high pressures and higher fields, the effect of electrode material becomes significant. For example, stainless steel is much superior to aluminum. In the same medium at high pressures, rough electrodes (sand papered but not polished) breakdown at lower voltages than polished, and prebreakdown currents are much higher. Similarly, electrode material effects have been noted in liquids, particularly for highly nonuniform geometries.

Dielectric coatings have been used effectively on electrodes to improve performance in vacuum, gases and liquids, presumably through the suppression of field emission. For example, Jedynak⁽¹⁶⁾ in vacuum experiments with coated cathodes showed that prebreakdown currents could be 2-4 orders of magnitude below that for bare electrodes, and that increases of 70% could be achieved in dielectric strength. Other workers have noted improvements in the performance of oil⁽¹⁷⁾ and high pressure gases using dielectric films.⁽¹⁸⁾

3.8 Frequency Effect

In general, the strength of dielectrics falls with frequency, the severity of the effect depending on the dielectric and other factors such as electrode geometry. With gases, for example, there is no real change in performance from dc to 60 Hz, but if frequency is raised to a value at which positive ions do not have time to cross the gap in a half cycle a positive space charge develops and the breakdown voltage is adversely affected. At even higher frequencies there are further complications in the breakdown process when the amplitude of oscillations by electrons in the gap becomes comparable

to the gap spacing and cumulative ionization occurs. For gases, until frequencies above perhaps 100 kHz are reached the effect is not strong, being most pronounced for accentuated (e.g., point) geometries.

In the case of liquids, for example oil, strength can be increased by as much as 100% in going from dc to 60 Hz, but falls with frequency in the megahertz range to almost zero at the highest frequencies (approximately 10 MHz), apparently because of thermal breakdown. With solids, strength falls with frequency, again usually because of thermal effects, although partial discharges where cavities exist can also be terminal.

3.9 Statistical and Formative Time Lags

Between the time of application of an overvoltage and the collapse of a dielectric there is a delay which is known as the time lag. It is a most significant feature where impulse voltage is concerned because the lag times are usually of the same order of magnitude as the duration or risetime of the pulse. There are basically two types of time lag. The first is known as the statistical time lag which exists because of the need for an electron to appear in the critically stressed region in order to initiate the discharge. The other is known as the formative time lag, and is determined by the time for the discharge once initiated to develop across the gap.

The statistical time lag is influenced by the degree of preionization or irradiation of the gap, and various techniques such as ultraviolet light or radioactive sources are used to remove or reduce this time lag, particularly where the dielectric is in a calibration gap. To obtain a statistically reliable design for an impulse system, it is obvious that the design data used should be free of perturbations related to statistical time lag.

Expressions have been developed for the formative time lag in gases based on cumulative α and γ (Townsend) processes in the gap. (6) One of the simpler of these is

where a, b are constants and V_0 is the direct breakdown voltage. For very short pulses, for example less than 100 ns, information is limited at high gas pressure, but Felsenthal and Proud have published valuable information in the range from one atmosphere down.

Formative time lag effects exist also in vacuum, liquids, and solids, the effect with vacuum being most dramatic at larger gaps with very short pulses (<100 ns). In this time range, breakdown strength in vacuum can increase by almost two orders of magnitude over dc strength. In practice, solids tend to have the shortest time lags, largely because the operating stresses are higher, which can lead to problems in insulation coordination—it is preferable to have flashover of the environment around a solid, which will recover, rather than have the solid puncture.

3.10 Tracking and Flashover

Tracking is a term describing action along the surface of a solid in vacuum, gas or liquid. It usually indicates a permanent loss of strength related to chemical change at the surface, the voltage being limited by conduction at the track. Flashover is used to label a discharge or spark close to, and influenced by, the solid surface which often leads to tracking, although tracking is not produced only by flashover. Tracking on a surface can develop by surface ionization or conduction at high fields, particularly in the presence of contaminants, and antitracking agents can be used for control. Some materials have much superior tracking properties than others.

The prevention of flashover requires good electric field design, particularly to reduce the stress at the dielectric terminations. In general, solids with low dielectric constants provide better flashover strength, because with a solid insulator the field at the terminations, where the dielectric meets metal, is increased according to ϵ_s/ϵ_a , where ϵ_s , ϵ_a are the constants for

the solid and ambient respectively. Lucite is an example of a good material, having a low dielectric constant and very high resistance to tracking.

SECTION 3

REFERENCES

- (1) Clark, Frank M., "Insulating Materials for Design and Engineering Practice," John Wiley & Sons, New York (1962).
- (2) Adamcewski, I., "Ionization, Conductivity and Breakdown in Dielectric Liquids," Barnes and Noble, New York (1969).
- (3) Kok, J.A., "Electrical Breakdown of Insulating Liquids," Centrex Publishing Co., Eindhoven, Holland (1961).
- (4) Whitehead, S., "Dielectric Breakdown of Solids," Clarendon Press, Oxford (1951).
- (5) Von Hippel, A., "Dielectric Materials and Applications," The Technology Press of MIT, John Wiley & Sons, New York (1954).
- (6) Meek, J. M. and Craggs, J. D., "Electrical Breakdown of Gases," Oxford Clarendon Press (1953).
- (7) Slivkov, I.N., "Electrical Breakdown in Vacuum," Moscow (1966), FTD-MT-24-123-71.
- (8) Hawley, R., "The Electrical Properties of High Vacuum," Ch. 4 of High Voltage Technology, Ed. L. Alston, Oxford University Press, London (1968).
- (9) Hawley, R., "Vacuum as an Insulator," Vacuum, 10, 310, 1960.
- (10) Charbonnier, F.M., "A Brief Review of Vacuum Breakdown Initiation Processes," Proc. III International Symposium on Discharges and Electrical Insulation in Vacuum," Paris, 1968, p. 15.
- (11) Hawley, R. and Maitland, A., "Vacuum as in Insulator: an Indexed Bibliography," Chapman & Hall (1967).
- (12) Fowler, R.M. and Nordheim, L.W., "Electron Emission in Intense Electric Fields," Proc. Roy. Soc. A119, 173 (1928) and A121, 626, (1928).
- (13) Tomaschke, M.E. et al, "The Role of Electrode Projections in Electrical Breakdown," Proc. International Symposium on Insulation of High Voltages in Vacuum, Boston, October 1964, p. 13.
- (14) Gumbel, E.J., "Statistical Theory of Extreme Values and Some Practical Applications," NBS Applied Mathematics Series, No. 33, Washington, Government Printing Office, 1954.
- (15) Hill, L.R. and Schmidt, P.L., "Insulation Breakdown as a Function of Area," AIEE Trans. 67, 442, 1948.

- (16) Jedynak, L., "Dielectric Coatings in Vacuum Gaps," Proc. International Symposium on Insulation of High Voltages in Vacuum, Boston, October 1964, p. 147.
- (17) Zaky, A.A. et al, "Influence of Electrode Coatings on the Breakdown Strength of Transformer Oil," Nature 202, 687 (1964).
- (18) McNeall, P.I. and Skipper, D.J., "Proc. Int. Con. on Gas Discharges and the Electricity Supply Industry." CERI, England (1962).
- (19) Felsenthal, P. and Proud, J.M., "Nanosecond Pulse Breakdown in Gaps," Phys. Rev. 139 A 1796 (1965).

SECTION 4

GAS DIELECTRIC

4.1 General Discussion

If electrical insulation were chosen purely on the basis of intrinsic electric strength, high voltage equipment would be otally encapsulated in a solid dielectric. However, although some smaller equipment such as isolation transformers are insulated in this way up to several hundred kilovolts, the difficulties in making homogenous solid dielectric structures on larger, extra high voltage equipment usually lead—to the rejection of the solid medium, and the use of liquids or gases as the main insulant from ground.

For continuous or low frequency applications at higher voltages and larger spacings, the use of liquid dielectrics, usually an oil, presents difficulties because of bubbles and other impurities (Section 5). As a consequence, gaseous dielectrics, usually electronegative gases at high pressure, are used extensively in low frequency very high voltage equipment and are being increasingly used also at moderately high voltages.

Advantages of gas dielectric, apart from a superior strength for some situations, are that it has a very low loss, is non-inflammable and clean, and is self-healing when breakdown occurs. It also is light, although at higher pressures the containment vessel can be heavy. The dielectric constant is close to unity, and for some applications, for example insulation with minimum energy storage, this can be advantageous. Disadvantages compared with liquids, include power heat transfer properties, and the presence at high pressure of significant compressive energy. Physical properties will be discussed later in Section 4.8.3.

Gas dielectric is used, for example, in high voltage, low loss precision capacitors, (1) coaxial power transmission, (2) switch gear, (3) transformers, (4) and power supplies, (5) and almost universally in very high voltage accelerators.

Several theories have been developed to explain the electrical breakdown of gases, and that which is applicable depends on the range of pressure and gap spacing. The first understanding of breakdown can be traced to Townsend at the beginning of this century. He defined a quantity α , known as the first Townsend ionization coefficient, representing the number of ionizing collisions made by one electron drifting one centimeter in the direction of the electric field. The value $1/\alpha$ is consequently the average distance between ionizing collisions. An initial electron current i amplifies to i $e^{\alpha x}$ in the field direction. The coefficient α is proportional over a distance to pressure (p) and consequently it is convenient to specify the value α/p , a function of E/p, for a specific gas. Townsend, in examining conduction through gas gaps, concluded that other processes could contribute to current growth, particularly by augmentation at the cathode, and he identified these, in combination, by a second Townsend coefficient y, defined as the number of secondary electrons produced at the cathode per electron produced in the gap by primary collisional ionization. This factor γ is a function of E/p.

These effects lead to the following expression for current across a gap with spacing $\boldsymbol{\delta}$

$$i = \frac{i_o e^{\alpha \delta}}{1 - \gamma (e^{\alpha \delta} - 1)}$$
 (1)

Current instability, i.e. breakdown, occurs when the denominator is zero, or

$$Y(e^{\alpha \delta} - 1) = 1 \tag{2}$$

and since usually $e^{\alpha \delta}$ >> 1 breakdown occurs at γ $e^{\alpha \delta}$ = 1. Townsend's equation can be used to justify Paschen's Law, which states that breakdown voltage depends only upon the product of pressure and gap (pd). Figure 4.1 gives Paschen's curve for several gases, including air. (7)

It is common to tabulate the intrinsic strength of a gas at atmospheric pressure, but these values should be used with care, particularly at

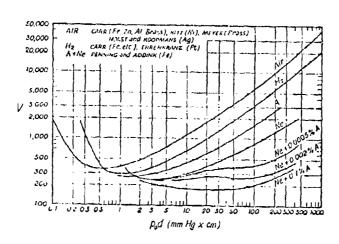


Figure 4.1 Typical breakdown voltage curves for different gases between parallel plate electrodes, $\rm p_{0}$ is the gas pressure in mm. Hg corrected to 0° C.

smaller spacings, below 1 cm perhaps, where breakdown fields can be significantly higher than at larger spacings (Figure 4.2). (7)

The speed at which insulation strength collapses under some situations, for example, when pulsed voltage is applied to a high pressure gap, requires explanation beyond that available from the Townsend mechanism alone. It has been postulated that the electric field in the gap can be significantly enhanced by the electron/ion pairs generated by the α process and thus lead to the development of "streamers" which can be both anode directed, and cathode directed. The electrons, of course, have high mobility, and ions low mobility, which leads to the type of field pattern shown on Figure 4.3.

A streamer, in contrast to the relatively weak and exponentially growing Townsend avalanche, is a conducting filament of highly ionized gas which constitutes the initial stage of a spark channel through which the external circuit discharges. The process of streamer development is shown diagrammatically in Figure 4.4. In the first phase a positive ion space charge, shown here at the anode surface (Figure 4.4(a)), is developed by avalanche effects. In the gas surrounding the avalanche photoelectrons are produced by photons emitted from the densely ionized gas in the avalanche stem. If the space charge field is significant compared with the external field, these electrons start auxiliary avalanches directed towards the main stem. Positive ions left behind by these avalanches effectively lengthen and intensify the space charge of the primary avalanche in the direction of the cathode (Figure 4.4 (b)) and the process develops as a self-propagating streamer. This transition from avalanche to streamer seems to occur in air when $e^{{m q}\cdot x}$ is the order e²⁰. The higher the overvoltage, the earlier the occurrence of the transition.

Apart from the observation that the avalanche is invisible and the streamer brightly luminous, there are large differences in the velocity of propagation. The avalanche progresses at perhaps 10⁷ cm/second whereas 10⁸ cm/second or higher is more typical of streamer propagation.

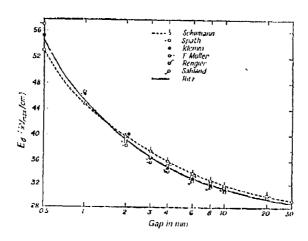


Figure 4.2 Breakdown voltage gradient in air at 1 atm, as a function of gap length between parallel plates.

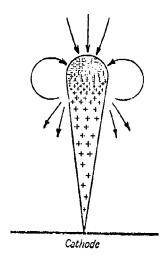


Figure 4.3 Representation of the distribution of electrons and positive ions in an electron avalanche. The arrows denote the direction of the resultant electric field surrounding the avalanche.

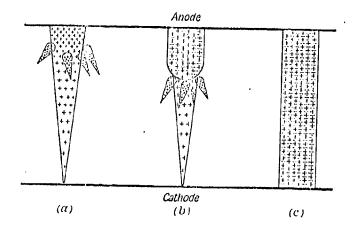


Figure 4.4 Transition from an electron avalanche to a streamer and the subsequent growth of a streamer across the gap.

In general, at smaller gaps and lower pressures breakdown can be attributed to the Townsend avalanche mechanism unassisted by streamer development. However at the larger gaps and pressures the space charge field attains a critical value before the avalanche reaches the anode, which generates mid-gap streamers. Raether has stated that above pd = 1000 torr cm streamers develop during the breakdown process, although even lower pd thresholds (approximately 500 torr cm) have been postulated. (9)

A concise treatment of the Townsend processes is given by Devins and Sharbaugh, and Meek and Craggs treat the streamer development process in detail.

With regard to the speed with which a gap breaks down, it is generally assumed that because of the relatively high speed of streamer propagation the elapsed time between the nonconducting and "fully" conducting state essentially consists of the time the avalanche mechanism takes to build up to the critical charge concentration for streamer development. This is important in switching gaps. If there is more than one free electron available at the start of the avalanching, for example if the gap has been overvolted with a fast risetime, or if laser initiation at the cathode is used to cause breakdown, multiple avalanches can develop together and the critical charge concentration is reached more rapidly than when only one avalanche propagates, i.e., the formative time lag is less because of multiple avalanching.

The breakdown strength of a gas is highly dependent on the value of α , the number of free electrons per centimeter produced by one electron. This in turn depends on the energy acquired between collision; the greater the number of collisions per centimeter the less the value of α for a given field strength. Consequently α falls and electric strength rises with increasing gas pressure. Further, the larger the gas molecule and its cross section the lower the value of α , which leads to higher strengths. However, a more important factor in obtaining high strength is the electron attachment process. The removal of electrons from the avalanche by attachment to a neutral molecule, produces relatively immobile negative ions and increases dielectric

strength considerably. The most important electronegative gas is sulphur hexafluoride which has a strength about 2.5 times that of air.

In general, it seems that the larger the molecular weight of a gas the higher its electric strength, as would be expected from the above comments. Unfortunately, the boiling point also tends to rise with increasing molecular weight and dielectric strength, so that some of the more interesting gases electrically, are liquid at room temperature. This can be seen from Table 4.1. (11) Reference 12 provides a valuable discussion of the several high strength gases which are of commercial interest. Table 4.2 is an extract from that reference.

To determine the best gas, pressure, and high voltage system configuration for a particular application, several important factors have to be considered. Generally, the requirement is a high voltage equipment design which will perform satisfactorily and with the best overall economy, including capital and operating cost considerations. Dielectric design usually starts with the given information on the temporal form of the voltage to be insulated, its amplitude and the general shape of the equipment at high voltage. The stress which can be supported may depend on the waveform of the voltage; whether it is continuous, alternating or pulsed. The breakdown stress can also be influenced by the magnitude of voltage to be insulated, and the area under stress. With a knowledge of these parameters (the area need only be roughly known) suitable gases, pressures, and materials for the stressed surfaces can be determined; the final selection usually being based on overall economic considerations. The usual stressed surface material is a metal, but interesting data has been obtained on dielectric covered metal surfaces. (13)

Because the high voltage parts have to be physically supported, it is impossible to design gas insulated equipment without considering the problem of solid dielectric flashover in the gas. Generally the distances required to be safe from flashover are much greater than for breakdown through the unbridged gap. In designing the stand-off insulation the wave shape of the voltage

Table 4.1 Values of relative electric strengths.

	T							i
* Relative Electric Strength	2, 5/760 mm	5. 5/600 mm	4.3/600 mm	3.6/753 mm	4.7/735 mm	5.8/550 mm	6.3/760 at 180°C	sure indicated (mm Hg) relative to air at the same pressure. The measureusing two polished brass spheres of diameter 1-inch contained in a glass cell acuated. The spark gap was generally 0.015 to 0.020 inch. The apparatus nently by the measurement of the relative electric strength of SF_6 . The this was found to be 2.5.
BP °C	-63.8	25	22	-63	-30	ı	101	at the same pressiameter 1-inch co
Molecular Formula	SF6	C476 C5F8	$C_{5F_{10}}$	CF_3CN	C2F5CN	C_3F_7CN	$c_{8F_{16}}$ o	sure indicated (mm Hg) relative to air at the same pressure. The measure using two polished brass spheres of diameter 1-inch contained in a glass cacuated. The spark gap was generally 0.015 to 0.020 inch. The apparatus uently by the measurement of the relative electric strength of SF_6 . The this was found to be 2.5.
Compound	Sulfurhexafluoride	nexalluorocyclobutene Octafluorocyclopentene	Decafluorocyclopentane	Trifluoroacetonitrile	Pentafluoropropionitrile	Heptafluorobutyronitrile	Perfluorobutyltetrahydrofuran	* Measured at pressure indicated (mm Hg) relative to air at the same pressure. The meas ments were made using two polished brass spheres of diameter 1-inch contained in a glas which could be evacuated. The spark gap was generally 0.015 to 0.020 inch. The appara was checked frequently by the measurement of the relative electric strength of SF6. The average value of this was found to be 2.5.

Table 4.2 Typical properties of gases at 760 mm Hg.

		Densit	Density, 0°C			÷				
Name	Formula	G per 1	Lbs./ cu ft	wolec- ular Weight	Point, C	Point ° C	Ke at we Diel. Str $(N_z = 1)$	Dielectric Constant	Specind Gravity, Air == 1	Flamma- bility
Air Hydrogen Nitrogen	# Z	1.2929 0.08988 1.250e	0.08018 0.005611 0.07807	28,952 2,0150 28,016	259.14	-194.0 -252.8 -195.8	1	*1.000590 *1.000264 *1.660580	1.00000 0.06952 0.96724	no yes no
Suffur Hexaffuoride	SF.	6.700	0.417	146.06		—63.8	23	16100 1,	5.19	ווכ
ordinations methane Perfluoropropane	CCLF. C.F.	6.33	•0.395	120.93 188.02	-158 -160	-29.79 36.7	2.46	31.00.1°		5 6
Octafluorocyclobutane Perfluorobutane	ر بر بر بر بر	29.6,	10.601	200.04	_41.4 _80.0	-5.85 -2.0	2.6	*1 0034	7.3323	2 2
Chloropenta- fluo-oethane	COLF	*3.37	0.522	154,48	-106	-38.7	2.54	1.0018		8
fluoroethane	C,CI,F.	•7.83	€84.0	176.94	76 H	- 377	2.8	1.0021		2
Hexafluoroethane Tetrafluoromethane	C.F.	'9 01 '7.62	'0.552 '0.476	138 02 88 01	100 6 184	- 78.2 -127 9e	2.02	"1.0020 "1.0006		011
1	42 42 12	4 Sat'd va 5 11 29 c 6 11 0 C	Satid vapor in bolitig point in 29% (0.5 atm) in 0.0	fried guil	7. ft. 8 1.2 9 ft	4 27.4°C .0 5 atm ¹ 12 atm & 26 8 C 4 23°C	atmi 3 C	10 1 11. S	10 12 atm & 24.6°C 11. Sublimes &63.8°C	6°C 63.8°C

is again important, as is the stand-off material, geometry, surface condition, end configuration, and of course the surrounding gas.

In the following section gaseous insulation under continuous stressing is discussed, with the subsequent sections treating in order the differences introduced by alternating and pulsed stressing. Section 4.7 separately identifies studies involving gas insulation which were prosecuted for specific DOD objectives and which consequently may be particularly relevant to the goals of this survey. The final section under gaseous insulation treats more general design considerations, including the important physical factors such as cooling properties and stored compressive energy. Typical operating stresses in equipment are given.

4.2 dc Properties

4.2.1 Air (Uniform Field)

The most commonly used gaseous dielectric is, of course, air, which has electrical properties equivalent to nitrogen for most practical purposes at atmospheric pressure, and being generally somewhat superior at higher pressures. The performance at pressures below one atmosphere can be determined from the appropriate Faschen curve on Figure 4.1. (7) Commonly the strength of air at atmospheric pressure is taken as 30 kV/cm, but as shown on Figure 4.2 the strength rises significantly above this value for smaller gaps, and falls slightly below 30 kV/cm for larger gaps. There have been many studies of the breakdown of air gaps in uniform fields, primarily for voltage calibration purposes: these studies have included the corrections required for humidity and density. (7) Most of these calibration experiments have been conducted using power frequency voltages, but the results differ very little from the direct voltage case. The curves on Figure 4.2 show closely corresponding ac and de results from several investigators.

At the relatively low electric fields supported by air at atmospheric pressure the breakdown voltage is usually highly reproducible. Bruce, (14) taking extreme care, reports maximum deviations of 0.15 percent. This indicates, as discussed later in Section 6, that area effects in this insulating environment should be very small.

As pressure is increased above one atmosphere the limiting electric field increases, at first in an almost proportional fashion. Howell (15) has obtained data for air at pressures up to 600 psig as shown in Figure 4.5. Trump et al. (16) present similar data for air and nitrogen/carbon dioxide mixtures which demonstrates the importance of electrode materials at the higher field strengths (Figure 4.6). Further data on high pressure air is given on Figure 4.7. Felici and Marchal (17) have shown that the cathode material is the more important factor, although it seems that the anode material also has a significance. (16) Surface roughness is another important factor. For example, careful polishing of an originally sandpapered surface can increase breakdown voltage by as much as 60%. (15)

At these high fields the scatter of breakdown values becomes large, indicating the presence of a significant area effect. Figure 4.8 is a typical sequence diagram from breakdown tests showing also that there is a pronounced conditioning effect. The final conditioned value after sparks have removed dust particles or surface contaminants can be 50% higher than the initial—an important design consideration.

4.2.2 Air (Nonuniform Field)

When voltage is increased in a nonuniform field gap system, corona is often initiated in the region of highest field at a potential appreciably below the breakdown voltage. The initiation voltage is determined by the degree of nonuniformity of the field. For example, with sphere to plane geometry it is impossible to distinguish between corona onset and breakdown when the gap is small and the field close to uniform, whereas at larger gaps when

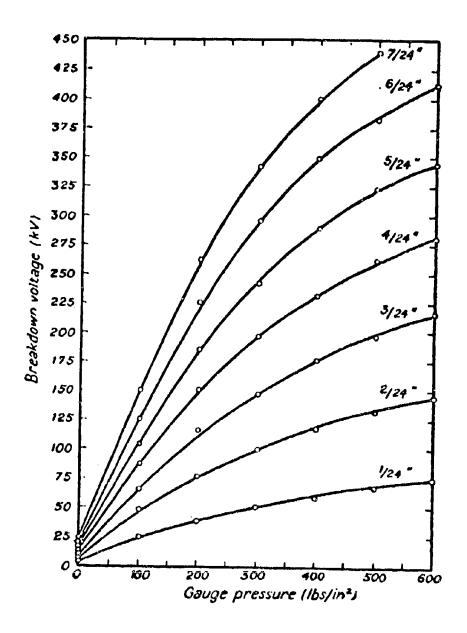


Figure 4.5 Breakdown voltages for plane electrodes in air at various constant spacings.

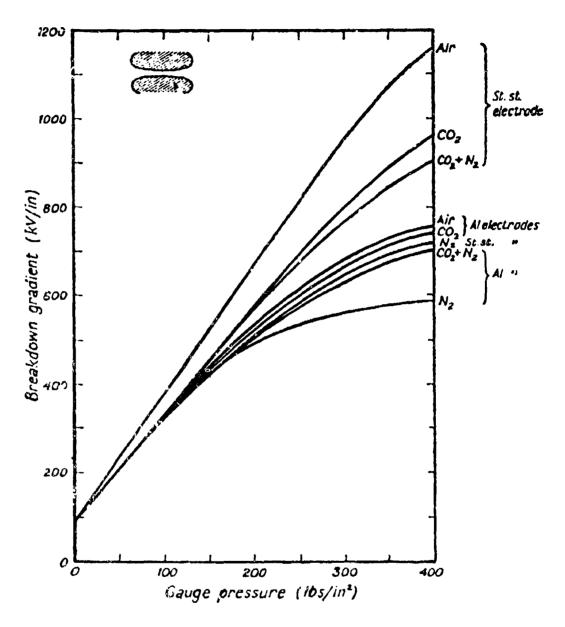


Figure 4.6 Br. akdown voltage gradients for several gases at high pressures for uniform fields between stainless-steel electrodes and between aluminum electrodes.

(Gradient is the mean values obtained from 1/4 inch, 1/2 inch and 3/4 inch gaps--no gap dependence was seen.)

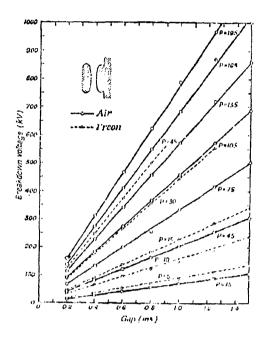


Figure 4.7 Variation of de breakdown voltage of air and of Freon-12 with electrode separation at several absolute pressures in pounds per square inch. Uniform field,

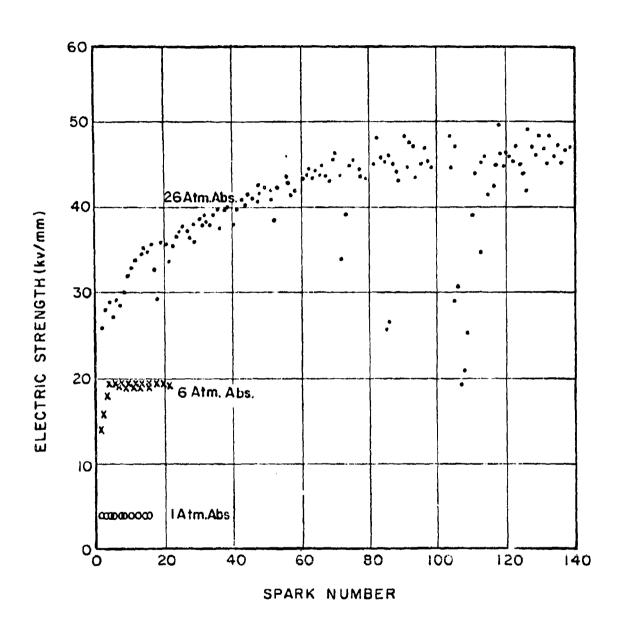


Figure 4.8 The effect of spark conditioning on the electric strength of compressed nitrogen, using parallel plane oxidized copper electrodes of 2-5 cm diameter at a spacing of 1 mm.

the situation approaches the point to plane configuration, corona develops at the sphere at voltages significantly below the breakdown value.

Nonuniform field geometries tend to fall into the following general configurations--coaxial, sphere to plane, point to plane and point to point (rod gaps). Examples of these arrangements will be treated in that order, progressing in general from atmospheric pressure to high pressure properties.

Coaxial geometries have been studied by Uhlmann using both de and ac. (18) The data on Figure 4.9 compares both polarities with ac, the broken curves showing that corona developed on the smallest diameter cylinders at voltages much below breakdown. In the absence of corona the maximum field supported on the inner wire is approximately 38 kV/cm. At the smaller internal cylinder diameters, the space charge produced by the corona modifies the electric field in the region critical to breakdown, which accounts for the high breakdown voltages at those geometries (Figure 4.9). Howell (15) has obtained curves of breakdown voltage at higher pressures for four different cylindrical arrangements (Figure 4.10). As shown, there is a distinct polarity effect with the smaller set of cylinders. With the larger cylinders Howell found it impossible to obtain satisfactory values for the positive polarity which ranged crratically between 50 and 80 percent of the negative value.

Sphere to plane geometries give field distributions which vary from near uniform situations when the gap is small compared to the sphere diameter to highly intensified fields around the sphere when the gap is large. Ganger (19) has studied sphere to plane gaps at pressures from zero to forty atmospheres (gauge) with results given on Figures 4.11 and 4.12. Figure 4.11 for a 5 mm diameter sphere, shows a pronounced polarity effect. It is worth noting that here, for example at 25 atmospheres gauge, the positive value is greater than the negative, whereas at lower pressures, for example at less than about 7.5 atmospheres, particularly for the more nonuniform field conditions (d large), the reverse can be true.

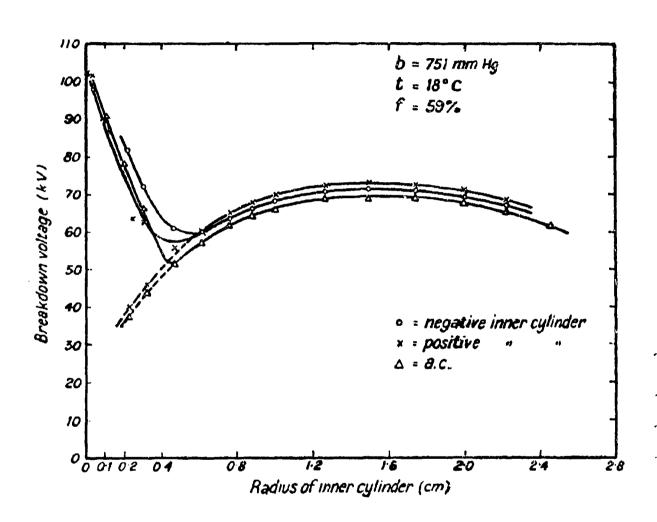


Figure 4.9 Breakdown voltage curves in air at 751 mm Hg between coaxial cylinders as a function of the radius of the inner cylinder. The radius of the outer cylinder is constant at 5 cm.

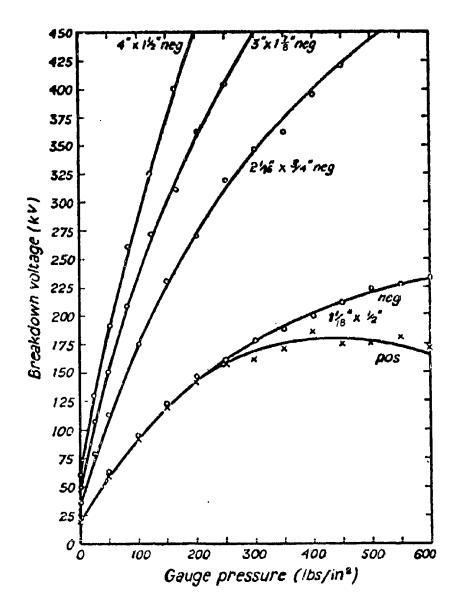


Figure 4.10 Breakdown voltage curves for coaxial cylinders in compressed air. The cylinder diameters, and the inner cylinder diameter, are shown.

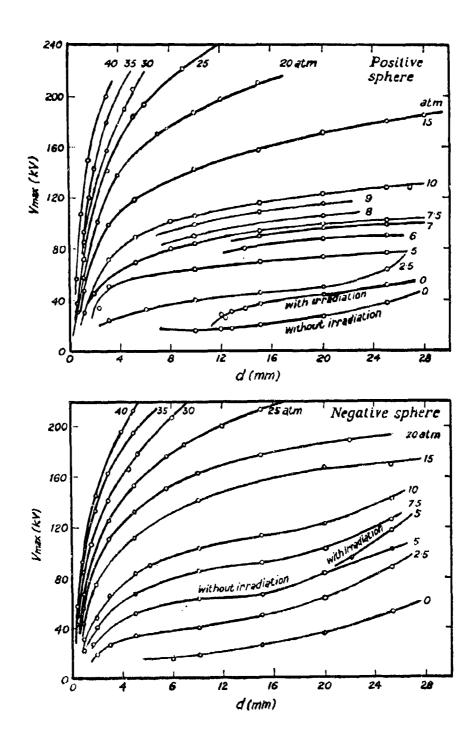


Figure 4.11 Breakdown voltage curves in air, at various gauge pressures in atm., between a sphere of 5 mm diameter and a plane.

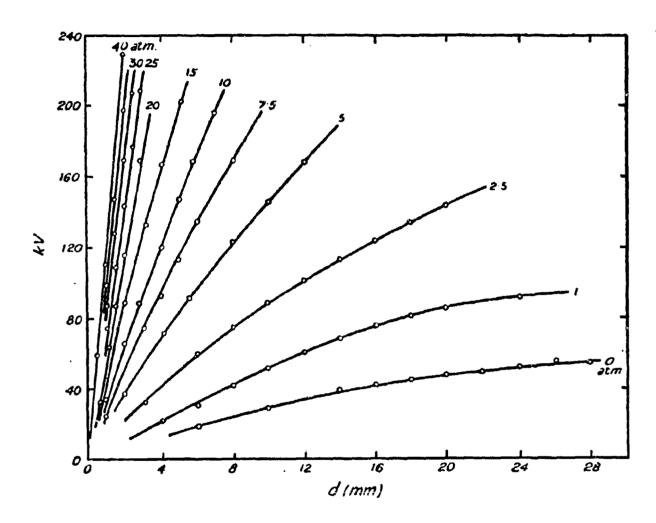


Figure 4.12 Breakdown voltage curves in compressed air, at different gauge pressures, between a 5 cm diameter sphere and a plane.

Point to plane gaps have been studied in several forms, in some cases the plane taking the form of a sphere of relatively large diameter. The "points" can be needles, hemispherically-ended rod, conical points or square rod (typically 1/2 to 5/8 inch in section when used in rod gaps). Uhlman (18) has reported for both polarities the performance of conically pointed and hemispherically ended electrodes at gaps up to 9 cm (Figure 4.13 and 4.14). The presence of field distorting corona below the breakdown level makes it difficult to determine before hand the performance of nonuniform field gaps, particularly where the gap is small. This is well illustrated by the information on Figure 4.15, (20) and is a further reason for designing high voltage equipment to be corona-free.

Howell (15) has obtained the data shown on Figure 4.16 for negative point to plane at pressures up to 550 psig. With positive points there is usually a pronounced peak in the breakdown voltage characteristic, as shown in Figure 4.17. This is attributed to a modification of field in the gap caused by space charge accumulation. The fact that nitrogen does not show this peak in contrast to the electronegative gases suggests the importance of negative ion space charge.

Point to point gaps generate a field distribution which is accentuated at each of the points. With points of similar geometry, the breakdown voltage is influenced by polarity with respect to ground, as would be expected since the field at the grounded point is less than that at the high potential point (Figure 4.18). (19) As the gap between points is increased, the breakdown voltage becomes less dependent on the geometry of the points and this has led to the use in commercial practice, for calibration and protection, of rod gaps of square section, typically of 1/2 inch or 5/8 inch side with square-cut ends.

4.2.3 SF₆ (Uniform Field)

Apart from air, the most widely used gas for electrical insulation is SF₆, a relatively dense, electronegative gas. Its dielectric constant varies

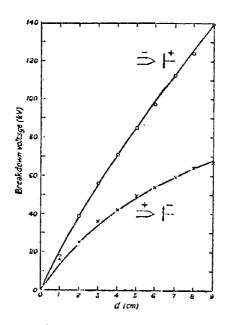


Figure 4.13 de breakdown voltage curves for air between a 30° conical point and a plane (atmospheric pressure).

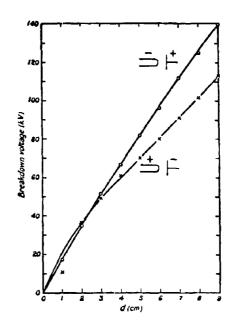


Figure 4.14 dc breakdown voltage curves for air between a hemispherically-ended rod, of 0.4 cm diameter, and a plane (atmospheric pressure).

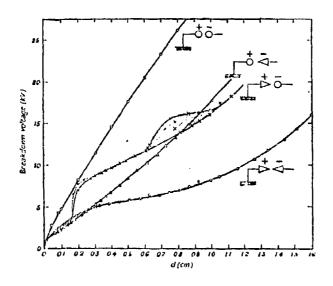


Figure 4.15 dc breakdown voltage curves in air at atmospheric pressure for various combinations of point and sphere electrodes. The sphere diameter is 5 cm. The shaded area indicates an unstable region.

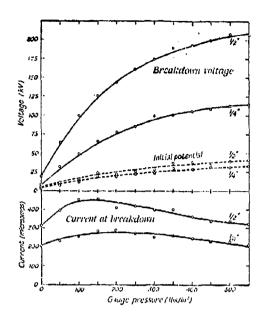


Figure 4.16 Voltage and current characteristics for a 0.25 inch and 0.5 inch gaps in air between a negative point and a plane. Broken curves show corona initiation potential.

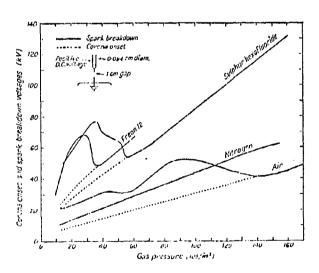


Figure 4.17 Voltage characteristics for a positive point-plane gap in compressed air, nitrogen, Freon, and sulphur hexafluoride.

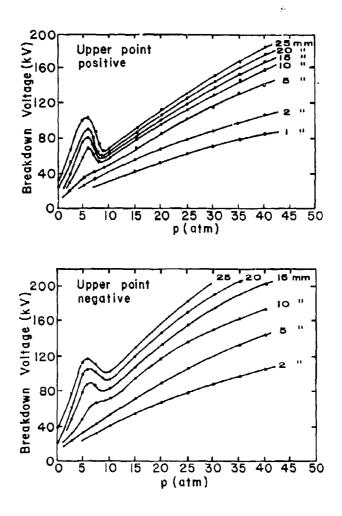


Figure 4.18 Breakdown voltage curves in compressed air between two points. The points are arranged vertically, the lower point being earthed. The figures against the curves give the gap lengths.

almost linearly from 1.00 to 1.07 over the range 0 to 22 atmospheres. (22) The Paschen curve for SF₆ is shown on Figure 4.19, (23) and Table 4.3 shows the de, ac and standard impulse breakdown voltage under near uniform field conditions at pressures up to four atmospheres. (24) There are no large differences in breakdown voltage at each pressure and gap as the temporal form is changed. A maximum difference of 22% exists between power frequency and impulse sparking at four atmospheres and 0.5 cm. The dielectric strength relative to air is seen to be close to 2.5.

For economy, sulphur hexafluoride is frequently mixed with other gases such as air or nitrogen, fractions of 10-20% giving dramatic improvements in strength over the base gas (but see Section 4.8.2). This is shown in Figure 4.20 where the strengths of ${\rm SF}_6$ and nitrogen mixtures are compared with those of the pure gases (upper curves). The lower set of curves shows the performance with ${\rm SF}_6$ and air mixtures. The large superiority of air over nitrogen at the higher pressures is worth noting.

Further data on the effect of mixing ${\rm SF}_6$ with gas at atmospheric pressure is given on Figure 4.21 and Figure 4.22 which show clearly for several total pressures that with a small fraction of ${\rm SF}_6$ performance approaching that of pure ${\rm SF}_6^{(25)}$ is realized. The curves also indicate that the same pressure and gas fraction characteristic pertains with an insulator bridging the gap, although at a lower voltage level. Figure 4.23 shows the effect of adding 5% ${\rm SF}_6$ to a high voltage accelerator insulated with 50% ${\rm N}_2$ and 50% ${\rm CO}_2$, and of adding 1% ${\rm SF}_6$ to an 80% ${\rm N}_2$, 20% ${\rm CO}_2$ mixture. This accelerator had a coaxial geometry of effective length about 10 feet, outside diameter 75 inches and inside diameter 29 inches. The inner conductor was negative.

Studies of high pressure ${\rm SF}_6$ at several hundred kilovolts have also been made by Nittrouer using electrodes consisting of a 12 inch diameter flat brass region surrounded by a 24 inch diameter "guard" ring. This ring was made of aluminum and had a Rogowski contour, to preserve

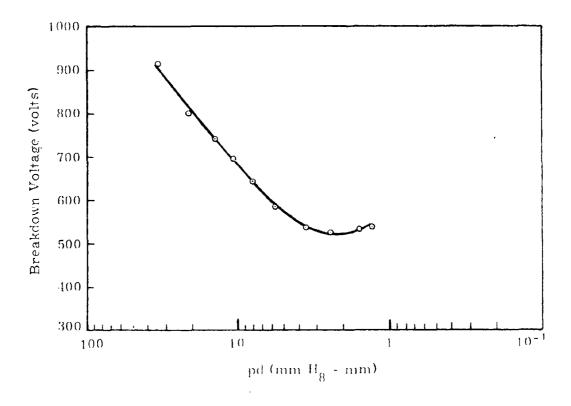


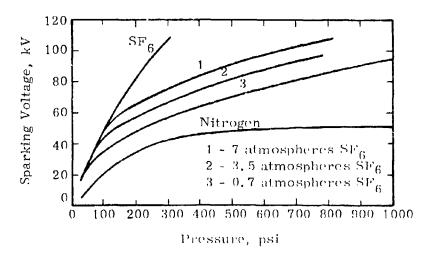
Figure 4.19 - Caschen curve for sulfur hexafluoride (gap 1 mm, parallel circular brass plates, 4 inches in diameter and 1/4 inch thick with rounded edges of 1/8 inch radius.)

Breakdown voltage between 5 cm diameter spheres in SF $_{
m 6}.$ Table 4.3

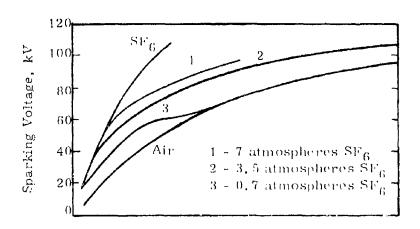
Breakdown Voltage, (kV)

Impulse Ratio*	1.0	90.	1.06	1.12	1.15
Imp Rat	0.5 1.0	1.05 1.06	1.15	1.19	1.22 1.15
Relative Electric Strength	1.0	2.7	2.87	2.68	2.53
Rela Elec Stre	0.5 1.0	2.6	2.47 2.87	2,48 2,68	2,47 2,53
tive ilse	ip, cm 1.0	47.7 91.3 2.6	171.0	244.0	306.0
Negative Impulse	Sphere gap, cm 0.5	47.7	0.19	134.5	175.0
Negative Direct	0.5 1.0	83, 5			
Negative Direct	0.5	44.0			
Power Frequency	1.0	86.0	79.0 161.0	218.0	268,0
Pov Freqi	0.5	45.0	79.0	112.5	143,5
Absolute Pressure Atm.		91	2	çç	4,
Compound		SF 6			

*Ratio of impulse to power frequency breakdown voltage.



Electrodes - bright mild steel Test gap - 1 mm



Pressure, psi

Electrodes - bright mild steel Test gap - 1 mm Field configuration - uniform

Figure 4.20 Dielectric strength of ${\rm SF}_6$ mixed with nitrogen (upper curves) and air (lower curves).

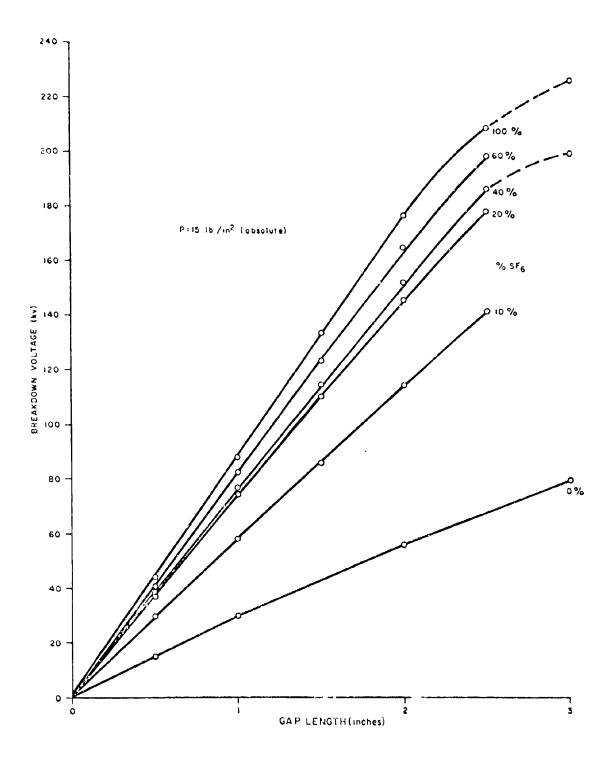


Figure 4, 21 dc breakdown versus gap length in SF $_6$ - $^{\rm N}_2$ mixtures (15 cm diameter uniform field electrodes).

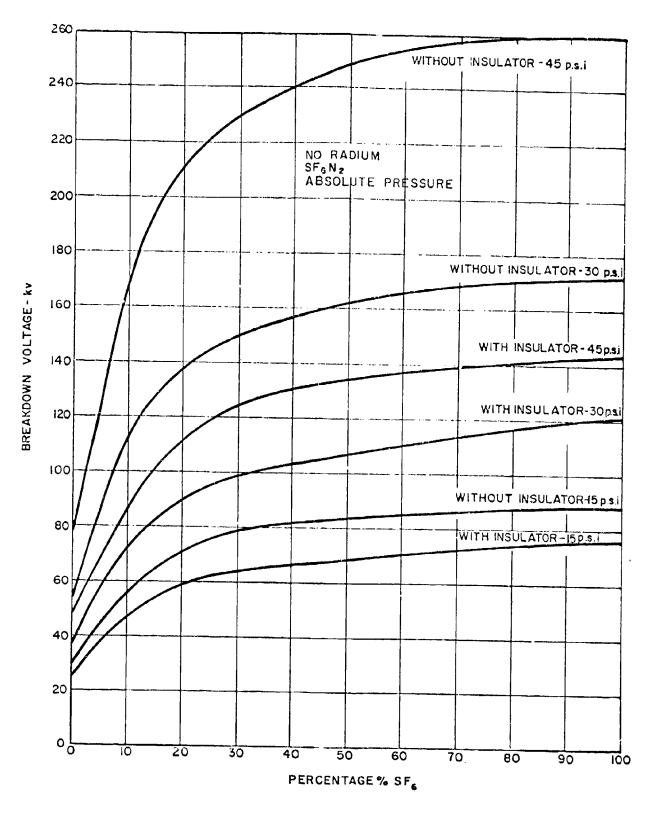


Figure 4.22 dc breakdown versus ${\rm SF}_6$ uniform field--1 cm gap (15 cm diameter uniform field electrodes and porcelain insulator).

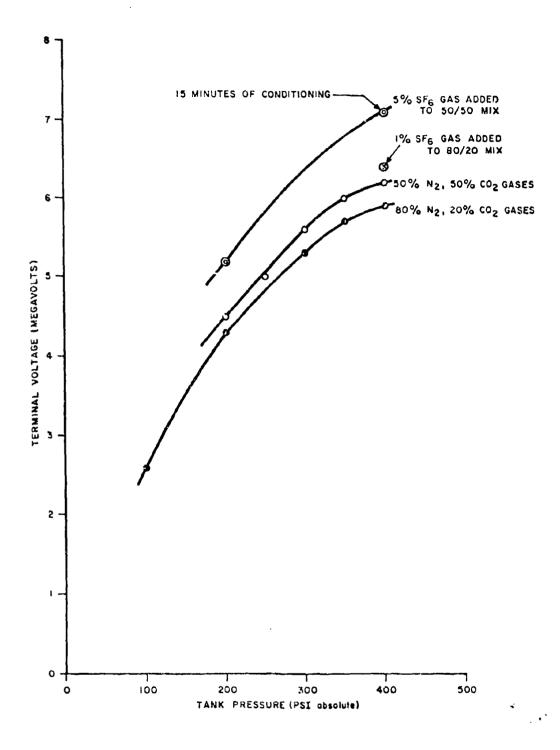


Figure 4. 23 Preliminary de breakdown characteristics for SF_6 , N_2 and CO_2 gas mixtures between concentric cylinder electrodes with a gap spacing of 58, 5 cm

uniform and maximum field conditions in the central region of the gap. Figures 4.24 and 4.25 show the data obtained. Comparatively few of the discharges occurred on the central brass electrode; most developing between the aluminum contours and at the junction between the brass and aluminum parts.

Several investigators have studied the effect on high voltage performance of a dielectric coating applied to the electrode surfaces. Figure 4.26 shows data obtained by Trump and Philp (28) when an inner coaxial conductor was coated with glyptol, glass or lucite to a thickness of 1.1 mm. It can be seen that with bare metal the maximum voltage insulated is higher when the inner, higher field, conductor is positive eather than negative, which might be expected from electron field emission and its potential effect on breakdown. The application of a dielectric to the high field (inner) conductor roughly doubles the insulation strength when the conductor is negative because of the suppression of field emission, and has little effect when it is positive.

For conditions where the field intensification is not great as evidenced by the corona onset approaching, or coinciding with, the breakdown voltage there is good agreement between the power frequency and deperformance, and power frequency data can be used for de design and vice versa. This is shown on Figure 4.27 for 1/2 inch sphere to plane electrodes. (29) This figure also shows the superior strength of the point to plane gap, relative to the sphere to plane gap, through space charge modification of the field. This is because of the intense corona in the point to plane gap, a most undesirable condition in most practical situations because of chemical deterioration of the SF_g.

4.2.4 SF₆ (Nonuniform Field)

Howard has studied extensively the dielectric properties of SF $_6$ at different pressures and with various electrode geometries. (24) Figure

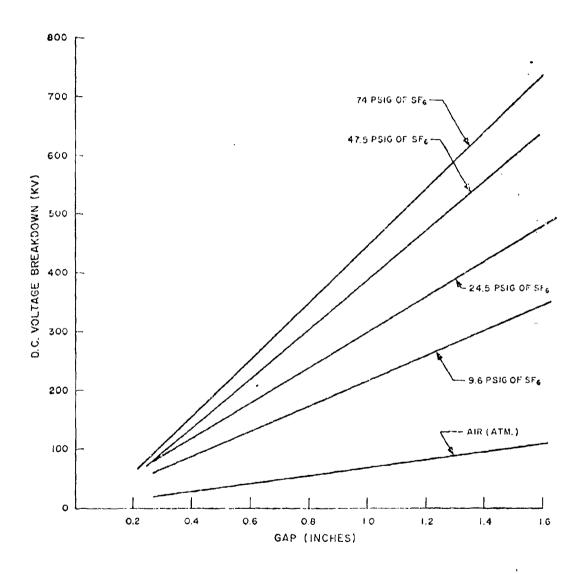


Figure 4. 24 de voltage breakdown versus gap spacing 'or 12 inch diameter brass parallel plane electrodes.

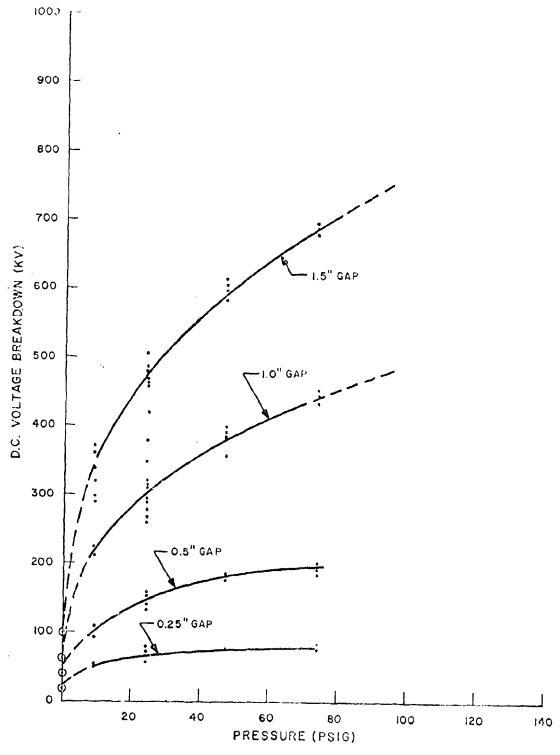


Figure 4.25 de voltage breakdown versus gauge pressure of SF for 12 inch diameter brass parallel plane electrodes at gap spacings of 0.25 inch, 0.5 inch, 1.0 inch, and 1.5 inch.

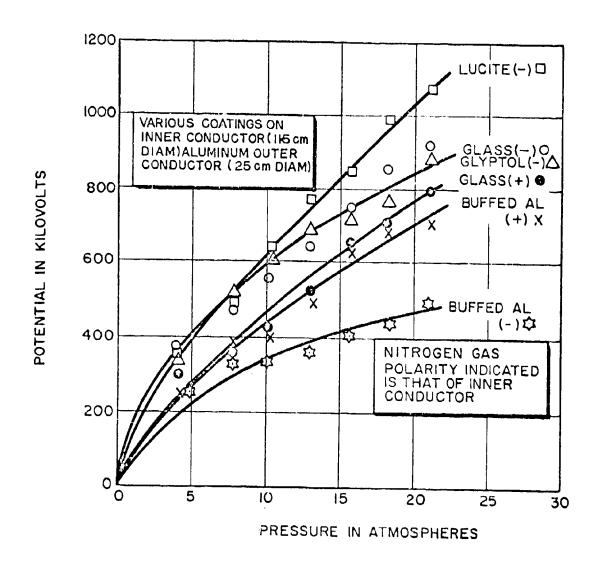
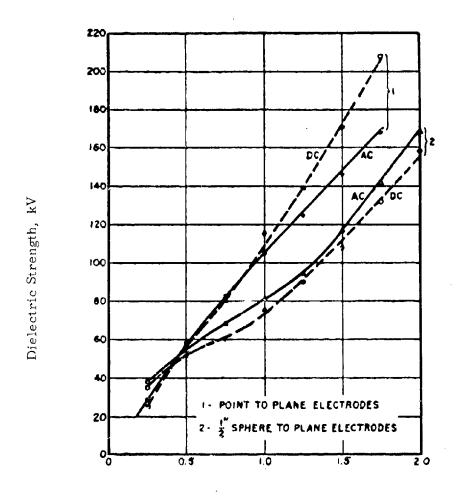


Figure 4, 26 Sparking voltage in concentric cylindrical system as function of gas pressure - various coatings on inner conductor (11,5 cm diameter) aluminum outer conductor (25 cm diameter)



Gap Distance, Inches

Figure 4.27 The comparative dielectric strength of sulfur hexafluoride gas tested under de and ac voltage at room temperature and pressure.

ac voltage - 60 cycles. dc polarity - positive. 4.28 shows do, ac and impulse breakdown voltages and corona inception levels plotted against the ratio of diameters for coaxial electrode arrangements, where the outer electrode had the diameter 3 cm. Figures $4.27^{(29)}$ and 4.29 to $4.32^{(29,30)}$ have been selected from the literature as representative data on other nonuniform field geometries, including small sphere/plane, point/plane and rod gaps under various pressure conditions.

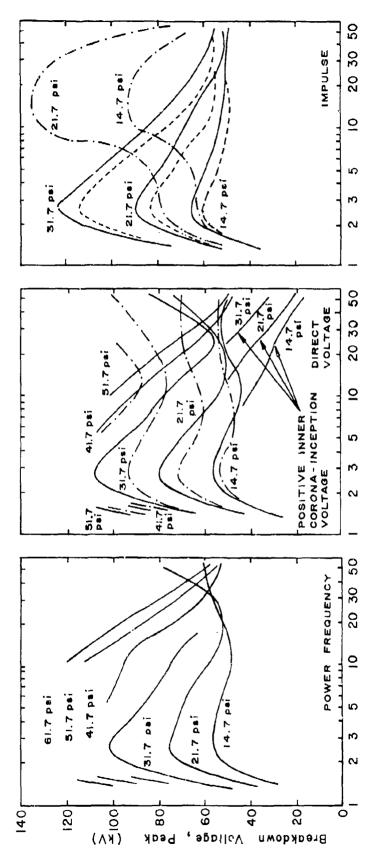
4.3 ac Properties

4.3.1 Air (Uniform Field)

As noted previously the performance of uniform field gaps under power frequency voltage is essentially the same as under continuous voltage. Tabulations are available, for example, in reference (7), giving data for uniform field gaps and for the quasi uniform field sphere gaps. At much higher frequencies (above the audio range) breakdown voltage falls below the de value, as has been discussed succinctly by Meek and Craggs. (7) The following is a condensation of their discussion which supplies the relevant references.

At the higher frequencies where positive ions have insufficient time to cross the gap in half a cycle, a space charge develops which distorts the field and reduces the breakdown strength below the de value. The breakdown process is further complicated where the frequency is sufficiently high to trap electrons which oscillate within the gap and produce cumulative ionization.

Studies of high frequency discharges in air have shown that for gaps up to 2.5 cm between spheres of 6.25 cm diameter there is no appreciable change in breakdown voltages for frequencies up to 20 kc/s. From 20 to 60 kc/s there is a progressive lowering of the breakdown voltage of a given gap as the frequency is raised but at higher frequencies, up to the maximum of 425 kc/s used, the breakdown voltage of a given gap is constant at about 15% below the value at 60 c/s.



Ratio of Diameter of Conductors

Figure 4.28 Breakdown voltage for sulfur hexafluoride between coaxial cylinders.

---- Power frequency, positive dc and impulse.
---- Ncgative dc and impulse.
---- Fositive impulse with radium.

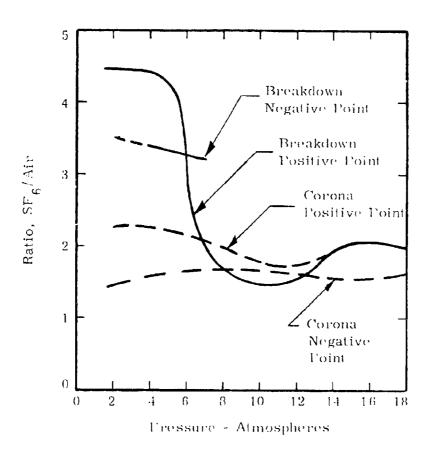


Figure 4.29. The ratio of the corona and breakdown voltages for air and ${\rm SF}_6$ as a function of the testing conditions in a nonuniform field.

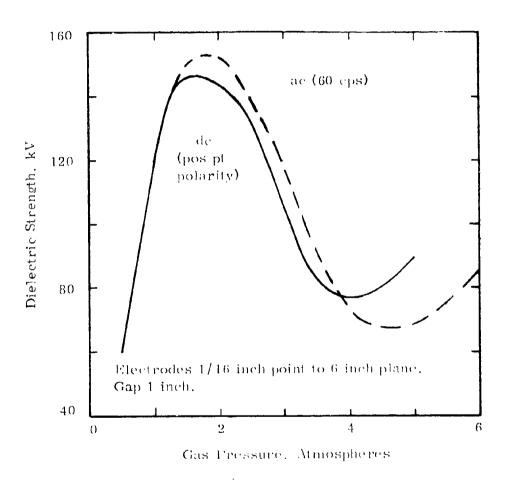


Figure 4.30 Dielectric strength as a function of gas pressure for dc and 60 cps ac voltage. Dielectric strength increases normally with pressure up to about 1 atm. Further increase in pressure produces a divergence from the straight line until a maximum strength is reached at about 2 atm. Increasing pressure beyond this point results in a drop in strength, the minimum occurring at about 5 atm.

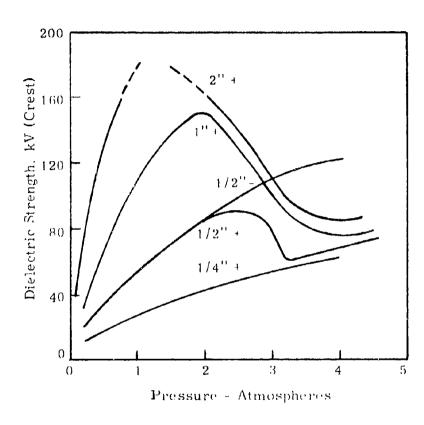
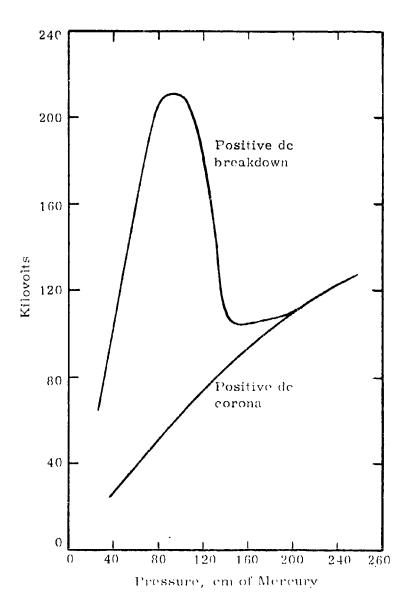


Figure 4.31 The effect of pressure on the dielectric strength of sulfur hexafluoride gas in a nonuniform (dc) electrical field for selected gap distances.

Electrodes - 1/16 inch point to 6 inch plane. Electrode polarity - point electrode as shown. Gap distance - as shown on curve.



411

Figure 4.32 The corona breakdown relation for sulfur hexafluoride as affected by pressure.

Electrodes - 1/2 inch square rods. Test gap > 2 inches. Similar results have subsequently been obtained with different types of gaps for higher frequencies and voltages. In several of the investigations voltages up to about 150 kV at frequencies up to 1 Mc/s have been used. The results show that the lowering of the breakdown voltage at the higher frequencies is appreciably greater for gaps in which point electrodes are present than for uniform or nearly uniform fields, as shown by the curves of Figure 4.33. Similar studies for point-plane gaps show the lowering at 370 kc/s being 46% for a 3 cm gap and 70% for a 25 cm gap, as compared with the power frequency values.

In the case of breakdown between spheres or plates, several of the investigators record a critical gap length below which the breakdown voltage is independent of the frequency, the critical gap length decreasing with increasing frequency. This gap is stated to be 0.45 cm at 110 kc/s and 0.09 cm at 995 kc/s. Consideration of positive ion mobilities shows that these critical gaps correspond roughly to those for which accumulation of positive ions may be expected to occur in the gap, with a consequent space-charge distortion of the field and a lowering of the breakdown voltage.

Ganger $^{(31)}$ has obtained data on the breakdown of air at pressures up to 40 atmospheres in near uniform field conditions at 1.05 x 10 Hz and compared it with the dc levels (Figure 4.34). It can be seen that particularly at the highest pressures, the rf breakdown voltage is considerably below the dc level. At higher frequencies, in the megacycle range, Bright $^{(32)}$ has investigated the breakdown of short gaps in air, nitrogen, oxygen, and C $^{(32)}$ at one atmosphere, and shown, as at the lower frequencies, that there is a critical, frequency-related, gap above which the breakdown voltage falls below the dc, or low frequency, level (Figure 4.35).

Again, the effect is attributed to trapped positive ions oscillating in the gap. In the frequency range between 100 to 300 MHz Pimm (33) has obtained the breakdown curves shown in Figure 4.36. At much larger gaps the breakdown gradient tends to a constant value of 29 kV/cm. When pressure

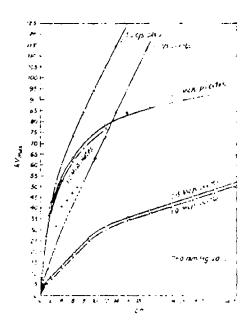


Figure 4, 33 Breakdown voltage in air at atmospheric pressure as a function of gap length between plates and between points for frequencies of 50 c/s, 0, 5 Me/s and 1, 0 Me/s.

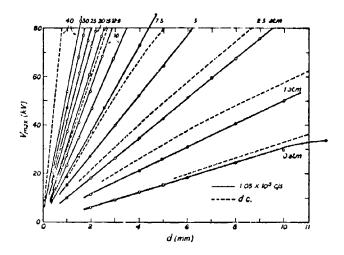


Figure 4.34 Breakdown voltage as a function of gap length between plates in compressed air for dc and 1.05 x 10^5 c/s voltages.

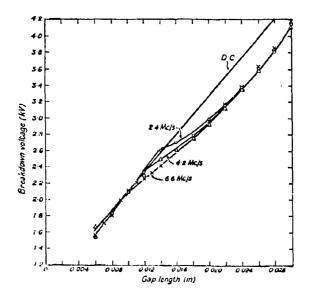


Figure 4, 35 Breakdown voltage curves in nitrogen as a function of gap length between spheres of 2, 0 cm diameter.

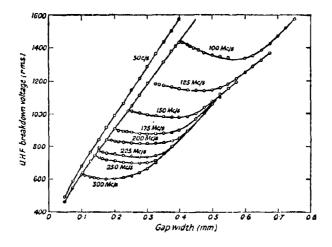


Figure 4.36 Variation of breakdown voltage with gap length between plates in air at different frequencies.

range over the range 59 to 1000 torr the breakdown voltage at 200 MHz varies with gap as shown on Figure 4.37. (30) The significance of this data to airborne packages in rarefied atmospheres is obvious. In the gigahertz range, Cooper (34) has studied the breakdown of coaxial lines and waveguides at wavelengths of 10.7 cm and 3.1 cm. Pressure was varied from 20 torr to one atmosphere with a microwave pulse duration of 1 microsecond repeated at 400 pps. One set of results compared with the positive dc case is shown in Figure 4.38. Using the same microwave frequencies I osin (35) has conducted breakdown studies with pulse duration varied from 0.3 microsecond to 5 microseconds. For example, with a 0.43 cm gap in air at one atmosphere the 3 cm breakdown voltage was independent of pulse duration above 4 microseconds and increased by about 30% for a 0.3 microsecond pulse. S. C. Brown and his colleagues have studied extensively the 9.6 cm microwave breakdown in cavities and coaxial lines at fractions of an atmosphere, and developed a new theory of ultra high frequency breakdown.

4.3.2 Air (Nonuniform Field)

In electric field systems where there is strong intensification at one of the electrodes, corona will be present over a considerable voltage range below the breakdown value. As has already been discussed, the space charge associated with this corona can strongly modify the initial field distribution and lead to surprisingly high breakdown levels. In the ac case, the presence of this corona space charge field can produce a gap current which is out of phase with the voltage across the gap.

It was noted previously for the uniform field case, that the frequency of the applied voltage can affect the breakdown level. Similarly in the nonuniform field case, the frequency can influence the voltage at which corona develops. This is shown on Table 4.4 where the corona onset voltage for wires mounted concentrically within a 5 cm diameter cylinder is given for frequencies up to 9.4 Mc/s. (32) The ac corona onset and breakdown voltage

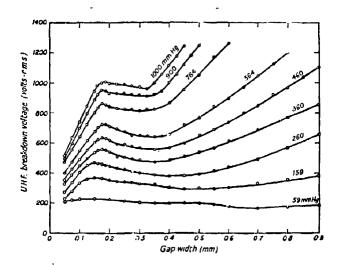


Figure 4.37 Variation of breakdown voltage with gap length between plates in air at 200 Mc/s for different gas pressures.

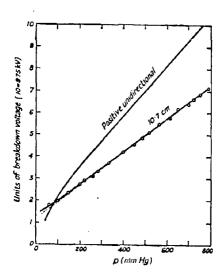


Figure 4.38 Variation of breakdown voltage with pressure for coaxial-line spark-gap.

Diameter of outer conductor = 1,04 cm. Diameter of inner conductor = 0,404 cm.

Table 4.4 Onset voltage at several frequencies for visual corona on wires coaxially within a 5 cm diameter cylinder.

	Frequency						
Wire Diameter in mm	50 c/s	1.6 <u>Mc/s</u>	3.0 <u>Mc/s</u>	3.5 <u>Mc/s</u> .	4.0 Mc/s	9,4 <u>Mc/s</u>	
0.316	7.95	7.0	6,85	6.40	6.15	6.01	
0.274	7.30	6.55	6.40	5,95	5.60	5.62	
0.234	6.75	5.90	5.85	5,50	5.00	5.10	

for sphere to plane gaps is shown in Figure 4.39. (37) The curves A correspond to the voltage at which the corona discharge can be detected, and it can be seen that at the smaller gap spacings where the field is most uniform breakdown occurs before the corona level is reached. At the larger gaps corona develops before the breakdown level is reached. The tendency to approach the point to plane gap breakdown voltage at the larger gap spacing and smaller sphere diameter is quite evident on the figure, and is further support for the comments on rod gaps for calibration and protection purposes in Section 4.2.2. Table 4.5 gives minimum 60 Hz breakdown voltage for 1/2 inch rod gaps in air at atmospheric pressure for various spacings, compared with the impulse voltage levles. Figure 4.40 shows the performance of rod gaps (for nitrogen) as the pressure is increased to 200 psia. (39)

4.3.3 Sulfur Hexafluoride (Uniform Field)

As already noted, the dielectric strength of SF relative to air in a uniform field situation is approximately 2.5, whether the applied voltage is ac or dc. This relative strength increases as the electric field departs from the uniform field condition as shown on Figure 4.41. (40) As pressure is increased from atmospheric, the electric strength increases, at first almost linearly (Figure 4.42). (41) The data on Figure 4.43 for 0.5 inch diameter sphere to plane electrodes (40) show the performance for near uniform field conditions (intensification approximately 70% for 0.5 inch gap) and for strongly nonuniform field conditions (intensification 7 for 1.5 inch gap). At atmospheric pressure the maximum breakdown stress on the sphere is 75 kV/cm for the near uniform field case and 194 kV/cm for the nonuniform field situation--showing again the high strength of ${\rm SF}_{\rm fi}$ nonuniform field geometries. The performance of SF, at 100° C over the pressure range up to 40 psig is given on Figure 4.44 (40) where it can be seen (cf Figure 4.43) that the increase of temperature has dropped the strength by 15% for the 0.5 inch gap. Howard has investigated the effect of frequency on the strength of SF_6 and

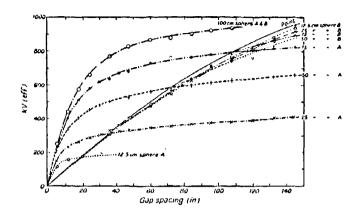


Figure 4.39 Breakdown voltage and corona onset voltage curves for sphere-plane gaps. The point-plane breakdown voltage curve is added for comparison. (Curves A are for corona onset. Curves B are for breakdown.)

Table 4.5 Minimum breakdown voltages in kV for 60 Hz and impulse voltages applied to gaps between 1/2 inch square rods in air. Polarity shown is that of the ungrounded rod. (barometer, 30 inches, temperature, 77° F, humidity, 0.6085 in vapor pressure)(38)

Gap in Inches	AC	1/5 usc	e Wave	1.5/40 u	sec Wave
		+	-	4.	-
0.5	16.5	22	23	22	23
1.0	32	38	38	38	38
6.0	105	143	146	128-141	143
15.0	210	340	335	275	309-342
40.0	545	835	875	650	740
70.0	940	1425	1515	1095	1235
100		2010		1530	

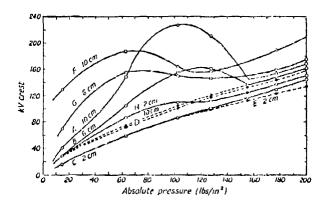


Figure 4,40 60 c/s and impulse breakdown vottage curves between 0.5 in. square-cut rods in compressed nitrogen. The figures against the curves give the gap lengths.

Curves A, B, and C Curves D and E Curves F, G, and H 60 c/s breakdown, 60 c/s corena onset, impulse breakdown,

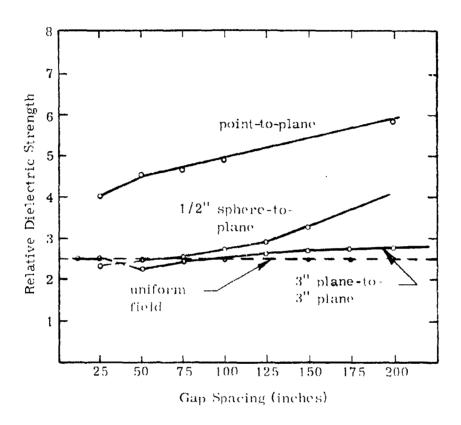


Figure 4.41 60-cycle relative strength of sulfur hexafluoride to dry air as a function of configuration and spacing of the electrodes. Gases at $25^{\rm o}$ C and at atmospheric pressure.

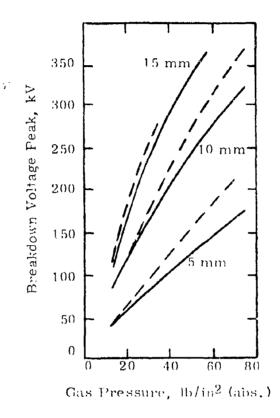


Figure 4.42 Breakdown voltage between 5 cm diameter spheres for sulfur hex illuoride.

--- Negative impulse Power frequency

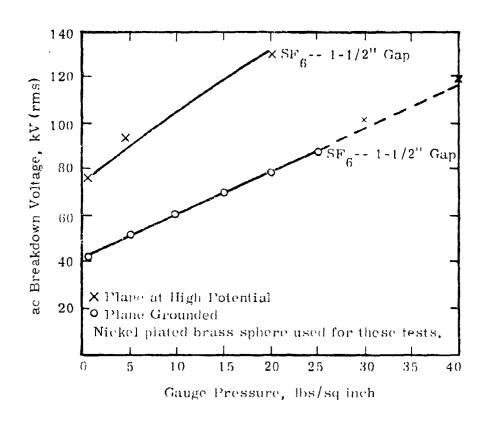


Figure 4.43 60-cycle breakdown voltages of SF₆ as a function of pressure. (Gas at room temperature.) Electrodes 0.5 inch diameter sphere to 3 inch diameter plane.

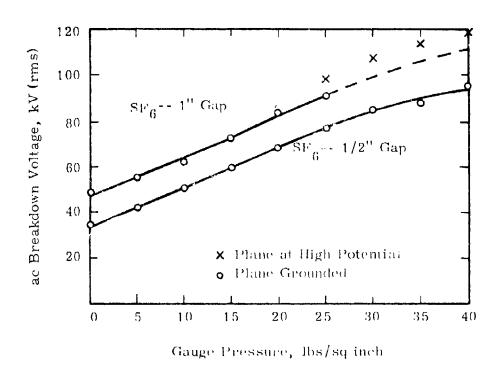


Figure 4.44 60-cycle breakdown voltages of SF₆ at 100° C as a function of pressure. Electrode: 0.5 inch stainless steel spheres to 3 inch diameter plane.

shown that it remains substantiany constant for uniform field geometries up to radio frequencies as shown on Table 4.6. (24)

As with the decase the ac strength of mixtures of SF_6 with air or nitrogen is relatively high for small percentages of SF_6 . Figure 4.45 shows, for example, that air with 15% SF_6 by volume has twice the strength of pure air. (22)

In general, with near uniform field conditions is pure SF or in mixtures with other gases, where breakdown is not preceded by corona, the dielectric strength corresponds to that of the dc polarity which has the lover value (usually negative). Kawaguchi et al. (42) have shown this in their study of the power frequency, switching impulse and standard impulse strength of SF, in near uniform field conditions (plane-plane, sphere-sphere, and coaxial). Voltages up to 1.5 MV were used. Over the pressure range examined, up to 4 kg/cm² (57 psia), they found that the positive impulse strength was given by the relationship $E/p = 86.1 \text{ kV/cm/kg/cm}^2$ as was the power frequency strength for pressures up to 2 kg/cm². Above 2 kg/cm² the power frequency strength versus pressure relationship showed a strong levelling off. This can be seen on Figure 4,46. They also concluded that polarity effects are prominent at pressures above 1 kg/cm² with the negative breakdown gradient becoming significantly less than that indicated by $E/p = 86.1 \text{ kV/cm/kg/cm}^2$. Electrode material and smoothness were not important in the pressure range examined. It was suggested that electrode area, duration of applied voltage, and gas pressure, are influential factors in the decrease of negative breakdown gradients below the positive values.

4.3.4 Sulfur Rexafluoride (Nonuniform Field)

Nitta and Shikuya $^{(43)}$ have studied both theoretically and experimentally the discharge characteristics of ${\rm SF}_6$ in nonuniform field geometries under power frequency voltages up to 600 kV peak. The strength of ${\rm SF}_6$ relative to air falls rapidly as the field becomes even slightly nonuniform as

Table 4.6 Effect of frequency on breakdown in SF₆.

Gap cm	990 kHz Breakdown Voltage (kV peak)	60 Hz Breakdown Voltage (kV peak)
0.3	26, 4	27.0
0.4	34. 3	36.1
0.5	44.3	45.0

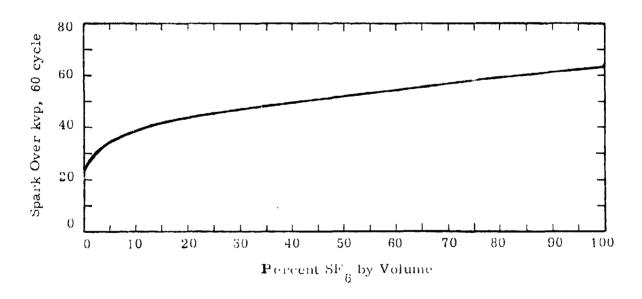
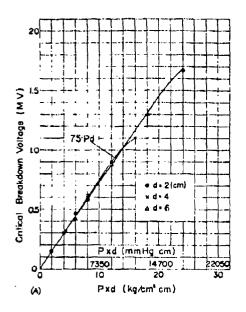


Figure 4.45 Effect of air on dielectric strength of SF₆.

1.0 inch diameter spheres--0.25 inch spacing
1200 cu. inch enclosed vessel
atmospheric pressure--room temperature
voltage increase 1 kV (peak)/minute



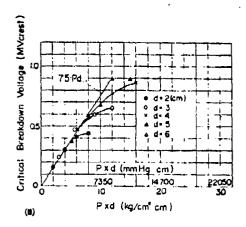


Figure 4. 46 Critical breakdown voltage between 43 cm diameter Rogowski profiled electrodes as function of p \times d (corrected to 20° C)

- (a) Standard 1. 1/40 microsecond impulse voltage
- (b) 50 Hz power frequency voltage

shown in Figure 4.47*. This is explained in terms of streamer formation when the avalanche population is of the order 10^8 . Good agreement was obtained between theory and experiment as shown by the curves for sphere and rod gaps given in Figures 4.48, 4.49 and 4.50. The expression they developed for the discharge voltage (V_d) for arbitrary electrode geometries is

$$V_{d} = (E/p)_{crit} upl \left(1 + \frac{k}{pR}\right)$$
 (3)

where $(E/p)_{crit} = a constant = 89 kV/cm atm$ E = field (kV/cm) p = pressure (atm) 1 = gap length (cm) k = 0.175 (atm 1/2 cm 1/2) R = radius of sphere or rod tipand u = E average/E maximum (Figure 4.51)

where pR is large this expression becomes

$$V_{cl} = (E/p)_{crit} upl$$
 (4)

It is questionable whether this expression can be used for all non-uniform field geometries, and as a consequence it is useful to have empirical information available. Examples from the literature for different geometries and pressure regimes are given in Figures 4.27, 4.28, and 4.52 through 4.56.

^{*}Strength here is defined as the voltage for either corona onset or breakdown, and should not be confused with the corona stabilized breakdown strengths discussed in the previous section (e.g., Figure 4.41).

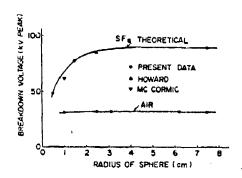


Figure 4.47 ac breakdown voltages of sphere-sphere gap as a function of sphere radius.

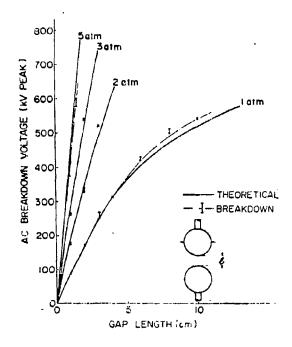


Figure 4.48 ac breakdown voltage for gap A (150 mm diameter spheres).

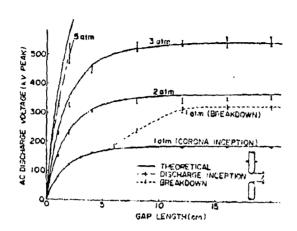


Figure 4, 49 ac breakdown or corona inception voltage for gap B (30 mm diameter rods).

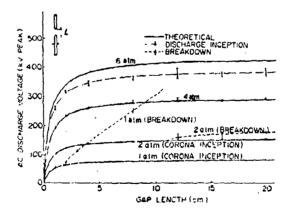


Figure 4.50 ac breakdown or corona inception voltage for gap C (10 mm diameter rods).

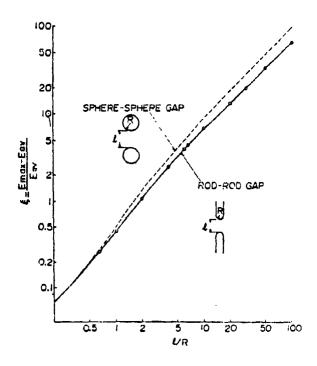


Figure 4.51 Field uniformity factor of sphere-sphere and rod-rod gaps.

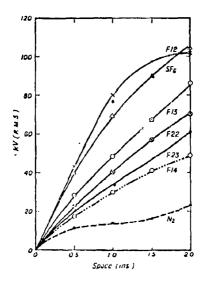


Figure 4.52 Breakdown voltage curves for various gases between a hemispherically-ended rod, of 0.1inch diameter, and a sphere of 1.0 inch diameter. The gas pressure is 1 atm.

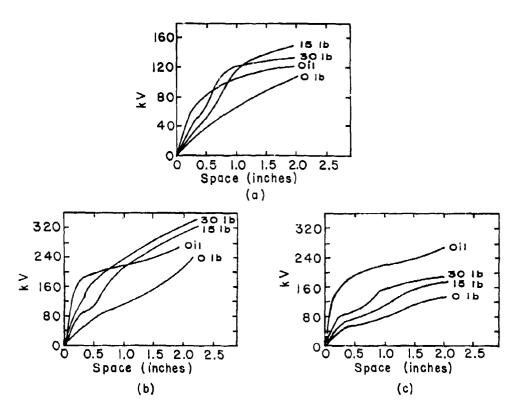


Figure 4.53 Breakdown voltage curves for SF₆ at various pressures at a function of the spacing between a hemispherically-ended rod (a) inch diameter and a sphere of 1.0 inch diameter.

(a) 60 /s. (b) Negative rod-plane (impulse).

(c) Positive rod-plane (impulse).

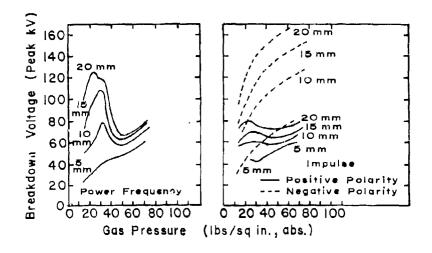


Figure 4.54 Breakdown voltage characteristics with point-sphere electrodes for ${\rm SF}_6$.

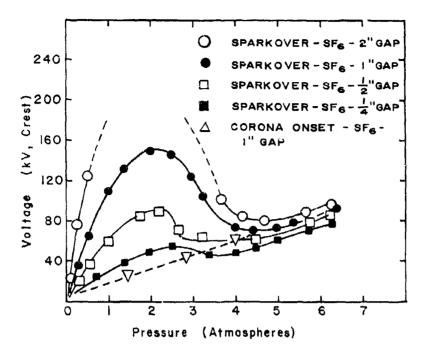


Figure 4.55 ac spark-over and corona onset voltages of sulfur hexafluoride for indicated gaps between 1/16 inch hemisphere point and 6 inch diameter plane in 12 inch diameter steel tank as a function of pressure.

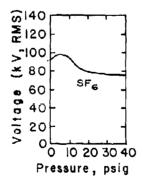


Figure 4.56 Breakdown voltage, nonuniform field, 1/5 inch rod.

4. 4 Impulse Properties

4. 4. 1 General

The impulse performance of gas gaps depends, to varying degrees, on time lag effects. As already discussed, the time lag can be separated into two parts, one (statistical) relates to the need for an electron to initiate the discharge, and the other (formative) to the time involved for the growth of the discharge once initiated.

The statistical time lag is determined by the amount of preionization, and where gaps are used for calibration purposes it is common to provide a source of preionization such as a uv lamp, a radioactive element, a corona source, or another discharge gap. The nature of the electrode surfaces also influences the time lag, as is shown on Figure 4.57. (44) In these plots the ratio $n_{\rm t}/n_{\rm o}$ represents the fraction of total impulses having a time lag greater than t. The statistical time lag has been shown to be related to the work function of the cathode and can be decreased as much as 10^3 in some situations by change of material. For example, in one case, a change of cathode surface from copper oxide to Elektron (a magnesium alloy) has been shown to decrease the statistical time lag from 560 microseconds to 0.16. (45)

The presence of intense illumination, for example that from a close electrical discharge of several joules, can lower the impulse strength significantly below the dc level (e.g. 20%). (46) This obviously is one way to trigger a spark gap (Section 9.3):

Felsenthal and Proud⁽⁴⁷⁾ have studied the formative breakdown of gases using nanosecond pulses. In their case statistical lag was eliminated by directing ultraviolet illumination from an adjacent discharge on to the cathode. Earlier investigators had theorized that formative time lag was based on streamer processes which involve space charge distortion of the initial field in the gap. Felsenthal and Proud within defined limits developed a theory based on the initial field remaining undistorted and showed that it

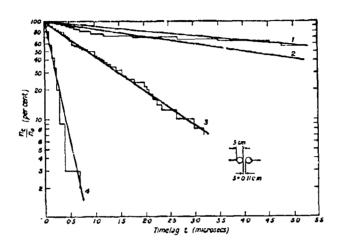


Figure 4.57 Influence of the nature of the electrode surfaces on the time-lag distribution curves for a gap of 1.1 mm between 5 cm diameter spheres. The gap is subjected to an impulse voltage of 6.5 kV, the dc breakdown voltage being 5.0 kV.

- 1. Oxidized copper electrodes, weakly illuminated, cleaned with alcohol.
- 2. Copper electrodes, unilluminated, cleaned with alcohol.
- 3. Copper electrodes, weakly illuminated, not cleaned with alcohol.
- 4. Copper electrodes, weakly illuminated, cleaned with alcohol.

agreed well with experiment. A summary of their formative time measurements in nine gases is shown on Figure 4.58.

Interest in impulse voltage strength can be roughly classified into three areas according to the pulse duration. These separate duration ranges are associated with switching surges, lightning transients, and faster phenomena such as flash X-ray pulses. Switching surges on power transmission lines typically have durations in the millisecond region and dielectric performance is generally similar to that under ac conditions. No standard switching surge waveform has been agreed upon to date, however, a wave with 200 microseconds risetime and 2000 microseconds falltime (200/2000) is a good average of the several shapes being used. Lightning transients on power lines usually generate surges at least an order of magnitude less in duration, which has led to the somewhat arbitrary adoption of the standard double experimental impulse testing waveform, with a 1.5 microsecond risetime (10-90%), and a 45 microsecond fall to the half amplitude. This waveform (1-1/2/45) is standard in the U.S. with the essentially similar 1/50 being more commonly used in the U.K. and Europe. Waves of 1/5 shape are also used occasionally for test purposes, with chopped waves also being of interest for some applications. Dielectric performance under even shorter duration pulses (<1 microsecond) is of interest for flash X-ray, electro-magnetic pulse generation, plasma physics and high power radar, and recently high power pulses in both the nanosecond and microsecond range have been required for laser excitation.

4.4.2 Air (Uniform Field)

The most extensively studied gap geometry is that between spheres, where essentially uniform field conditions exist for small gaps (spacing much less than the sphere radius). For impulse voltages with wavefronts at least 1 microsecond, the wavetails greater than 5 microseconds, there is close agreement with power frequency and dc values. The positive strength tends to be slightly higher than the negative. The differences are significant for

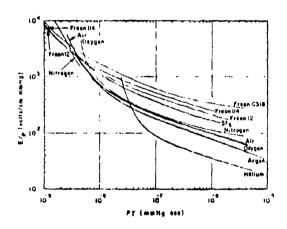


Figure 4.58 Summary of formative-time measurements in nine gases.

calibration purposes (48) but hardly so for design. At the shorter pulse durations the improved performance over dc or power frequency voltages, because of time lag effects, can be determined from Figure 4.58. For example, these curves relate the formative time of the discharge for each gas for each field strength at a given pressure, and there is thus a relation between the ouration of the pulse and the electric field necessary to cause breakdown in that clapsed time. Several investigators have studied the overvolted breakdown of sphere gaps in air. For example, Bellaschi and Teague (49) found a ratio of breakdown voltage at 0.2 microsecond time lag to that at 2 microseconds time lag of about 1.7 for their more uniform field situation (e.g., with d = 2R).

4.4.3 Air (Nonuniform Field)

Very significant differences can be obtained between positive and negative impulse breakdown voltage for strongly nonuniform field geometries as shown on Table 4.7, (50) which is for 1.5/40 microsecond wave breakdown in air. The impulse strength of rod to plane gaps at specific clapsed times for the same impulse wave can be compared with the 60 Hz value on Figure 4.59. (51) Further voltage time characteristics obtained by Udo et al. (52) and Bowdler et al. (53) are shown on Figures 4.60, 4.61, 4.62, and 4.63. Figures 4.60 and 4.61 show also the voltage which caused breakdown with 50% of the applications of a 1/50 microsecond wave. Figure 4.61 shows time to flashover values for the typical multiple unit suspension insulator strings used on high voltage power transmission lines. The performance does not differ markedly from that of long rod gaps (Figure 4.60) when the 5 inch per unit spacing is used to calculate the length of the string. Figures 4,62 and 4,63 present the impulse volt-time characteristics for parallel wire conductors (geometry on Figure 4.63), the polarity indicated (with respect to ground) being that for the conductor furthest from ground. In this very nonuniform field situation (as with rod gaps) the geometry, i.e., diameter, of the conductors is not important.

Table 4.7 Positive and negative impulse breakdown voltages of point-plane gaps, rod gaps, and wire-plane gaps in air at 20° C, 760 mm Hg, and absolute humidity 11 gm/m³, 1.5/40 microsecond impulse wave. Voltages given in kV.

Gap in cm.	Point	Point-plane		Rod gap		Wire-plans	
	+	_	+	-	+	-	
100	539	945	682	720	570	912	
125	673	1,140	803	885	705	1,140	
150	807	1,305	945	1.045	841	1.328	
175	941	1,502	1,090	1,205	976	1.515	
200	1,075	1,670	1,230	1.370	1.112	1.682	
225	1,209	1,830	1,370	1,530	1,247	1.845	
250	1,343	1,980	1,515	1,695	1,383	2.000	
275	1,477	2,125	1,655	1,855	1,518	l '	
300	1,611	2,260	1,800	2,020	1.654		
325	1,745	.	1,940	2,155	1,789		
350	1,879		2,080	2,285	1,925	١	
375	2,013		2,210	2.400	١.,	١	
400	2,147	.	2,320			١	
425	2,281		2,425	٠			
450	2,415	ļ ,.	2,512	!		١	

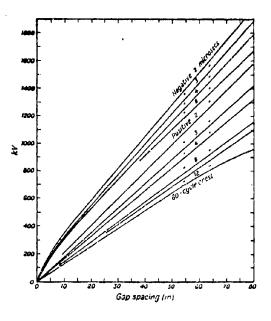


Figure 4.59 Positive and negative impulse voltage characteristics of rod-to-plane gap.

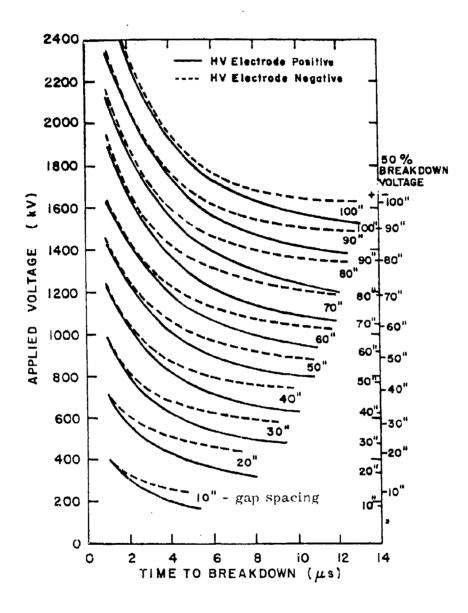


Figure 4.60 Time-lag curves of standard rod gaps (1/50 microsecond wave) and spacings to give 50% breakdowns vs. voltage.

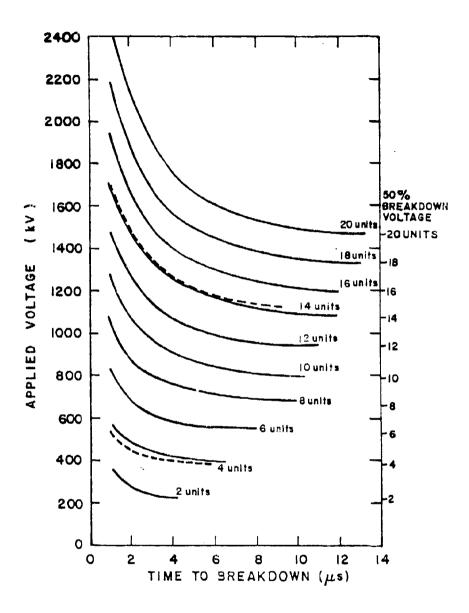


Figure 4.61 Time-lag curves of suspension strings of insulators, 10-inch diameter by 5-inch spacing, without arcing fittings (1/50 microsecond wave).

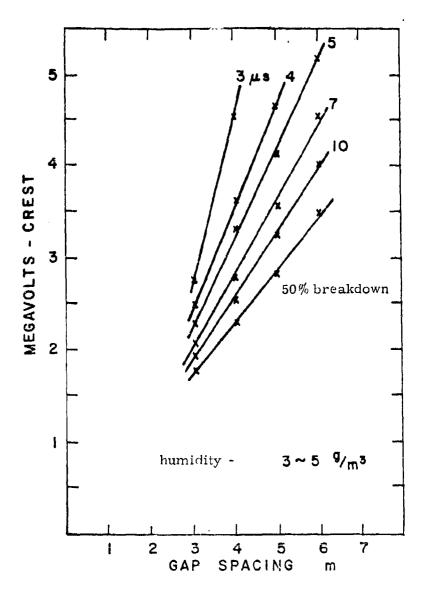


Figure 4.62 Impulse volt-time characteristics of parallel conductor - conductor gaps (at 760 mm Hg, 200 C, not corrected for humidity conditions (with negative impulse)).

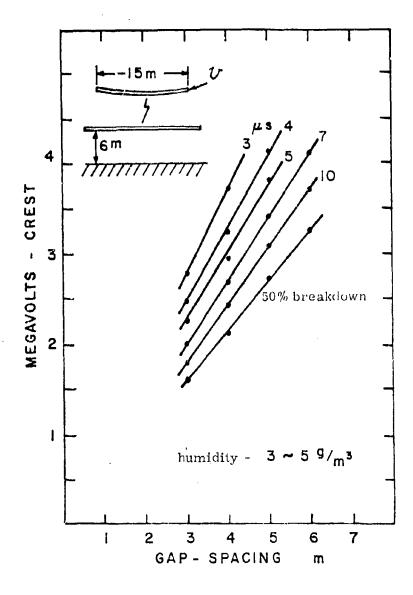


Figure 4.63 Impulse volt-time characteristics of parallel conductor - conductor gaps (at 760 mm Hg, 20° C, not corrected for humidity conditions (with positive impulse)).

At the higher pressures Nonken (39) has studied the breakdown of rod gaps in nitrogen. Some of his results are shown on Figure 4.40. It can be seen that at the lower pressures for the larger gaps (e.g., 6 and 10 cm) the impulse strength exceeds the 60 Hz strength, whereas in an intermediate pressure range, for example at 120 psi the reverse is true.

In the time regime below one microsecond Martin (54) and colleagues have studied the breakdown of highly nonuniform gaps (point or small sphere to plane) during the development of precision switching techniques. They found, that for positive points or spheres prediction within 10% is given by the expression

$$k = Ft^{1/6} d^{1/10}$$
 (5)

where Is the "average" field strength (voltage divided by gap specing) in kV/cm.

1 is the clapsed time above 88% of the maximum voltage in microseconds.

d is the gap in cm.

and k is a constant given on Table 4.8.

Table 4.9 gives the constant k for negative points or spheres.

The above expression determines the field to give breakdown at a specific gap after a given elapsed time, primarily on a rising wavefront. Crewson (55) has discussed the streamer development considerations used by Martin to justify expression (5). He pointed out that in the case of a fast rise and exponentially falling wave, where the requirement is to withstand stress, the time (t) which should be used in expression (5) is one sixth of the decay time constant. Crewson develops information out to 1000 microseconds to show safe distances for an exponentially falling wave. However, experimental information for air above one microsecond (e.g., Figure 4.59) for large gaps shows that the weak dependence of breakdown on the gap length,

Table 4.8 Values of $k \approx Ft^{1/6}d^{1/10}$ for positive point or small sphere.

р	absolute p.s.i.	15	25	35
AIR	Point	24	33	37
	Small Sphere	20	28	33
FREON	Point	4 0	43	46
	Small Sphere	4 5	51	55
SF ₆	Point	48	55	59
	Small Sphere	60	66	69

Table 4.9 Values for k--for negative point and small sphere.

р	absolute p.s.i	1.5	25	35
AIR	Point Small sphere	25 17	38	49 28
FREON	Point . Small sphore	67 4 7	84	100 77
SF6	Point Small sphere	79 49	-	116 93

implicit in expression (5) does not exist in these ranges, and although a logarithmic plot can indicate at t^{1/n} relationship at a fixed gap (e.g., from Figure 4.59 or 4.60), n is not a constant as the gap is varied. For example, empirical information on rod gaps (Figure 4.60) with a 1/50 microsecond wave gives an average stress of 6 kV/cm at 200 cm for breakdown on 50% of the trials. The Crewson data indicates that approximately 8 kV/cm should be withstood (equivalent time approximately 12 microseconds). In general the use of expression (5) should be confined to the range over which it has been tested—and for which it was developed. The empirical information available at longer pulse durations is a better design guide.

4.4.4 SF₆ (Uniform Field)

The uniform field breakdown of SF_6 and mixtures with nitrogen under impulse conditions has been studied by Muleahy. His data taken with 1/50 waveform shows (Figure 4.64 and Table 4.10) the linear variation of breakdown voltage in SF_6 up to three atmospheres for gaps in the range 0.5-2.5 cm. The effect of dilution with nitrogen and of the presence of an insulator (porcelain) across the gap is also shown. This is in good agreement with the near uniform field sphere gap data presented earlier (Figure 4.42) where the comparison with power frequency performance is shown.

Kawaguchi and colleagues have studied the impulse (1.1/40) breakdown voltage of uniform fields at gaps up to 6 cm, and pressures to 4 kg/cm² (approximately 4 atmospheres). Plots of critical breakdown voltage against pd are linear up to 1.7 MV (Figure 4.46) and in good agreement with an extension of the lower voltage data of Figures 4.64 and 4.42. They concluded from experiments with Rogowski, sphere/sphere, and coaxial geometries that breakdown in configurations which do not develop strongly nonuniform field conditions, occurs at gradients close to a limiting value given by $E/p = 86.1 \text{ kV/cm/kg/cm}^2$. This is particularly so for positive impulse, both 1/40 microsecond and standard switching impulse. Negative impulse breakdown

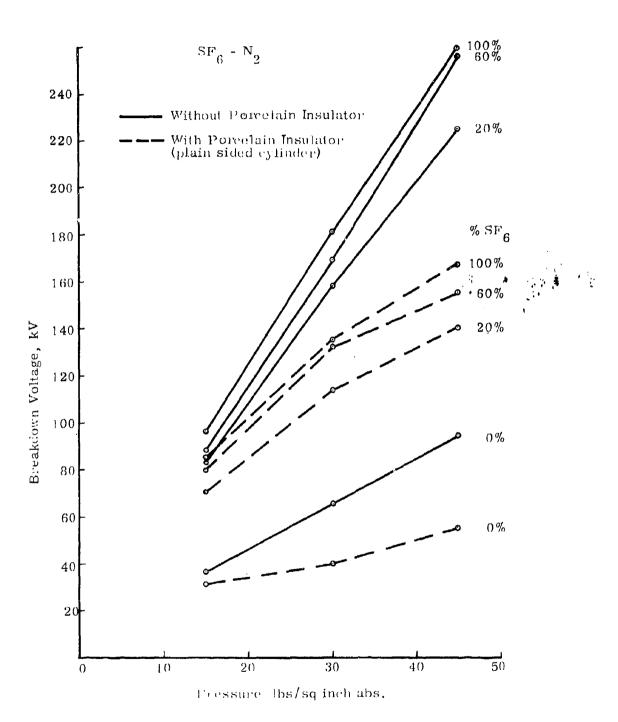


Figure 4.64 Negative impulse breakdown versus pressure. Uniform field 1 cm gap. No radium.

Table 4.10 de breakdown voltage (kV) of ${\rm SF}_6$ in uniform field gap.

Press	Del and dire	No Radium Gap (cm)				Radium		
lb/in2 Polarity (abs.)		0.5	1.0	1.5	2.0	2.5	0.5	1.0
15	+	44	88.3	132.9	174.6	213.0		
	-	44.3	88.3	133.8	176.1	208.0		
30	+	85.2	171.0	251.7			85.6	170.0
	-	84.5	170.6	251.4			84.2	170.0
45	+	132.0	260.0					

voltage falls below the positive value, particularly above 1 kg/cm². It is worth noting that stainless steel, copper and aluminum electrodes were studied, and over the pressure range examined the metal used was not a significant factor.

The performance of ${\rm SF}_6$ in uniform field geometries at pulse durations less than one microsecond can be determined from the data of Figure 4.58 which was experimentally determined at voltages less than 25 kV. Mulcahy and his colleagues (57) have examined the breakdown of uniform field gaps in ${\rm SF}_6$ mixtures when subjected to a rising wave front. The mixture used was 10% ${\rm SF}_6$, 40% ${\rm N}_2$, and 56% Argon at 150 psig. The Argon was present to improve the discharge switching of the mixture in a particular pulse power application. Figure 4.65 shows the results obtained (dc breakdown level 195 kV). Assuming an effective time given by the voltage duration above 63% of the breakdown value, (after Martin, ${\rm (58)}$) the authors showed that their data when replotted fitted well with an extension of Figure 4.58 to higher values of p τ , for example to 10^{-2} tore second.

Sulfur he aftuoride is used to inhibit the breakdown of high power waveguides. Examples of this are given in reference (59) for both quasi uniform field and nonuniform field conditions within guides for pulsed microwave frequency (2 microsecond duration of typically 2.82 GHz).

Operating temperature can have a significant effect on the performance of gases and ${\rm SF}_6$ is certainly no exception. Apart from chemical stability, which will be discussed later, the electrical strength of sulfur hexafluoride falls quite rapidly as temperature is raised above the normal ambient. This is shown in Figure 4.66 where the impulse strength is compared over the range to 100° C with the unvarying strength of air. (29)

4.4.5 SF₆ (Nonuniform Field)

The influence of field uniformity on the strength of ${\rm SF}_6$ has been discussed by ${\rm Clark}^{(29)}$ using the data on impulse strength at one atmosphere

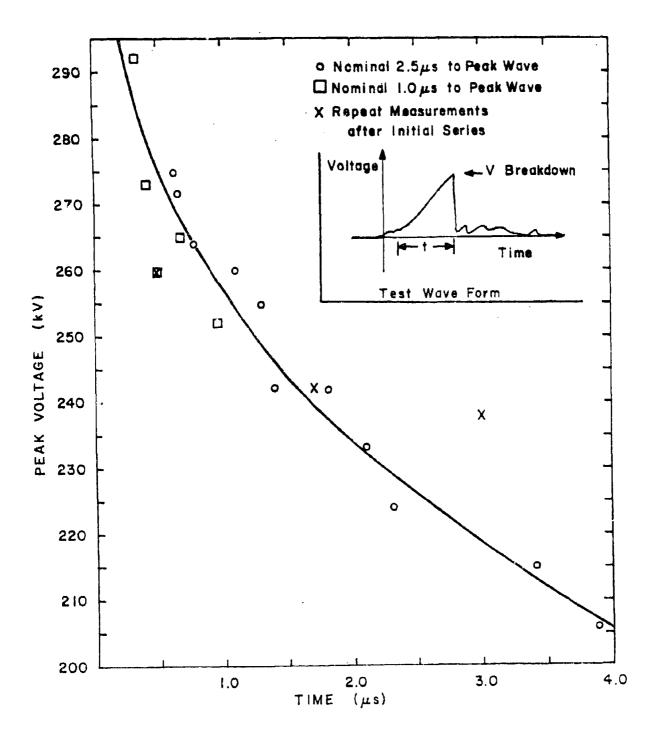


Figure 4.65 Time and voltage dependence of breakdown under impulse conditions for uniform field stainless steel in 150 psig, 10% SF $_6$, 40% N $_2$, 50% Ar gas mixture - 0.58 cm gap.

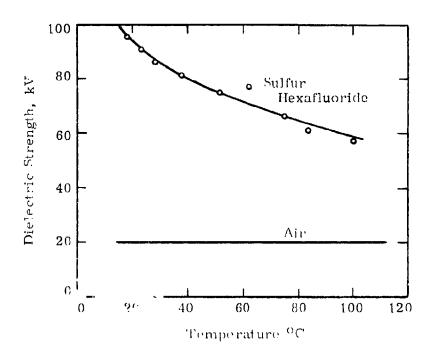


Figure 4.66 The dielectric strength-temperature relation for sulfur hexafluoride tested at atmospheric pressure.

Electrodes - 1/2 inch sphere-to-plane.

Gap distance - 1/2 inch.

Voltage - 1-1/2 x 40 microsecond waveform.

given on Figure 4.67. The electric field increases in nonuniformity as the gap is increased, and a replot of the data on Figure 4.67 showing maximum electric field versus gap is shown on Figure 4.68. It can be seen that at the larger gaps the dielectric strength tends to a limiting value of 40 volts per mil (approximately 1.6 MV/m).

As noted earlier Kawaguchi et al. (42) have studied the impulse breakdown of SF, at up to four atmospheres in uniform and modestly nonuniform field conditions. Their uniform field performance at atmospheric pressure is in reasonable agreement with that of Figure 4.67. Data from tests at pressures up to about 4 atmospheres with coaxial cylinders at voltages up to 1,2 MV is shown on Figure 4,69. Standard deviations are less than 5%, except for the switching impulse case which is 8%. It can be seen that the positive impulse (1.1/40) breakdown gradients increase almost linearly with pressure, while the negative impulse gradient has a marked reduction in its rate of increase with pressure at about 1 kg/cm². The positive switching impulse breakdown gradient increases with pressure in a similar fashion to the 1, 1/40 wave gradient up to about 2 kg/cm 2 and then the rate of increase with pressure decreases. The slope of the negative switching impulse curve has a similar change, but at only 1 kg/cm² and approaches the power frequency performance. There appears to be an area effect, since the breakdown gradient is highest with the smaller diameter cylinders.

Klewe and Tozer $^{(60)}$ have studied the high pressure impulse breakdown of SF $_6$ in strongly nonuniform fields using a point to plane geometry. Both "standard" (2/50) and switching (200/3000) impulse voltages were used. The 50% breakdown values which they obtained at different pressures are shown on Figure 4.70 (1 atmosphere equals 0.098 MN/ 2). The authors discussed the results obtained with a positive point in terms of expansion of corona around the point to a characteristic radius. If, at that radius, α , the first Townsend coefficient, is greater than η , the attachment coefficient, breakdown occurs. As discussed earlier, Martin has studied the pulse

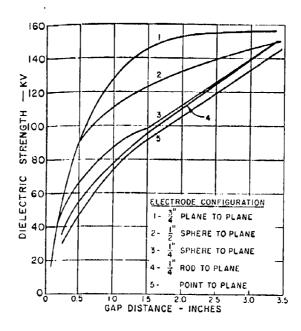


Figure 4, 67 The dielectric strength-gap distance relation for sulfur hexafluoride gas as a function of the electrode configuration measured at atmospheric pressure.

Test temperature - 250 C. Voltage wave form - $1-1/2 \times 40$ microseconds. Polarity - positive.

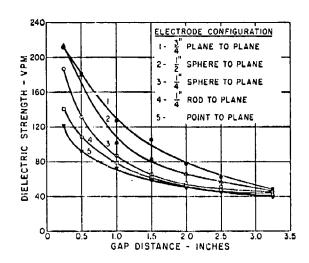
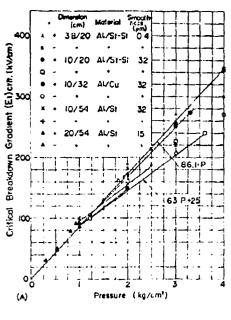
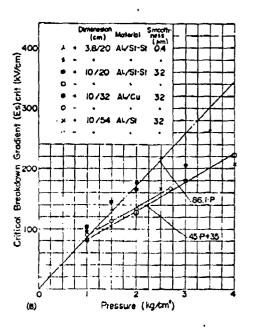


Figure 4.68 Showing the decrease in the voltage gradient at breakdown which accompanies the increase in the test gap for different electrode configurations for sulfur hexafluroide when tested by impulse voltage at atmospheric pressure.

(VPM-volts per mil)





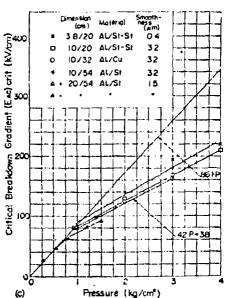


Figure 4.69 - Critical breakdown gradient $\mathbf{E}_{\texttt{crit}}$ between coaxial cylinder electrodes as a function of pressure (corrected to 20° C).

- (a) Standard 1.1/40 microsecond impulse breakdown gradient $(E_{\tilde{I}})_{\text{crit}}$.
- (b) Switching impulse breakdown gradient $(E_S)_{crit}$. (c) 50 Hz power frequency breakdown gradient $(E_{AC})_{crit}$.

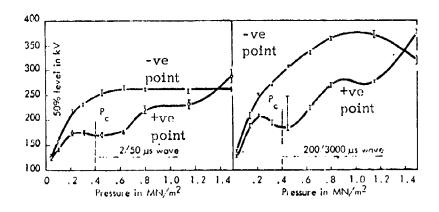


Figure 4.70 - 50% breakdown voltage for point to plane geometry as a function of pressure. The errors shown are 90% confidence limits. (1 MN/m 2 = PSI x 6.89 x 10 $^{-3}$)

breakdown of point to plane gaps in several gases, including SF_6 , in the time regime below one microsecond. The constant relating time to breakdown and average field for SF_6 is given in Tables 4.8 and 4.9.

4.5 Freons (dc/ac and Uniform Field)

4.5.1 Freon-116 and C-318

Apart from sulfur hexafluoride the major special dielectric gases are the freons hexafluorocthane (${\rm C_2F_6}$) and octafluorocyclobutane (${\rm C_4F_8}$). They have been labelled Freon-116 and Freon C-318 respectively by DuPont, and fortunately are usually discussed using this nomenclature. These compounds have been known for about three decades, and were first used commercially as insulants in the early 1960s. They have a significant advantage over SF_6 for high temperature applications, since they are stable chemically to at least 300° C⁽⁶¹⁾ and consequently are used in equipment, such as transformers, which operate at high overall temperature or with hot spots. The commonly used refrigerant gas Freon-12 has also been used quite extensively as a dielectric where lack of chemical stability, either at higher temperature or under electrical discharge conditions, is not a limitation. Its dielectric properties are discussed after the following treatment of F-116 and F-C318.

The boiling points of these special dielectric gases are F-116 (-78° C) and F-C318 (-6° C) and as a consequence in low temperature situations, there would be difficulties with the latter, which has the better dielectric strength. However, mixtures of these two can be used to give adequate performance in such situations. (61) Freon-116 can be compressed at room temperature to higher pressures than ${\rm SF}_6$ (500 psia of 330 psia) although no dielectric studies appear to have been made at these higher pressures. In general, at atmospheric pressure under uniform field conditions F-116 has a dielectric strength somewhat less than ${\rm SF}_6$, although it has been suggested that under nonuniform field conditions the reverse is true. (62)

Before proceeding to a more detailed discussion of the dielectric properties of the above two gases it is worth noting the boiling point and high electrical breakdown strength of some of the other Freons, which are liquid at room temperature but may be used in equipment at higher temperatures. This information is given on Table 4.11 (0.1 inch gap sphere to plane).

Many Freengases have been examined as potential dielectrics and much of the data is on types which are not available in commercially useful quantities. It seems reasonable to assume that those now obtainable, in particular F-116 and F-C318, represent the optimum selection from a performance and economic point of view. However, the many varieties which have been examined, and their relatively short technical history, leads to a poorer definition of their overall performance than is possible with SF₆. This is particularly true for some geometries and for higher frequency applications. The hazards implicit in extrapolating from the performance of one electronegative gas to that of another is well illustrated on Figures 4.71 through 4.73.

As with other gases, the strength of uniform field gaps under power frequency and direct voltage conditions is basically the same. Figure 4.74 shows the uniform field performance of F-116 (C_2F_6) and F-C318 (C_4F_8) under power frequency conditions at pressures up to three atmospheres absolute. Experiments on F-116 with N_2O added, have been made to much higher pressures and voltages, using a short coaxial transmission line with the results shown in Figure 4.75. The small percentage of nitrous oxide was added to the F-116 to inhibit the formation of deposits under discharge conditions. Until recently it was believed that electrical discharges in Freon gases would lead to greater contamination problems than in SF₆ because of the carbon produced. This is not necessarily so, even with uninhibited Freons. (63) A 90/10 mixture of F-116 with N_2O is now available commercially. At the lower pressures the strength of F-116 and F-116/ N_2O (90/10) is essentially the same, at least for small gaps (Figure 4.76), and at higher pressures in

Table 4.11 Strength of Freon vapors at their boiling point (atmospheric pressures).

Freon	E1	E2	E3	C-51-12	TF			
Boiling Point ^o C	40.8	104, 4	152.3	45	47			
Breakdown voltage* kV (rms)	22	27	35	32	28			
* cf N ₂ - 7 kV, SF ₆ - 17 kV								

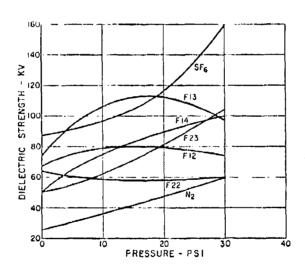


Figure 4.71 Comparing the impulse dielectric strength of fluorinated hydrocarbon gases.

Electrodes - tungsten rod to sphere. Test gap - 1 inch. Wave form - 1-1/2 x 40 microseconds. Polarity - positive.

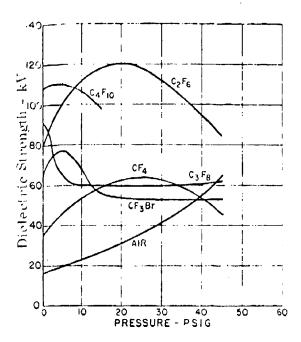


Figure 4.72 The dielectric strength of the fluorinated hydrocarbon gases as affected by pressure, tested under nonuniform field conditions.

Electrodes - 1/4 inch square rods. Cap distance - 1 inch. Voltage - 60 cycles.

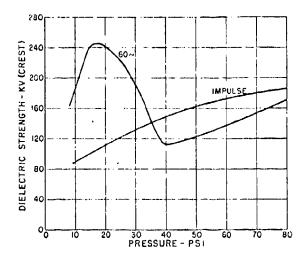


Figure 4.73 The effect of gas pressure on the breakdown of dichlorodifluoromethane (Freon 12).

Electrodes - 1/2 inch square rods.
Test gap - 6 cm (2.362 inch).
Test voltage - standard impulse (1.5/40) and 60 Hz.

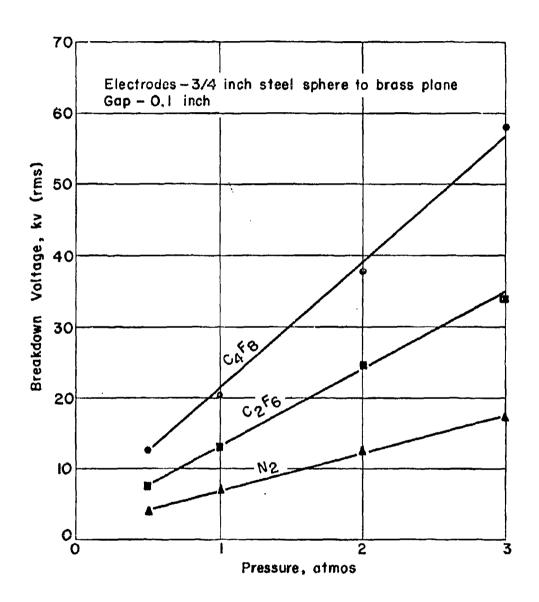


Figure 4.74 Breakdown voltages versus pressure.

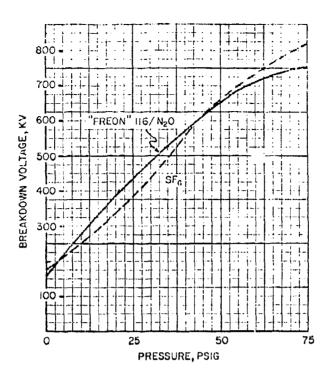


Figure 4.75 Comparison of breakdown voltage as a function of pressure for Freon $116/\mathrm{N}_2\mathrm{O}$ (90/10 by wt) and SF_6 in a section of coaxial gas-filled transmission line. Inner conductor diameter - 3 inches, outer conductor diameter - 6 inches. The effective line length was 30 inches and the electrode gap was 1.5 inches.

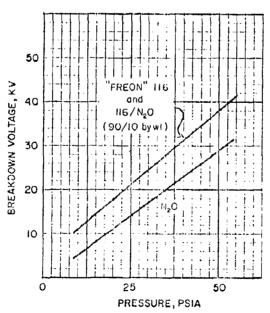


Figure 4.76 Breakdown voltages measured in a Seavy cell, ASTM D-2477-66T. The electrode gap was 0.1 inch, steel sphere (0.75 inch diameter) to brass plane (1.5 inch diameter). In this test pure

Freon 116 and a mixture of Freon 116 and nitrous oxide

(90/10 by wt) gave equivalent results.

larger area systems the presence of the N_2O degrades the performance of F-116 less than 20% (Figure 4.77).

Examples of the performance of these gases under nonuniform field conditions are given in Figures 4.78 through 4.82. (61) Figures 4.78 and 4.79 are for square rod to plane gaps, 4.80 and 4.81 for cylindrical rod electrode and Figure 4.82, showing only corona inception, is for a needle point to plane. (61)

4.5.2 Freon 12

Because of its ready availability and cheapness, the dielectric properties of Freon 12 have been studied quite extensively. It is one of the two most commonly used refrigerant gases, and has a strength relative to air usually quoted at 2.42. The other common refrigerant F-22 has a relative dielectric strength of 1.4 and is less useful as a dielectric. The main limitations of Freon 12 are that it is chemically unstable when in contact with commonly used electrical materials at a relatively low temperature (250° F) and disintegrates badly under arcing conditions. Nevertheless, it is interesting as a cheap material for insulation at room temperature, or for laboratory test purposes, such as in a dielectric immersion bath for quick tests, or for spraying around an insulating structure in air to improve temporarily its flashover properties.

Figure 4.83 shows a Paschen curve for Freon 12 obtained by Howard (24) over the pressure range 0 to 60 psig. Figures 4.84 and 4.85, showing the ac and standard impulse strength for almost uniform field conditions at pressures up to 30 psig, indicates that the impulse strength which varies linearly with the pressure is significantly higher than the 60 Hz strength. (64) Figure 4.86 (24,65) shows further power frequency and impulse data obtained under near uniform field conditions at higher pressures and voltages. Freon 12 has also been used mixed with nitrogen, for operation well beyond the pressure where the pure gas liquifies at room temperature

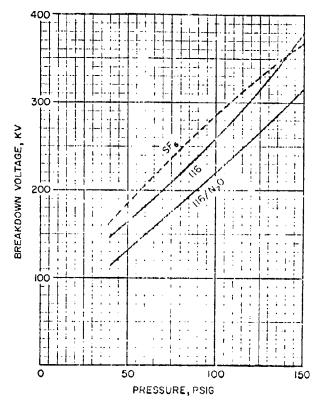


Figure 4.77 Breakdown voltage with ${\rm SF_6}$, Freon 116, and Freon 116/ ${\rm N_2O}$ (90/10 by wt) in a uniform field as a function of pressure in a steel tube, 36 inches long and with an ID of 20 inches. The electrodes were discs 4 inches in diameter and made of stainless steel. Electrode gap at 0.5 inches.

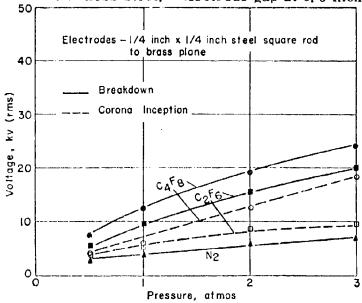


Figure 4.78 Corona inception and breakdown voltages versus pressure at power frequency. Gap spacing 0.1 inch.

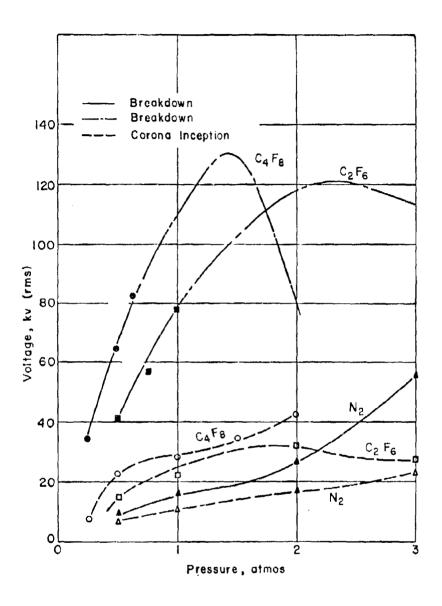


Figure 4.79 Corona inception and breakdown voltages versus pressure. Gap spacing 1.0 inch.

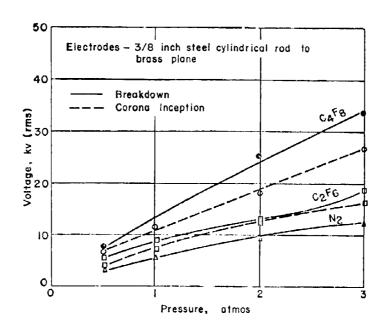


Figure 4, 80 Corona inception and breakdown voltages versus pressure. Gap spacing 0, 1 inch.

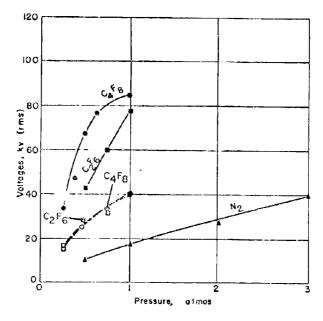


Figure 4.81 Corona inception and breakdown voltages versus pressure. Gap spacing 1.0 inch.

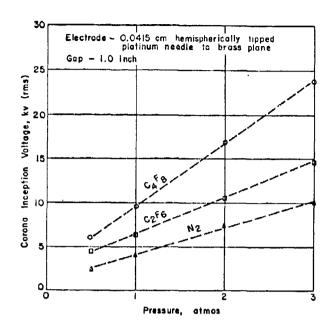


Figure 4.82 Corona inception voltages versus pressure.

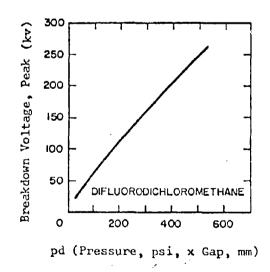


Figure 4.83 Paschen curve for Freon 12.

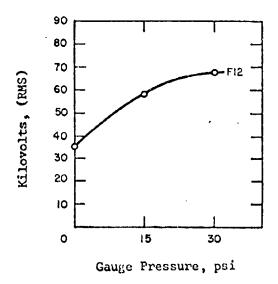


Figure 4.84 60 cycle dielectric strength of Freon 12, tested between two 1 inch diameter spheres spaced 1/4 inch.

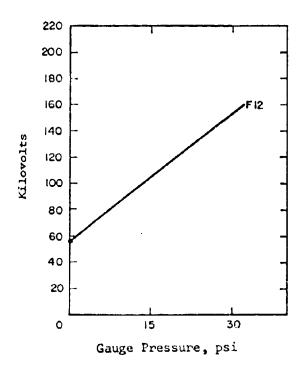


Figure 4.85 Impulse dielectric strength of Freon 12, tested between two 1 inch diameter spheres spaced 1/4 inch.

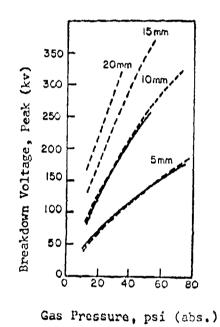


Figure 4, 86 Breakdown voltage between 5 cm diameter spheres

for Freon 12 as a function of pressure. Gaps as noted.

Power frequency
Negative impulse

(82 psia). Data from tests on mixtures, again under near uniform field conditions are shown on Figure 4.87. The authors found a linear relationship for the sparking voltage (V) according to

$$V = (88 PS + 1.9) (1 + 1.08 F)$$
 (6)

where V is in kilovolts

P is pressure in atmospheres

S is spacing in inches

F is fraction of Freon by volume

This expression is not accurate for small fractions of Freon, e.g., less than 5% or pressures above about 7 atmospheres.

With regard to nonuniform field conditions, it is difficult to predict the performance of a given geometry without specifically related empirical data. Figure 4.88 shows data obtained by Howard (24) for various coaxial arrangements. It can be seen that for these systems where the field is nonuniform, but not intensified to the degree obtained with other geometries, the strength increased with pressure, whether the voltage is power frequency, direct or impulse. This is not necessarily the case for the more intensified field geometries as shown on Figures 4.89 and 4.90. (64) The futility of increasing pressure to improve performance with these geometries is fairly obvious. It is also interesting to compare this nonuniform field data with that for uniform fields shown on Figures 4.84 and 4.85 where in contrast the impulse strength is higher than the power frequency. Figure 4.91 shows breakdown strengths obtained for half inch square rod gaps over a wider pressure range. (39) To conclude for Freon 12, Figure 4.92 shows the power frequency, direct and impulse voltage performance, of a point to plane gap at various spacings. (24)

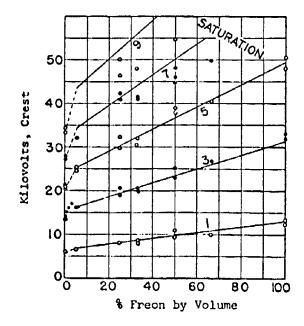


Figure 4.87 Sparking voltages in mixtures of Freon 12 and nitrogen.

Spherical electrodes; length of spark gap: 0.050 inch; pressure in atm. as noted on curves; points are experimental; lines are computed from V = (88 PS + 1.9) x (1 + 1.08 F) kv. (see text)

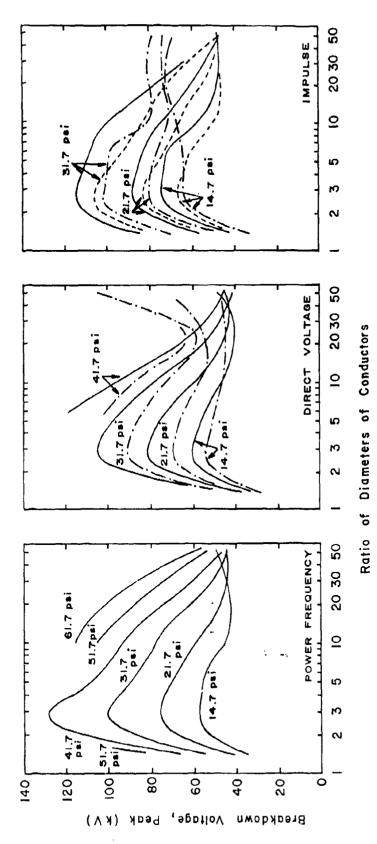


Figure 4.88 Breakdown voltage for difluorodichloromethane between coaxial cylinders.

Power frequency, positive dc and impulse.

Negative dc and impulse.

Positive impulse with radium.

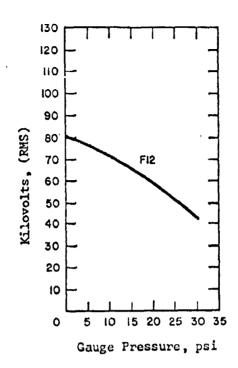


Figure 4.89 60 cycle dielectric strength of Freon 12, tested between tungsten rod and 1 inch diameter sphere spaced 1 inch.

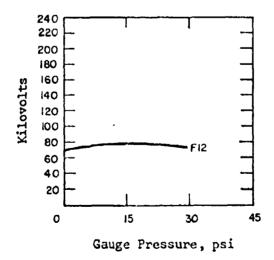


Figure 4.90 Impulse dielectric strength of Freon 12. Positive tests made between tungs in rod and 1 inch diameter sphere spaced 1 inch, 1.5/40 microseconds wave form.

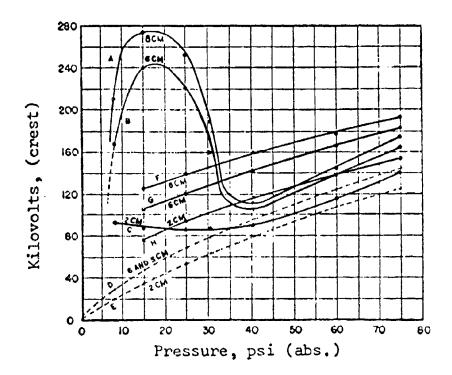


Figure 4.91 - 60 cycle and impulse breakdown between 1/2 inch square rod gaps in ${\rm CCl}_2{\rm F}_2$.

Curves A, B, & C = 60 cycle breakdown.

Curves D & E = 60 cycle corona starting voltage.

Curves F, G, & H = impulse breakdown.

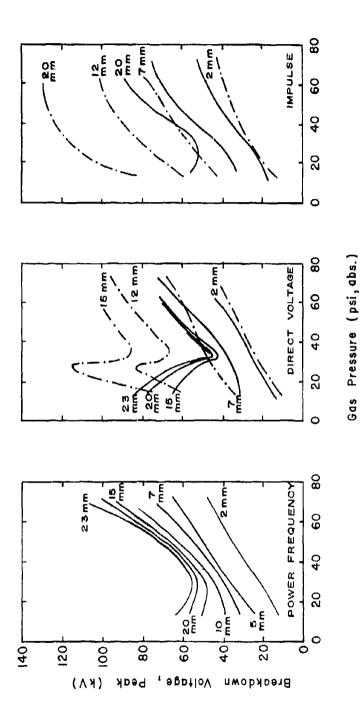


Figure 4.92 Breakdown voltage with difluorodichloromethane and non-irradiated point-sphere electrodes.

---- Fower frequency, positive dc and impulse.

4.6 Flashover of Solid Dielectrics in Gas

Without using solid dielectrics in the gas environment for support it is impossible to design gas insulated high voltage equipment. In many cases the voltage limit in the system is reached when these solid supports break down electrically. This usually occurs across the surface in the ambient, which is generally self-healing. The term "flashover" is used in this discussion only to denote breakdown across the surface of solid diclectric, although it is used more loosely elsewhere. Apart from the Hashover strength of a solid dielectric, its are resistance and tracking properties are also relevant to high voltage design. Are resistance describes the ability to resist physical or chemical deterioration because of electrical action such as flashover or arcing along surfaces. This deterioration usually is evidenced by failure to support voltage, either because of excessive leakage current or total collapse of insulating properties. Tracking denotes the development of a conducting path (usually carbon) along the surface of solid insulation. The subject of deterioration is dealt with later in the section on solid dielectries, and the discussion here is restricted to flashover strength.

When an electrically stressed gap is bridged with a solid dielectric the flashover strength is almost invariably less than that of the unbridged gap. Commonly, the flashover performance of a solid dielectric is given in terms of the ratio of bridged to unbridged gap performance, and this ratio is known as the spacer efficiency. Frequently, test samples take the form of a right cylinder which is placed in a uniform field gap, although the growing interest in gas transmission lines has led to many tests on coaxial samples.

Any effect which changes the surface resistivity of the dielectric can influence the flashover strength by modifying the electric field along the surface. This is particularly important—when insulators are used in an atmosphere where they are subject to contamination. Even changes in humidity can have a significant effect (Figure 4.93). (29)

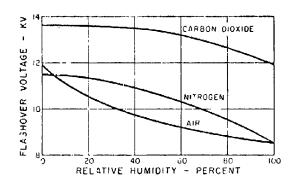


Figure 4.93 The flashover of procelain insulators as affected by the surrounding gas and its moisture content.

Gas pressure - 760 mm of mercury Gap distance - 12 mm (0,472 inch)

The most critical region in the design of solid insulation is at the terminations where the high voltage or grounded metal parts are attached, in particular at the region where metal, solid dielectric and the ambient (fluid) dielectric meet. The term "triple point" has been coined to describe this region. Where the solid dielectric butts against a metal surface in a gas, a small gap exists between the insulator and the metal where the dielectric constant is unity. Figure 4.94 shows a representative situation. It can easily be shown that the stress in the small gap is greater than that in the solid by a factor &, where & is the dielectric constant of the solid. This intensification can cause ionization and premature flashover of the solid dielectric. (67) Figure 4.95 shows the importance of good cohesion between solid dielectric and metal. (68) In this instance the dielectric had a coaxial configuration. In another approach to eliminating field intensification at the triple point, a conducting film (metal, graphite) is applied to the solid dielectric where it "contacts" the metal electrodes. Figure 4.96 illustrates the benefit of metallizing the terminations of a cylindrical sample, (a geometry that is conducive to obtaining flat and smooth ends.) (56)

With regard to the significance of the solid dielectric material on the flashover strength, there is a tendency for materials of lower dielectric constant to perform better than those of higher dielectric constant, particularly for ac and impulse voltages, as might be expected from the triple point considerations discussed previously. Table 4.12 shows spacer efficiencies for a variety of materials in SF ander de, 50 Hz and 1/50 impulse voltage. (69) In these tests the samples were cylindrical with the end surfaces coated with a metal film. Parallel experiments where the dielectric samples were given various shapes, such as cylinders with corrugations, or truncated cones, always gave lower flashover values than plain sided cylinders bridging the same gap. Other authors, (68,70) using coaxial samples, agree that plane dielectric sides are best in a carefully controlled dust-free environment, but this is often impracticable, and then corrugations, or other departures from

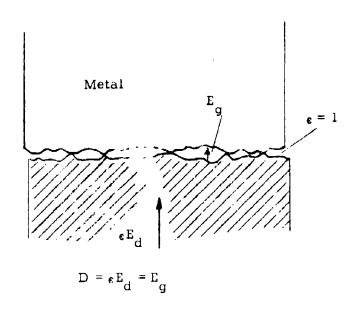


Figure 4.94 Representation of Dielectric/Metal Interface

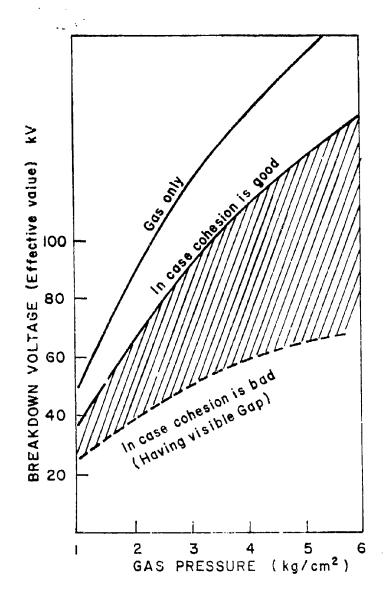


Figure 4.95 Effect of cohesion in case of coaxial electrode.

No Radium

_____ Copper Copied Ends

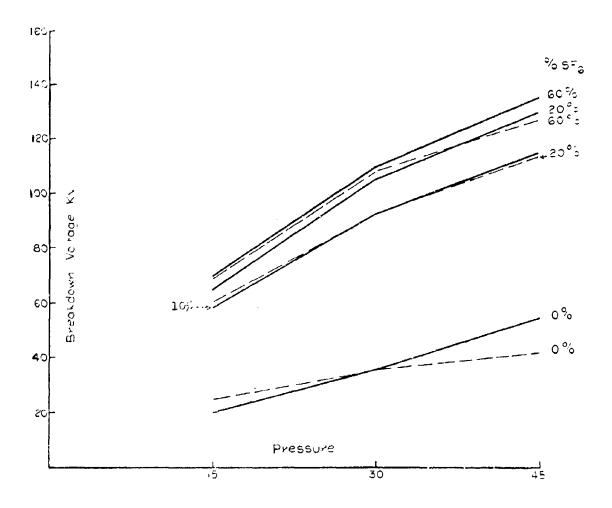


Figure 4.96 de breakdown versus pressure across 1 cm porcelain insulator in mixtures of SF $_6$ with $\rm N_2$.

Table 4.12 Mean spacer efficiencies for the flashover of cylindrical insulators in a uniform field in SF.
(1 or 2 cm long spacers - temperature 200 cf)

Applied Voltage		हैं।			ac			Impulse		+
Fressure psia	15	30	45	15	30	45	1.5	30	45	į
Polymethy Imethaciviate	. 93	98.	. 65	06.	.84	89.	1.0	. 94	i	3, 57
Polypropylene	16.	88.	.75	. 94	t ₀ .	. 93	.94	1.0	68.	2.2
Folytetrafluoroethylene	98.	.87	. 81	. 92	88.	98.	0.1	. 92	ı	2.1
Nylon 11	.77	1	ı	. 95	62.		10.	. 97	ı	3.7
Epoxy Resin	. 95	ı	i	o ∞.	1	. 78	ı	ı	ı	4.5
Glass/Epoxy Laminate	. 91	σ: •	. 71	.74	. 62	. 54	.93	. 84	.76	4.8
Glass	.87	# 1.	I	.77	. 72	09.	ı	ı	I	5.0
Glazed Porcelain	. 84	92.	ı	•	1	1	ı	I	ı	6.5
Unglazed Procelain	.71	.57	.51	.78	. 63	. 52	ı	ı	ı	6.5
SRBP* Rod	. 47	ა გ	. 25	.72	. 60		i.		.79	8°.
SRBP* Tube	10	.31	. 23	.61	48	44	.87	.67	. 59	
Synthetic Resin Densified Wood	.37	ı	1	ı	1	i	ŧ	1	1	i

^{*}Synthetic resin bonded paper.

⁺Typica! values--may be frequency dependent--care should be taken in using these numbers--generally similar materials (e.g., epoxies) can have quite different values.

the plane sided geometry, ⁽⁶⁸⁾ are desirable. It may be that metalizing the surface of the solid dielectric which is in contact with the terminating electrodes is necessary to obtain the better performance reported with plain sided over corrugated samples. Corrugations are also preferable where flashovers are likely to occur, since they help to prevent permanent degradation of strength. Figure 4.97 shows data obtained for one "corrugation" under both power frequency and impulse conditions. ⁽⁷¹⁾

Perhaps the most useful technique for optimizing dielectric flashover is that of using shielding electrode, as discussed by Itaka and Ikeda. (68) One method for internal shielding the triple point which is discussed in detail by these authors is shown in Figure 4.98. The benefits obtained by using this technique can be seen on Figure 4.99.

As might be expected, the flashover voltage of a solid dielectric in gas depends on the properties of the gas. In general the better the performance of the gas in the unbridged gap, the better it is when an insulator is present. This is demonstrated on Figure 4.64, which shows the performance of a uniform field gap at several pressures and varying fractions of sulfur hexafluoride and nitrogen. The data compares gap performance with, and without, a cylindrical porcelain insulator present.

The significance of the temporal form of the applied voltage to spacer efficiency cannot be explicitly defined (see Table 4.12, for example). Initial field distributions in the dc case are influenced by the dielectric constant of the material, by conductivity, and possibly, by charging of the surface due to ionization effects. In general, with appropriate field design as described above to remove high stresses from the terminations, and a suitable choice of material, it is possible to achieve spacer efficiencies in excess of 80%.

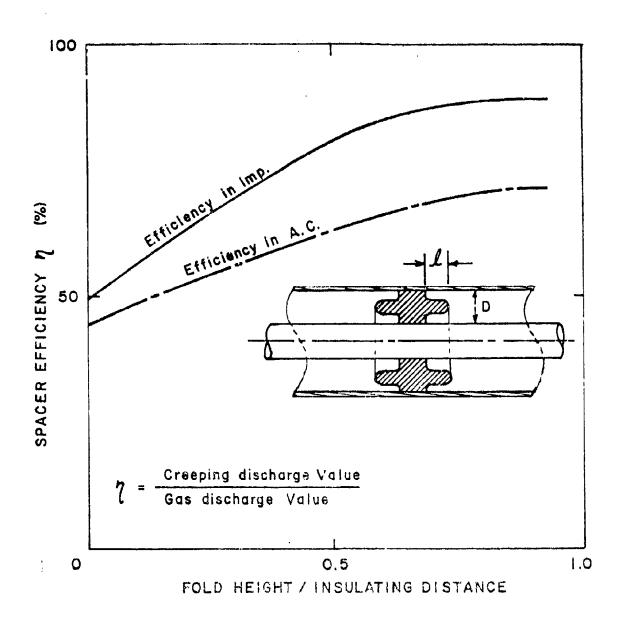
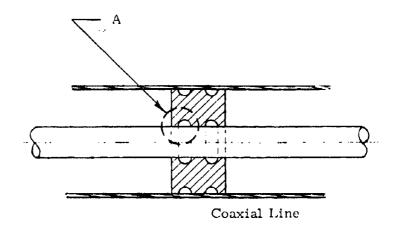


Figure 4.97 Effect of crease length extension on coaxial line spacer characteristics.



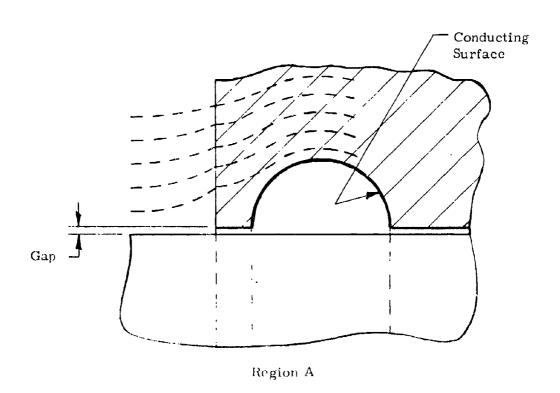


Figure 4.98 Concept of internal shielding.

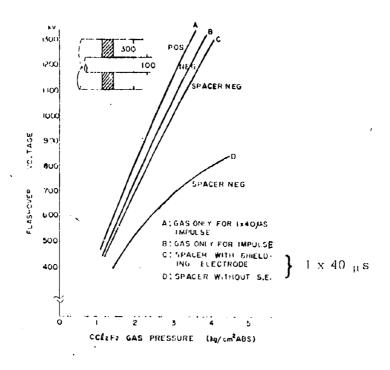


Figure 4.99 The effect of the shielding electrode. (300 mm od, 100 mm id, coaxial line)

4.7 Government Supported Design Studies (Gas Dielectric)

The pursuit of weapon simulation systems in recent years has required many design studies involving dielectrics to support pulse power technology. Several of these studies relate to gas dielectrics, and are treated in this section. They are segregated because they answered special government needs in the past, and may be equally relevant in the future, and if integrated into the general text their particular significance to DOD might be lost. Further, in some cases the special objective of the studies would be inconsistent with the more general treatment in the rest of the text.

In the following, only sufficient outline is given of the relevant material to direct the reader to a particular reference. Most of the studies were on pulsed flashover and breakdown, and related to emp simulation activities. The first study treated is an exception to this because the material has been roughly arranged in order, starting from the dc case then proceeding to the shortest pulse length. Gas breakdown studies which are directed towards improvements in the switching art, are not included in this material, but will be covered later in a corresponding section when switching is discussed. Table 4.13 summarizes the following discussions.

Experiments have been conducted to determine the optimum high pressure gas mixtures (SF $_6$, N $_2$, CO $_2$) for the dc insulation of large coaxial line flash X-ray machines (26). In one case a FX-45 flash X-ray machine was used, having a coaxial line of outer diameter 75 inches, inner diameter 29 inches, and length about 120 inches. The equipment has a maximum voltage capability of 6.5 MV. Figure 4.100 shows the performance after conditioning for several gas mixtures as a function of pressure (line negative). Experiments were also made in a smaller coaxial line machine (FX-25) with 5% SF $_6$ added to a 50/50 N $_2$ /CO $_2$ mixture at a total pressure of 300 psi. Performance compared with the FX-45 for the same mixture was:

Table 4, 13 Dielectric design studies (gas).

Geometry	Maximum Voltago	Voltago	Waveform	Application	Reference
Coaxial line	9.	6.5 MV	ာပူ	FX machines	28
Cylinder to plane with lucite interface	276 KV	kV	1/140	EMP	<u>π</u>
Dielectric cylinder flashover	C 17	κV	1/50	FX machines	*7 1
Dielectric disk flash- over	1140	kV	1/50	FX machines	empe Prop
Thin dielectric inter- face Hashover	485	kV	die -	FV machines	
Strip line and rod to plane with and without lucite interface	525	kV	0.5/30	EMI	7.5
Cylinder to plane	440	kV	0.5/30	EMP	7.5
Strip line to plane with and withour lucite interface	300	kV	su oot	ьмы	76

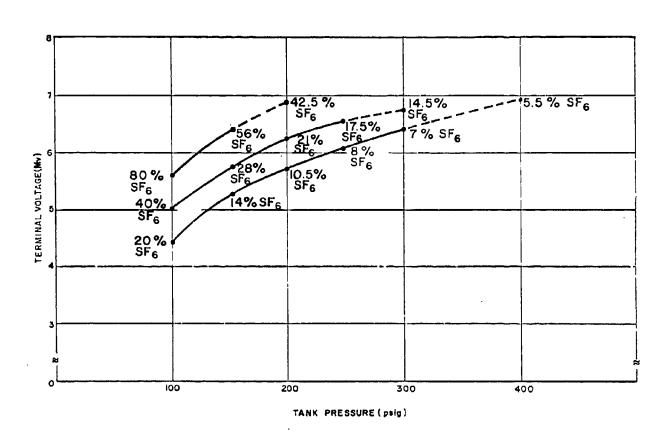


Figure 4.100 Effect on breakdown voltage of adding N_2 to fixed pressure of SF_6 .

Maching	Voltage (MV)	Fiela (MV/m)	Electrode Area (sq. inches)
FX/25	3.6	19.9	8,200
FN-45	6.4	18.0	13,000

Reference 72, although containing no original data, contains a good review of gas, liquid and solid dielectrics in support of the design of a low impedance emp simulator at the 2 MV level. The section on gas dielectrics is particularly comprehensive and summarizes the impulse investigations of McNeal and Skipper. (13) This reference also discussed the importance of good design to obtain optimum solid dielectric flashover performance. cited some examples, and emphasized the importance of good cohesion at the junction of solid dielectric and metal electrodes. Table 4.14 (a) shows maximum de stresses obtained in Ion I hysics Corporation's gas insulated coaxial line flash X-ray machines together with the area of the more highly stressed conductor. (72) Table 4.14 (b) gives operational stresses in two megavolt electromagnetic pulse (emp) systems developed by the same company. Both cmp systems generate fast rising (~ 10 ns) and exponentially falling wave forms, the emp-10 system having a 100 ns e-folding time and the emp-28 a 130 ns e-folding time. Both systems are similar in concept, the design details being given in "Report on the Development of Five EMI Generators, AFWL-TR-70-6, Air Force Weapons Laboratory, July 1970. In Table 4.14 (b) column A is the pulsed stress in a coaxial oil transmission line, which in the case of the emp-28 system is 12 inches od, 1.25 inches id and about 20 feet long. Columns B and C refer to a lucite sheet interface (oil/SF $_{
m B}$ at 1 atmosphere) with a spacing of 20 inches for emp-10 and 48 inches for emp-28. Columns D and E refer to the output interface of the systems, again a lucite sheet, with spacings of 45 inches for emp-10 and 96 inches for emp-28.

In support of their SIEGE II development, I hysics International has studied the pulsed insulation strength of lucite interfaces in 50/50 air/
Freon 12 at one atmosphere with the conclusion that their interface design stress of 33 kV/cm was safe. (73) The test geometry was a positive 11.4 cm

Table 4.14 (a) Maximum dc Stresses in FX Machines -- Chaxial Line Geometry

Area of Inner Conductor (sq. inches)	8,200	13,000	37,000	00°00
Maximum Radial Sress at Inner Conductor (MV/m)	22	18.6	18.2	٠ ٣
Polarity	⇔ ∧ -	9 > -	e)	θΛ-
Total Voltage (MV)	4.0	6.5	e: 17	12.8
Gas Mixture	5% SF6 80/20 N ₂ /CO ₂	5% SF6 80/20 N ₂ /CO ₂	5% SF6 80/20 N ₂ /CO ₂	20% SF6 80/20 N ₂ /CO ₂
Total Fressure (psi)	400	400	U0†	300
System	FX-25	FX-45	FX-75	FX-100

Table 4, 14 (b) Operating stresses in emp systems.

E SF ₆ , Air Edge Interface MV/m	5.5	2.03
D SF ₆ /Air Center Interface MV/m	0.92	0.813
C Oil/SF ₆ Edge Interface C MV/m	12.2	1.63
B Oil/SF ₆ Center Interface MV/m	2.22	1.63
A Ott Line MV/m	20.6	24.0
e-fold Time	100	130
Peak Volts (MV)	1.1	2.0
System	emp-10	emp-28 2.0

dia wher and spaced 9.9 cm from the ground plane which gave a field enhancement of 1.53 at the rod. The test voltage used had a fast risetime, and a 140 microsecond decay. The minimum voltage at which breakdown occurred was 276 kV, corresponding to a maximum stress at the rod of 42.7 kV/cm. Measurements of the de strength of 50/50 Freon 12/air at various pressures up to one atmosphere are also given.

In a DASA supported program to develop low impedance electron beam simulators Ion Physics Corporation has examined the potential of decharged solid dielectric lines for the storage of energy with very low output inductance. (74) To do this it was necessary not only to study the strength of interesting solid dielectrics but also to examine flashover strengths in high pressure gas. Flashover studies were conducted on epoxy cylinders in ${\rm SF}_c$ mixtures using a 1/50 microsecond lamples generator. The samples were 1 inch diameter cylinders of several types of epoxy with lengths between 0.5 and 9 inches. For cylinders of length 2 inches and below, flashover tests were carried out between 6 inch diameter stainless steel electrodes in a pressurized gas mixture of 10% ${\rm SF}_{\rm g}$, 40% ${\rm N}_2$ and 50% ${\rm Ar}_{\rm c}$. For cylinders of length 8 inches and above, flashover tests were carried out in Latmosphere of $\mathrm{SF}_{_{\mathrm{S}}}$ between large plane electrodes of 18 inches diameter. Table 4,45 summarizes the data on the smaller samples for both maximum and mean flashover. strength. Figure 4, 101 shows flashover voltage versus sample length for one of the materials. Mean flashover field strengths up to 600 kV/inch are obtainable in 300 psig; 10 SF $_6/40~\mathrm{N}_2/50~\mathrm{Ar}$ mixtures for small ungraded lengths. Flashover tests were also made on flat plastic and epoxy samples using the same 1/50 waveform. The shape of the samples and the data obtained is shown on Table 4.16. One method which eases the problem of fabricating a long coaxial line of solid dielectric, is to make several short lengths of coaxial section and butt them together. However, this produces narrow radial interfaces between the pieces where they contact which tend to flashover. Interface flashover tests were made to determine the feasibility of this

Table 4,15 Flashover data for enoxy materials.

Sample	Length	Pressure (psig)	Average V _{BD} (kV)	Maximum V _{BD} (kV)
Permali	1/2-inch	150	220	230
Permali	1/2-inch	150	248	25 9
Permali	1/2-inch	150	235	235
Permali	1/2-inch	150	237	24 8
Permali	1-inch	150	400	42 8
Permali	1-inch	150	331	3 59
Permali	1-inch	150	372	414
Permali		1		
(Sand-Blasted)	1-inch	150	403	> 469
Permali	2-inches	25	436	> 469
Stycast	1/2-inch	150	103	110
Stycast	1/2-inch	150	110	124
Stycast	1/2-inch	150	120	124
Stycast	1/2-inch	150	115	132
Stycast	1-inch	25	152	1 66
Stycast	1-inch	25	155	1 66
Stycast	1-inch	150	257	2 90
Stycast	1-inch	150	340	3 59
Stycast				
(Sand-Blasted)	1-inch	150	345	345
Stycast	2-inches	25	363	41 4
Styca st	2-inches	25	375	4 14
Stycast	2-inches	25	314	345
Styca st	2-inches	25	362	414
EC-1 339	1/2-inch	150	124	124
EC-1039	1-inch	150	309	331
E-170	3/4-inch	150	186	207
E-170	1-inch	150	317	34 5
System's Resource	2-inches	25	37 3	373

All tests carried out in a gas mixture of 10% SF_6 , 40% N_2 and 50% Ar .

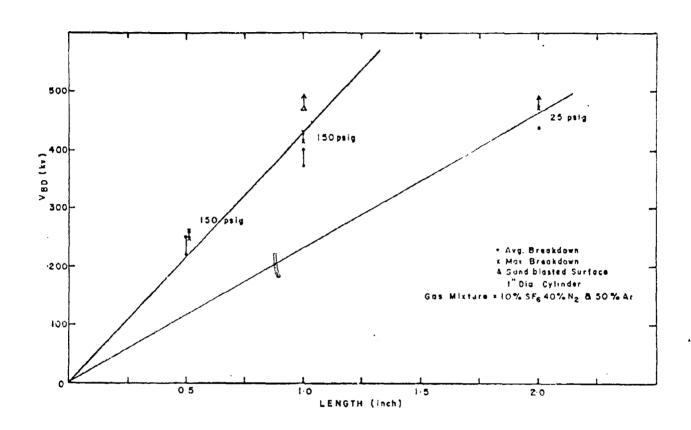
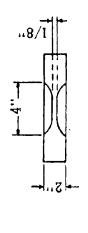


Figure 4, 101 Surface flashover data for Fermali material.

Table 4.16 dc puncture strengths and flashover of machined plastics tested in high pressure gas.



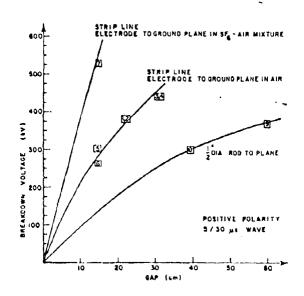
Material	Sample	Gas Conditions	First Surface Flashover	First Surface Flashover Strength	Puncture Voltage	Puncture Strength
Stycast 2850 Ft.	2-inch sidus straight and parallel with electric field	75 pet SF ₆ 215 pet A	260 kV	136 eV/inch	320 kV 280 304	2. 56 MV/znch 2. 24 2. 43
Lucite	Annealed 1) Straight once after 2) Straight machining 3) Straight Coringated	75 pei SF; 140 pei N2 } 50.50 SF ₆ /N2, 215 pei A	860 410 620 780	420 205 310 390	1909 410 780	8.0 3.28 6.24
Lucite	Annealed 1) Straight three times during 2) Edge Radius machining 3) Straight	$ \begin{cases} 75 \text{ pa: } SF_6 & 140 \text{ pai } N_2 \\ \\ 50 50 50 5F_6/N_2 & 215 \text{ pai } A \end{cases} $	370 > 580 420 > 380	185 > 290 210 > 190	550 860 380	4.64 6.88 3.04
Styrene	1) Straight Corrugated Corrugated and Acrylic Astmachined Repeat - No Acrylic Corrugated Corrugated Acrylic Acrylic Acrylic Acrylic Acrylic Acrylic	75 pei SF ₆ 140 pei N ₂	360 260 700 380 300 660	180 130 350 190 150 330	>820	9.12
Cast* Aprylic	1) Type A (095") 2) Type A (095") As machined 3; Type C (097") 4) Type C (095") Repeat	50.50 SF ₆ /N ₂ 215 pet A	620 7 740 660 540 860	31.5 > 37.5 > 37.5 27.0 43.0	740 740 860 940	1 10 8 8 0 1 0 0

• C-LEC/N.J.

 $_{\rm SP}$, each using a 0.002 inch interface gap and a radial flashover distance of 2 inches. The ambient gas was 10% SF $_{6}$, 90% N $_{2}$ at 285 psig and flashover voltages greater than 485 kV were achieved. It was concluded that interface flashover strengths in excess of 250 kV/inch (dc) can be achieved with careful field design.

Impulse flashover and breakdown studies in support of emp development are reported in reference (75). The breakdown strength between a high voltage strip line and a ground plane with edge field enhancement of 0.5 on the strip was determined for 0.5/30 pulses with and without a lucite interface. Data for air and SF environments are shown on Figure 4.402 along with the results from 1/2 inch rod to plane tests. Experiments were also made with cylinders of several radii, spaced 20 and 30 cm above a ground plane in air, with the results (positive pulse) shown in Table 4.17. Impulse tests were also made on a 1 inch gap in SF and Freon 114 at atmospheric pressure with the conclusion that Freon 114 is consistently 25% higher in strength than SF barge ceramic standoffs were also designed and tested to 1.1 MV de in air.

The ARES emp system is based on a nigh pressure coaxial line energy storage unit de charged to several megavolts. (76) In support of the design Ion I bysics Corporation supplied information on maximum radial stresses and gas mixtures in their FX machines (Table 4.14 (a)). Tests were conducted on the flashever of striplines spaced 10 and 13 cm from the ground plane, with and without lucite interfaces, using a 200 ns e-folding (decaying) pulse. The results are shown on Figure 4.103. The discussion also covers the effect on flashover of solid dielectric barriers normal to the interfaces and of dielectric covered ground planes. With positive polarity at the smaller spacings very pronounced current loading limited the voltage which could be achieved. Studies of this current loading were made with several geometries. It disappeared completely when a slight trace of SF 6 was added to the air.



- 1. Electrodes Without Interface in Air 1.8 µs to B/D
- 2. Electrodes With Lucite Interface in Air 1, 4 μs to F/O
- 3. Electrodes Without Interface in Air 1.8 μ s to B/D
- 4. Electrodes With Lucite Interface in Air 1.5 µs to F/O
- 5. Electrodes Without Interface in Air 0 9 μ s to B/D
- 6. Electrodes With Lucite in Air 0.7 pt to F/O
- 7. Electrodes With Lucite in SF_{0} 3.2 μs to F/O
- 8. 1/2 Inch Rod-to-Plane 3 μs to B/D
- 9. 1/2 Inch Rod-to-Plane 6µs to B/D

Figure 4.102 Breakdown voltage vs gap for test electrodes in air and ${\rm SF}_{6}$.

Table 4.17 Entured field stress for breakdown or flashover-cvilleders to ground plane in air (EV/em).

	•		Junction	Junction Radius (End of Cylinders)	linders)
Gap (cm)	Cylinder Radius (cm)	Interface	25% of Diameter	~5% of D:ameter	~1% of Diameter
		Without	38.5	:11.5	>43
	Ŋ	Lucite	38.5	35	32.4
,		Fiberglass	38.5		19.2
0		Without	45	óŦ	46.5
	2.5	Lucite	òř	40	28
		Fiberglass	32.6	23.3	28
-		Without		39.4	28.8
	'n	Lucite		37.3	24.5
Ć		Fiberglass			18.6
07		Without	43.4	38	46.5
	2.5	Lucite	43.4	30.2	. 24.8
~		Fibertgass	30.2	21.7	19.4

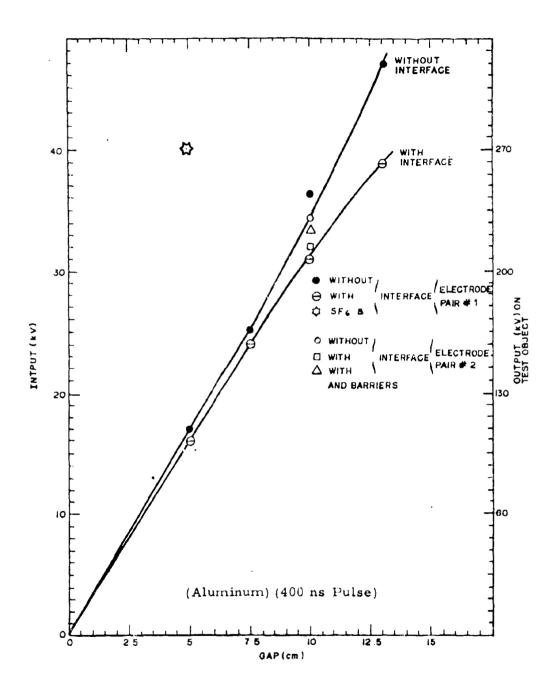


Figure 4.103 Test results of negative polarity on electrodes.

1.8 Design Considerations

4.8.1 Dielectric Performance

The several gases of particular interest for electrical insulation have been listed with their important physical properties on Table 4.18. The relative strength column presents an average of the dielectric strengths relative to nitrogen as found in the literature, but it should be borne in mind that this information is for do or power frequency voltage and near uniform field conditions. Relative strengths can change under impulse and nonuniform field conditions. The pressure at which the gases liquify at room temperature is also given together with the maximum temperatures at which they should be used from considerations of chemical stability in the presence of typica, construction materials. The next column indicates the cost per pound of each of these insulants and the final column indicates the cost to fill a specific volume (1 m³) to three atmospheres.

For designing in very nonuniform field situations where corona space charge effects make field calculations difficult, for example with wire geometries and particularly at higher frequencies, it is advisable to refer to the experimental breakdown data, some of which is included in the earlier treatment. Where the electric field is nonuniform, but not strongly so, typically a sphere gap at a few gap/radius ratios, it is possible to use a semi-empirical approach to determine breakdown voltage. This approach is based on streamer theory which predicts that breakdown develops when a certain critical number of ions are reached in an electron avalanche. (77) For SF_6 , Pedersen developed the relationship

$$\int_{0}^{N} (\alpha - \eta) dx = k = 18 \tag{6}$$

where α is the first Townsend coefficient and η is the attachment coefficient (SF₆). To use such a relationship in general it is necessary to know:

Table 4.18 Properties of several insulating gases.

-,	128		375	
\$/1p.	3.00	1.10	5.75	.72
Max. Temp.	150	300	300	120
Max. Press.	22	32	5,0	5,8
Rel. Strength	2.4	2.0	3.0	2.6
Formula	${\rm SF}_{6}$	$^{\mathrm{C}}_{2}^{\mathrm{F}}_{6}$	$C_{1}F_{8}$	$C C I_2 F_2$
Gas	Sulfur Hexafluoride	Freon 116	Freon C318	Freon 12

- (1) Uniform field breakdown potential gradients.
- (2) α and η values.
- (3) Potential gradient distribution across the nonunitoral field gap.

Blackett et al. $^{(78)}$ have developed a general purpose digital computer program which uses the factors from 1, 2 and 3 and Pedersen's relationship to determine breakdown levels. Figures 4, 104–4, 110 show the agreement between this method and experiment at 50 Hz for several useful geometries. Also, from considerations of ionization and attachment, Bortnik and Cooke $^{(79)}$ have determined a similarity law for SF at extra high voltage. Their expression, relating field, pressure, and geometry agrees with experiment up to 150 kV/cm-200 kV/cm. Unfortunately information on the α and η values for the better freons does not seem to be available.

An approach based on I edersen's or Bortnik's resitionships is valuable for design, but it is necessary to consider also factors such as clear trode area, and the non-ideal situations which develop in engineering conditions (particulate contembacion etc.). The information on as a effect in a six is limited, although I hilp and Trump (2) have assembled data which demonstrates well the severity of the effect (Figure 4, 111). This shows then the residuction of strength with creasing greaters at the highest pressures (in the season of a line with the greater scatter in remaits obtained with small area less sort to higher electric fields, so colours of either on the subject of area effect (Section 2). Bortnik and Chobs (79) also present unormation showing a significant area effect in Short at a consequence in the change below one square meter.

Small particle of debris, both conducting and conconducting, will inevitably be present to come extent in any gas insulated so stem of significant size. Such particles will charge up when they contact electrically stressed surfaces, then be "repelled" and move to the oppositely charged surface, where their charge is reversed and they return and so on. To periments indicate that diefectors particles (such to a lucite dust) have little, if the

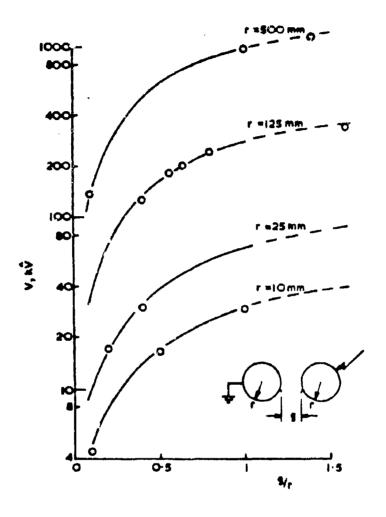


Figure 4.104 Sphere/sphere, air, 1 atmosphere.
-- B.S. 358:1960, o estimated.

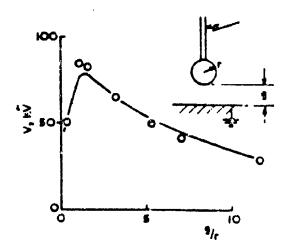


Figure 4.105 Sphere/plane, air, Latmosphere rt g = 80 mm. \sim experimental, o estimated.

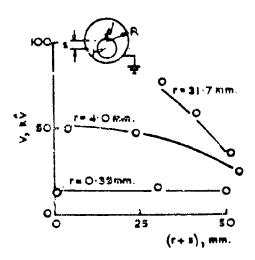


Figure 4.106 Concentric and eccentric cylinders, air, 1 atmosphere R = 63.5 mm. —experimental, o estimated.

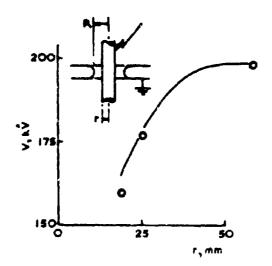


Figure 4.107 Conductor and earthed metal plate, air, 1 atmosphere, R = 140 mm. - experimental, or timated.

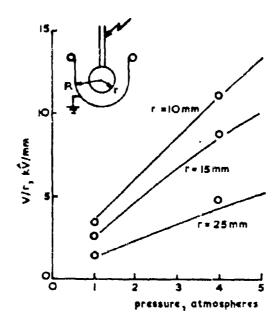


Figure 4.108 Concentric sphere/hemisphere, air,
R = 38.1 mm.
--experimental, o estimated.

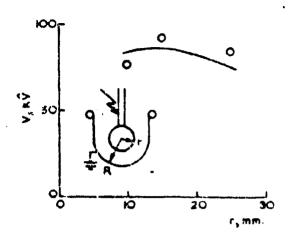


Figure 4.109 Concentric sphere/hemisphere, SF_6 , 1 atmosphere, $R \simeq 38.1$ mm. --experimental, o estimated.

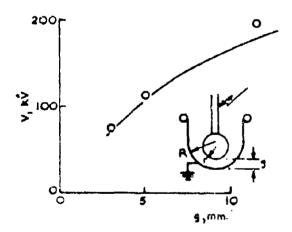
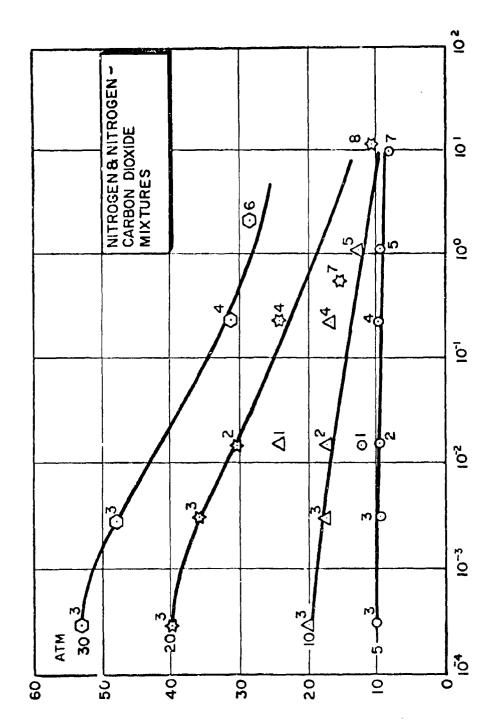


Figure 4.110 | Eccentric sphere/hemisphere, SF₆, 3 atmospheres, r = 15 mm, R = 38.1 mm. - experimental, o estimated.

MAXIMUM GRADIENT - MV/meter



ANODE AREA IN SQUARE METERS

Figure 4.111 Effect of electrode area on the maximum gradient in compressed gas insulation.

have examined the effect of free conducting particles on the strength of nitrogen and SF in a coaxial electrode system several feet in length at voltages up to 1.25 MV. Aluminum particles of size less than 0.7 mm were used. Figure 4.112 and 4.113 show the results for positive and negative polarity in SF in a curves labelled L are the threshold at which significant conduction current was detected with particles, S is the sparking voltage with particles, and H is the performance of a clean system. Obviously, sparkover at positive polarity is more sensitive to contaminating particles than negative, although conduction current starts at a higher voltage. Diesner found that perforating the outer electrode removed particles from the electrode region and improved performance. This data shows the strongly adverse effect of particulate contamination for dc or low frequency applications. As might be expected from consideration of particle movement, such contamination is less significant for the pulse case.

Designers of gas insulated equipment face the problem of determining operational stresses from test data, mostly from small electrode tests. What "factor of safety" is required to design for larger areas? This is particularly critical at higher field strengths (high pressures) because area effects are much greater, as is the effect of contaminants. The question of design stresses for different types of operation is perhaps best answored by a tabulation of experience in relatively large equipment. Before using, or extrapolating, from these stresses the following features of gas insulation in situations where corona space charge effects are not significant are worth summarizing. For defor power frequency conditions:

- (1) At least for small areas of the order 100 ${\rm cm}^2$, electrical strength increases linearly with pressure up to about 10 atmospheres for ${\rm SF}_6$.
- (2) Again for small areas, electrical strength becomes dependent upon electrode material above about 10 atmospheres.

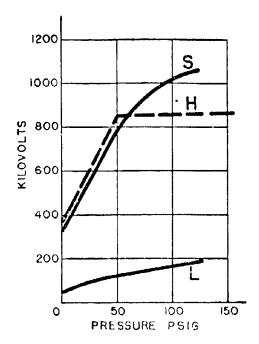


Figure 4.112 $\,$ Negative inner conductor, ${\rm SF}_6.$

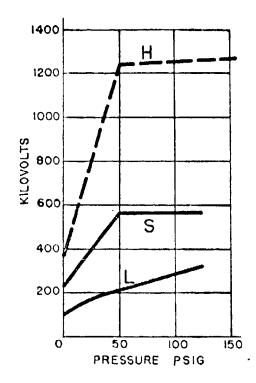


Figure 4.113 $\,$ Positive inner conductor, $\,$ SF $_{6}$.

- (3) There is a significant area effect at the higher stresses.

 For example, conditions giving 50 MV/m at areas of several square centimeters will allow about half this stress at one square meter.
- (4) Particulate contaminants of a conducting nature have a strongly deleterious effect on dielectric performance. For example, where contamination is likely a coaxial system arranged vertically will perform better than one arranged horizontally because in the former case particles fall out of the high field region. The effect of contaminants can be reduced by using particle extraction grids or dielectric coatings.
- (5) The performance of pure electronegative gases can be approached by using mixtures of these gases (e.g., 20%) with nitrogen.
- (6) The performance of gas gaps bridged with insulators can approach that of the unbridged gap if good design technique is used (material, cohesion, shielding).
- (7) For pulse conditions with effective duration in the microsecond range (e.g., 1/50 wave) performance is usually slightly above (10-20%) the dc or power frequency performance. The effect of contaminants is less significant, and one would expect the area effect to be less severe. For pulses less than a few microseconds effective duration formative time lags become important, as discussed earlier.

Information from several publications on the performance of SF 6 in larger area systems is given on Table 4.19. In general, these studies are related to the growing interest in the use of gas insulated lines for underground transmission. Reference (81), for example, discusses the performance of three separate phase lines, each 155 meters long, forming a 345 kV transmission

Table 4.19 Larger area studies with ${
m SF}_{6}$.

Comment	Precision gas capacitor Peak ac strength > 1830 kV	3 min. withstand dc 450 kV ac 540 kV	clean lab condition, standard deviation (δ_s)8%, δ_{max} 20-25%	I min. withstand 590 kVac withstand ±900 kV(I/46 imp) withstand ±720 (170/200 imp)	clean lab conditions $\delta_{\rm S}\sim 5 r_{\rm S}$	
Breakdown Field MV/m	16 imp	7.1 ac	21 de	9, i ac	21	14.6
Area (m^2)	12.5	رج ر	0.3	10.4	0.3	0.3
Gas (ab. atmos.)	SF ₆ /2.7	SF ₆ /2.5	SF ₆ /4.4	SF ₆ /4.85	$\mathrm{SF}_{6}/3.9$	$SF_6/2.5$
Breakdown Voltage (kV)	2650 imp.	540 dc >540 ac	900 dc	590 ac	725 ac	505 ac
Operating Voltage (kV)	870 ac	270 ac		225 ac		
Ref.	H	80	49	83	42	

factor of safety of about 2 (references (81) and (82)) has been determined as adequate at these pressures and field strengths. The relatively high breakdown strength of the gas capacitor (reference (1) cf. references (81) and (42)) is surprising. It may be due to the vertical orientation of the coaxial arrangement, or perhaps to special care in handling the SF_E (dew point control etc.).

Fortunately, the applications at higher voltages tend to be for experimental equipment where a self-healing breakdown is not a disaster, and as a consequence, factors of safety can be much less than for the power industry. At these elevated voltages higher electric fields are usually required to keep equipment size within reasonable limits, and as a consequence higher pressure is used. Often advantage is taken of the fact that, for example, 20% of SF_6 in nitrogen approaches closely the performance of pure SF_6 (Figure 4.22). Examples of operating stresses in megavolt equipment operated close to breakdown are given in Table 4.14. Probably the largest area multimegavolt system is the FX-100 unit installed at AFWL. This unit has a horizontal terminal of area $60~\text{m}^2$ and operates at 12 MV (19 MV/m) with 10-20% SF_6 in nitrogen at 300 psi.

4.8.2 Chemical Stability and Toxicity

Although SF₆ and the freens discussed here are chemically and physiologically inert gases, special care has to be taken at higher temperatures or where electrical discharges may exist because of breakdown of the gas into less desirable products. Sulfur hexafluoride will be discussed before proceeding to the breons. Although the pure gas can be heated in an inert container such as quartz to 500° C without decomposition, it reacts with certain metals at temperatures as low as 150° C. This can create problems, for example, with a hot spot in a transformer. Information is available from the manufacturer (83) on the rating of various materials for use at high temperature.

Electrical arcing, or even corona, will degrade sulfur hexafluoride, producing mostly lower fluorides of sulfur. Highly corrosive products may be formed, particularly in the presence of water vapor. Table 4.20 lists some typical materials in order of increasing resistance to chemical attack by decomposition products (ref. General Chemicals Research Laboratories). Decomposition products can be absorbed by circulation through a 50-50 mixture of soda lime and an activated alumina.

Sulfur hexafluoride is not toxic, but of course will not support life and suffocation is possible. Because it is very dense, leaking sulfur hexafluoride will tend to fill pits or other depressions in the vicinity. The decomposition products are toxic, in some cases highly so. As a consequence it is sound practice either to vent SF_6 insulated equipment to the outside atmosphere or to pump, via absorbers of the decomposition products, into storage cylinders. Ashbaugh et al. (6) have discussed the use and handling of SF_6 in a large volume electrostatic accelerator at 60 psig.

The Freon gases F-116 and C-318 have better thermal stability than ${\rm SF}_6$ and are relatively inert chemically. They can be used without degradation with a variety of metals and insulating materials at temperatures up to 300° C. (61) Neither of these Freon gases is toxic or flammable, in fact C-318 is approved by the Food and Drug Administration as a food propellant. However, the products produced at excessive temperature, or under electrical discharges may be toxic, and the comments earlier on the handling of sulfur hexafluoride from high voltage systems apply also to the Freons. Considering the carbon content of the Freons it could be expected that electrical discharges in these gases would produce more conducting deposits than in ${\rm SF}_6$. However, this does not seem to be so for F-116 and C-318. (63) The conducting deposit can be reduced even further by introducing a gaseous inhibitor such as nitrous oxide, (63) and a 90/10 by weight mixture of F-116/nitrous oxide is available commercially from DuPont.

Freon 12 is the most commonly used refrigerant gas, and in the literature where the label "Freon" is used in an unqualified fashion the term

Table 4.20 Resistance to attack by ${\rm SF}_{\vec{6}}$ (decomposed).

Least resistant

Most halogen absorbing plastics

Sulfur and sulfur bearing compounds

Selenium (rectifiers)

Silicon steel

Steel

Brass

Copper

Stainless steel

Aluminum

Silver plate

Activated alumina, soda lime, alkalis and most

non-metalic elements

Most resistant

Platinum

usually refers to Freon 12. As already noted it has excellent dielectric strength but is rather unstable chemically. It degrades at temperatures above about 140° C in the presence of several common structural materials such as oil, steel and copper, and is highly unstable in the presence of electrical discharges. Because of its low cost relative to other dielectric gases Freon 12 is very attractive for temporary tests, but should not be used in scaled equipment for permanent operation.

4.8.3 Physical Considerations

The use of high pressure gas as an insulating medium requires a carefully designed containment vessel. Because the stored energy in a pressurized gas is high, the consequence of vessel failure can be disastrous. For this reason containers designed for pressures above one atmosphere gauge are subject by state law to the ASME Unfired Pressure Vessel Code. Where the pressurized housing is a dielectric, design becomes particularly difficult-less well understood or controlled. One attractive approach for very high pressures is to use a fiber wound vessel, but care must be taken with the orientation of fibers with respect to the electric field. Correct selection of materials and quality control is very important. (84,85)

Table 4.18 shows the pressures at which ${\rm SF}_6$ and the Freens of particular interest here will liquify at room temperature, and Table 4.2 shows other physical properties, such as density, and the temperature at which the gas will liquify at atmospheric pressure.

In many applications of dielectric gases the ability to transmit heat from a hot region, often at high voltage, to an external cooled surface is most importnat. Fortunately, largely because of their high density, the electronegative gases transfer heat well by natural convection. They are not, of course, as effective as a liquid, but are significantly better than air. At the higher pressures the increased density enhances heat transfer. In tests with a heated coil in ${\rm SF}_6$ at atmospheric pressure, (40) it has been found that

the heat transfer to the containing tank was 0.005 watts per square inch per degree, independent of the temperature difference between coil and ambient. The coefficient of transfer was about 1.6 times that of air. Both Freon 116 and Freon C-318 have greater densities than SF_6 and better heat transfer properties. Freon 116 and Freon C-318 have heat transfer coefficients respectively 2.13 and 2.29 times that of air. Freon 12, with a density closer to SF_6 than to Freon 116 or C-318, presumably has heat transfer properties closer to those of SF_6 . The earlier warnings on the high temperature limitations of Freon 12 should be borne in mind.

SECTION 4

REFERENCES

- (1) Lucas, H.R. and MacCarthy, D.C., "Outdoor 2550 kV-BIL Shielded Precision Gas Capacitor," IEEE Trans. Power Apparatus and Systems, PAS-89, No. 7, p. 1513, (1970).
- (2) Philp, S.F. and Trump, J.G., "Compressed Gas Insulation for Electric Power Transmission," Conference on Electrical Insulation, National Academy of Sciences, p. 100, (1966).
- (3) Friedrick, R.E. and Yeekley, R.N., "A New Concept in Power Circuit-Breaker Design Utilizing SF₆" AIEE Transaction, Vol. 78, p. 695, (October 1959).
- (4) Goodman, E. V. and Posner, G. C., "Trends in Gas Insulated Transformers," Insulation, p. 39, January (1965).
- (5) Reinhold, G. et al, "High Power Cockeraft Walton Generator," IEEE Trans. Nuclear Science, NS-18, 3, p. 92, (1971).
- (6) Ashbaugh, P.G. et al, "Sulphur Hexafluoride Its Properties and Use as a Gaseous Insulator in Van de Graaff Accelerators," IEEE Trans. Nuclear Science, NS-12, 3, p. 266, (1965).
- (7) Meek, J. M. and Cragget, J. D., "Electrical Breakdown of Gases, Oxford, Clarendon Press, (1953).
- (8) Raether, H., Elektrotech Z, 63, 301, (1942).
- (9) Petropoulos, G.M., Phys. Rev. 78, 250, (1980).
- (10) Devins, J.C. and Sharbaugh, A.H., "The Fundamental Nature of Eleccrical Breakdown" Electro-Technology, p. 403, February 1961.
- (11) Alsron, L.L. et al, "Some Novel Gases of High Electric Strength," Colloq. on Gaseous Insulation, IEE, London, (1965).
- (12) Staff, "Gaseous Dielectrics," Insulation/Circuits, Directory/Encyclopedia, p. 14, June/July 1971.
- (13) McNeal, P. I. and Skipper, D. J., "The Impulse Flashover Strength of Solid Insulators in Compressed Gases," Proc. Int. Conf. on Gas Discharges and the Electricity Supply Industry, C. E. R. L. England, (1962).
- (14) Bruce, F.M., J. Instn. Elect. Engrs., 94, (11), p. 138, (1947).
- (15) Howell, A.H., "Breakdown Studies in Compressed Gases," Trans. AIEE, 58, p. 193, (1939).

- (16) Trump, J.G. et al, Elect. Engrig., 69, p. 961, (1950).
- (17) Felici, M.N. and Marchal, Y., Rev. Gen. Elec., 57, p. 155, (1948).
- (18) Uhlmann, E., "The Electrical Breakdown of Air Between Concentric Cylinders," Arch. Elektrotech 23, p. 323, (1929).
- (19) Ganger, B., Arch. Elektrotech 34, p. 633, p. 701, (1940).
- (20) Strigel, R., Arch. Elektrotech 27, p. 377, (1933); Strigel, R., Elektrische Stobfestigkeit, J. Springer, Berlin, (1939).
- (21) Foord, T.R., "Positive Point to Plane Spark Breakdown of Compressed Gases," Nature, 166, p. 688, (1950).
- (22) Allied Chemical Corp., Sultur Hexafluoride, Tech. Bulletin TB-65602, (1955).
- (23) Schreier, S., "On the Breakdown Voltages of Some Electronegative Gases at Low Pressures," NASA TN D-1761, (June 1963).
- (24) Howard, P.R., "Insulation Properties of Compressed Electronegative Gases," Proc. IEE, 104, p. 123, (1947).
- (25) Sharbaugh, A.H. and Watson, P.K., "Breakdown Strength of Perfluorocarbon Vapor (FC-75) and Mixtures of the Vapor with SF₆" IEEE Laper 63-922, (1963).
- (26) Ion Physics Corporation, Final Report on Contract DAAG39-67-C-9081 (Harry Diamond Laboratories) - Supplementary Insulation Study. August (1967).
- (27) Nittrouer, C.A., "Design of a High Energy Fast-Pulse Power System" WI, TDR 64-94, (1965).
- (28) Philp, S. F. and Trump, J. G., Conference on Electrical Insulation, National Academy of Sciences, p. 100, (1966).
- (29) Clark, F.M., "Insulating Manerials for Design and Engineering Practice," N.Y. Wiley, (1962).
- (30) Clark, F.M., "The Newer asulating Gases," Materials in Design Eng., 53, 2, o. 95, (1961).
- (31) Gameer, B., Arch. Elektrotich 24, 525, (1930),
- (32) Bright, A.W., Brit. Elect. and arcical find. Res. Assoc. Report, Ref. L/T 229, (1950).
- (33) Pimm, J.A., J. Inst. Elect. Engrs. Part III, 96, 117, (1949).
- (34) Cooper, R., ibid, 94, 315, (1947).
- (35) Posin, D.Q., Phys. Rev., 73, 496, (1948).

- (36) MacDonald, A.D. and Brown, S.C., ibid, 76, 1634, (1949).
- (37) Coodlet, B. L. et al, J. Instn. Elect. Engrs., 69, 695, (1931).
- (38) Electrical Engineering 56, 712, (1937).
- (39) Nonken, G.C., "High Pressure Gas as a Dielectric," Trans. Amer. Inst. Elect. Engrs., 60, 1017, (1941).
- (40) Camilli, G. et al, "Gaseous Insulation for High Voltage Transformers," AIEE Trans. III 71, 348, (1952).
- (41) Howard, P. R., "Compressed Gases as Insulants in High Voltage Equipments," Electrical Times 132, 683, (1957).
- (42) Kawaguchi et al, "Dielectric Breakdown of Sulfur Hexafluoride in Nearly Uniform Fields," IEEE Trans. Power Apparatus and Systems, PAS-90, 3, 1072, (1971).
- (43) Nitta, T. and Shibuya, Y., "Electrical Breakdown of Long Gaps in Sulfur Hexafluoride," ibid, 1065.
- (44) Strigel R., Elektrische Stossfestigkeit, J. Springer, Berlin, (1939).
- (45) Strigel, R., Arch. Elektrotech 27 379, (1933).
- (46) Brinkman, C., Z. Phys. 111, 737, (1939).
- (47) Felsenthal, P. and Proud, J.M., "Nanosecond Pulse Breakdown in Gaps," Phys. Rev. 139, A1796, (1965).
- (48) Meek, J. M. and Craggs, J. D., "Electrical Breakdown of Gases," Oxford, Clarendon Press, p. 307, (1953).
- (49) Bellaschi, P. L. and Teague, W. L., Elect. J. 32, 120, (1935).
- (50) Gorev, A.A. et al, Conf. Int. Gr. Res. Elect., Paper N0142, (1948).
- (51) Bellaschi, P.L. and Teague, W.L., Elect. Eng., 53, 1638, (1934).
- (52) Udo, T., IEEE Trans. on Power Apparatus and Systems, PAS-84, No. 4, 304, (1965); Udo, T. and Watanake, Y., IEEE Winter Power Meeting, Paper N031PP 67-106, (1967).
- (53) Bowdler, G. W. and Hughes, R. C., The Institution of Electrical Engineers (London), Paper No. 33175, (1960).
- (54) Martin, J. C., "Pressure Dependence of the Pulse Breakdown of Gases," AFWL Dielectric Strength Note 15, (1967).
- (55) Crewson, W.F., "Operating Theory of Point-Plane Spark Gaps," AFWL Switching Note 11, (1971).
- (56) Mulcahy, M.J., Personal Communication.

- (57) Mulcahy, M. J. et al, "Breakdown and Flashover in Electronegative Gas Mixtures - Insulator Evaluation, Time Lag and Impulse Ratio Measurements," Proc. Elect. Ins. Conf., p. 300, September 1971.
- (58) Martin, J.C., "Comparison of Breakdown Voltages for Various Liquids Under one Set of Conditions," AFWL Dielectric Strength Note 15, (1967).
- (59) Anon, "Sulfur Hexafluoride Waveguide Dielectric Breakdown Curves," Space/Aeronauties, 31, No. 5, 138, May 1959.
- (60) Klewe, R.C. and Tozer, B.A., "Impulse Breakdown of a Point-Plane Gap in SF₆," International Conference on Gas Discharges, September 1970, IEE Conf. Pub. #70.
- (61) Dupont, "Electrical Insulating Gases: Hexafluoroethane and Octafluoro-cyclobutane," Freon Technical Bulletin EL-5.
- (62) Dupont, "Freon 116 Dielectric Gas," Freon Technical Bulletin EL-15.
- (63) Dupont, "Inhibitors for Carbon Deposition in Dielectric Gases," Freen Technical Bulletin El. 10.
- (64) Camilli, G. and Chapman, J. J., "Gaseous Insulation for High Voltage Apparatus," Gen. Elec. Rev., 51, No. 2, 35, (1948).
- (65) Howard, P.R., "Compressed Gases as Insulants in High Voltage Equipments," Electrical Times 132, 683, October 1957.
- (66) Skilling, H.H. and Brenner, W.C., "The Electrical Strength of Nitrogen and Freon under Pressure," Electrical Communications 20, No. 4, 287, (1942).
- (67) Trump, J.G. and Andrias, J., "High-Voltage DC Flashover of Solid Insulators in Compressed Nitrogen," Trans. AIEE 60, 987, (1941).
- (68) Itaka, K. and Ikeda, G., "Dielectric Characteristics of Compressed Gas Insulated Cables," IEEE Trans. Power App. and Systems, PAS-89, No. 8, 1986, (1970).
- (69) James, A.G. and Norton, C.S., "Flashover of Insulators Between Parallel Plane Electrodes in Sulfur Hexafluoride," Colloq. on Gaseous Discharges, London, (1966) - unpublished.
- (70) Hampton, B. F., "A Flexible, Compressed Gas Insulated Cable," IEE Conf. Pub. #41, 61, (1968).
- (71) Ikeda, G. et al, "A Spacer for a New Gas Insulated Cable." Sumitomo Elect. Industried Ltd., Japan, Report No. TD-1-5633, (1967/8).
- (72) Ion Physics Corporation Final Report (Appendices) on "Design of an Advanced Siege Pulse Generator, Phase I," AFSWC Contrast F29601-69-C-0054, Project No. 133B, February (1969).

- (73) Physics International Co., "Design of an Advanced Siege II Pulse Generator, Phase II," AFWL-TR-69-79, June (1970).
- (74) Ion Physics Corporation, Final Report, "Low Impedance Simulator Studies," Contract No. DASA01-69-C-0091, (1970).
- (75) Ion Physics Corporation, Siege II, Phase II, Vol. III Phase II Study, AFWL TR-69-81, Vol. III, (1969).
- (76) Ion Physics Corporation, "Electromagnetic Pulse System", AFWL-TR-69-15, Vol. I, (1969).
- (77) Pedersen, A., "Criteria for Spark Breakdown in Sulfur Hexafluoride," IEEE Trans. PAS-89, No. 8, p. 2043, (1970).
- (78) Blackett, J., et al, "Breakdown Voltage Estimation in Gases Using a Semi-Empirical Concept," International Conference on Gas Discharges, September 1970, IEE Conf. Pub. #70, (1970).
- (79) Bortnik, I.M. and Cooke, C.M., "Electrical Breakdown and the Similarity Law in SF₆ at Extra High Voltages," IEEE Trans. Paper T72, 116-7, (1972).
- (80) Deissner, A. and Trump, J.G., "Free Conducting Particles in a Coaxial Compressed-Gas-Insulated System," IEEE Trans. PAS-89, No. 8, 1970, (1970).
- (81) Williams, J.A. et al, "Installation of 345 kV SF₆-Insulated, Phase Isolated Underground Bus," IEEE Conf. Paper C72, 117-5, (1972).
- (82) Fukuda, H. et al, "EHV Pipe Type Cable Insulated with SF₆ Gas," Proc. Conference Progress on Overhead Lines and Cables for 200 kV and Above", IEE Conf. Pub. 44, 338, (1968).
- (83) Allied Chemical Corporation, "Sulfur Hexafluroide for Gaseous Insulation," Technical Bulletin TB-85603.
- (84) Maxwell Laboratories Inc., "Final T.R. for Investigation of Radiation Fields from a Distributed Source," MLR-83, (1970), (AFWL EMP-HAS 302).
- (85) Renwidek, W.J. and Blewitt, R.H., "Fibrous and Non-Fibrous Insulators for Use in High Voltage Power Equipment," Trans. Plastic Inst. 26, 23, (1968).

SECTION 5

LIQUID DIELECTRICS

5.1 The Attributes and Applications of Liquid Dielectrics

Insofar as is technically and economically possible, atmospheric air is used for the general insulation of electrical apparatus. This apparatus may be concerned with the generation, transformation, storage, transmission or utilization of electrical energy. Generally, for these functions, provided that electrical stresses of 20-30 kV/cm, energy storage of $\sim 0.5 \times 10^{-4}$ joules/cm³ and specific dissipations of ~ 0.5 watts/cm² are acceptable, then there is no incentive to resort to superior dielectric media.

For increasing electrical stress requirements, the simplest change can be effected by replacing atmospheric air with an atmospheric electronegative gas (sulfurhexafloride, Freon, etc.). This can raise the electrical stresses by a factor ~2 and the stored energy by a factor ~4 but without materially increasing the allowable heat dissipation within an equipment.

Beyond the general performance which can be achieved by this means a designer can resort to:

- (1) Pressurized gases or gas mixtures.
- (2) Liquid dielectrics.
- (3) Solid dielectries.
- (4) Mixed dielectric:, liquid/solid, gaseous/solid.

For judicious choices of these media, and under certain modes of operation, one might expect to advance equipment performance such that electrical stresses of the order 10^5 volts/cm, energy storage of the order 0.1 joule/cm³ and specific dissipations of ~100 W/cm² are possible. Of course, these levels of performance are earely, if ever, required simultaneously.

The general selection of a liquid insulating medium is governed by a number of electrical, mechanical and thermal considerations. The

important factors for most equipment designs are reliability and cost. Relating to these, liquids provide self-healing media, that is, the dielectric properties are recoverable after a breakdown. Gases are likewise self-healing but solid dielectric media are permanently impaired after volume breakdown. Further, electrical damage is cumulative for solids so that they have a predictable "lifetime" in a sense that liquids and gases do not. Assuming the technical suitability of the three phases of matter for an insulating task, the economic arguments for selecting or preferring one over the others are complex. One is concerned with the handling, installation and maintenance of the dielectric as these factors relate to the environment of the equipment, manufacturing capabilities, legal restrictions and even personal preferences.

In these respects, the characteristics of liquids are mostly attractive; the simple containment, case of transfer, volume filling and impregnating properties associated with liquids build a strong economic case. Additionally, the cost of insulating oil at $\sim 50 \phi/\mathrm{US}$ galprovides a cost reference for all superior dielectric media.

Over the whole field of applications for which liquids are commonly chosen there exists a greater diversity of dielectric technology than for gases and solids. This is largely explained by the chemical activity of the liquid phase, together with its ability to absorb gases and provide a vehicle for the solid particles which are inevitably present. The division of the technology is determined by the influence of these characteristics upon the dielectric properties of the liquid and it will be evident in the ensuing sections that the nature of the electrical stress to which the liquid is subjected is the criterion.

As a consequence, equipment operating at high duty cycles, such as transformers, power switch gear, certain liquid filled power cables, etc. demand a different specification for the various properties of a liquid dielectric from the specification which might be placed for low duty cycle equipment. By low duty cycle it is implied that the equipment operates in an

intermittent or pulsed mode with low repetition. For high duty cycles, greater emphasis will be given to the chemical and mechanical properties of a liquid rather than the electrical properties which are, in any case, largely governed by impurities. In contrast, for low duty cycles, the emphasis is more likely to be on the electrical properties which will tend to be more intrinsic to the liquid for this mode.

The concern here is for the dielectric properties of liquids under certain conditions of duty and electrical stress. However, the cooling properties of liquids and cooling techniques are most important to the electrical and electronic industries and represent a considerable separate technology. For this, there exists a useful literature review carried out for the USAF Materials Laboratory under the EPIC Reports. (1)

5.2 Properties of Liquid Dielectrics

5.2.1 General Properties of Liquids

The important properties of liquid dielectries may be separated into three classes: electrical, physical and operational. For any given application different weightings will be placed on the importance of these various properties and the liquid(s) selected should have properties which are most appropriate but always within the acceptable cost range.

 Λ non-exhaustive listing of these properties are as follows:

(1) Electrical Properties Range of Values

Dielectric Strength (E)
$$+10^5$$
 V/cm $- \sim 5 \times 10^5$ V/cm

Dielectric Constant (ϵ) 2 - 80

Dissipation Factor (Tan δ) 0.0001 - 0.05

Volume Resistivity $10^6 - 10^{13}$ ohm/cm

(2) Physical Properties

Density

Coefficient of Thermal Expansion

Specific Heat

Thermal Conductivity

Viscosity

Molecular Structure

(3) Operational Properties

Chemical Stability

Compatibility

Flash Point

Toxicity

Cost

If, as in the previous subsection, one assumes that electrical equipment may be separated into two broad classifications according to its intended operational duty cycle, then certain distinctions can be made between the liquid dielectric property requirements of these classifications. For the high duty cycle equipment, maintenance of any of the electrical properties, with the possible exception of dielectric constant, will depend upon the chemical stability of the liquid in the equipment environment, and this can often be associated with the degree of compatability which the liquid has with the materials used in the fabrication of the equipment.

Again, assuming that the more obvious liquid properties for design, manufacturing and performance have been evaluated - such as dissipation, viscosity, etc., then the value of the dielectric constant is of fundamental importance. This determines the level of energy storage within an equipment at the operating peak voltage, according to:

$$W = 1/2 \epsilon_0 \epsilon_r E^2$$
 (1)

ε = Permittivity of free space

ε = Relative permittivity (dielectric constant) of liquid

E = Electrical stress

For reasons of efficiency, system safety and cost, equipments associated with energy transformation and transmission require the least possible stored energy and therefore a liquid with the lowest dielectric constant. On the other hand, components intended for energy storage, that is capacitors, require a liquid impregnant with a relatively high dielectric constant which is also electrically compatible with the solid dielectric which it is impregnating.

For the low duty cycle, or pulse, equipments it can be broadly stated that the electrical characteristics of liquid dielectrics are given prime attention. Dielectric strength is of foremost importance, the higher the value the more compact the equipment can be. This, together with a high value of dielectric constant yields the greatest stored energy density within the equipment. This is often a desirable characteristic of the class.

For both these classifications, there are operational properties which are related to safety and economies which must be taken into account. The flash-point and degree of toxicity of the liquid are factors of interest particularly as the required volume increases. Apart from any legal restrictions the costs of handling and protection could be significant.

The cost of a fluid could well influence the dielectric choice. In practice, provided that the general properties are reasonably acceptable, mineral oils are used for large volume applications. It is only for small volumes or special applications that the choice of a liquid may be made on purely technical grounds.

5.2.2 Particular Properties of Certain Liquids

The liquids or classes of liquids which find common application are not too numerous. For a given type of duty, the dielectric stresses which may be assigned do not vary greatly under practical conditions. The superiority of one liquid over another depends more upon the properties of dielectric constant, dissipation factor, viscosity, flash-point toxicity, etc.; the weighting given to the various properties will be in accordance with the equipment specification and the manufacturing processes. With a few exceptions, one of which may be water, the characteristics and properties of liquids are evaluated against those of mineral oil, the commonest and cheapest of all. Further, to a first approximation, the statistical data available for the dielectric strength of mineral oil under various conditions may be taken as a design guide for most liquids.

5.2.2.1 Mineral Oil (Table 5.1 and 5.2)

These oils are derivatives of crude petroleum, classified as heavy distillates. The oils are therefore complex hydrocarbons and the refining processes are controlled to obtain distillates which exhibit the desired compromises between best dielectric properties and best chemical stability from a given crude oil.

Being a significant byproduct of a gigantic industry this insulant is in abundant supply with a powerful marketing base. The relative cheapness and overall satisfactory properties have ensured that this family of oils have the widest application of all liquid insulants. Mineral oils are extensively used for transformer, capacitor, switch gear, and many other applications.

The major problem with mineral oils is that they are susceptible to oxidation. The rate of oxidation depends upon temperature and other environmental factors.

Oxidation brings all the tribulations such as acidity, water, sludge and evolved gases which, together reduce the initial effectiveness of the oils

Table 5.1 Typical properties of liquids.

).i			Polybulenes -				- Askarels -	1	-
	dinnib- ted transf.	Capac- tor	Pipe cable	ficury cable oil	P:pe cable liquid	Paper imprestiant	Capac- itor Irquid					
7 Section 20 25-6 37.8 6 46.183 7	58.24	် ကွော် (၁)	7635 406	2365.		8.666	300 000-	+0-42 30-31	44-51	82-92 34-35	185-240 36-37	1300 7500
1 Scorty, 1s, 26 C Scorty, 2s, 2c, 26 C Scorty, 2s, 25 C	9.73	15.5	. ??	2.	!	1)	1.8	69	17.2	45.3	45.4
Flashpoint Oper tup. 'C. Acidity, mgn. KOH. gn.	24. 94. 15.59.	151.5. 0. 25.66	96.1 .0 - 26.1°	245.3:	154 · 0.01 ·	163: 9.01: -23:	252 9.01: 1.7:	0.010 max	0.010 max - 35.5	182.2× 0.010 max -19.0	192.8> 0.010 max -7.0	None 0.010 max 10.0
Specific gravity, 15.6 °C		0.907	0.928	0.926:	0.862	5.870	0.965	813	1.26	1.38	1.45	1.54
Coef. of expan. cc cc ·C Thermal conduc. (gm-cal secXcm-X C cm) (810 hrxftX F.	3.00063 3.00031m 3.076*	0.00031:n 3.376	0.00030**	0.00080 0.072	0.00078	3.66076	60.0	3.33071	0.063	0.058	0.000/0	. !!!!Jbb 3.054
Boring point at 760 mm. C Volatility, weight loss Delectric strength, kv. J." (0.254 cm.		: , à !	ا عن:	: 8 		- 	7.357	275.0	290.0	325.0	340.0	35.0
Urelectric constant, 60 Hz 10 Hz. 25°C 10+ Hz	 - - -				2.14~	2.16'	2.22 ~	មា *1	5.7	5.8	5.6	:
Evisipation factor, 60 Hz	5.0014	0.001	0.0014	0.001	0.00051≝	3.0005 :-	0.000514	0.001	0.001	00.0	0.001	1.00
Volume resistivity ohm-cm					x10.4	· lxic···	> IxI0:4 p4	>5x10:=	>5x10:-	> 5x10"	>5x10 ¹²	> 5x:0

For key to superscripts, see Table 5.5.

Note: For definitions of viscosity units and conversions see "Handbook of Chemistry and Physics" (in 38th Edition, 1956-57, p. 2029), Chemical Rubber Publishing Company.

Table 5.2 Comparison of oil testing techniques and requirements for the dielectric strength of transformer oil.

		ELECTROD	ES	_	Specified
Country and Specification	Size (Inches)	Shape	Spacing (Inches)	Voltage Rise	Value for New Oil
British (BS148)	.5512	spheres	.157	0 to sp. value in 10" - hold for 1 minute then increase 1 kv/sec	drums 30 kv bulk 40 kv
USA (D877)	1.00	disks	.100	3 kv/sec	26 kv
Belgium (#13)	.394	spheres	.079	1 kv/5 sec	18 kv
France (CIR-C103)	.472	spheres	.196	Hold 1 minute at each 5 kv rise	40 kv
Germany (0370/4)	.985	calottes	.098	0-BD/20 sec	50 kv (dried)
Italy (CEI 10.1)	.394	spheres	.196	1 kv/sec to 40 kv hold 5 minutes	40 kv (dried)
Sweden (SEN14.07)	.472	spheres	.118		100 kv/cm
		or conc. cyls.	.197	_	roo kyem
Switzerland (SEV124)	.49.2	spheres	.196	1 ky/sec to 30 ky - hold for 30 seconds	30 kv (dried)

as electrical insulants and coolants. Much of the development and research activity is directed towards the formulation of additives or retardants which can reduce the rates of oxidation.

The use of mineral oils in large volumes is regulated by the Board of Fire Underwriters. (2)

5.2.2.2 Askapels (Table 5.1 and 5.3)

This is a family of synthetic liquid dielectrics which are chlorinated derivatives of aromatic hydrocarbons. Being synthetic, members of this class have proprietary trade names, such as Pyranol, Arochlor etc. The breakdown products are assumed to be only hydrogen chloride and carbon for correctly synthesized liquids. These liquids are intended to replace mineral oils where fire hazards are restrictive and, because of their chemical stability with greatly reduced rate of oxidation, to provide lower maintenance costs than are normal for mineral oil insulated systems.

Additionally, the dielectric constant of askarels is in the range 4.0-6.0, providing a better match to paper than unineral oils ($\varepsilon = 2.0-3.0$) for impregnation purposes.

This improved match results in higher energy densities for capacitor units and a wide acceptance of the askarels as impregnants.

These liquids are therefore used primarily in capacitors and transformers. As for most liquids, there are shortcomings. There is a higher degree of toxicity than with mineral oils and more thought must be given to compatability with other materials. (3)

5.2.2.3 Polybutenes (Table 5.4 and 5.4)

The polybutenes are a family of synthetic liquids which are polymers of butene (butylene). They have a wide viscosity range, 60-3000 ssu at 212°F, which makes them mechanically suitable for volume filling and impregnation.

Table 5.3 The characteristics of General Electric Company pyranols.

Askarels

	#1476 (A13B1)	# 1499 (A13B1B)	#1478	# 1467	#1470
Specific Gravity (65/15.5°C)	1.495-1.515	1.405-1.415	1.460-1.465	1.560-1.568	1.563-1.571
Refractive Index (25°C)	1.6370-1.6390	1.6290-1.6310	1.5695-1.5705	1.6137-1.6147	1.6075-1.6085
Total Acidity (MgKOH/gr) max	0.010	0.010	0.01	0.01	0.014
Free Chlorides (ppm) max	0.1	0 1	0.10	0.10	0.10
Free Sulfates	None	None	None	None	None
Water Content (ppm) max	35	35	30	30	30
Viscosity (SSU) seconds					-
37.8°C 98.9°C	44-48	195-205 38-40	38-31	52-56	40-43
Pour Point (°C) max	10	0	10	-32	-44
Fire Point (°C) max	None	310	None	None	None
Color (APH) max	100	150 .	150	150	150
Dielectric Stiength (25°C Ky) min**	35	30	30	35	35
Dielectric Constant (100°C)	4.15-4.35	4.6	3.7	3.5-3.8	3.8-4.1
Resistivity (ohm-em, 100°C) min	500 x 10°	500 x 10"	50 x 10°	190 x 10°	100 x 10 ⁿ
Distillation Range (°C) First drop 10% Point 50% Point 90% Point Dry Point	366-378 371-379 379-391	310 365	200 210·215 220	200 385-400	210 232-240 275-300* 390-400
Specific Heat (cal/gr at 30-35 °C)	262		2.61	2.51	2,55
Thermal Conduc- tivity (30°C)		281 x 10 ⁻⁶	346 x 10 ⁻⁰	298 × 10-6	*****
Coef. of Expansion (15.5-100°C)	.000661	.000702	.00073	.00070	.00070

^{*} This value is the 55% point

^{**}Gap 0.1 inch.

Table 5.4 Polybutenes--properties, thermal aging and mixtures.

	(;ı) <i>1</i>	ropertie	s of	o Plan			
Property	w			To dia	Table V		49 - 249	
Glean fAoI set Viscondy, ep. 37 8-9 160-0	3.00 20 3.4	470 93 10	470 · 188 15.8	55Vn 624 30/5	10/	51: 14: 30 5(1)	14 0 27,100 585	28,40° 18,23°C, 3560
Pour Point, 10 Sp.a. Gr.a., 15-10 Flack Point, 10	- 51 0 - 1 151	37 03 7 155	. 32 0.854 160	. 70 017 171	1.2 0 1 - 3 216	2 6391 21a	4 0 ⁶⁰ 1 2 <i>6</i> 0	24 0.545 272
Poder Lact, 30 76 5 50 cps, 78 C 70 °C 5	(: 0; 0.0?	9 01 0 02	0 01 0 0,	0 l 0 2	0 l 6 2	0 J 0 4	0 1 0 5	0 ? 0 's
Driff Coast, 2016 70 C	2.20 2.14	2.21 2.15	2.14 2.14	2 21 2 16	2.21 2.15	7 * t 2 1/	2.24 2.17	2 23 2 16
& ashvity, ohn cm, >; 10°° 70°C 70°C	[160 [43]	160 160	160 169	100 100)/n 80	100 90	100 yıı	0°1 80

[&]quot;As supplied by "Asset a Chila seas Corp., "Oronto Dec., Chisago Chemical Co., and W. R. Grate, Ud.

11	×	r Fact, 10 °	Diel (20 C	Con+1 70 C		helty. i = 10°° 70 C	Acadety, g-o kud g	Vis contry, cp, 25 C	Harkins Spiread Coult dyon Cm, ZO C
Baterral	20%	/// U	20 (.	70 L		-/U C	run r		/ 17 Li
Paneral Oil,									
Virgin	Ui	0.2	2 76	2.21	ηŊ	10	(i (ii) (j	20.2	8.8
Arril	1.9	15.5	2.25	2.20	10	2	0.03	70.4	14.5
April a j Copyrer	3 5	145	2.78	7.72	1.5	01	0.15	50 g	250
2 (m.: 1B,									
Vitgin	0 (+1	0.07	2 70	2.14	- 160	11.)	0.025	3-1-1	IJί
Accid	0.05	0.37	2.30	7.23	£υ	9.0	0.31	41.5	25.3
Agod will Coper of	0 :	20	2.28	2.3	0.9	C 12	0 17	417	24.5
4.50 mg, 1°B									
Virgin	9.01	0.02	7.71	2.15	-160)(0	0.005	252	3.7
Arcil	0.01	0.13	2.31	2 "	5.0	0.5	0.33	26%	23.5
April v. Copin r	01	0.3	2 30	113	70	0.65	0 04	261	20 0
420 nov PB.									
Vition	0.01	0.01	2.00	2.13	>160	-100	n 0u'-	4.1	. 75
April	0.0.	0.18	2.28	2.21	110	7.5	0.23	432	70.2
Zicelw Cepper	0.4	0.1	231	2.27	0.11	Üь	0.12	411	20.3

		. da ce	1	Power Fa	et sala	ke -t obnici	
Mixture				20 C		1.0	
Missister, Voyen Ap. 4	30° -	/6	13.9	0.03 0.6	0.1	100 7 0	la 0 0.3
Montral Ind. (1977) of 100 (19 mw FB) Virgini Aged	370	240	 15 -	0.02	0 1 0.8	160 9.8	12.0
Maneral G 1 (1 Y 1); of 10 0 (1 a w 1) to Virgin (A); et	le'e n	675	143	0 0? 0.1	0 1 0.7	160 160	12 C
Chinesel of 1 (1 (1)), of 15 of text (1), Virgin Appel	14,6 0	310	61	0.01	6 1 6 8	160 17.0	9(

They are characterized by their good electrical properties, having excellent power factors and dissipation factors at supply frequencies. Under their normal applications, as pipe and cable insulants, it is claimed that their electrical properties are not deteriorated by oxidation.

Polybutene can be mixed with mineral oils to provide for adjustments to viscosity characteristics.

5.2.2.4 Fluorocarbons (Table 5.5 and 5.6)

These can be obtained in gaseous and liquid form and are derivatives of organics with the hydrogen replaced by fluorine and/or chlorine. They are rarely used in large volumes, being more confined to electronic applications for which their excellent coolant properties provide a significant space advantage.

These liquids are chemically inert, non-flammable and have low viscosity. Electrically they are equally attractive, having a low dielectric constant (~2.7), extremely low dissipation factor over a wide frequency range, high resistivity and a published dielectric strength 50% higher than "pure" mineral oil.

For volumes where the dielectric cost is small compared with that of the contained equipment the fluorocarbons are excellent.

5.2.2.5 Silicone Oils (Table 5.5 and 5.7)

These oils can be obtained in a wide range of viscosities $(1-10^6)$ cs). For any given oil the viscosity change with temperature is much less than for mineral oil.

They are particularly useful for applications requiring low dielectric losses over a wide frequency range at elevated temperatures. Even at temperatures in the 200°C range the liquids retain their characteristics and are chemically stable.

Table 5.5 Typical properties of liquids.

										singer	Cotors				
	(C.F.) N	(C.f.) N *n = 1 n = 5	C.F.e0		Ses — — —	Silicones		Diefectric Grade Castor Oil	Glyceryl Tri- acetoxy- Stearate	Butyl Butyl Stearate Sebacate	Butyl Sebacate	Butyl Naphth- enate	Tetra Hydro- furfuryl Diente	Ethylene Glycol	Suicate Ester Base Fluid
Viscosity, SUS, 25°C 37.8°C		33.			360	720	180			848	9		19		
Viscosity, cs, 25°C	253	- 2.7	0.82	10.5	ig & 8	200 160	005 004 1	00		7	ھ		10		12.2 3.95
3-001-66	0.43	- 0.88	1.33		: ₹, 66, ^ _	>315	>325			167.8	175.0		203.9	116	187.8 0.15 max
Acidity, mgm KOH gm	1 503	154 -84	- 100.0	р <u>6</u> –	- 55	-52.7	~ 50.0	- 23	4.4	21.7	-10.0		-17.8		<-59.5
Specific gravity, 15.6°C	1.88	1.57 1.82	1.79	0.540	0.970	0.971	0.973	0.959	0.955					1.1154	0.887
Coef, of expan., cc cc 2C		20084 .00036	.0016	0.00095	76000	0.00097	0.00097	0.00056	0.00066					7000370	2000
Thermal conduc., (gm-cal sec)(cm²)('C.'cm)	,			0.00034	3000	0.00037	9000	0 103	0.103					.00063	0.080
(BTU-ht)(ftX°F) Boiling point at 760 mm, °C	0.359	40.8 224.2	102.2		1		 							196.206	>371.1
Volatility, weight loss Dielec strength ky 1" (0.254cm.) 35 min	tem.) 35 min	28 50	35 min	31%; 35:	1%r 32	35%	33						3		27.
Dielectric constant, 60 Hz	2.1 1.89	3.02 2.45	1.84	2.7.2	2.75	2.75	2.75	3.74**	3.57**	m m	\$		3	4	2.65
10° Hz Dissipation factor, 60 Hz 103 Hz	0.0005	-<0.00000 -<0.00000	<0.0005 <0.0005 <0.0005	F-51000.		10000>	1000:0>	0.06	0.0097	0.01	0.01	0.016	0.019		0.0336 0.0042
10. Hz	3x10	- >4x10 :	:0.0005 6xI0-4	: 00000;	1x10-11	0.00005 7 IXIO:4	> Ix10.4	3×10	6.3x1010	5x10!:	210000	1×10.:	<1x10::		9x1010

F(CFCF_O)_CHFCF_

a ASTM D446
b ASIM D92
c ASTM D92
c ASTM D93
c ASTM D92
d ASTM D1250
e ASTM D1250
e ASTM D924
e ASTM D924
c ASTM D924
g ASTM D936
g ASTM D

Table 5.6 General properties of fluorinated liquids.

Property	$(C_2H_8)_8N$	(C ₃ F ₇) ₃ N	(C,F,)3N	$(C_iF_g)_2O$	(C ₄ F ₁₃) ₂ O	c-C ₆ F ₁₂ O	c-C ₈ F ₁₆ O
Pour Point (°C)	******		50		90	*******	- 100
Boil Point (°C)	69	129	178	101	172	56	103
Specific Gravity (25°C)	1.73	1.82	1.87	1.71	1.81	1.69	1.77
Viscosity-CS (25°C)	0.50	0.80	2.74	0.61	2.11	0.47	0.81
Surface Tension- dynes/cm (25°C)			16.1	13.0	16.3	••••••	15.2
Coef. of Expan- sion x 10 ³ (25°C)	*******		1.2		4		1.6
Specific Heat (cal/gr/°C)			.27		*******	•••••	.25
Refractive Index No (25°C)	*******	*******	1.2910	******	*******		1.2769
Heat of Vaporiza- tion (cal/gr)	*******		16.5				20.9
Vapor Pressure (mm) (25°C)			.3	******	*******		estimat.
Dielectric Constant (25°C)	1.89	1.85	1.86	1.77	1.85	1.85	1.85
Resistivity (ohm-cm)	1016	1016	1018	10 ¹⁰	1016	1014	1018
Dissipation Factor (25°C)	.0005	.0005	.0005	.0005	.0005	.0005	.0005
Dielectric Strength Kv (25°C)*	39	44	40	40	45	41	37

^{*}Gap 0.1 inch.

Table 5.7 The physical properties of selected silicone fluids manufactured by the General Electric Company.

Property	SF96(40)	SF96(100)	SF96(500)	SF96(1000)
Viscosity at 37.8°C Centistokes Saybolt Universal	40 189	100 460	500 2260	1000 4620
*Viscosity Temperature Coefficient	0.588	0.590	0.599	0.599
Pour Point (°C)	- 54	- 53	49	49
Specific Gravity (20/20°C)	0.964	0.965	0.969	0.969
Flash Point (°C)	315	320	320	323
Specific Heat (26.6°C)	0.374	0.370	0.365	0.352
Coefficient of Expansion (°C)	0.00098	0.000968	0.000932	0.000920
Color	Water white	Water white	Water white	Water white
Condition	Clear	Clear	Clear	Clear
Reaction (mgKOH/gram)	0.04	0.04	0.04	0.04

[&]quot; Viscosity temperature coefficient = 1 - viscosity at 210°F viscosity at 100°F

Property	Liquid		Virgin	Aged	Aged w Copper
	Mineral	20 C	0.03	1.9	3.5
	Orl	7 0 C	0.2	15. 5	45
Power Factor	800 mw	20°C	0.01	0.02	0.02
≤ 10 °	Silicone	70°C	0.04	0.04	0.08
	5000 mw Silicone	70. C	0.01 0.03	0.01 0.03	0.01 0.04
	Mineral	20 C	2.26	2.25	2.28
	Oil	70 C	2.21	2.20	2.22
Dielectric	800 mw	20°C	2.73	2.12	2.69
Constant	Silicone		2.56	2.57	2.53
	5000 mw	20°C	2./3	2.71	2.75
	Silicone	70°C	2.56	2.55	2.58
	Mineral	20°C	90	10	1.5
	Oil	70°C	10	2	0.1
Resistivity, Ohm-cm \times 10 $^{\rm cr}$	800 mw Schoone	20°C	160 80	60 11	35 5
	5000 inw Silicone	20°C	160 65	47 16	50 10
Acidity, mg KOH g	Mineral Oil 800 nw Silicone 5000 mw Silicone		0.008 0.005 0.005	0.03 0.005 0.006	0.15 0.007 0.005
Viscosity. cpa-25' C	Mineral Oil 800 niw Silicone 5000 niw Silicone		20.2 19 9/	20.4 20.2 98	20.6 20.1 98
Harkins	Mineral Oil		-8.8	14.5	25.0
Spr Coeff,	800 mw Silicone		9.3	7.2	7.7
dynes cm	5000 mw Silicone		8.3	8.5	8.1

Silicone oils are expensive compared with mineral oils and other liquids but can perform unique insulating and cooling functions.

5.2.2.6 Castor Oil (Table 5.5)

This is one of the more important vegetable oils. After proprietary treatments, this oil is often selected as the impregnant for energy storage capacitors. For economic reasons these capacitors are more highly stressed than filter or power factor correction capacitors and therefore subject to partial electrical discharges at peak charge which cause dissociation of the impregnant.

Under these conditions, hydrogen is evolved from castor oil which recombines to form a wax of similar dielectric properties to the liquid. Capacitor life is enhanced by this process when compared to the effects on other impregnants operating under similar conditions.

5.2.2.7 Research Liquids

These are liquids of known molecular structure which can be obtained in very pure form. They are ideally suited for experiments which are concerned with understanding the "intrinsic" breakdown mechanisms in liquids and any dependences of electrical performance due to molecular structure. Proprietary liquids are too complex for use in this fund mental work.

Commonly, the liquids used are aliphatic hydrocarbons of the alkane series--pentane, hexane, heptane, octane, decane, etc. and the published data for these liquids are only of practical value in a qualitative sense. The test electrode geometries and dimensions, coupled with the dielectric treatments normally used do not permit extrapolations to operational systems.

5.3 Factors Influencing the Properties of Liquids

There are intrinsic factors which influence the various properties of liquids. These factors can be appreciated by study of the data taken from research fluids (4,5) in which, for example, the properties of dielectric strength, viscosity and thermal conductivity are seen to be dependent upon molecular structure or molecular weight.

In engineering practice, the selection of a liquid is only indirectly based on these fundamentals. The performance of a liquid is strongly influenced by its physical environment and most importantly upon the nature of the applied electrical stress factors.

5.3.1 Environmental Factors

Because of the nature of liquid dielectrics many environmental factors influence their properties and the more important of these factors must always be included in the selection process and/or in the assignment of a design stress.

In no particular order, some of the factors may be listed as: temperature, pressure, type of containment, electrode material, electrode area - or dielectric volume, radiation environment.

5.3.1.1 Electrode Area/Dielectric Volume

There is some justification for selecting electrode area/dielectric volume as the most interesting of these factors because an estimation of its effect upon the assignable dielectric stress involves and recognizes the statistical nature of dielectric breakdown.

Briefly at this stage, if a number of dielectric breakdown measurements are taken under identical conditions between the same pair of electrodes, the observed data may be given a mathematical description. The mean value of breakdown voltage is:

$$\overline{\mathbf{X}} = \frac{\sum_{i=1}^{n} \mathbf{X}_{i}}{n} \tag{2}$$

where

n = number of breakdown measurements.

The "Modal" value of breakdown is the value which has the highest occurance frequency and can be different from the mean value.

The dispersion of the data about the mean value is measured from the variance, \boldsymbol{s}^2 :

$$S^{2} = \frac{\sum_{i=1}^{n} (x_{i} - \overline{x})^{2}}{n-1}$$
 (3)

The standard deviation, S, is the square root of the variance. A theoretical relationship between breakdown voltage and electrode area has been derived $^{(6,7)}$

$$V_{A1} - V_{A2} = 1.80 \text{ S log A}_2/A_1$$
 (4)

where

 V_{A1} is modal B/D voltage from electrode area A_1 . V_{A2} is modal B/D voltage from electrode area A_2 . S is standard deviation for one of the areas.

This equation is precise if the value of S can be assumed independent of area. (6,7)

The effect of this area factor upon the assignable dielectric strength of a liquid (leaving aside the esoteric arguments on dielectric volume at this

stage) is illustrated in Figure 5.1. Approximately, an increase in area of three orders of magnitude reduces the breakdown strength of a liquid by a factor of 2. This is typical under a wide range of stress conditions.

5.3.1.2 Temperature

The temperature of a liquid dielectric has influence on both its electrical and mechanical properties and is certainly a factor in selection and stress assignment.

(1) Effect on Dielectric Strength

The ambient or operating temperature of a liquid dielectric medium can have two kinds of influence upon the dielectric strength. Long term, the products of chemical activity are cumulative and detrimental; approximately, this activity is doubled for every 10° C rise in temperature. For mineral oils this will be exhibited by the rate of oxidation. In the shorter time scales, an increase in temperature appears to reduce the electric strength of liquids under most stress conditions, de, ac and impulsive, certainly in the 10⁻⁵ sec range. This is held to be due to the change in level of absorbed gases with change with temperature and under applied stress. The formation of microbubbles upon the electrode and within the bulk of the fluid is suggested as the initiator of the breakdown process. This lends support to the gas breakdown theory for liquids.

Examples of the temperature effect are given in Figure 5.2 for mineral oil under ac stresses and Figure 5.3 for impulsive stresses, in n-alkanes.

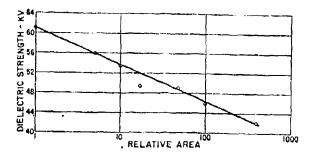


Figure 5.1 The electrode area effect on the dielectric strength of transformer oil.

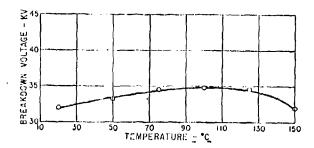


Figure 5.2 The effect of temperature on the breakdown voltage of transformer oil.

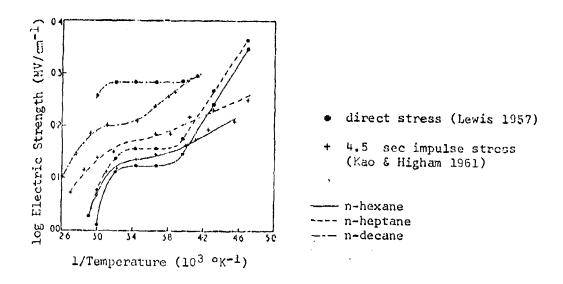


Figure 5.3 Temperature dependence of the electric strength of n-alkanes.

(2) Effect on Dielectric Losses

In general, dielectric losses are increased with increasing temperature over the range 0°-100° C. Relative to other liquids the silicone oils, or certain viscosity grades of these oils, are least affected by temperature change.

Figure 5.4 shows the effect on mineral oils for a wide frequency range, Figure 5.5 for askarels at power frequency and Figure 5.6 for a silicone liquid SF 96 (40) over a frequency range 10^2 - 10^6 cps.

(3) Effect on Dielectric Constant

This property is affected by temperature change to varying degrees dependent upon the liquid. The askarels are subject to significant change over practical ambient temperature ranges, Figure 5.7, whereas the silicone oils show a smaller percentage linear decrease in s with temperature rise.

This change in a can be important for impregnation applications where a match of values of a leads to optimum electrical stress distributions. For energy storage applications in general, the adverse effects of temperature upon dielectric strength and dielectric constant reduce the obtainable values of energy density within the store.

5.3.1.3 Pressure

The environmental pressure to which a liquid is subjected has been found to have a first order effect upon its dielectric strength from de applied stresses to the microsecond range - that is, certainly over the range in which the gaseous content has influence on the breakdown strength.

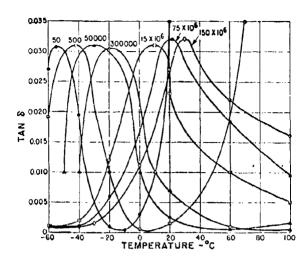


Figure 5.4 The effect of temperature on the dissipation factor of a typical European transformer oil over a range of frequency (cps).

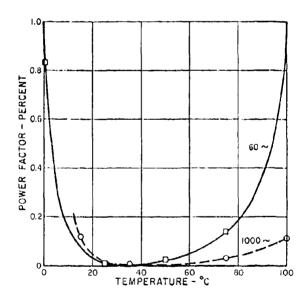


Figure 5.5 The power factor of pentachlor diphenyl (1476 Pyranol) tested under 3 kV (30 vpm).

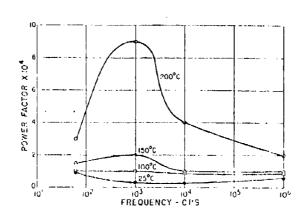
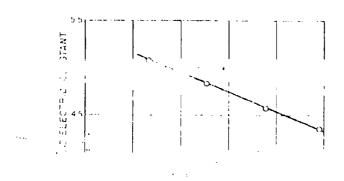


Figure 5.6 The effect of frequency on the power factor of SF96(40) silicone liquid a selected temperatures of test.



4.50

Figure 5.7. The dicter via constant of prescullor diproner tested a requestion in the range from 500 to 5000 cycles per accord.

For ambients of below atmosphere, in the hundreds of microns region, liquids exhibit a form of Paschen relationship, Figure 5.8; while for over-pressures to many atmospheres the dielectric strength increases, although not linearly, Figure 5.9.

There is an important influence here upon assignable design stresses and therefore, as for area effect, the subject will be expanded upon in the main section of the review.

There are other environmental factors which can influence the long and short term properties of liquid dielectrics, such as electrode and solid insulation materials, containment and radiation environment. These are treated in reference (4) and other texts. They can be important in an engineering sense and their effects will be evident in some of the major experimental work.

5.3.2 Electrical Stress-Time Effects

The electrical stress as a function of time could well be regarded as an environmental factor for the dielectric media. For liquids, more than for the others, the nature of the stress is of such significance that a separate treatment is justified.

The interest lies in the ability to assign reliable design stresses to liquids under a variety of environmental conditions for electrical stress times of thousands of hours (de/ae) down to times of less than a microsecond.

In practical scales and conditions, liquids can rarely be obtained and retained in a pure state. They are contaminated with solid particles, moisture and dissolved gases. These contaminants are unevenly effective in reducing the dielectric performance of a liquid as the period of stress is varied over the range of interest.

For dc or prolonged ac stressing the dielectric strength of any liquid is solely dependent upon the level of contamination. At the other end

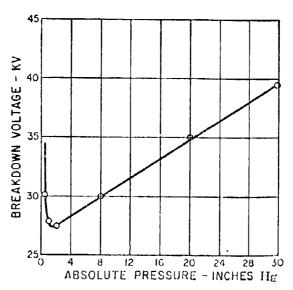


Figure 5.8 The breakdown voltage of transformer oil as affected by the absolute pressure.

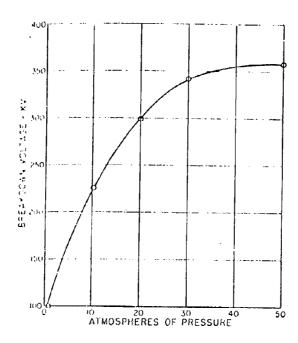


Figure 5.9 The effect of high values of air pressure on the breakdown voltage of mineral oil.

of the time scale, the single sub-microsecond stresses obtainable are independent of the contaminant level, being more dependent upon electrode conditions and breakdown streamer velocities through the liquid.

In between these extreme cases there are difficult conditions of long single pulse operation (10^{-5} - $10^{-4}\mu$ sec) and repetitive stressing with short pulses (10^{-6} sec - 10^3 pps), for examples, for which the level of contamination might be influential in varying degrees.

Figure 5.10 illustrates this stress-time effect over a large range of stress times. The division of the technology is essentially explained by the significance of contaminants over the stress-time range.

5.4 Dielectric Performance

Due to the varying influence of contaminants on the breakdown strength of liquid dielectries with changing stress time, it would seem reasonable to divide the the experimental data into three categories - direct stress, alternating that and impulsive stress. Such a division does not necessarily separate on the time areas of interest which exist in the application of liquids and therefore gives little guide to the relevance of data to specific designs. For example, experimental data obtained for hexane in small volumes and under carefully controlled conditions cannot be applied to practical designs. These data are probably directed to the determination of a breakdown theory for liquids and are of limited use.

The majority of data can be separated into three main areas of interest and application and each of these areas exhibit different treatments and requirements.

- (1) Power frequency and dc applications with associated impulse testing $(10^{5}-10^{4})$ second range.
- (2) Low repetition impulsive stressing (10⁻⁹-10⁻⁶ second range) applied to energy storage systems.

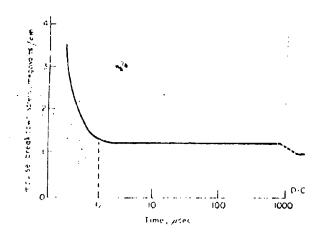


Figure 5.10 Breakdown strength of liquids as a function of applied pulse length.

(3) Miscellaneous, small scale research projects.

High repetition impulsive stressing, >>1 pps, could fall into categories (1) or (2), but the little data that exist—will be included in (2).

In general, the work in category (1) has been carried out in industrial research labs; (2) has been carried out under government military contracts, stimulated by defense needs and (3) is largely of university origin.

5.4.1 Prolonged Stress and Associated Impulse Experimental Data

This quite distinct section of the technology has been primarily advanced by R&D activities in the power industry. The concern is to obtain long term equipment reliability by the assignment of dielectric design stresses which are also consistent with reasonable equipment costs and routine maintainence. These design stresses must take all environmental factors into account, including the voltage 'surge' conditions which can be expected in practice. Because of this, it is reasonable to include relevant impulse testing data in the sub-section. The equipment, pulse specifications and motivations are, after all, quite different from those treated under the Pulsed Stresses subsection.

It is generally agreed that this facet of dielectric technology is the most complex and difficult to present coherently. The influence of contaminants is strong and any reasonable data must accrue from testing conditions which relate to contaminant levels that are economically obtainable in practice.

There are other subtleties in design. The steady state to impulse strength must be retained at the correct relative level. With extensive purification of the liquid, the economic temptations to raise the steady state design stress may impair relative performance under impulse.

According to Clark, not only are the performances of all liquids similar under prolonged stresses but also, with some exceptions, the

performances of liquids under alternating (ac) and direct (dc) stresses are comparable.

The peak AC stress ($\sqrt{2}$ x rms. for sinusoids) is the equivalent delevel with the exception that a distinct polarity effect exists for destressing, when higher breakdown values are obtained for a negative electrode. Figure 5.11 illustrates this polarity effect. As a practical confirmation of this, for large H.V. rectifier units a major manufacturer uses design stresses in oil of 100 KV/in for positive polarity outputs and 150 KV/in for negative outputs.

It would therefore seem reasonable to use ac data for de designs taking the advantage of ... 50% increase in these breakdown values for the negative electrode case.

This approach is suggested because the important publications in the field are mainly based on ac stressing and treat the data statistically, providing the only sound approach to the selection of an appropriate design stress.

5. 4. 1. 1 ac Stressing -- Experimental Data

The basis for much of the developing experimental data—can be found by reference to the work of K. H. Weber and H. S. Endicott (7). Automated testing equipment was prepared to yield a large number of oil breakdown data for electrodes of varying area both in the horizontal and vertical planes. The aims of the investigations were stated to be:

- (1) to present a sufficient quantity of data for oil breakdown, under stated conditions, for adequate statistical analysis;
- (2) to analyze the effect of electrode size on oil breakdown for uniform fields;
- (3) determine the theoretical distribution which best fits the data and derive—from it the relationship of area to strength.

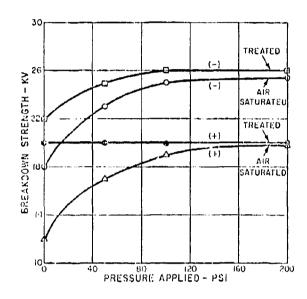


Figure 5.11 The de voltage strength of transformer oil as affected by electrode polarity in nonuniform fields, including the effect of oil treatment.

A complete tabulation of the data is given in Table 5.8 together with a fisting of the experimental conditions and electrode relationships. These data are summarized statistically in sections A and B of Table 5.9. Histograms of these breakdown voltages are presented in Figure 5.12 (a) with smooth curves calculated from the modes and slopes given in Table 5.9, section C. It is noted that the positional effect of the electrodes, in this case between horizontal or vertical, is insignificant. Further, the skewness of the distributions is noted to be characteristic of an extremal rather than a normal, symmetrical distribution.

Area effect is examined in detail. Three methods of estimating this effect are possible:

- (1) Physical area effect.
- (2) Minimum of groups area effect.
- (3) Theoretical area effect.

Estimates by these three routes are shown to be in close agreement in Figure 5.12 (b).

The physical area effect (1) is obtained directly by testing electrodes of significantly different areas. In Figure 5.12 (b) the modal values from Table 5.9 (c) are plotted against the logarithm of the relative areas.

The estimate by minimum of groups is made by simultaneously testing different numbers of identical electrode pairs. It is stated as follows.

What is frequently referred to as area effect is the result of a series of inferences, if N breakdowns have been obtained on a gap of area A, and m and n are numbers such that N = mn, then:

(1) Taking the m minimum voltages of m groups of n breakdowns each is equivalent to connecting n such identical pairs of electrodes of area A in parallel, and measuring the breakdowns of this system m times.

Table 5.8 Test conditions and breakdown data.

Control Data

Elapsed Time, Hours	Cumulative No. of Breakdown Cyrles	Gas Content, % by Volume	Water Content, Parts per Million	Ambient Temperature, Degrees Contigrade	Atmospheric Relative Humidity,	Acid, Milligrams KOII per Gram	Color, National Petroleum Association	Test Temperature	Power Factor,	Resistivity, Ohm- Centimeters	Interfacial Tension, Dynes per Continueter
24	. 65	1 0	25	23	40			-			
96 112		2 98	22	., .,.21.,	54	0 006	1/2	32 8		4×10 ¹⁴	50

Relative Electrode Areas

Fro testication (1) 4 Experience (1) (2) (doi: 1) 2 (d)

Note: Electrode $\#4 \sim 50 \text{ cm}^2$.

Table 5.8 (Continued)

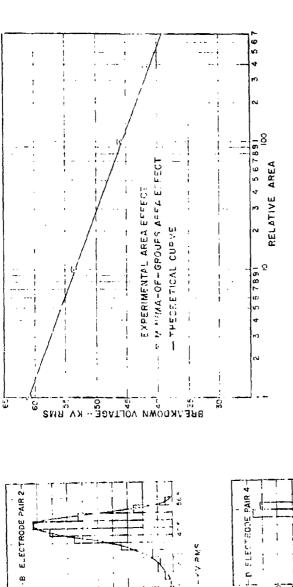
Breakdown Voltages, Kv, of Transformer Oil with Use of Rogowski Electrodes, 0.075-Inch Specing Vertical (V) and Horizontal (H)

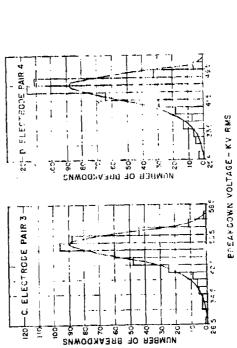
53 50 48 00 17 50 30 33 10 63 56 48 40 44 45 15 38 67 57 41 60 48 51 39 44 44 66 61 10 63 51 51 52 41 61 52 51 51 51 51 51 51 51 51 51 51 51 51 51	V II												Fie	elds											
53 50 48 00 17 50 33 10 63 50 48 40 44 45 45 38 57 57 41 60 48 51 58 44 44 44 65 66 61 61 63 41 30 48 11 50 00 67 41 60 60 38 46 48 64 64 64 64 67 40 67 40 40 40 40 40 40 40 40 40 40 40 40 40	18		1		2		3		•				2		3				ı	- 2	!	3		- 4	
44. 66*	44. 60	v	н	V	u	v .	н	v ·	н	v	н	V	н	V	11	v	H	٧	н	V	н	Ÿ	н	v	н
$\begin{array}{cccccccccccccccccccccccccccccccccccc$	00 01 47 48 17 40 43 47 58 60 50 51 52 51 47 41 53 51 54 41 13 16 50 50 50 48 40 45 17 47 41 53 16 50 57 30 43 18 44 63 43 43 60 61 49 4 49 43 40 65 61 61 50 17 12 35 42	44, 40	501. 503. 504. 505. 506. 507. 507. 508. 508. 509.	488 481 481 481 481 481 481 481 481 481	40 40 40 40 40 40 40 40 40 40 40 40 40 4			48	10	40 00 00 00 00 00 00 00 00 00 00 00 00 0	566 47 567 568 47 569 569 569 569 569 569 569 569 569 569	48, 48, 48, 48, 49, 49, 49, 49, 49, 49, 49, 49, 49, 49	444 447 448 444 447 448 444 447 448 444 447 448 448	44. 600 44. 64. 64. 64. 64. 64. 64. 64. 64. 64.	48, 374, 42, 43, 44, 44, 44, 44, 45, 45, 45, 45, 45, 45		388 447 447 447 447 447 447 447 447 447 4	57. 569. 569. 569. 569. 569. 569. 569. 569	57. 57. 57. 57. 57. 57. 57. 57. 57. 57.	414 488 483 484 484 484 484 484 484 484 48	. 50.0 . 40.7 . 61.1 . 40.4 . 46.4 . 46.4 . 46.4 . 46.4 . 46.4 . 51.6 . 50.6 . 51.7 .	- 448	544 - 436 - 436 - 456 - 457 - 458 - 456 - 456 - 457 - 458 - 456 - 457 - 458 - 456 - 457 - 458 - 456 - 457 - 458 - 456 - 457 - 458 - 456 - 457 - 458 - 456 - 457 -	. 38.5 1.6 1.6 1.6 1.6 1.6 1.6 1.6 1.6 1.6 1.6	437 450 138 300 1437 442 444 400 800 1437 443 453 444 453 445 114 445 100 2

Table 5.9 Statistical values for breakdown voltage distributions.

All Gaps at 75-Mil Spacing

	νδ	ection A :	Section A: Horizontal Field	ntal Fiele	1		Section	Section 3: Vertical Field	al Field		Section	C: Com	bined Ho	rizontel es bons	Section C: Combined Horizontal and Vertica Field Positions	Sect	ion D: C	Combined Groups of	d Date, 1 f Ten	Section D: Combined Data, Minima of Groups of Ten
Electrode Number	-	7	1 2 3 4	1	Composite	-	7	*	7	omposite	-	2	~		Composite 1 2 3 4 Composite 1 2 3 4 Composite	-	2	F.	•	1 2 3 4 Composite
Mode Fm, kv Menn F, kv St. 33. 49.71 48.43 45.56 49.80 55.79 49.08 48.56 45.56 49.70 Menn F, kv Standard deviation Sr, kv 4.67 3.71 43.7 428 426 507 408 2.75 401 423 Coefficient of variation 16.75 St. 7 7 9.4 9.8 89 95 87 80 92 88 Stope L/st, kv/decade area ratio 2.78 3.00 200 200 200 200 200 200 200 200 800	55 53 53 39 8 7 8 7 8 7 8 7 8 7 8 7 8 7 8 7 8 7 8 7	49 71. 48 01. 3 71. 7 7 . 3 00.	48 43 46 42 4 37 9 5 4 200	45.56 43.60 4.28 9.88 3.46	47 86 47 86 4 26 8 9 3 44 800	55.79 53.46 5.07 9.5 4.10	47 20 47 20 4 09 8 7 8 3 31	45 25. 46 84 3 75. 8 0	45 25 4 01 9 2 3 24	27 + 4 5 8 8 8 8 8 8 8 8 8 8 8 8 8 8 8 8 8 8	55.65 53.45 4.88 9.1	45 39 39 39 39 39 39 39 39 39 39 39 39 39	46.63 46.63 4 08 4 08 7 25	45.56 43.66. 4.15. 9.5. 3.31.	55-55 49 39 48 49 45.56 49.77 46 58 42 45 41 46 38 99 42 14 53 43 47 80 42 14 54 67 83 avg 44 45 40 75 39 28 85 95 40 11 avg 48 8 3 92 4 08 4 15 4 27 rms, 4 48 3 57 4 58 4 48 4 30 rms 3 9 1 8 2 8 7 9 5 3 3 3 3 3 3 3 3 3 3 3 3 3 3 3 3 3 3	46.58 44.45 4.48 10.1 3.92 40	42 45 45 45 45 45 45 45 45 45 45 45 45 45	41.46.3 39.28.3 4.38. 11.7 10.4	38 09. 55 95. 12 5 48. 10 5 93.	5 4 5 11 4 5 5 5 5 5 5 5 5 5 5 5 5 5 5 5





(b) Electrode area effect.

(a) Distributions of test results for various electrode areas.

Breakdown distribution and area effect. Figure 5.12

BPEAKDOWN VOLTAGE--77 PMS

B 30 R3PMUP 일 후 후 발

NUMBER OF BREAKDOWNS

BBEAKDOWNS

ŝ

(2) These n hypothetical, identical pairs of electrodes of area A are equivalent to one electrode pair of area n x A; and the m breakdowns obtained are taken to be a random sample of breakdowns for this new area n x A.

Complete data for minima of successive groups of ten breakdowns are shown in Table 5.9, section D, the differences between the corresponding modal voltages of sections C and D correspond to a 10:1 area ratio. The plot in Figure 5.12 (b) shows the mean area effect for the four sets of data with area ratios of 1-10-100-400.

Figures 5.13, 5.14 and 5.15 represent the distributions of interest taken from the data of Table 5.8 plotted on extreme value probability paper.

A theoretical argument is developed for a weak-link dependence of breakdown where the distributions are best fitted to an exponential, or extremal, rather than a normal distribution.

The work is summarized as follows:

- (1) The breakdown of transformer oil follows extreme value theory rather than normal probability.
- (2) The distributions of breakdowns for different areas are similar exponential distributions shifted successively toward zero for increasing areas. Area effect is essential to the specification of dielectric strength.
- (3) Extreme value theory yields a precise equation for predicting the breakdown for electrodes of any area in uniform field, once the modal voltage and the standard deviation are known for any one area in the oil used. This relationship is:

$$V_{A_1} - V_{A_2} = 1.80 \text{ S}_{v} \log_{10} \frac{A_2}{A_1}$$
 (5)

where

 V_A , V_A are the modal voltages for the two areas A_1 , A_2 . S, is the constant standard deviation.

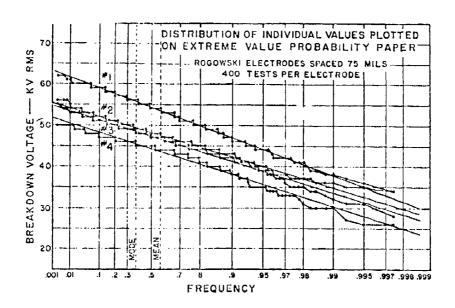


Figure 5.13 Breakdown voltage distributions of transformer oil for electrodes of four different areas.

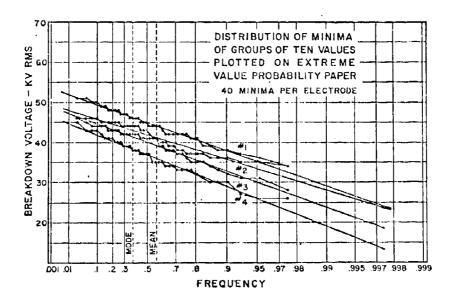


Figure 5.14 Minima-of-groups area effect. Breakdown voltage distributions of transformer oil for minima of successive groups of ten for data of Figure 5.13.

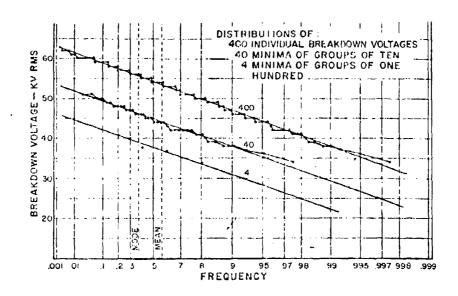


Figure 5.15 Minima-of-groups area effect. Comparison of the distribution of individual breakdown voltages for electrode pair 1 with those of minima of successive groups of 10 and 100 breakdown voltages.

(4) For the particular oil used, a 10:1 increase in area results in a 16% decrease in dielectric strength from the higher value.

The statistical arguments and treatments used in the evaluation of these experimental data may be best understood by reference to Gumbel's collected lecture series on the statistic theory of extreme values.

Weber and Endicott published in 1956; fifteen years later differences of opinion on the distribution of breakdown measurements still exist.

J.K. Nelson agrees that the distribution of breakdown data will be extremal under the following conditions:

- (1) "Idealized" electrodes are used.
- (2) Time effects are permitted to influence breakdown.
- (3) The liquid is homogeneous and stationary.
- (4) The testing technique is exactly reproducible.
- (5) There are no errors of measurements.

His argument is that there will always exist random environmental factors which tend to "normalize" the distribution of data. He therefore puts the hypothesis that the probability of breakdown will be the result of two random processes:

- (1) Bulk liquid breakdown as characterized by a weak-link concept having an extremal distribution (skewed).
- (2) Random environmental errors with an assumed normal (symetric) distribution.

The distribution he suggests is of hybrid form, the support for (8) which has been accumulated from an experimental program—in which the liquid was optionally circulated between the electrode structure. Figure 5.16 illustrates the relative probability densities exhibited.

E. Simo (10) has carried out significant large-scale tests of transformer oil under 60 cps stress conditions. Doubting the statistical significance of the number of tests required by ASTM, B.S. (British) and V.D.E.

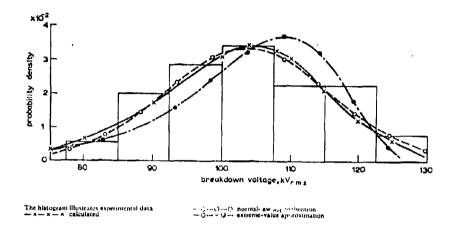


Figure 5.16 Breakdown probability density for circulating liquid subjected to 20s step-by-step test.

(German) testing procedures for measuring the quality of oil, Simo designed an experiment to evaluate the effects of electrode area, electrode material and oil treatment via thousands of breakdown tests. There is no discussion of a possible hybrid form of the cumulative distributions, the data are plotted on extreme value probability scales with tabulated values for the 0.999 and 0.001 probabilities.

The configuration of the test equipment and physical properties of the oil are shown in Figure 5.17, the tabulated data on Table 5.10 and the cumulative distribution plots in Figure 5.18.

A separate experiment to determine the effect of oil treatment on the breakdown strength was carried out with small volume and 3.16 cm diameter brass electrodes. These results are reproduced in Table 5.11 and Figure 5.19.

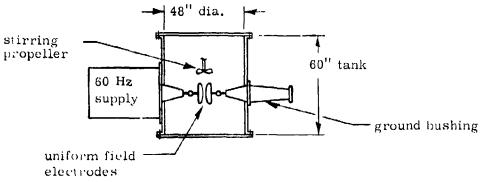
The conclusions drawn were:

- (1) Breakdown values depend on both the oil and the test conditions.
- (2) Electrode materials influence the breakdown values, brass being superior to aluminum, for example.
- (3) Breakdown values are a function of electrode area.
- (4) Breakdown values did not appear to be a function of volume.

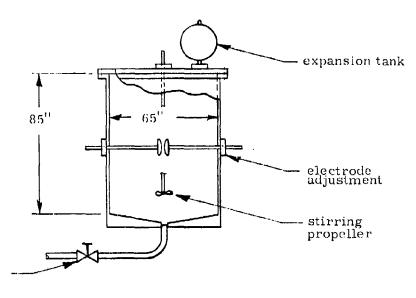
The statistical method based on no fewer than 200 tests is advocated for the evaluation of oil.

The interpretat on of Simo's data appears to be slightly conflicting with the conclusions drawn by Nelson et al. (8) from their large electrode area tests in transformer oil. The conflicts arise in the assignment of influences due to dielectric motion and volume. In any event, both these test data are important in that they treat practical electrode areas and dielectric conditions.

Nelson et al. initiated their testing programs for electrode areas up to 2 m 2 under near uniform field conditions with the purpose of providing



400-gallon test vessel



for filling & draining

0.9-gallon test vessel

Physical Properties of the Oil Tested

Specific gravity 60°F	0.854
Viscosity SUS 100°F	57
Flash point *F	315
Pour point °F	60
Interfacial tension dyn/cm	43
Total acid number mg KOH/gm	Nil
Loss index, room temperature	0.0008
• • • • • •	

TABLE II
ELECTRODE DIAMETERS AND SPACINGS AS TESTED

Outside	Area of		
Diameter (cm)	Flat portions (cm²)	Spacing (mm)	Electrode Mate rial
3.16	1.11	2	Rod aluminum
3.16	1.11	$\overline{2}$	Rod brass
15	25.6	4	Brass composition
30	102	5	Cast aluminum
30	102	5	Forged brass

Figure 5.17 Conditions of the oil dielectric test bed.

Table 5.10 Breakdown values obtained under varying electrode conditions.

BREARBOWN VALUES OFFAINED WITH 3.16-CM-DIAMETER ALUMINUM FLECTRODES AT 2-MM SPACINGS

	rithme tic	Statistical	
Number of Volume Minimum Maximum	Mean	Distribution	
Tesis (gal) (kV) (kV)	(k V)	Λ	B
y district the transfer of the department of the second of			
3072 0.9 33.2 68.5	59.1 3	2.2 76	
886 400 34.2 71.8	60.5 3	0 73	2.7

A = minimum kV 0.909 probability, B = maximum kV 0.001 probability.

BREAKDOWS VALUES OBTAINED WITH 3, 16 CM-DIAMLTER BRASS ELECTRODES AT 2-MM SPACINGS

				m 15*		ಚರ್ಷಗಳಲ್ಲಿ ಮ	
	Specimen	Aes	ાતા	Arithmetic	State	stical	
Number of	Volume	Minimum	Maximum	Menn	Distri	nglaon	
Tests	(gal)	(k V)	(kV)	(kV)	Á	B	
	•	÷ •		•• •	4.0		-
2904	0.9	36	77	62.6	35.2	73.5	
2145	0.9	25	76	61.2	30.5	73.4	
820	400	40.5	75.8	63.5	34	74.5	
				· · · · · · · · · · · · · · · · · · ·			_

A minimum kV 0.999 probability, B maximum kV 0.001 probability.

BID AKDOWN VALUES OUTAINED WITH 15- AND 30-CM BRASS AND 30-CM ALUMINUM ELECTRODES

2. *			SECTION 1	in de n i e e e e e e e e e e e e e e e e e e		Electrode	.aaa 	istical
Electrodes	Number of Tests	Specimen Volume (gal)	Minimum (kV)	tual Maximum (kV)	Arithmetic Mean	Spacing (mm)		ibution B
15-em Brass	250	400	67	122	107.4	4 -	02.8	125.2
	281	400	45	118	104.1	4	56.2	123.3
	284	400	60	123	105 1	4	56.8	124.8
	250	400	47	126	106/2	4	52.0	127.5
30-cm Brass	200	400	59	138	111		37	140.5
	:1001	400	30	131	105.8	5	28.2	139.9
	200	400	48	129	108.8	õ	30.1	140-2
	300	400	50	128	108.3	ā	39.9	135.9
30-cm Aluminum	2.40	400	50	100	80.4	ā	26.2	102.1
	250	400	47	100	81.4	ô	33.2	101.8
	300	400	50	110	87.4	5	28 6	110.9
	319	400	50	112	89.4	ភ	30.2	113.1

A = minimum kV 0.999 probability, B = maximum kV 0.001 probability.

BREAKDOWN VALUES FOR BRASS AND ALLMINUM FLECTRODES

· •	••	* <u>*</u>	-		72.3		
Electrode Diameter (em)	Electrode Material	Electrode Spacing (mm)	Minimum	Statistical Maximum (kV/mm)	Menn	Number of Tests	Coefficient of Variation Percent
3.16	Rod Aluminum		15.7	35.7	30.1	3100	9,6
3.16	Rod Brass	$ar{2}$	16.6	37	31.1	6069	9.8
30	Cast Aluminum	ã	5.8	21.7	17 1	1019	12.5
30	Forged Brass	5	7.5	27.6	21.8	3400	13.5
	- · · · ·						

Table 5.10 (Continued)

PERCENT INCREASE OF BREAKDOWN VALUES FOR BRASS ELECTROPES

	f	1 15			
(cin)		Minimum Percent	Maximum Percent	Mesn Percent	
$\begin{array}{c} 3.16 \\ 30 \end{array}$		$+5.7 \\ +29.3$	+3.6 +27.2	$+3.3 \\ +27.5$	

	Electrode	. War waren i om	Electrode	Transcription of the	Statistical	-	77.1
	Diameter (em)	Electrode Material	Aren (cm²)	Menn	Minimum	Maximum	
	3.16	Brass	1.11	1	1	1	
	15	Brase	25.6	0.862	0.903	0.851	
	30	Brass	102	0.702	0.457	0.745	
	3.16	Aluminum	1.11	1	1	l	
h =	30	Aluminum	102	0.569	0.370	0,608	

Electrode	Electrode	Electrode	Oil Volume		ente successione de la marche successione	. 1	- =
Diameter	Area	Spacing	Tested	9.81 1	Maximum		
(em)	(em²)	(intn)	- (cm³) 	Minimum	(kV/mm)	Menn	
3.46	1.11	2	0.22	16.6	36.9	31	
$\frac{15}{30}$	$\begin{array}{c} 25.6 \\ 102 \end{array}$	1 5	$\frac{10.2}{51.2}$	15 7 5	31.3 27.7	$\frac{26.8}{21.8}$	
						21.0	_

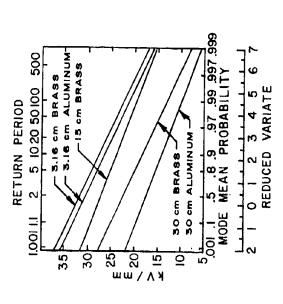


Figure 5.18 Cumulative distribution of all results.

Table 5.11 Test results for oil of varying quality with and without motion.

	· ···		Still Oil,	Still Oil, Electrode Spacing-2 mm	pacing-	-2 mm				Contrac	ous Stirred	Continuous Stirred Operation Fleetends Spaning	Plentande	Spacine	8	
												· functional and		•	*****	
Source	Number Nu of Samples T	mber of ests	Minim	akdown kV Maximum	Mean	Breakdown kV Coefficient Water by of of of of length Number Number of Variable ppm Volume Samples Tests N	Water ppm	Gass Percent by Volume	Number of Samples	Number of Tests	Bre Minimum	Gas Breakdown kV Coefficient Water by Minimum Maximum Mean of Variable pom volume	Mean	Coefficient of Variable	Water Dom	Ger Percent by
Open Tanks	<u></u>	5600	22.8	6.2	49.7	42 .9 4 9.7 10.9 24-36 9-11	22-36	9-11	=	2200	15.5	15.5 57.5 45 13.5	4 5	13.5	24-36 9-11	9 -11
Oil Treatment Plant	*	908	28.7	70.1 61	61	1~	01>	<10 <1	9	1200	25.	4 19	57.0	61 4 57 5 7 7 7 10	5	,
Production											- 1				;	;
Transformer	ន	999	ង	65.5	56.2	65.5 56.2 7.9 10-14 1-1.2	10-14	1-1.2	6	1800	33.3	66.2 56.9	56.9	œ	10-14	10-14 1-1.2

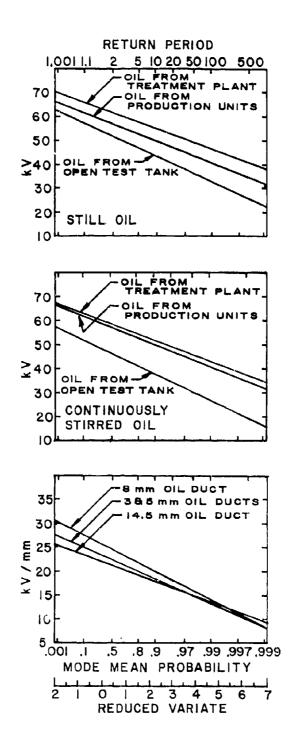


Figure 5.19 Breakdown strengths under various conditions.

practical design data for mineral oils. Both ac and impulsive stress conditions were investigated.

The test vehicle which was in coaxial form with provision for circulating the oil is illustrated in Figure 5.20.

In preliminary tests and using smaller scale equipment, the effect of moisture content and time between discharges upon the electric strength of the oil were measured. These effects are shown in Figures 5.21 and 5.22. It is noted that the electric strength of the oil falls rapidly with increasing moisture content until the saturation condition is reached. Further increase did not appear to have a significant influence upon the strength.

Using the main test vehicle with an electrode area of 1.885 mm² and a gap length of 11.7 mm, 100 breakdown measurements were taken for both stationary and circulating oil; oil which was filtered and dry air saturated. It was observed that the distribution of data was extremal for stationary oil but that a degree of normalization of the data occurred with movement of the dielectric which was proportional to its speed. (Typical speed range, 3-4 mm/second). The influence of circulation is illustrated in Figure 5.23 where the data are plotted on both extreme value and normal paper; Table 5.12 gives a tabulation of the distribution indices. Accompanying the change of distribution an increase in the mean breakdown strength was obtained with circulation.

It was observed that the relative effect of circulating the oil was strongly dependent upon temperature, see Figure 5.24, and, for still oil, the gas content was important. Simo also noted, Figure 5.19, that the relative performance was dependent upon the quality of the oil, therefore a designer should be cautious in the expectations of improved dielectric performance through liquid circulation. In most equipments the liquid will be in motion due to convection of heat. For practical electrode geometries, complex thermal gradients will often exist which, together with the difficulties of precisely defining the electrical stresses prevailing at all points, make a number of these claims academic.

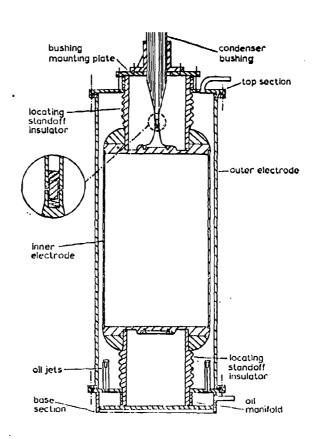
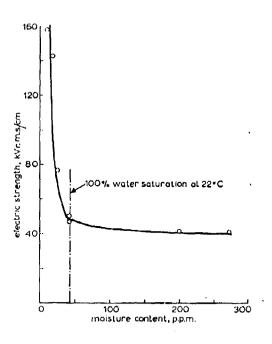
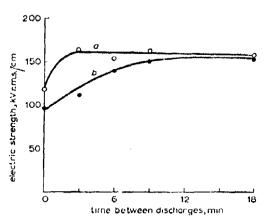


Figure 5.20 Sectioned view of large electrode system.



127 mm-diameter aluminium flat-plate electrodes 5 mm gap

Figure 5.21 Variation of electric strength with moisture content (supply-frequency voltages) at 22° C.



a For new oil
 b For oil maintained at 100°C for 500h
 127 mm-diameter aluminium flat-plate electrodes
 5 mm gap

Figure 5.22 Influence of time between discharges (supply-frequency voltages).

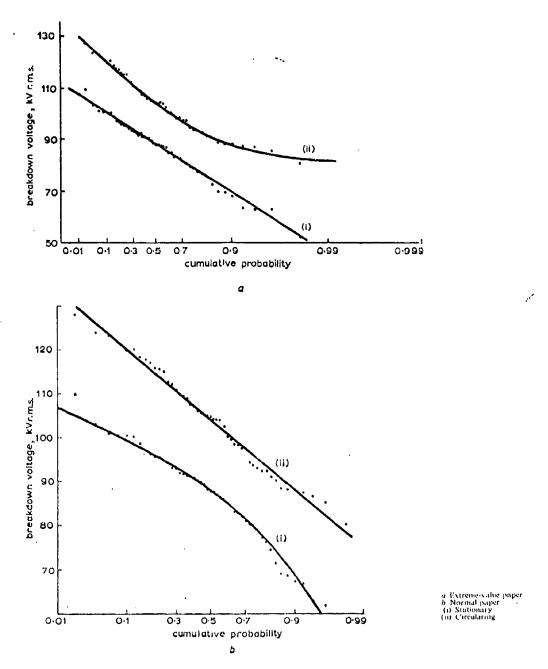
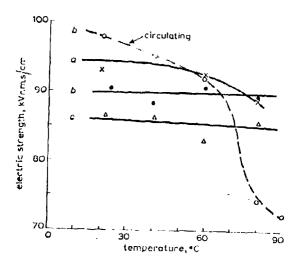


Figure 5.23 Cumulative probability for stationary and circulating-oil samples.

Table 5.12 Distribution indices for stationary and circulating oil

	Pawer f	requency	1/50-25	impulse		<u>-</u>
	Stationary	i Circulating	Stationary	Circulating	Gaussian	1 stre 44
Mean stress, kV/mm Standard deviation, kV/mm Coefficient variation "/ stew Kurtosis	7:3 1:2 16:5 1-35 5:9	8-9 1-1 12-2 0-00 2-32	18-9 2-3 12-4 0-64 2-92	,	!	
*						



Gap - 11-7 mm Area - 1-885 m² Moettre - 5 7 p.p.m. Applied voltage - 2kV c.m.s./s ramp

Figure 5.24 Effect of nature of gas in solution (supply-frequency voltages).

The paper further deals with impulse testing data, to be treated later, arguments for a volume rather than an area effect upon the liquid breakdown stresses and more discussion of the cumulative probability distributions.

For the latter, it would seem advisable to accept an extremal distribution for it is shown by Weber and Endicott (7)--Figure 5.25--that this gives a safer estimate of the size effect.

5.4.1.2 Impulsive Stresses--Relevant to Equipment Testing

Under long term operation, power equipment is periodically subjected to abnormal surge stresses which may be associated with switching transients or atmospheric disturbances. Equipment must be designed to survive these sporadic extremes with the aid of arrestors, suppressors and other protective devices. Knowledge of the dielectric performance under these impulsive conditions is therefore as necessary as knowing steady state performance.

Tests are performed using pulses of standard amplitudes relative to the normal equipment working voltages and of standard shape and durations which are reasonably representative of the expected surges.

The standard impulse for USA and Canada is the 1.5 x 40 $\,\mu\,sec$ waveform and the International Standard is 1.2 x 50 $\,\mu\,sec$

There is no significant performance difference between these waveforms. The usual impulse level for power equipment is 4-5 times the peak
line-to-ground voltage. Figure 5.26 illustrates the impulse and defines the
risetime and duration.

5.4.1.3 Experimental Results

It is emphasized by many workers that the experimental results obtained have a significant dependence upon the preparations and test procedures adopted. Less frequently, the significance of much of the accumulated data to practical applications is guestioned. Hancox and Tropper (11) in their

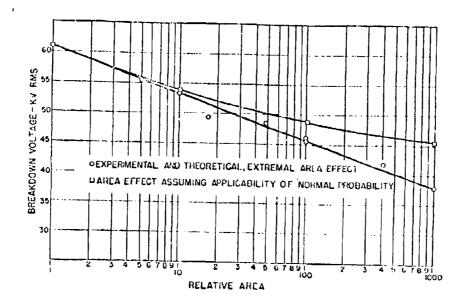
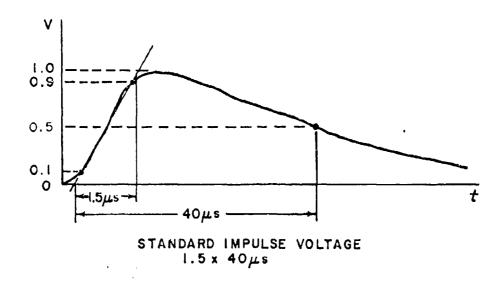


Figure 5.25 Deviation of normal-probability area effect from the experimental and theoretical values.



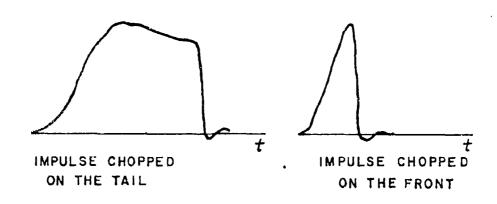


Figure 5.26 Impulse waveshapes.

reported impulse testing with an oil medium, show sensitivity to both matters. These workers carried out impulse tests up to 500 kV using mostly 2/60 μ sec pulses between electrodes of 2-7 cm diameter with gaps of less than 1 cm.

They refer to three testing procedures, two of which they adopted for their experiments:

- (1) Normal testing technique: The application of a series of impulses of increasing magnitude until breakdown occurs.

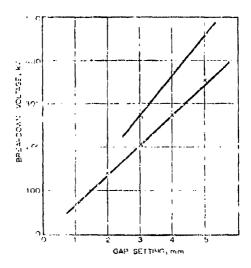
 (12)
 Harrison has suggested that the assigned impulse strength under this testing procedure is optimistic.
- (2) The Sorenson technique: First impulse is greater than required for breakdown. Successive pulses are reduced and the last breakdown level is recorded. This is shown to reveal lower breakdown strengths for the medium than would the normal testing technique.
- (3) The first impulse technique: Similar to normal technique, except that the value of the first impulse of each successive series is progressively increased and the first breakdown on the first pulse of a series is recorded. This technique yields comparable results to the Sorenson technique.

The relative results of normal and first impulse testing, using 6.25 cm diameter electrodes with 2.5 mm gap, are shown in Table 5.13 and a plot of B/D voltage against gap setting is shown in Figure 5.27. It is seen that the first impulse technique yields $\sim\!25\%$ lower breakdown levels than the normal technique.

The phenomenon of "conditioning" is discussed and a serious question is raised--should the initially low breakdown data be rejected? Since operating high power systems cannot normally be "conditioned" the inference is that the "preconditioned" data may be of prime importance. Figure 5.23 illustrates the typical "conditioning" effect obtained by Hancox

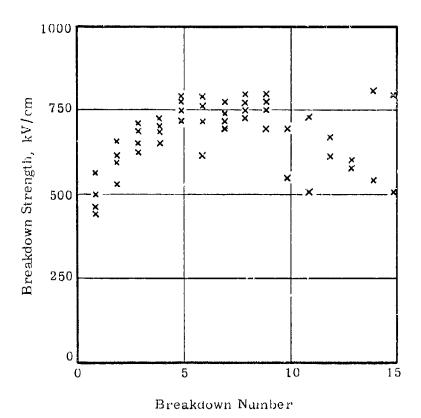
Table 5.13 Dependence of electric strength on testing technique.

N.	mont fiste.	In timmeter
	e od marc	α by $a \phi$
Mean break in strength, kV/cm	5()t)	60.00
Maximum brea down strength, kV/cm		710
Minimur . Fr akdown strength kV/cm	(1(1 ₁)	4-(/()
Coefficient (variation,)	14	



Brass electrodes, 6.25 cm diameter. oo Normal testing technique. xx First impulse technique.

Figure 5.27 Variation of breakdown voltage with gap setting.



Brass electrodes, 6.25 cm diameter, 2.5 mm gap.

Figure 5.28 The conditioning effect.

and Tropper. It can be assumed, unless there are statements to the contrary, that the breakdown data provided by the great majority of workers have been obtained after the "conditioning" process.

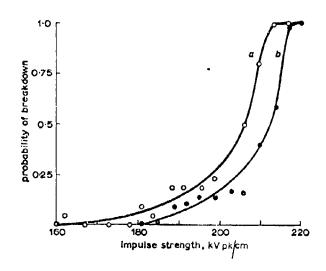
These workers note the existence of an electrode "area effect" and no "volume effect". The strengths corresponding to electrode diameters of 6.25 cm, 2.5 cm, and 13 mm were 75.0 kV/mm, 99.0 kV/mm and 145.0 kV/mm for the 1/50 µ sec impulse.

Nelson et al., in the impulse testing section of their tests, (8) the ac part of which has already been treated, have followed the work of Hancox and Tropper in providing an estimate of the probability of breakdown on application of the first impulse. The results are summarized in Figure 5.29 in comparison with transformed data from the normal technique. The value of the work by Nelson et al. is that it provides a direct comparison of power frequency and $1/50~\mu$ sec impulse data taken from the same test bed. The areas are orders of magnitude greater than for Hancox and all tests were carried out with gas-saturated oil, a condition most likely to prevail in practice.

The results confirm the work of Endicott and Weber in that the "area effect" is found to be the same order for impulse as for power frequency. Table 5.14 gives the relative performances of 50 cycle and $1/50~\mu$ sec impulse voltages for varying electrode areas and gap spacings and Figure 5.30, the relative performances as a function of stressed volume.

In the discussion it is noted that movement of the dielectric has no influence upon the pulsed strength of the liquid and it is suggested that other thermal and mechanical processes which influence 50 cycle performance are still influential in the $1/50~\mu$ sec time scale, resulting in comparable size effects and relatively low impulse ratios of 1.5-1.8. In summary, it is suggested that contamination in the form of gas bubbles and solid particles is a controlling factor.

In the pulse duration range useful to industrial testing there is a body of work which has been performed for the $USAF^{(14)}$ weapons simulation



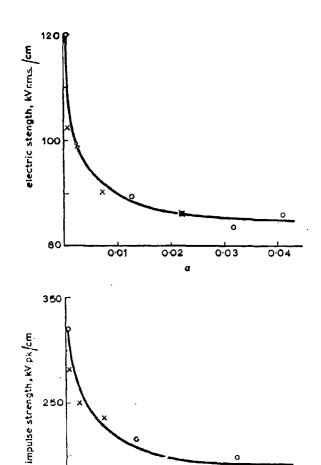
a Direct experiment b T

b. Transformed date of normal testing technique

Figure 5.29 Ogive curves for first-impulse testing technique.

Table 5.14 Electrode gap and area effects for power-frequency and surge voltages.

		İ	Power frequency				1/50 ps impulse			
Area .	Gap	Voltage	I lectric strength	Standard error	Standard deviation	Voltage	l lectric strength	Standard error	Standard deviation	
m²	mm	kVr.m.s.	kV/mm	kV/mm	kV/mm	kVr.m.s.	k V/mm	k\/mm	kV/mm	
1 - 885	21.9	195	8.6	0.18	1.3	410	18 · 7	0.52	3 · 66	
1 - 885	16.9	141	8 · 4	0.15	1.26	342	20 - 2	0.38	3 - 32	
1.885	11.7	100	8.6	0.23	1:13	220	18.9	0.65	2.05	
1 · 885	6.8	61	8.9	0.11	0.78	148	21 · 7	0.42	2.96	
0.631	11.5	104	9.0	0.22	1 - 54	270	23 · 6	0.49	3 - 45	
0 - 211	11.3	112	9.9	0.17	1.48	280	24.9	0.51	4.46	
0.070	10.9	112	10.3	0.16	1.11	304	28.0	0.63	4.48	
0.070	6.0	72	12.0	0.13	1 · 2	192	32-0	0.58	4.52	





150

Figure 5.30 Volume effects.

0-01 0-02 0-03 stressed volume, m³

0.04

program. The work is interesting since it represents an extension of technique and data analysis used in those Government programs which are mainly concerned with the short pulse performance ($\leq 1.0~\mu sec$) of energy stores. As such, it forms a bridge between the technology of this section and the one which follows on pulsed stresses in low duty cycle equipment.

In this program the strength of oil was investigated using parallel plane electrodes, both coated and uncoated, of areas in the range 600 cm 2 -3600 cm 2 , with applied exponential pulses having e-fold times in the range 60-130 μ sec. The electrode coatings were acrylic or epoxy; the bare electrodes aluminum.

The intent of the program was to find the dependency of the mean breakdown field strength (\overline{f}) upon electrode area and pulse length. (\overline{f}) was defined as the field intensity at which 50% of the tests caused breakdown. In general, the following relationship was found:

$$f_{\tau}^{0.0041}\sqrt{A} = K$$
 (6)

where

τ is the e-fold time in microseconds

 Λ is electrode area in cm²

 $\frac{1}{f}$ is kV/cm

K is an arbitrary constant

The results of these experiments are shown in Figure 5.31 for bare electrode area relationship at a fixed pulse duration and in Figure 5.32 for the time dependence for coated and bare electrodes with several areas.

It has been the general experience that little long-termed advantage is to be gained by the coating of electrodes; although the idea has not been rejected and techniques by no means exhausted.

In side experiments it was found that within the temperature range of 60-105° F, no perceptable change in f took place. Generally, the oil is stated to be "clean" and typically, for this field interest, one can assume that the oil was given little treatment.

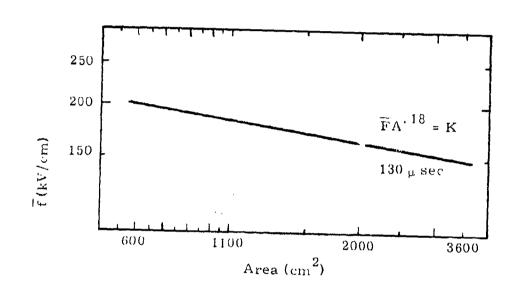


Figure 5.31 Plate area versus mean breakdown field strength.

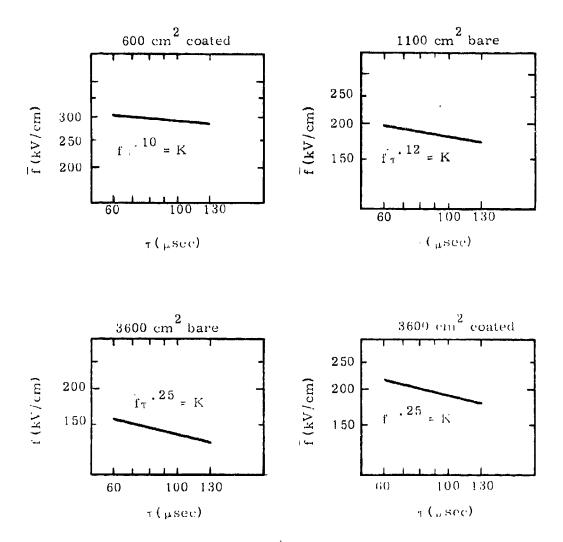


Figure 5.32 Fulse length versus mean breakdown field strength.

5. 4. 2 Impulsive Stresses--Low Duty Cycle Equipment

Government-sponsored programs have provided the major part of the design information treated in this section. Contributions have been made by service laboratories, university groups and private industry in the USA, sometimes in joint action with UK agencies. The prime interest is in the insulation properties of liquids under pulsed stresses of a few microseconds and less. Such conditions exist for the transient storage of energy within the electric field between electrodes of various areas and geometries.

There are significant differences in equipment requirements and dielectric behavior which distinguish this technology from power frequency technology and the like.

(1) System duty cycles are low--typically a few applied stresses per minute.

4 4

- (2) Equipment lifetime is often measured in thousands of "shots"-or the acceptable mean-time-to-failure may be of that order
 or less.
- (3) Dielectric behavior is almost independent of solid contamination levels.
- (4) The effective stress-time to breakdown is strongly influenced by interelectrode streamer velocities under conditions where the propagation time for these breakdown streamers is of the same order as the pulsed stress duration.

Whereas for prolonged stressing claims could be made that the performances of all liquids are similar, for this short impulsive mode all liquids do not perform equally and the search for a liquid with a high value of ε combined with superior dielectric strength is valid.

Much of the material presented for impulsive stresses is low duty cycle equipment essentially divided into two parts:

- (1) The work of J. C. Martin and his team at AWRE, Aldermaston, England, in which simple voltage generators and electrode structures have been used to provide the maximum of design data and relationships which can be economically obtained in a laboratory environment.
- (2) Large electrode area work carried out in US facilities which was associated with the design phases of large pulse power systems. This work can be regarded as a verification of the AWRE work. Certainly the treatment of the data is the same.

5.4.2.1 AWRE Techniques and Programs

Before presenting the AWRE work some background information is necessary to a balanced understanding of its broad scope.

The limited objective at AWRE was to provide design data for pulsed generators, with particular emphasis on the efficient storage of energy within these generators.

The keys to successful accomplishment of these goals lay in the provision of easy-to-operate, small pulse generators and cheap, quick methods of manufacturing useful test electrode shapes. These permitted rapid experiments in liquid dielectrics at significant voltages and with relatively large spacings which, combined with the inherent scatter in liquid breakdown results (typically $\sim 10\%$), produced useful results without the significant costs of formally engineered test systems.

For the early experiments, charging generators of the pulse transformer type were used. These worked in the voltage range of 1.0-3.0 MV, handling energies of ~1 kJ. Marx generators were used to study the larger volumes of liquid with energies to 50 kJ. The 1-Cos type waveform generally used was considered to be a fair representative of the stress conditions for most practical pulse charged systems.

The test electrodes, which are often expensive and difficult items for a dielectrics program, were, in some cases, simply fabricated by forming copper sheet over wood forms. The advantage of this construction was that the copper was driven into the wood at a discharge site to form a smooth profiled pit. This allowed the electrodes to be used for many discharges before recovering was necessary. This pragmatic approach to electrode construction was typical of the procedures used.

An experimental advantage to using large electrode spacings was that simple optics could be used to study the breakdown processes. Open shutter photography was often used in conjunction with a voltage clipping point-plane gap so that time-resolved information on the growth of the breakdown streamers, or bushes, could be obtained.

As a result of these techniques, AWRE formed an early conviction of the possibility of a breakdown model based on a streamer mechanism; at least in the time scale of 0.1-1.0 µsecs. The observations made, although not published, were used internally to guide experiments and to provide estimates of breakdown conditions where experiments were not possible.

It is tentatively suggested by this group that breakdown initiates on very small whiskers on the metal electrode surfaces--accounting for the inherent scatter of liquid breakdown data and the small influence of the macroscopic finish of the electrodes. With an applied field these field enhanced surfaces emit current and heat the liquid locally. Of the possible consequences, it is favored that the temperature rise reduces the surface tension to a low enough value for a bubble to form. This micro-bubble then elongates in the electric field from its initial dimension of 10^{-5} - 10^{-4} cm to 10^{-3} - 10^{-2} cm length in highly ellipsoidal form. At this length a streamer can propagate from the pointed tip of the bubble which contains ionized gas. The streamer then moves with a velocity which is characteristic of the medium and the applied voltage. For typical breakdown fields, it has been estimated that the electrostatic pressures causing the elongation of the bubble were about 30-100 atmospheres and that the elongation could be damped by a liquid viscosity

in the order of a megapoise. This notion was verified experimentally by reducing the temperature of various liquids until this viscosity range was obtained. A dramatic increase of dielectric strength was obtained with a significant decrease in the time-dependence of breakdown.

It is concluded that the difference between liquids and solids as dielectric media is a viscosity of about a megapoise. It is claimed that this model can account for a pressure effect, since an applied pressure, of the order of the electrostatic pressure at the whisker tip, can inhibit the hydrodynamic phase.

Three methods are suggested for improving the dielectric strength of a liquid by inhibiting the hydrodynamic phase:

- (1) A high viscosity layer (coating or cooling).
- (2) External pressure.
- (3) Reducing the largest whiskers by conditioning.

With respect to the latter, it is thought that the area and time dependencies of breakdown can be drastically reduced; the standard deviations of breakdown data reducing from the normal $\sim 10\%$ to $\sim 2\%$.

5.4.2.2 Streamer Propagation and Time Dependence

Much of the initial work which lead to the tentative theories, described in the previous subsection, was performed by Herbert. (15) This work was concerned with obtaining integral relationships for the mean streamer velocities in several common liquids as functions of the applied voltage and, in some cases, time of the applied voltage. Herbert used needle-to-ball electrode geometries, so that the streamers would be initiated very early in the applied waveform, and generators which could apply square type pulses as well as the 1-Cos type waveform. Applied voltages were in the megavolt range and pulse durations $\sim 0.5~\mu sec$ and $\sim 50~nsec$. An analysis of his results with coefficients of correlation are given in Table 5.15. He noted that

Table 5.15 Streamer velocities.

Oil, positive	$\overline{v} = (90 \pm 12) V^{1.75 \pm 0.12}$
Oil, negative	$\ddot{v} = (31 \pm 5.5) \text{ V}^{1.28 \pm 0.15}$
Carbon tetrachloride, positive	$\bar{v} = (168 \pm 28) v^{1.63 \pm 0.15}$
Carbon tetrachloride, negative	$\hat{\mathbf{v}} = (166 \pm 29) \mathbf{v}^{1.71 \pm 0.19}$
Glycerine, positive	$v = (41 + 1.5) V^{0.55 + 0.03}$
Glycerine, negative	$\tilde{v} = (51 + 8) V^{1.25 + 0.13}$
Water, positive	$vt^{1/2} = (8.8 \pm 0.4) V^{0.6 \pm 0.03}$
Water, negative	$vt^{1/3} = (16 \pm 0.25) V^{1.09 \pm 0.02}$

- v is measured in cm/microseconds
- V is measured in megavolts
- t is measured in microseconds

the mean velocities were proportional to the applied voltage and not to stress at the electrodes. It is suggested by the first three results that:

$$\overline{V} = \frac{d}{t_{eff}} \quad \alpha \quad V^{n} \tag{7}$$

where \overline{v} = mean velocity, cm/ μ sec

d = gap spacing, cm

V = applied voltage in MV

t_{eff} = effective stress time

and n lies between 1.2 and 1.8

The effective stress time depends upon the value assigned to n. For a square voltage pulse, the effective time, $t_{\rm eff}$, is obviously the time of the whole pulse to breakdown. For pulses other than square, $t_{\rm eff}$ is not obvious—in practice it is some function akin to 1-Cos for which we must define $t_{\rm eff}$.

Let the applied voltage be a ramp function, which is reasonably close to 1-Cos.

$$\frac{\mathrm{dx}}{\mathrm{dt}} = A V^{\mathrm{n}} \tag{8}$$

$$\frac{d}{t_{eff}} = \Lambda V_{max}^{h} \tag{9}$$

$$V = kt$$
 (as defined) (10)

$$d = Ak^n \int_0^t t^n dt$$
 (11)

$$G = A \frac{k^n}{n+1} \cdot \lim_{m \to \infty} (12)$$

$$d = \frac{t_{\text{max}}}{n+1} \Lambda V_{\text{max}}^{n}$$
 (13)

$$t_{\text{eff}} = \frac{t_{\text{max}}}{n+1} \tag{14}$$

If n = 1.5 (within the suggested range 1.2-1.8), then term = 0.4 term or, for a ramp, measured from 60% of $V_{\rm max}$ to $V_{\rm max}$.

Herbert's definition of teff is the time of 63% $V_{\rm max}$ to breakdown. This definition of teff stems from the original AWRE estimates of a t $^{2/3}$ time dependence for n = 1.5;

$$\frac{d}{t_{eff}} \propto V^{3/2} \tag{15}$$

$$V_{t} \frac{2/3}{eff} \sim d^{2/3}$$
 (16)

$$F t_{\text{eff}}^{2/3} \propto d^{-1/3} \tag{17}$$

where F is the stress, MV/cm.

The data from later experiments using larger electrode geometries showed that a much better fit could be obtained by a power law of t $^{1/3}$.

For n = 3;

$$V + \frac{1/3}{\text{eff}} = \omega \cdot d^{1/3} \tag{18}$$

$$F_t^{1/3} \propto d^{-2/3}$$
 (19)

For this, $t_{\rm eff}$ = 0.25 $t_{\rm max}$, or $t_{\rm eff}$ should be measured from $\sim 75\%~V_{\rm max}$ to breakdown.

It was recognized that, from experimental evidence, $t_{\rm eff}$ should be taken at the ~75% level and not from 63%, as originally defined. However, it was less confusing to accept the latter since only a 10% change of predicted breakdown level was involved for times in the range 0.1-1.0 μ sec. Crewson supports the validity of this judgment in a very thorough examination of Martin's definition of the "effective stress time".

The apparent electrode spacing dependence (d) should not be weighted with too much significance at this point for subsequent experiments show a rather weak relationship.

It can be appreciated that Herbert's experiments contributed much to a general understanding of the subject and to the derivation of subsequently well-used relationships for stress and time.

Plots of mean streamer velocities against applied voltage are shown for several liquids in Figures 5.33, 5.34 and 5.35. It will be noted that, in general, there are distinct polarity effects, that is, the velocities for the positive streamer (the streamer initiating from the +ve electrode) and the negative streamer (the streamer initiating from the -ve electrode) are not equal. For the particular case of water, the positive streamer is faster than the negative.

5.4.2.3 Figures of Merit for Various Liquids

As previously stated, the ability to store electrical energy between electrodes at the highest densities is a major interest in this time regime. This implies that liquids of high dielectric constant (ϵ) and high dielectric strength are interesting candidates. In a series of experimental programs which were closely directed to the development of the energy

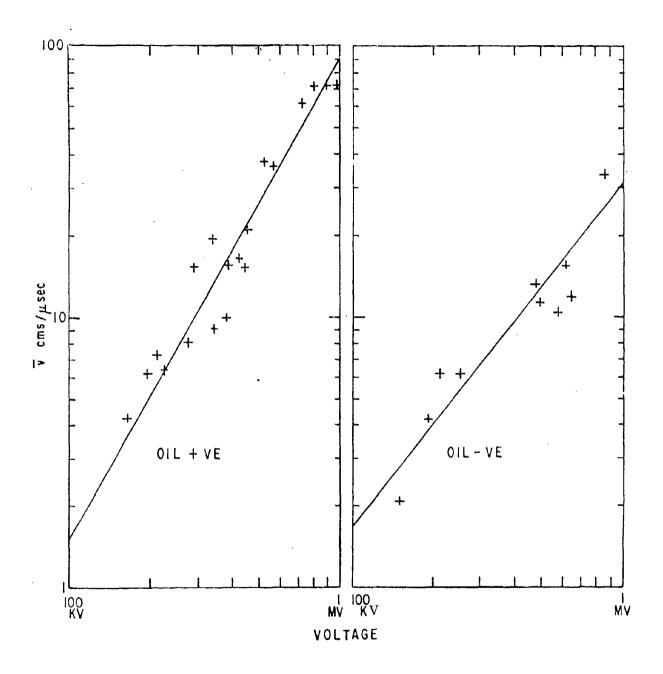


Figure 5.33 Oil streamer velocities.

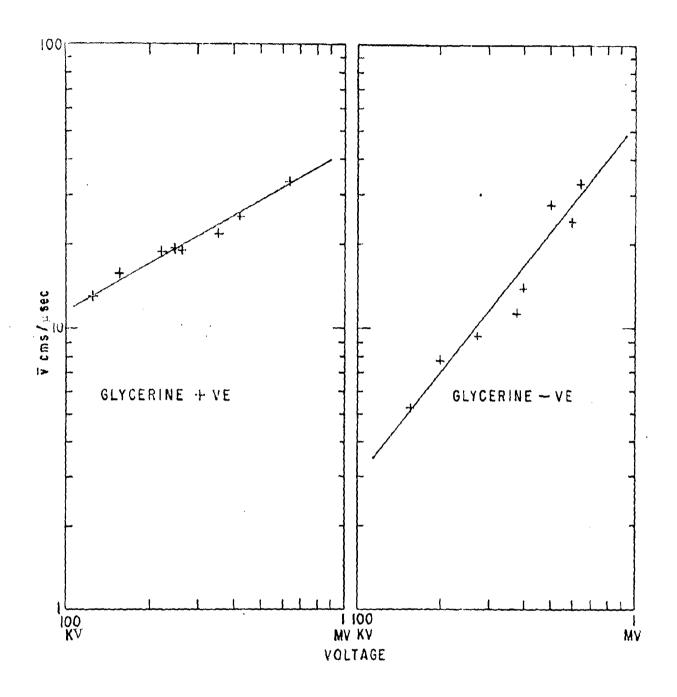


Figure 5.34 Glycerine streamer velocities.

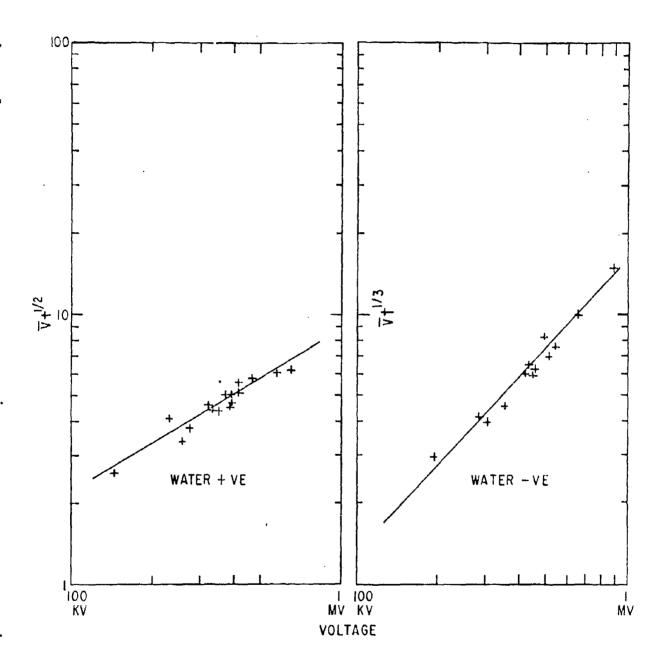


Figure 5.35 Water streamer velocities.

Stores for pulse power systems, J.C. Martin and his co-workers at AWRE, Aldermaston, England, provided much of the basic data and many of the relationships which are currently used in this field. The development programs associated with large US projects have confirmed and augmented Martin's work.

In an exploratory phase, Martin (17) assigned figures of merit to a selected number of liquids for energy storage applications. These figures were assigned via breakdown tests performed under a common set of conditions.

The relation to which the breakdown voltages were fitted was:

$$F^{3/2} t = K \tag{20}$$

where F = the breakdown stress in MV/cm

t = the effective stress time or time of the pulse above 63% of peak amplitude

K = a constant

The figure of merit tabulated was ϵ K^{4/3}, which is proportional to the energy stored per cc at breakdown stress for a constant charging time.

Table 5.16 gives the listing of these figures of merit, from which one can appreciate the potential importance of water and other high dielectric constant liquids.

5.4.2.4 AWRE Data and Stress Relationships

The liquids which are operationally and economically acceptable are not numerous. The Aldermaston team have provided data for low ϵ , oil; medium ϵ , Ethylene Glycol and high ϵ , deionized water.

(1) Transformer oil: Smith (18) of AWRE has reported breakdown data for unprocessed transformer oil. The experiments

Table 5.16 Figures of merit.

Values of
$$F^{3/2}$$
 $t_{eff} = k$

Area of plates : 16 square inches The dielectric constant, taken from standard tables, not measured. 111

Material	k	٤	ε k ^{4/3}
Ethyl Alcohol	.057	24)	
" + 1% water	.059	24.6)	0.56
" + 10% water	.052	29.6)	
Methyl Alcohol	.052	33	0.65
Ethylene Glycol	.03	38	0.34
Glycerine	.010	44	0.10
Castor Oil	.11	4.7	0.25
Transformer Oil	.08	2.4	0.09
Water	.03	80	0.72

Note: Values of k are good to perhaps 10 to 15%.

were carried out for a wide range of electrode areas, with uniform and nonuniform fields and with fast and relatively slow pulse generators. The data are fitted to two relationships:

$$Ft^{1/2}d^{-1/4} = k (21)$$

where

 \boldsymbol{F} and \boldsymbol{t} are as previously defined.

d is electrode spacing in cm.

and

$$Ft^{1/3} = k \tag{22}$$

k is an area dependent constant in both cases.

Figure 5.36 gives these plots against area, the full lines are based on all uniform field experiments and the broken lines on fast pulse data only. On the whole the ${\rm Ft}^{1/3}$ fit is preferred and there is speculation that the d dependence might be as low as ${\rm d}^{1/6}$.

(2) Ethylene glycol: Smith (19) has tested this medium, although much less extensively than transformer oil. On the basis of sparse data the assumption is:

$$Ft^{1/3} = k \tag{23}$$

The negative assymetric field data is noted to have a higher value of k and to show little area effect. Figure 5.37 shows a plot of the results.

(3) Deionized water: Because of the high figure of merit assigned to water as an energy storage medium, the work done with this medium has been extensive and international. Smith (20)

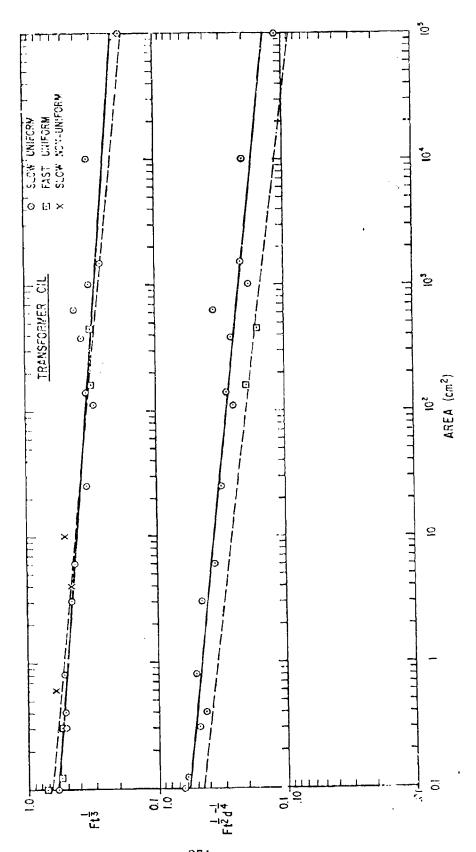


Figure 5.36 The effect of electrode area upon the impulsive breakdown strength of transformer oil.

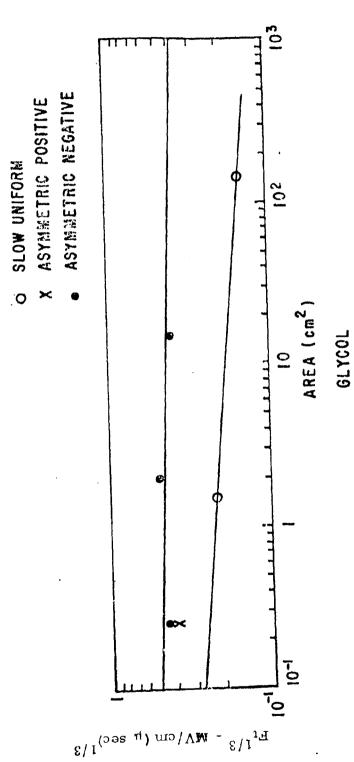


Figure 5.37 The effect of electrode area upon the impulsive breakdown strength of ethylene glycol.

1,1

has again contributed substantially with experiments in this medium. Experiments were carried out for a wide range of electrode areas and effective stress times. In the discussion of the data. Smith concludes that $Ft^{1/3} = k$ is a reasonable approximation and notes the strong polarity effect exhibited by water under asymmetrical field conditions: the negative electrode giving approximately twice the value for constant k. The point is made that the relationships obtained in Herbert's work with point-point and point-to-plane gaps should apply in some form to the plane-plane gaps. It is recognized that the breakdown is associated with the establishment of a streamer-initiating, threshold field and the velocities of these streamers when moving between the electrodes under an applied voltage. Smith makes estimates of this threshold field for various electrode geometries. (see Figure 5.38), and concludes that for long gaps with high voltages the streamer transit time must be dominant over the initial bubble formative time and that it is under these conditions that water becomes outstandingly attractive for energy storage. The relationships for uniform field and negative asymmetrical field are plotted against area in Figure 5.39. Thus

$$Ft^{1/3} = constant-uniform field$$
 (24)

and
$$\frac{Ft^{1/3}}{T}$$
 = constant--negative, asymmetrical field (25)

where α is a measure of the asymmetry = 1 + 0.12(F /F max/F mean -1)^{1/2}

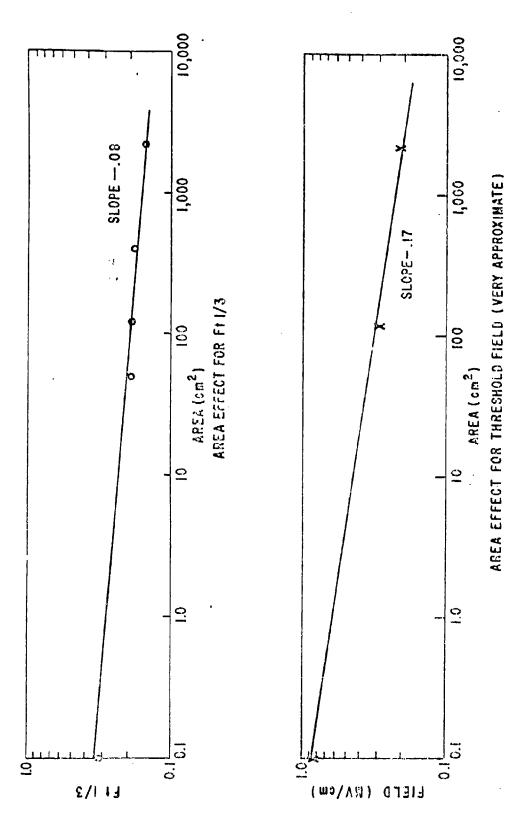


Figure 5,38 Area effect for deionized water.

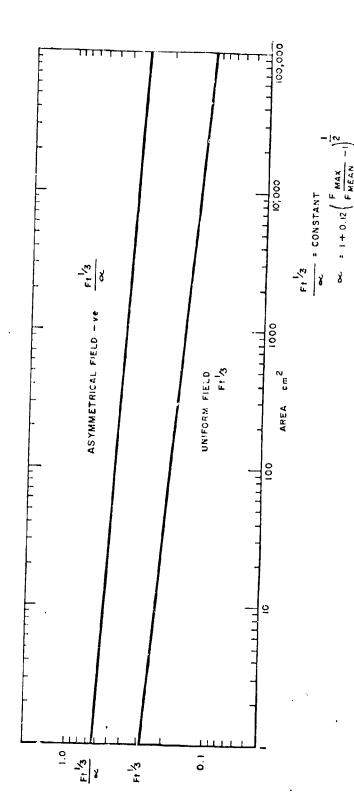


Figure 5.39 Impulse Breakdown of Deionized Water

Smith notes that data obtained by USSR workers (22) for small areas and gaps is in essential agreement (Figure 5.40), and he also observes (19) that the higher values shown for the smaller length gaps confirm AWRE experience for liquids other than water.

5.4.2.5 Summary of AWRE Programs

Martin (23) summarizes the outcomes of AWRE liquid dielectric programs in his overview of nanosecond pulse techniques.

Generally, any finish less than gross roughness of electrode surfaces is unimportant; solid impurities and additives to the liquid media have little effect upon pulse breakdown, in submicrosecond times.

For uniform fields the breakdown field is approximated by:

$$Ft^{1/3} \Lambda^{1/10} = k \tag{26}$$

where F is in MV/cm, t in μ see, and A is the electrode area in square centimeters.

The values of k for the various liquids are given as:

Transformer oil	k = 0.5
Water - Uniform field	k = 0.3
Negative asym. field	k = 0.6
Methyl and ethyl alcohols	k = 0.5
Glycerine	k = 0.7
Castor oil	k = 0.7

For point or edge-plane conditions mean streamer velocities are given for voltages $10^5 \text{--} 10^6 \text{ V}$ by:

$$\overline{\mathbf{v}} = \mathbf{d}/\mathbf{t} = \mathbf{k}\mathbf{V} \tag{27}$$

Experimental Conditions

t psec .25 .5 1.0 2.0 .25 .5 1.0 2.0 .25 .5 1.0 2.0 .25 .5 1.0 2.0 F MV/cm 1.7 1.3 .7 .5 1.6 1.0 .9 .8 1.6 1.3 1.1 1.0 2.3 2.0 1..5 1.3 A (cm²).01 .002 .001 .0006

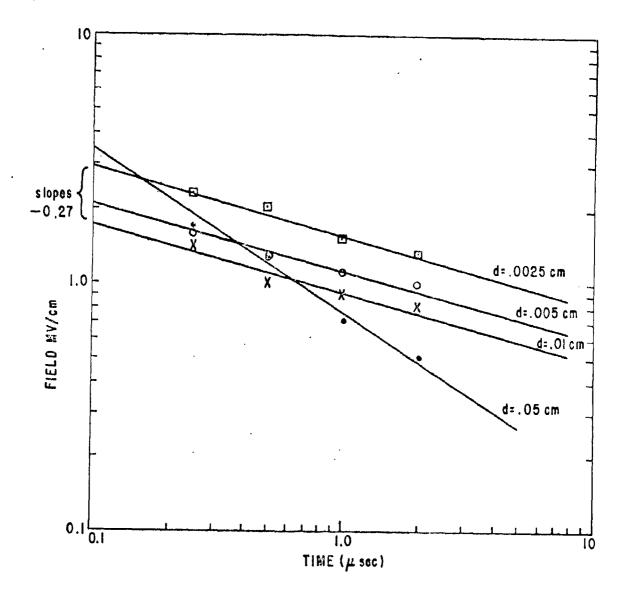


Figure 5.40 Russian data for small ball gaps.

where visin cm per usec, Visin MV

Table 5.17 gives values of k and n for three liquids. Velocities for water are as given by Herbert (Table 5.15).

An additional relationship is given for oil, in both polarities, for the 1 MV-5 MV region:

$$\frac{1}{v_{+}} d^{1/4} = 80 V^{1/6}$$
 (28)

5.4.2.6 US Experimental Data for Large Areas

Although the work of Martin et al. has provided most useful relationships for the engineering applications of liquid dielectrics under single pulse mode, very extensive support for dielectric programs has been provided by US Government agencies and laboratories. In particular, the Defense Nuclear Agency, the Air Force Weapons Laboratory and the Naval Research Laboratory have sponsored or carried out significant programs.

In the development program for a large pulsed system sponsored by DNA, some of the aims were stated as follows:

- (1) To investigate the time dependence of breakdown in oil.
- (2) To establish the effect of oil contamination.
- (3) To establish the effect of electrode surface finish.
- (4) To establish the effects of temperature.
- (5) To investigate the effects of surface coatings.
- (6) To investigate surface flashover of oil-solid interfaces.

The experiments were carried out with relatively small scale planar electrodes of approximately 4 ${\rm ft}^2$ and large scale coaxial electrodes of 900 ${\rm ft}^2$ area.

At the outset of the report on this work, the meaning of teffective stress time, is discussed. Additionally, the importance of the

Table 5.17 Streamer velocities.

$$\overline{v} = d/t = kV^n$$

Where \overline{v} is in centimeters per microsecond and V is in MV. Values of k and n for transformer oil and two other liquids.

	k+	n+	k-	n-
oil	90	1.75	31	1.28
carbon tetrachloride	168	1.63	166	1.71
glycorine	41	0.55	51	1,25

dielectric testing method is stressed. In experiments where the risetime of the applied pulse is fixed, t can be varied by a factor of 3 or more by applying different levels from the pulse charger; the higher input will lead to more rapid breakdown. This point is illustrated in Figure 5.41. It is apparent that the general wave shape varies with level under these conditions.

A preference is expressed for a testing mode where the break-down is observed in the same "phase" of the pulse, independently of level. Thus the breakdowns will all be recorded at peak volts or 90% of peak volts. To accomplish this, at each testing level, compensating reactances must be placed between the generator and the energy store under test.

For the first tests reported, using planar, aluminum electrodes it is claimed that, by adopting the latter testing method, a smaller time dependence than $t^{1/3}$ was obtained. The results plotted in Figure 5.42 certainly show less than a third power dependence and it is claimed that Ft $^{1/6}$ or Ft $^{1/5}$ equal to a constant would be a better fit. On the other hand, similar test procedures using planar, steel electrodes yielded a much closer fit to Ft $^{1/3}$ equal to a constant; see Figure 5.43.

The results with planar electrodes in oil are summarized as follows:

"The time dependence of the breakdown strength of oil, in uniform fields, could not be uniquely described but was always 'weak'. Time dependence was less in clean oil, or conversely, the oil condition was more important for long pulses. The strongest time dependence observed was in proportion to the inverse cube root of time. Other results were more consistent with the inverse sixth root of time".

For the large, coaxial experiments, results for which are shown plotted in Figure 5.44, the experimenters' comments are as follows:

"The results fit an equation of the form Ftⁿ = C, where n was 1/3, or less, in all cases. The most proper test, in which the charging inductance is varied and comparison is made of breakdowns at the same 'phase' on the waveform, gave an exponent for t of 1/4 to 1/5. With fixed Marx

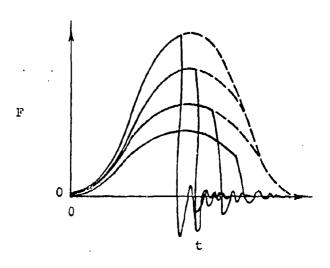


Figure 5.41 Variability of waveshape for constant risetime.

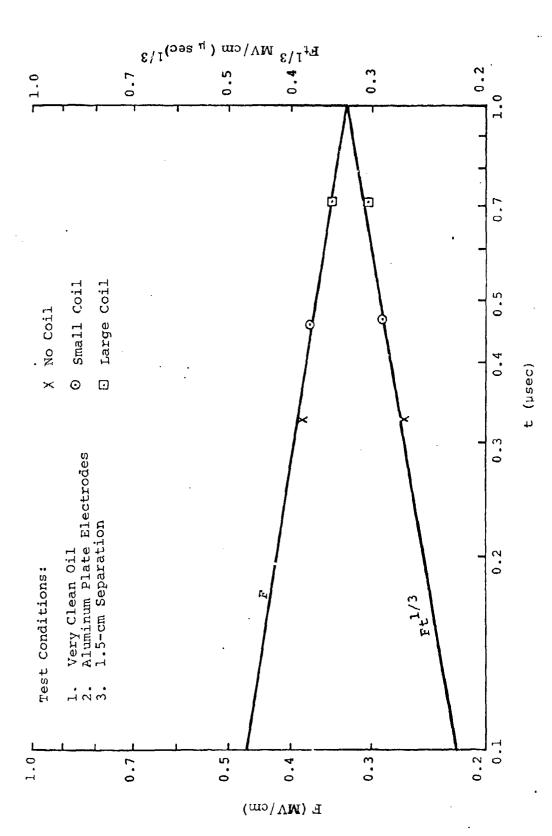


Figure 5.42 Breakdown strength of oil with aluminum electrodes constant breakdown phase.

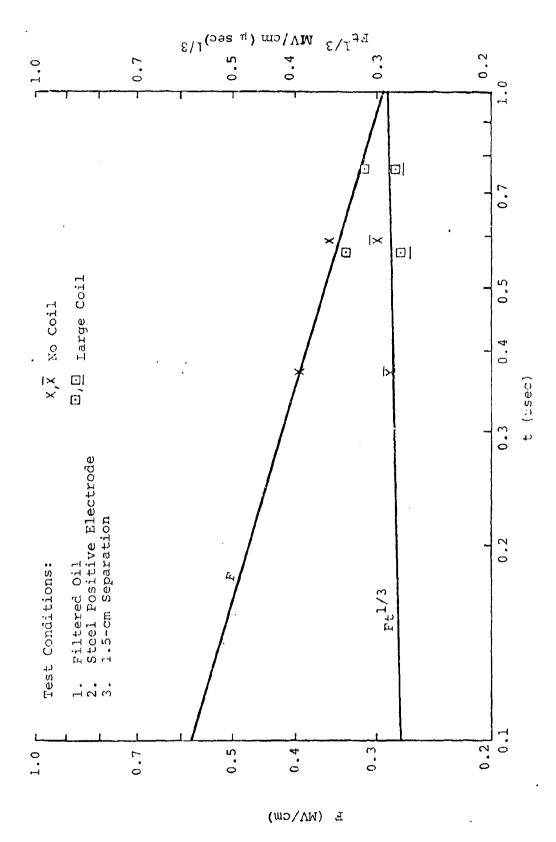
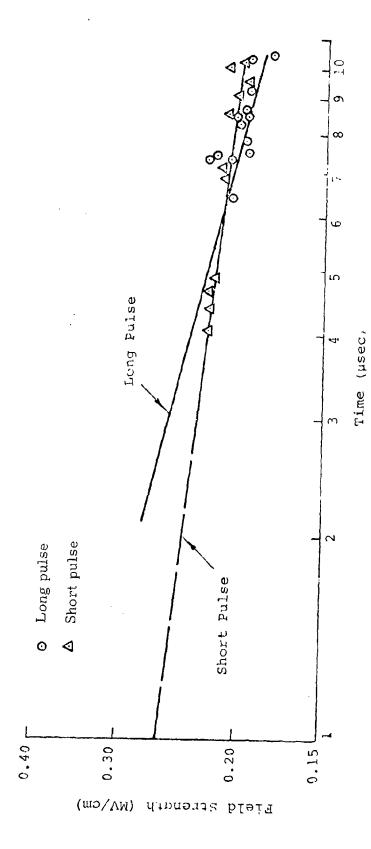


Figure 5.43 Breakdown strength of oil with a steel positive electrode.



The dependence of Lange and on creakdowr.

anductance (fixed risetime), the dependence on t $_{
m eff}$ for short charging time was similar. With long charging times, the exponent of t could vell have been as much as 1/3.

The designer should not be confused by the arguments on $\frac{1}{e^{44}}$ and testing methods. The testing methods adopted should always relate to the operating conditions of the pulse system under design. Further, it seems safe to adopt a $t^{1/3}$ dependence for design purposes, since the work of AWRE is reasonably confirmed for large electrode areas.

Side experiments in this testing series are summarized as follows:

- (1) Finish on electrode surfaces was not critical
- (2) A temperature variation of 15° C from ambient cut not effect results.
- (3) Effects of solid contaminants could only be detected unring the small scale experiments. This was attributed to the practical difficulties of processing range volumes or equid.
- (4) Plastic coating of the electrodes improved the value of the constant by 10-15%.

Major engineering applications of d ionized water as a nucled dielectric have been undertaken at the US Navar Research Laboratory. In a Final Electrical Design Report, (25) a comprehensive system d sign for accompanied water is presented based on Martin's relationships for time and area dependence. Refined relationships used are:

(1) For breakdown due to streamers from positive electrode

$$F_{(+)} t^{1/3} = 0.287 A^{-0.911}$$
 (29)

(2) For breakdown due to streamers from the negative et circle:

$$\frac{F_{(-)}^{-1/3}}{a} = 0.579 \text{ A}^{-.0911}$$
(30)

where

F, t and A are as previously defined

and

o is a field enhancement factor

where

$$_{\odot} = 1 \pm 0.12 \left(F_{\text{max}} / F_{\text{mean}} - 1 \right)^{1/2}$$

By the careful control of the maximum fields within machine electrode structures so that they were in accordance with values suggested by these relationships, satisfactory reliability was obtained.

5 4.2.7 Repetitive Pulsing

The foregoing has treated the street pulse strength of equal when the formation and propagation of streamers are determining factors. For repetitive pulsing, streamer growth must not be cumulative and herestore the assignable stress must be reconsidered.

There is not much guiding information for these conditions and it would seem to be a suitable topic for future programs. Ameen carried out experiments to 15 pps in various grades of oil. He carried out a preliminary selection of oils and oil treatments at a fixed repetition rate of 0.3 pps with near sinusoidal pulses at tell ~1.0 asec. These results are shown in Table 5.18. Tests were then carried out in the selected, treated oil, at increasing repetition rates. The results of these tests are shown in Figure 5.45. In the course of the tests degradation of the oil occurred and it was noted that there was a tendency for the alignment of carbon particles—as would happen for de and ac application.

Relatively small scale tests have been carried out with fluorocarbon liquids at 250 pps (27) -- a repetition rate of interest for radar. At this constant frequency, the effect of gap spacing was evaluated at one pulse duration (Figure 5.46); also at one gap spacing the pulse duration was varied to

Table 5.18 Breakdown voltage (V_B) for various transformer oils in different initial states.

V_{B62} = Breakdown Voltage of Gulf Transcrest 62

V_{B33} = Breakdown Voltage of Esso Univolt 33

VB42/46 = Breakdown Voltage of Esso Special Marcol 42/46

Initial State of Oil	V _{B62} (kV/cm)	V _{B33} (kV/cm)	V _{B42/46} (kV/cm)
Crude	370 + 20	43 0 ± 20	410 ± 20
Filtered	370 ± 20	430 ± 20	410 1 0
Pumped	595 ± 30	475 ± 25	500 + 35

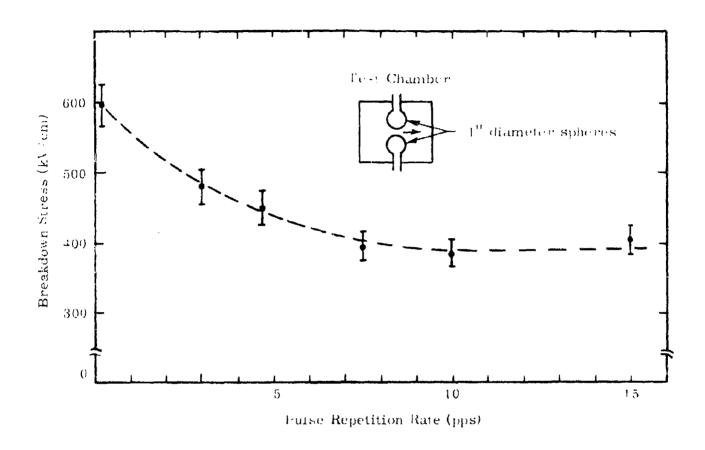
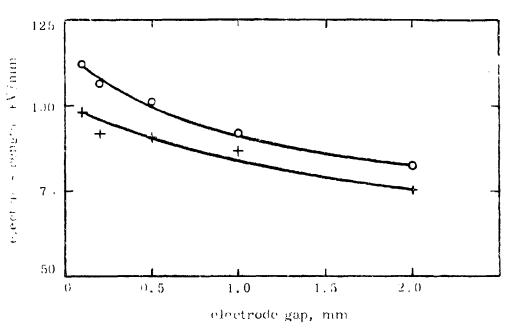


Figure 5, 45 Breakdown stress as a function of pulse repetition rate for Gulfcrest 62,



Variation in electric strength with electrode of rong

Fulse-top duration - 2.8% s Repetition frequency : 250 pulse/s Temperature = 20° C

- O PPT
- + 142

Figure 5.46. Strength of 4 rooms under repeative page.

15 see (Figure 5.47). Two fluorocarbon equids were tested, the type and characteristic for which are given in Tuble 5.19.

It is concluded that a reduction in electric strength of 25% sulted from a gap increase of 0.1-2.0 mm, or, as the pulse duration w s increased from 0.4-16 μ secs.

5.4.2.8 Liquid Performance Under Pressurization

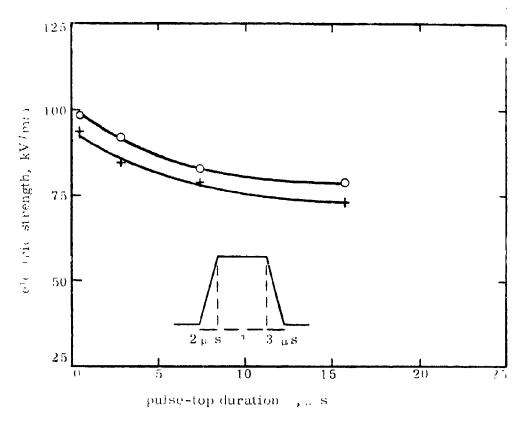
It is evident that workers in the USSR have long accepted the advantages of pressurizing liquid dielectrics. (28) Publication of work cone at Eirmingham University, England, indicated that the electric strength of transformer oil (29) and pure hydrocarbon liquids are dependent upon hydrostatic pressure over the range 5 mm. Hg to 350 psig.

Stressing the significant advantages which may be gained in the transient storage of energy, USSR workers have made recent claims for supporting stresses of 700 kV/cm in deionized, pressurized water (31) for periods of 10-15 microseconds. In these experiments, water was pressurized to 150 atmospheres. For an assumed electrode area of ~1.0 cm², this is 3-4 times the stress which could be predicted for atmospheric water and, in terms of energy stored, an order of magnitude increase. It is enumed that pressurization of a liquid significantly affects the initiation and growth of breakdown streamers.

For pulses in the microsecond range, one can examine the results of Kao and McMath. These workers performed tests with oils, measuring time to breakdown and electric strength for different rates of applied stress over a pressure range of 0-200 psi. The experiments were conducted with spherical electrodes, 2.0 cm diameter, ~0.1 cm gap spacing and ancarty rising pulses. Their results for transformer oil are shown in Figure 5.48.

Using Martin's relationships, the data may be written $\hat{\tau}$

$$F_t^{1/3} = 1.0$$
 (one atmosphere pressurization) (30)



Variation in electric strength with pulse-top duration

Repetition frequency = 250 pulse/s Electrode spacing = 1 mm Temperature = 20° C O 1-P1 + PP2

Figure 5.47 Strength of Freons under repetitive purses.

Table 5.19 Physical properties of the freens.

Liquid type	PPI	PP2
Chemical formula Boiling point at latm, °C Densit at 21°C, kg/m³ Viscosity at 25°C, m²/s Molecular weight	C ₆ F ₁₄ 57 1·695 × 10 ³ 0·39 × 10 ⁻⁶ 338	27F ₁₄ 76 1.788 × 10 ³ 0.88 × 10 ⁶ 350

• Pressure 0 Psig X Pressure 200 Psig Electrodes - 2 cm SS Spheres; Gap 0.091 cm

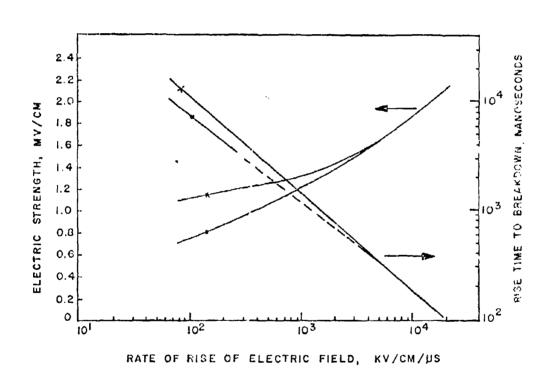


Figure 5.48 Pressure effect in oil.

Ft^{1/5} = 1.45 (14 atmospheres pressurization) (31) (using previous definitions of t and assumed stressed area $\sim 1.0 \text{ cm}^2$).

It can be seen that for t of 1 μ sec, there is a 50% increase in dielectric strength and for t of 10 μ sec, the gain is 2.

At this time the Air Force Weapons Laboratory is sponsore a further programs for pressurized liquids.

5.5 Theory of Breakdown

Although there is no uniquely accepted theory of preakdown of liquid dielectric media, there is a wide acceptance of an initiating field-on-hanced, or, field emission process. (11, 33, 34, 35, 36) Many workers have contributed in this search for a theory through investigations of concurrance currents and electron-ion mobilities (5) under various dielectric environmental conditions. Small volumes of pure liquids have been used to oppose to approach the intrinsic properties with a freedom from the mask of effects of contaminants.

Watson's work on the onset of thermal breakdown (3.0) extractions provides a convincing analysis of what he calls, the "New Thermal Model." It is claimed that high mean current densities exist in liquids at ficial close to breakdown. These currents originate at the tips of asperities on the lithrode surface due to the field emission process, providing energy injections which could lead to the vaporization of small volumes of the liquid in microsecond time durations. Local discharges within these low strength volumes of vapor could lead to breakdown in the interelectrode volume.

Through estimates of the space-charge-limited current from a point-plane approximation and the local field at a reasonable cathode radius, it is shown that adequate power can exist for local boiling of the liquid. The required power density of 5×10^8 waits/cm³ is claimed to be consistent with asperity radii of ~ 0.4 microns. The propagation of the breakdown from

these localized volumes of high power density is claimed to be via high velocity streaming of the liquid away from these cathode points. It has been shown that ion drag forces (37) can promote an efficient pumping process for these streamers. Streaming due to plasma effect (38) and heating have also been suggested to explain observed and calculated velocities in the range $10^3 - 10^4$ cm/second. If a streamer, or filament of vapor, has enough nergy to propagate across the gap, or a major portion of it, complete breakdown can be expected through the low strength vapor or heated liquid column.

It is observed by other workers that this model, or something similar to it, is consistent with the effects obtained by pressurization—a raising of the boiling point and pressurization of the vapor resulting in higher electric strengths for the liquid.

Workers in the USSR have observed these breakdown mechanisms and have shown growth processes using high speed photography which are consistent with the general contemporary understandings of liquid dielectric behavior.

SECTION 5

REFERENCES

- (1) Milek, J.T., "Heat Transfer and Cooling of Electronic Components and Equipment," (A Literature Guide), EPIC Interim Report No. 18-73, Air Force Materials Lab, AFSC, (September 1970).
- (2) National Electric Code, American Standards Association, Article 450, (1956).
- (3) Insulation Directory/Encyclopedia Issue, Sect. C-2, (June/July 1970).
- (4) Clark, Frank M., Insulating Materials for Design and Engineering Practice, J. Wiley & Son, (1962).
- (5) Milek, "Electron Mobility in Aliphatic Hydrocarbons as Related to Organic Insulation Breakdown" Hughes Aircraft Co., EPIC Report No. S-5, (February 1965).
- (6) Gumbel, Emil J., "Statistical Theory of Extreme Values and Some Practical Applications." National Bureau of Standards, Applied Mathematics Series 33, (1954).
- (7) Weber, K.H. and Endicott, H.S., 'Area Effect and Its Extremal Basis for the Electric Breakdown of Transformer Oil," Transactions of AIEE, (June 1956).
- (8) Nelson, J.K., Salvage, B. and Sharpley, W.A., "Electric Strength of Transformer Oil for Large Electrode Areas," Proc. IEE 118, (February 1971).
- (9) Nelson, J.K., "Statistical Effects of Environmental Factors on Liquid Breakdown Measurements," Proc. IEE 118, (November 1971).
- (10) Simo, E., "Large Scale Dielectric Test of Transformer Oil with Uniform Field Electrodes," IEEE Trans. on Electrical Insulation EI-5, (December 1970).
- (11) Hancox, R. and Tropper, H., "The Breakdown of Transformer Oil Under Impulse Voltages," Proc. IEE 105A, 250-258, (1958).
- (12) Discussion on "Surge Voltage Breakdown Characteristics for Electrical Gaps in Oil," Trans. Am. AIEE 59, 82, (1940).
- (13) Zein El Dine, M.E. and Tropper, H., "The Electric Strength of Transformer Oil," Proc. IEE 103C, 25, Monograph No. 1358, (June 1955).
- (14) SIEGE II Pulse Generator Report No. PIPR-180-10, to AFWL, Kirtland AFB, Under Contract F29601-69-C 0150, (November 1969).

- (15) Herbert, H.G., "Velocity of Propagation of High Voltage Streamers in Several Liquies," Dielectric Strength Notes, Note 10, AWRE, AFWL, (October 1966).
- (16) Crewson, Walter F., "Operating Theory of Point-Plane Spark Gaps," Switching Notes, Note 11, AFWL, (March 1971).
- (17) Martin, J.C., "Comparison of Breakdown Voltages for Various Liquids Under One Set of Conditions," Dielectric Strength Notes, Note 1, AWRE, AFWL, (November 1965).
- (18) Smith, I.D., "Breakdown of Transformer Oil," Dielectric Strength Notes, Note 12, AWRE, AFWL, (November 1966).
- (19) Smith, I.D., "Breakdown Strength of Ethylene Glycol," Dielectra Strength Notes, Note 9, AWRE, AFWL, (1966).
- (20) Smith, I.D., "Impulse Breakdown of Deionized Water" Die eetric Strength Notes, Note 4, (November 1965), Note 13, (November 1966), AWRE, AFWI.
- (2) Champney, P.D.A., "Impulse Breakdown of Deionized Water with Asymmetrical Fields," Dielectric Strength Notes, Note 7, WRF, Al Wi., (October 1966).
- (22) Rudenko, N.S. and Tsvetkov, V.I., "Study of Pulse Electrical Strength of Some Liquids," Sov. Phys. -Tech. Phys. 9, 837, (December 1964).
- (23) Martin, J. C., "Nanosecond Pulse Techniques," Circuit and Electromagnetic System Design Notes, Note 4, AFWL, (April 1970).
- (24) Design Review III, Design, Development of the Aurora Facility, Under Contract DASA (now DNA) 01-68-C-0175, Defense Nuclear Agence, Washington, D. C. 20505, (July 1969).
- (25) Final Electrical Design Report of the Gamble II Pulse Generator NRL Memorandum Report 2212, Naval Research Laboratory, Washington, D.C., (March 1971).
- (26) Ameen, D.L., "Impulse Breakdown Studies on Liquid Dimeetrics of High Repetition Rates," Ion Physics Corporation, Burlington, Mass., Internal Report No. 808-TR-340, (1968).
- (27) Whalley, G. W. and Salvage, B., "Electric Strength of Fluorocarbon Liquids Under Repetitive Pulse Voltages," IEE Electronics Letters 5, No. 19, (September 1969).
- (28) Vorobyev, A., Vorobyev, G.A. et al., "High Voltage Testing Equipment and Measurements," Technical Documents Liaison Office, MCL 1265/142, English Translation, (July 1962)

- (29) Watson, P.K. and Higham, J.B., "Electric Breakdown of Transform of Oil," Proc. IEE, Part 3A, 100, 168-174, (1953).
- (30) Kao, K.C. and Higham, J.B., "The Effects of Hydrostatic Pressure, Temperature and Voltage Duration on the Electric Strengths of Hydrocarbon Liquids," J. Electrochem. Soc. 108, 522-528, (1961).
- (31) Alkimov, A.P. et al., "The Development of Electrical Discharge in Water," Soviet Physics, Doklady 15, No. 10, (April 1971).
- (32) Kao, K.C. and McMath, J.P., "Time Dependent Pressure Effect in Liquid Dielectrics," IEEE Transactions on Electrical Insulation, EI-5, No. 3, (September 1970).
- (33) Watson, P. K., "High Field Conduction and the Onset of Thermal Breakdown in Liquid Dielectrics," Electrical Insulation Conference, 1965, National Academy of Sciences, NRC, p. 39, (1966).
- (34) Sharbaugh, A.H. and Devins, J.C., "Electrical Breakdown in Solids and Liquids," Electro-Technology, (October 1961).
- (35) Kao, K.C., "Electric Conduction and Breakdown in Laund Dielectrics," Electrical Insulation Conference, 1965, NRC, p. 44, (1966).
- (36) Sletten, A. M. and Lewis, T. J., "Influence of Dissorved Gases on the Electric Strength of N-Hexane," Brit. J. Appl. Phys. 14, 883, (1963).
- (37) Stuetzer, O.M., J. Appl. Phys. <u>30</u>, 984, (1959)
- (38) Chadband, W.G. and Wright, G.T., Brit. J. Appl. Phys. 16, 305, (1965).
- (39) Ushakov, V. Ya., "Development of a Discharge in a Liquid Dielectric with Ramp Function Voltage Pulses," Soviet Physics-Technica: Physics 10, No. 10, (April 1966).
- (40) Ryabchikov, S. Ya. et al., "The Effects of High Voltage Pulsed Discharges on the Dielectric Strength of Liquids," Translation from Elektronnaya Obrabotka Materialor, No. 5 (29), pp. 58-62, (September-October 1969).
- (41) Abramyan, Ye. A. et al., "A Megavolt Energy Densifier." Sov. Phys. Dokiady 16, 983, (May 1972).

SECTION 6

SOLID DIELECTRIC

6.1 Introduction

Solid insulation is expensive and not self-healing. At high voltage, a puncture failure is catastrophic. This partly explains why the electrical power industry makes use of air insulation for the bulk transmission of electrical power at high voltages. Underground cables (paper/oil or high pressure gas insulated) are used when other circumstances dictate the choice e.g. in cities. The designer normally attempts to keep the quantity of highly stressed solid insulation to a minimum by reducing the number of suspension points and increasing the length of the insulator string.

Where it is necessary to reduce the spacing between high- and low-voltage electrodes or conductors, the designer turns to high-vacuum, high-pressure gas, insulating liquids, solids, solid/high-pressure gas or solid/liquid insulation. Typical applications where this need arises include underground cable, high-voltage transformers, switch gear, capacitors, power supplies and pulse generators (particularly of the low inductance type). Even where vacuum, gas or liquid is the main insulant, solid dielectrics are required for supporting the high voltage structures. Flashover and tracking are then usually the important factors affecting clearances.

The theoretical electric strength of solid dielectrics, based on ionization and bond breakage, is very much higher than that of other media, and reported intrinsic strengths (measured under closely controlled conditions) fall in the range 2 to 20 MV/cm. Operating stresses, however, are usually one or two orders of magnitude lower than this (Table 6.1). In this respect, electrical insulation does not differ from materials used for their structural properties where the design stress is far removed from the mechanical intrinsic strength. In principle, the reason for both is the same -- the presence

Table 6.1 Typical working stresses in practice. (Whitehead(1))

Material	Crest Value of Working Stress
Paper impregnated withoil or compound at normal pressure	70 kV/cm ac
As above but at 200 psi	150-220 kV/cm ac
Capacitor paper, oil impregnated	$150-220~\mathrm{kV/cm}$ ac and de
Capacitor paper, wax impregnated	$100\text{-}200~\mathrm{kV/cm}$ ac and dc
Rubber, pvc	30-40 kV/cm ac
Polyethylene	100-150 kV/cm ac 50 kV/cm ac HF
Porcelain	5-20 kV/cm ac
Mica - stacks - single plates	150 kV/cm ac 300-500 kV/cm ac

of defects which give rise to scatter in strength results and an ensuing "area" or "volume" effect. More will be said about this later.

Frequently, other properties of the dielectric are more important than the dielectric strength, for example: cost, compatibility, mechanical properties, thermal properties, processability, and electrical properties such as loss angle. Table 6.2 provides a convenient checklist when assessing the suitability of several materials for a particular application. (2) For example, many excellent plastics are seriously affected by mineral oil or themselves degrade demineralized water.

It is obvious therefore that great care is needed in selecting the solid dielectric for a particular application, especially at high voltage. Environmental and mechanical factors alone may eliminate an otherwise attractive material. Due consideration must be given to expected life, material and processing costs, normal and abnormal stresses on the system, and factors of safety. The real cost of failure will affect the reliability specified. Having selected a material the designer must take care with the electric field configuration, particularly at nonuniform field regions and solid/liquid, solid/gas and solid/vacuum interfaces.

To produce an effective design, the engineer should be aware of the mechanisms of breakdown and the factors which affect breakdown. These are discussed in later sections. Finally, a word of warning; ASTM test figures for solids are of little value to the designer. The small spread in strengths for a wide range of materials obtained by this test method emphasizes the fact that materials should be evaluated under conditions closely simulating those experienced in practice, with due allowance for area and volume effects.

6.2 Breakdown Mechanisms

Solids usually break down due to one of the following mechanisms, acting singly or in combination (see also Table 6.3).

Table 6.2 Properties of interest for insulating materials.

Miscellaneous	Density Refractive index Transparency	Color Porosity	Permeability Moisture	sorption Surface	atsorption of water	Resistance to fungi	Resistance to light and UV	Cost Radiation resistance
Chemical	Electrochemical stability Solubility Solvent crazing	Resistance to reagents	Compatibility with other materials	Aging and oxidation	stability			
Thermal	Conductivity Expansion Primary creep	decomposition Plastic flow	Spark, arc and flame resistance	Temperature coefficients	Melting point Pour point	Vapor pressure		
Mechanical	Tensile, shearing, compressive, bending strengths Elastic moduli	Hardness Impact and tearing	strengths Viscosity	Extensibility Flexibility	Machinability Fatigue	Abrasion resistance	Stress crazing Bonding ability	Processing techniques available
Electrical	Electric strength Surface breakdown strength Tracking resistance	Volume and surface resistivities	Permittivity Loss angle	Insulation resistance Effect of frequency	Discharge resistance			

Consistency

Table 6.3 Breakdown processes in solids.

Breakdown Mechanism	Comment
Intrinsic	Material disruption due to electron processes.
Electromechanical	Forces resulting from electrostatic field.
Tracking	Conducting channels forming on the surface.
Partial discharges	Discharges in non-solid regions, e.g., voids.
Thermal instability	Heat generation rate due to losses exceeds dissipation rate.
Electrochemical	Increase in chemical activity due to electric field.

- (1) Intrinsic
- (2) Electromechanical
- (3) Tracking or surface breakdown
- (4) Partial discharges
- (5) Thermal instability
- (6) Electrochemical deterioration

The final collapse of voltage is usually intrinsic.

6.2.1 Intrinsic Breakdown

Intrinsic breakdown of solids is generally assumed to be electronic in nature, and either of the avalanche or collective electron type. (3, 4, 5) Cooper (6,7) discusses these and some of the difficulties in intrinsic strength measurements. Early attempts at measuring intrinsic strengths showed a variation of strength with thickness. However, by taking care with the electrode edges and reducing thermal effects, intrinsic strength was found to be almost independent of thickness and electrode material. Techniques, using recessed electrodes or high quality encapsulants, (8) have replaced the earlier disc shaped specimens and curved electrodes which were limited by the electrical strength of the surrounding medium. For example, test stresses were limited to 100 kV/cm in air, 500 kV/cm in oil, 3 MV/cm in high-pressure gas and 15 MV/cm in distilled water. The use of pulse voltages, with breakdown occurring in less than a few microseconds, has reduced thermal and surface flashover problems. However, some materials exhibit reduced strength under fast pulse conditions; this is believed due to the absence of electric stress relieving which can occur on do and slow pulse.

Intrinsic strength is associated with the physical structure and temperature of the material. Above a critical field strength, free electrons are accelerated, increasing their number in a runaway manner, leading to catastrophic failure. Free electrons will always be present in solid dielectrics due to imperfections and impurities, thermal effects, radiation absorption and field emission. In gases, the energy loss mechanism for electrons

below the breakdown stress is based on inelastic collisions with the gas molecules, kinetic energy being converted to excitation. In solids, due to the band structure, excitation and ionization are almost the same. The energy loss mechanism for free electrons below the breakdown stress is based on molecular vibrations.

Tables 6.4 and 6.5 show some values of measured intrinsic strength for several common insulating materials.

Artbauer (9) has investigated some factors which prevent the attainment of intrinsic electric—strength in polymeric insulation. In particular, increasing size, and time at stress, reduce the measured breakdown stress. Sample data fit extreme value theory better than normal or log-normal distributions.

6.2.2 Electromechanical Breakdown

The electrostatic pressure exerted by the applied field on the dielectric $(0.5 \ \epsilon_0 \ \epsilon_r E^2 \ n/m^2)$ causes mechanical strain. At any dielectric/dielectric or dielectric/metal interface, this electrostatic pressure puts the surface in tension. Should this exceed the tensile strength of the material it will fail mechanically. For structures where the dielectric supports the electrodes, the electrostatic pressure compresses the material. Materials with low clastic modulus can be thinned considerable even to the point of mechanical failure. The effect is more pronounced at temperatures approaching the softening point. Polyethylene is an example of such a material and mechanically initiated breakdown usually occurs at temperatures above 40° C. (See Figure 6.1.) Fava, $^{(11)}$ working with polyethylene, concluded that electromechanical failure occurred at elevated temperatures when a dc stress was applied. The impulse strength was only slightly reduced.

Table 6.4 Electric strengths of various polymeric organic materials measured at or near ambient temperature (Cooper (67)).

Polymer	Voltage Type	Electrical Strongth MV/cm
Epoxies	de	5-9
Polyethylene	de	5-8.7
Polyethylene	de crest	7.9-9.4
Polystyrene	de	5.9-6.7
Lucite	de	9.8
Polypropylene	ac crest	8.0
Nylonite	ac crest	6. 6
Polytetrafluoroethylene	ac crest	>8.8
Polyethylene-)	dc	5.9
$ ext{Polyethylene-} \left. ight. ight. $	ac crest	5.5

Table 6.5 Intrinsic strengths of organic polymeric materials (McKeown 8),

Materia: and Treatment		Average Thickness (Microns)	Nange Range	MV/cm Peak	Standard Deviation	Number of Samples
Polyethylene						
Extruded film A. Surface treated 60 Hz with $K_2Cr_2O_7$ and conc. H_2SO_4 . Oil immersed.	2 60 Hz	76	6-9.2	8.1	16%	10
Low density extruded film A. \} Cast in epoxy.	60 Hz dc	79 87	8.1-9.3	0.8	% L % 9	c 0
High density pressed film A.	ZH 09	30	8.7-11.1	9.6	8 %	9
Polystyrene						
Isotactic extruded film (pressed).	2H 09	69	3.1-6.0	4.9	23%	-
Atactic extruded film (pressed).	60 Hz	99	5.2-8.1	7.1	9%6	9
Nylon						
Nylon 6 extruded film.	60 Hz	. 81	5.6-8.4	6.8	16%	2
Nylon 66 extruded film.	60 Hz	23	6.2-7.6	6.6	8%	4
Polyethylene Terephthalate						
Extruded film	2H 09	46	4.6-6.8	5.7	9%	22
PVC						
Extruded film.	2H 09	13	2.8-6.4	٠ <u>.</u> ت	27%	æ
PTFE						
Extruded film.	2H 09	48		>9.0		

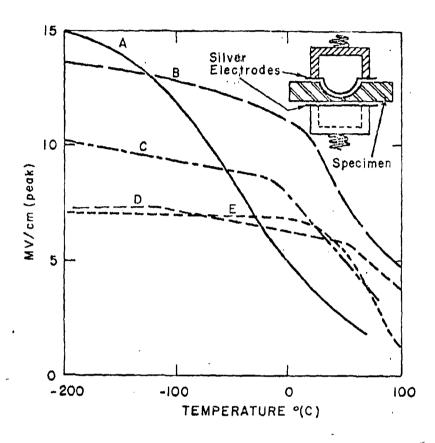


Figure 6.1 Electrical breakdown of some polymeric materials.

Polar: A, polyvinyl alcohol; B, polymethyl methacrylate;

C, chlorinated polyethylene (8% chlorine); nonpolar:

D, polystyrene; E, polyethylene. (Reference Mason (10)).

6.2.3 Tracking or Surface Breakdown

Solid insulation may fail by surface breakdown which can be of two types, tracking and flashover. Tracking consists of the formation of a conducting path (usually of carbon) on the surface. Surface flashover is a breakdown in the gas (or liquid) along the surface; it is therefore a gas (or liquid) discharge phenomenon and has been discussed in detail in Section 4. Unlike tracking, flashover does not necessarily permanently impair the dielectric surface, although it may be eroded. Tracking is essentially a long term process usually starting as an ionic conduction current in the insulation, or developing from surface deposits or damage caused by nearby discharges. Conducting channels usually form as the current concentrates due to local variations in the surface. Semiconducting films can be used to reduce this effect somewhat by grading the surface. The alternative is to choose surface treatments which provide good insulation and are discharge resistant and hydrophobic e.g. silicone and antitrack varnishes. Billings (12) has shown that the tendency of polymers to fail by tracking depends on the chemical structure. Teflon, for example, is extremely good on both dry and dust/fog type tests. In general, polymers based on aromatic compounds or with weakly bonded or easily oxidized chains, are susceptible to track formation. Aliphatics tend to be more track resistant, except where side chain losses occur, as for example with polyvinyl chloride. Cycloaliphatic epoxies tend to fail by erosion rather than tracking.

Polymers which do not track under normal conditions are those which give off volatiles and therefore crode. Any carbon formed is normally amorphous. For example, polymethylmethacrylate decomposes by chain seission.

The Dust Fog Test (ASTM D2132-6T) is used to compare materials as to their suitability for outdoor insulation. Billings gives the following figures for a surface one inch long, coated with a saline contaminant and exposed to artificial fog. Test voltage is 1500 volts.

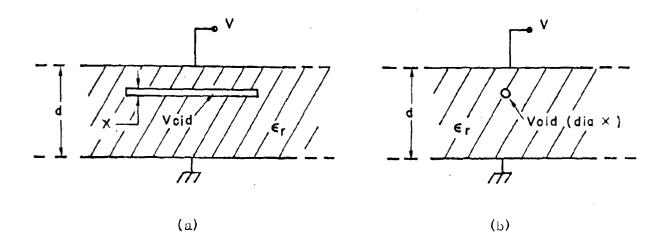
The numbers in parenthesis are the hours to failure when tested as described above. Polytetrafluoroethylene (600), Polypropylene (191), Perspex (Methylmethacrylate) (162), Polyethylene (33), PVA (1.0), Polystyrene (0.9), Polyvinyl Chloride (0.3), Polycarbonate (0.3). Nylon ranks low under track tests.

6.2.4 Partial Discharges

The mechanism of insulation failure by partial discharges has received a lot of attention during the past few years. (1,13,14,15) It is one of the most important factors determining the life of insulation when operated at medium to high stress.

In practical solid insulation systems, it is virtually impossible to remove all voids. A void is a region where solid or liquid is unintentionally absent; this region may contain gas at pressures varying from a few torr to a few atmospheres. Above a certain stress, often labelled the corona inception voltage (CIV), gas discharges occur in the void. Continuous operation above this level (ac and pulse especially) eventually leads to insulation failure, in addition to generating radio interference. The stress at which discharges occur in the void depends on several factors, the most important of which are void size, shape and location, gas pressure and type of gas, dielectric constant of surrounding medium, and waveform. Two simple void shapes are shown in Figures 6.2 (a) and 6.2 (b). For x << d, the electric field in the voids under ac stress are $\frac{1}{6}$ V/d and 3 $\frac{1}{6}$ V/d(1 + 2 $\frac{1}{6}$) respectively. Figure 6.2 (a) could arise due to a crack or incomplete impregnation of a laminated structure while 6.2 (b) could be a bubble in a solid or liquid dielectric. Two other common discharge sites are shown in Figures 6.2 (c) and 6.2 (d).

The effect of void size depends on the pressure and nature of the gas in the void. It is found that the breakdown voltage of a void follows closely the Paschen curve. Air, for example, shows a minimum of 300 volts at a pressure times gap product (pd) of 0.6 torr-cm. Thus 50 micron diameter



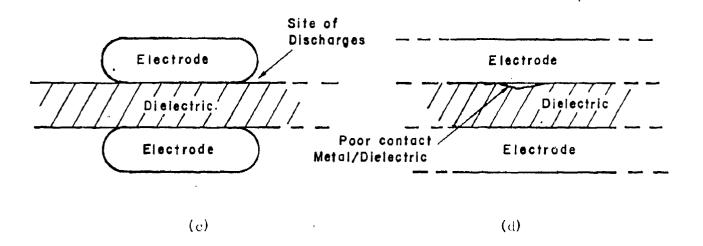


Figure 6.2 Various locations for partial discharges.

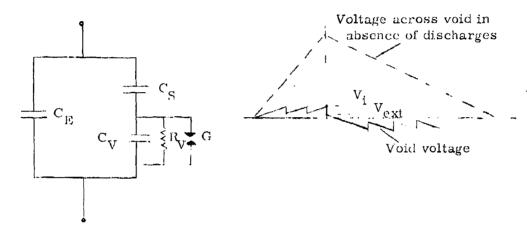
spherical voids containing air at NTP will break down in most solid dielectrics operating at 100 kV/cm and greater.

The discharge repetition rate is very sensitive to the applied voltage waveform. For dc stress, above the CIV, the rate of discharges is usually counted in number per hour, e.g., in polyethylene insulated cable operating on dc. For other waveforms, repetitive discharges occur only when the voltage is changing, i.e., increasing or decreasing. Figure 6.3 shows the equivalent circuit and void voltage waveform for an applied triangular voltage. C_E is the bulk capacitance of the sample, C_V is the void, C_S is the capacitance in series with the void, C_V is the equivalent leakage resistance of the void, and gap C_V represents the breakdown of the void. Note that the gap C_V ignites when the void voltage is C_V and extinguishes when it drops to C_V ; the result is a relaxation phenomenon.

Successive breakdowns in the void cause material erosion and degradation by thermal damage, UV radiation, ion and electron impact or by thin are channels fed by transverse discharges. Garton (16) examined these and concluded that electron and ion impact are the most likely cause of erosion. There will be microscopic areas where erosion is more rapid than average. These develop into channels which propagate by local intrinsic breakdown at their tips.

The erosion rate, besides depending on material, voltage waveform, void geometry and location, also depends on the chemical nature of
the gas in the void and whether or not the void is vented. For example, when
both nitrogen and oxygen are present, nitric acid is formed which is very
deleterious to both insulation and electrodes.

The life of insulation, operating under partial discharges, is thus limited. For example, lucite is reported to crode at $3-5 \times 10^{-7}$ mm/picocoulomb. Discharge inception measurements give an indication of the soundness of the insulation, and quite sensitive detection equipment is now readily available. ASTM D 1868 describes one standard method.



- (a) Equivalent circuit of sample with a void present.
- (b) Void voltage in presence of discharges for triangular waveform applied voltage.

1 1 1

Figure 6.3 Equivalent circuit and typical voltage waveform of a void.

6.2.5 Thermal Instability

Under an applied electric field, some currents flow in dielectrics which generate heat. These currents are of the conduction (ionic and high field) and hysteresis loss component types. The rate of heat generation is an increasing function of temperature, electric field and frequency. Other potential sources of heat in insulation are partial discharges and nearby hot metal conductors. The temperature distribution in the insulation depends on the location and magnitude of the heat sources as well as the geometry, temperature and thermal properties of the medium and heat sinks.

Thermal instability can occur at any point where the rate of heat generation exceeds the ability of the material to dissipate. The critical voltage at which thermal runaway occurs in a system depends on the voltage waveform (dc, ac, pulse), ambient temperature, geometry, and material properties.

The following equation has to be solved for each particular problem, putting in the appropriate boundary conditions.

$$C_V dT/dt + div (k, grad T) = \sigma (E) E^2$$
 (1)

 $C_{_{m{V}}}$ = specific heat per unit volume

k = thermal conductivity

g = electrical conductivity (effective value for given E and frequency)

E = electric field

T = temperature

Analysis (17) shows that there is a maximum thermal voltage for an indefinitely thick specimen. For example, under do stress and with the assumption that the material electrical conductivity o increases exponentially with temperature, the maximum thermal voltage is given by

$$V^{2}_{TH} \propto \frac{kT_{o}}{\sigma_{o}}$$
 (2)

where k = thermal conductivityand $T_0 = ambient temperature$

Note that the temperature dependent conductivity results in a certain amount of stress relieving on dc and is one of the reasons for the higher thermal voltages.

Calculated maximum thermal voltages for several materials are shown in Table 6.6. The general indication is that continuous solid insulation thicknesses greater than 10 cm are of little electrical benefit. With good design, thermal instability should not be the limiting factor on de. On high voltage, high frequency service the thermal voltage is probably the limit, although poor quality control may result in breakdown by partial discharge. Greater thicknesses and voltages should be attainable for low repetition rate impulse stresses; life will probably be limited then by partial discharges. Analysis of thermal breakdown under pulse conditions can be carried out using the above equation modified by omitting the second term, since usually thermal conduction heat losses are negligible and the heat input goes into raising the local temperature.

6.2.6 Electrochemical Deterioration

Electrochemical deterioration is just one aspect of the general problem of chemical stability of the insulation. Chemical processes can be initiated or accelerated by the ionic current resulting from the applied electric field. The deterioration rate is affected by the current density, the nature of the ions, temperature, moisture, contamination and the voltage waveform. The effect is greatest on dc, particularly with mixed dielectrics.

Chemical changes can also come about due to elevated operating temperatures and exposure to radiation (either from external source or local corona).

Table 6.6 Maximum thermal voltages.

	Thermal Voltage (MV) (20°C)					
Material	dc	50 Hz	1 MHz			
Mica	24	7-18				
Rock Salt	38	1. 4				
Borosilicate Glass		4. 8				
High Grade Porcelain		2.8				
Polystyrene		5	0.05			
Polyethylene		3-5	0.05			
Acrylic		0. 3-1				

6.3 Factors Affecting the Breakdown Voltage of Solids

The aim of good electrical insulation design is to provide the required electrical characteristics and life at minimum cost. The number of suitable materials can often be quickly narrowed down to three of four because of various constraints, e.g., compatibility, temperature, mechanical loads, shape and size. In making the final selection of material and deciding on thickness and shape, the designer is seldom fortunate enough to have before him dielectric strength data directly applicable to his design. Because of this, industrial designs change slowly both in shape and material usage. Only after extensive research, development and field trials (which may take from three to seven years) are radical changes introduced. When time and financing are available, materials should be evaluated under conditions representing, as closely as possible, those eventually experienced in practice. Unfortunately this is seldom possible. Often the designer can only refer to insulation manufacturers' literature, company reports and publications in journals. The former are usually ASTM test figures which are seldom of much value and the latter two are usually limited in the range of test conditions.

This section is written to help the designer by indicating the main factors which influence the breakdown voltage of solid insulation. Thus, available dielectric strength data, although not immediately useful, can be modified to suit the new design. For example, material X is known to have operated at a stress of 100 kV/cm for 1000 hours; how long is it likely to last at 150 kV/cm?

The main factors affecting the breakdown voltage are shown in Table 6.7 and discussed further below. It will be assumed that by correct choice of material and system geometry, failure by electrochemical deterioration, tracking and thermal instability has been eliminated.

6.3.1 Time at Stress

For economic reasons, high voltage insulation is often operated above the corona inception voltage (CIV), with partial discharges occurring

Table 6.7 Factors affecting the breakdown voltage of solids.

Factor	Comment
Time at Stress	Small reduction in stress often increases life considerably.
Insulation Thickness	In practice, operating stress is usually reduced for thicker sections.
Area and Volume	An increase in area (or volume) by 10 ³ reduces stress by factor 2 (typically).
Environment	Can result in failure by tracking, chemical deterioration, thermal breakdown, radiation effects.
Waveform	Peak to peak voltage important.
l'olarity	Point to plane: negative breakdown voltage greater than positive for most solids.

in voids or near the electrode/dielectric interface. The useful life of the insulation under this condition is very much affected by the working stress level (Figure 6.4). Most solids appear to have a voltage-life characteristic of the form

$$P = constant \times (V_1/V)^n$$
 (3)

where P is the number of cycles or pulses to breakdown, V is the applied voltage and V_i the corona inception voltage (CIV). The value of "n" depends on the material and typically lies between five and eight. Thus, measuring the lives at higher stresses enables the longer life at reduced stress to be predicted. Mylar, for example, has $n \simeq 7.5^{(18,19)}$ and polyethylene between 6.5 and 8.5.

Another method of accelerating tests is to raise the test frequency. To date, this method has given inconsistent results when the test frequency exceeds a few kilohertz; the results usually predict an optimistic 60 Hz life. For frequency acceleration, the assumption is generally made that the number of cycles of applied voltage to failure is constant. This is not true for internal and scaled voids since the equilibrium pressure in the void depends on the discharge rate; and the equilibrium pressure affects the corona interaction. With open voids, frequency acceleration can usually be used if humidity is kept low and sufficient gas flow is maintained. Figure 6.5 shows some results for polystyrene.

For many insulations operating on pulse duty the peak to peak voltage of the pulse determines the life. For example, polyethylene insulated cable operating under pulse conditions has its life reduced by 90% if the pulse reversal is increased from a nominal 25% to 85%. Increasing the peak stress of a unidirectional pulse by 50% reduces the life by approximately 95%.

It is clear from the above relationship that the insulation designer should attempt to raise the discharge inception level by good electric field

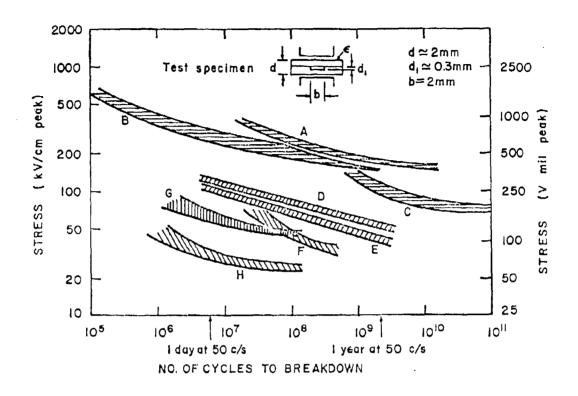


Figure 6.4 Life data for plastics with internal discharges (Ref. 15).

Code	Mate	rial		Discharge Inception Stress kV/cm peak
Α	Polyethylene		cable	137
В	Polyethylene			100
С	Polyethylene		disc	35 - 50
D	Poly sty rene		plasticized	28
E	Poly sty rene		non-plasticized	28
F	Phenolformaldehyde		molded cavity	18
G	Nylon			20
Н	(nylon + cellulose filler)		machined cavity	18

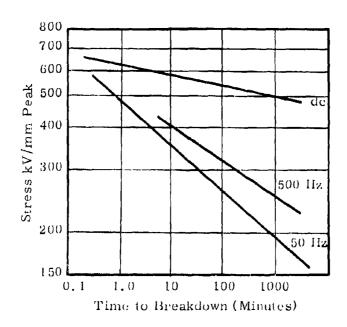


Figure 6.5 Life/stress for polystyrene (uniform field). (22)

control and elimination of voids and discharges (particularly in high field regions). High quality control is essential during manufacture and assembly. In applications using tape or sheet, vacuum impregnation is normally necessary for long life. For cast insulation there now exist guidelines for producing high quality, low void content castings. (23,24,25) Low dielectric constant materials clearly have advantages.

The benefits of removing partial discharges are seen in Figure 6.6 which compares the life of PTFE when operating with and without corona. (26) Paper insulated cable is similarly improved when oil impregnated or filled with high pressure gas.

The waveform of the applied voltage has a considerable effect on the life. This is discussed more fully later.

6.3.2 Insulation Thickness

Most published data on the dielectric strength of solid insulation suggests that the dielectric strength falls with increasing thickness. This is probably due more to the method of measurement than to some inherent characteristic of the material. ASTM D149 for example suggests that the standard test method gives a square root law i.e. V α d^{1/2}. This test method, and many methods used in the literature, are based on a geometry which permits discharges at the electrode/material interface. Under these conditions, something less than a linear relationship between spacing and breakdown voltage is to be expected. (10) By improving the test geometry (see section on "intrinsic breakdown") the voltage/spacing relationship becomes almost linear.

Figure 6.7 shows some data for crosslinked polyethylene cable with multiple layers extruded in tandem. The impulse breakdown stress level of 0.7 MV/cm at a 1 cm wall is of interest. Impulse strength data (28) for polyethylene, EP rubber and butyl rubber insulated cable show an approximate linear dependence on wall thickness (at least up to the 15 mm reported). Epoxy resin (29) shows an almost linear dependence when the

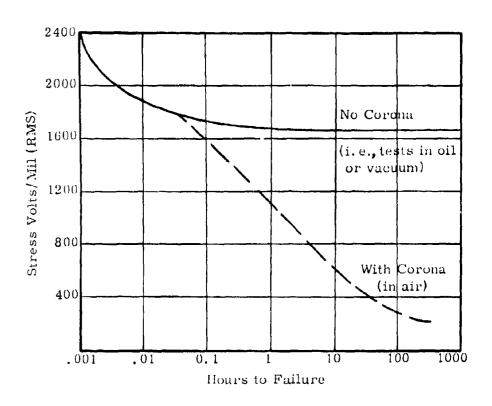


Figure 6.6 Life of PTFE with and without corona. (26)

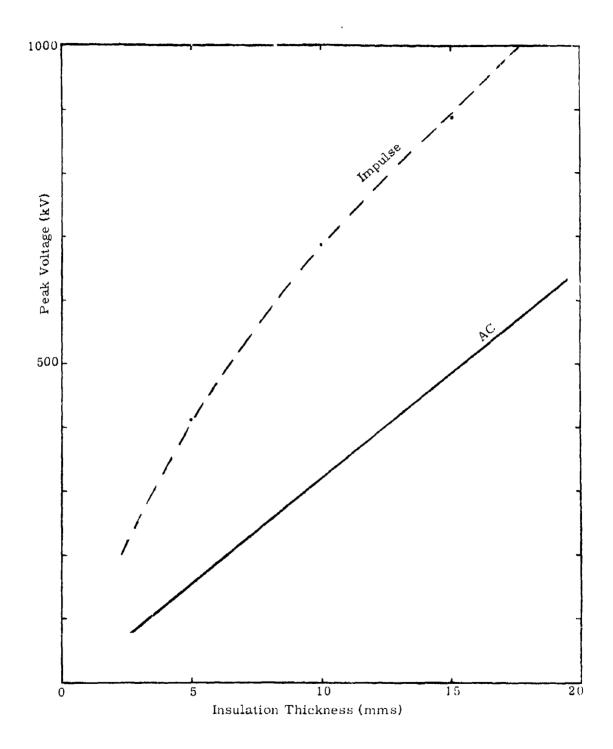


Figure 6.7 Breakdown voltage versus insulation thickness for polyethylene cable (27) (two layers extruded in tandem).

electrodes are properly encapsulated. Figure 6.8 illustrates the linear dependence (curves 3a and 3b) and the square root result (curve 1) when the electrodes are external to the test sample. Curve 2 shows the effect of reducing the sample volume and area (see later).

With the following exceptions, therefore, it may be concluded that in a well designed system, the breakdown voltage increases almost linearly with thickness. Exceptions are where:

- (1) Samples are extremely thin and the thickness is of the order of electron mean free path.
- (2) Breakdown occurs by the "thermal" mechanism e.g. high frequency operation. Temperature increases with thickness.
- (3) Allowance must be made for increasing stressed volume.

6.3.3 Electrode Area and Stressed Volume Effects

The area or volume effect on dielectric strength has been discussed earlier, both in general (Section 3), and in particular with regard to gaseous and liquid dielectrics (Sections 4 and 5). The effect is most important to the application of solid dielectrics and will be discussed in further detail here, particularly as it effects solids.

Electrical insulation of commercial purity usually fails at stresses well below those measured on small samples under closely controlled conditions of purity and preparation. Experiment shows this to be true, at least for solids, liquids, vacuum and gases at high pressure. The observed reduction in mean breakdown strength with increasing sample size (volume or area) points to the presence of imperfections (impurities and voids for example) in the stressed region. Thus the probability of breakdown in an elemental region will depend on both the probability of finding an imperfection in that region and on the distribution of imperfection size. Increasing the size of a sample under stress clearly increases the probability of finding increased imperfection size, i.e., reduced breakdown stress.

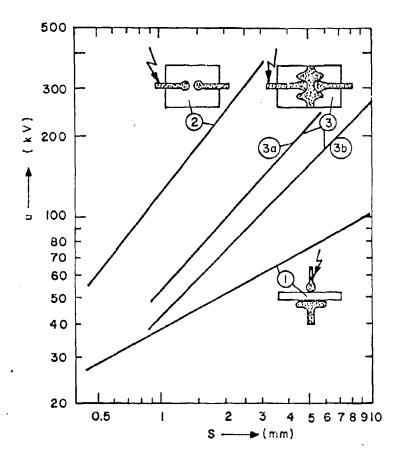


Figure 6.8 Breakdown voltage U in kV of epoxy resin moldings vs wall thickness S in mm. Arrangement (1): Test sample 200 mm diameter between a spherical electrode (20 mm dia) and a flat electrode (50 mm dia). The wall thickness is reduced to S with a spherical deepening. The insulation surface under the electrode has a conductive painting. Stressed area is smaller than 1 cm². Arrangement (2): Spherical steel electrodes (10 mm dia) molded in an epoxy cylinder (80 mm dia x 150 mm long). Stressed area is smaller than 1 cm². Arrangement (3): Rogowski electrodes (50 mm dia) with a stressed area of 20 cm² and with a) a graphite painting on the insulation surface, and b) an iron cloth in the epoxy surface. (Ref. 29)

The statistics used to describe this effect can best be described as "weak link" theory since breakdown, by definition, occurs at the weakest spot. Extreme value probability theory (30) has been applied to this type of problem with considerable success, (31, 32, 9) enabling the diffective strength of larger specimens to be predicted.

Breakdown due to imperfections gives rise to statistical fluctuations in the measured breakdown strengths. For example, if apparently similar samples are tested under identical test conditions, they will not fail at the same voltage. It is usual therefore to quote the mean value of dielectric strength E and the standard deviation σ , for the tested material, although it would be better to give the cumulative probability of breakdown P(E) as a function of E and the test geometry. This information can be used to predict the strength of samples of another size.

A simple, but perfectly general, approach is the following. If $P_1(U)$ is the eumulative probability of breakdown up to voltage U for an elemental sample, and $P_1(U)$ the corresponding value for "n" such samples tested in parallel, then by using the binomial distribution function

$$P_n(U) = 1 - (1 - P_1(U))^n$$
 (4)

This result makes no assumption concerning the form of the basic distribution involved. Figure 6.9 gives the results in a useful form. For a normal distribution, the effect of n=10, $100\,\mathrm{and}\,1000$ is to reduce the observed mean strength by approximately $1.75\,\mathrm{o}$, $2.6\,\mathrm{o}$ and $3.25\,\mathrm{o}$ respectively.

In all cases, the magnitude of the size effect is very dependent on the variability of the insulation (standard deviation). Creedon (33) has developed the ideas generated at the Atomic Weapons Research Establishment, Aldermaston, England, by J. C. Martin (34) and derives a volume effect which is dependent on the standard deviation. Figure 6.10 has been derived from his theory to show the dependence on σ .

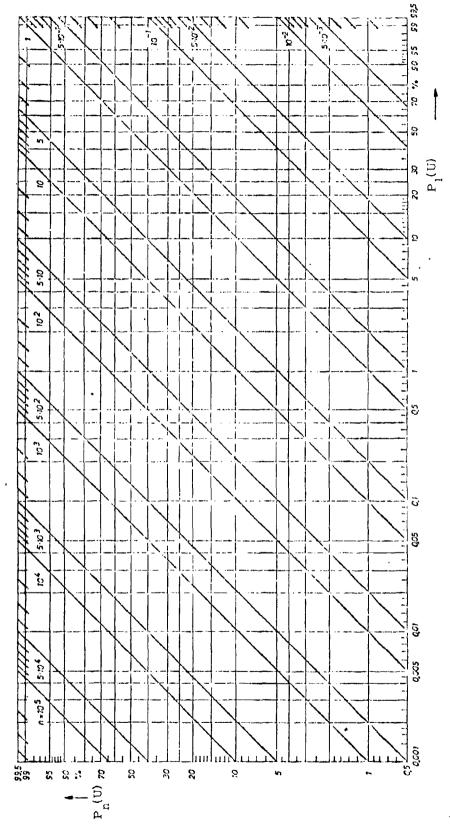
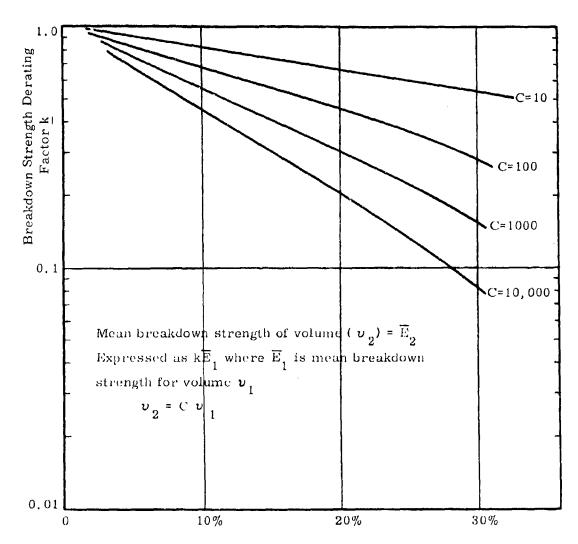


Figure 6.9 Relation between the distribution functions of a model and of an object n times larger.

 $P_n(U) = 1 - (1 - P_1(U))^n$



Standard Deviation (Percentage of Mean)

Figure 6.10 Effect of increasing volume and standard deviation on mean breakdown strength.

There still seems to be some confusion as to whether to use "area" or "volume" for the size effect. Intuitively one expects a volume effect if the imperfections causing breakdown are distributed throughout the insulation, and an area effect if breakdown is initiated by imperfections on the electrode surface. Martin (34) concludes that for many plastics, a volume effect exists. Some of his data for pulse breakdown are shown in Figure 6.11. Note that volume refers to the actual volume stressed to 90% or greater of the maximum field strength. Figure 6.8 also illustrates a volume effect for epoxy resin. Comparing curves (2) and (3a) a reduction in strength of approximately 50% is observed. The corresponding volume change is approximately 250:1. For the given $\sigma = 15\%$, Figure 6.10 predicts a similar reduction in strength. Using Figure 6.10 and the results of Eustance (35) for polypropylene film, where an increase of 10⁴ reduces the breakdown strength to 0,55, the standard deviation is 7.5%. This is remarkably low for solid insulation and is indicative of the cleanliness of the polymer and the quality of the film making process. In this respect, plastic film is usually superior to paper for impregnated capacitor insulation.

Some filled epoxy resins were studied at Ion Physics Corporation, Burlington, Massachusetts, as to their suitability for highly stressed, high voltage insulation. (36) Tests on small samples (2 inches diameter, 1/4 inch thick) gave $\overline{^{12}}_{BD}$ = 2.4 MV/inch and σ = 18%. Two large samples (approximately 200 inches 3, 0.5 inch thick) broke down under similar test conditions (dc) at a mean stress of 0.97 MV/inch. Figure 6.10 predicts 1.03 MV/inch for these conditions, assuming a volume effect.

The volume dependence reported by Morton and Stannett (37) for mylar, polystyrene and polyethylene are equivalent to a standard deviation of 12% (from Figure 6.10).

Milton, using casting resins, concludes that an area dependence exists. His results are shown in Figure 6.12. Other tests, using Rogowski profile electrodes, failed to show a thickness effect. It should be noted that the work was done with unfilled polymers and relatively small stressed volume

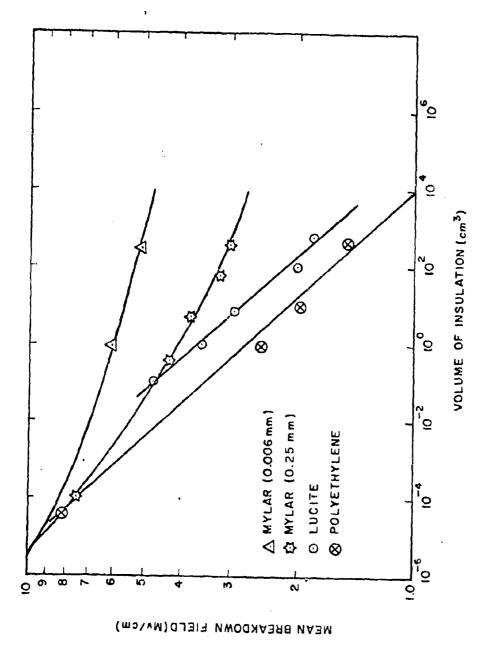


Figure 6.11 Volume effect: electrical breakdown in plastics.

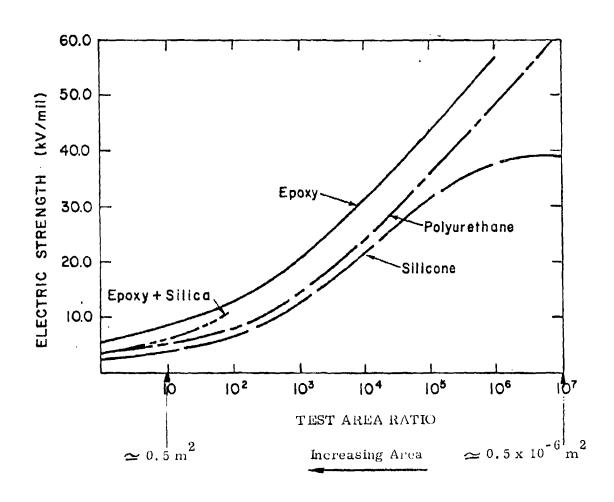


Figure 6.12 Electric strength of the three encapsulating materials relating to test area. (Ref. 38)

(.03 inch maximum gap, 10 in² area). Even the lowest measured stress for epoxy (5 MV/inch) is high by normal commercial standards. It is possible that breakdown was electrode dominated for his tests with a consequent area dependence. Support for this appeared in later work by the same author in which the mold material was found to have a large effect on the breakdown strength. (39)

To summarize, a size effect results from inhomogeneity in the insulation. Commercial insulation will contain imperfections, the type, size and number of which will determine the standard deviation of the mean breakdown strength. The standard deviation of common solid dielectrics appears to be in the range 5 to 40% (plastics 5-15, filled epoxies 15-25, mica 10-40). The larger the standard deviation, the greater is the size effect. Thus plastics, with say $\sigma = 12\%$, will show a reduction in mean breakdown strength of 50% when the volume is increased by a factor of one thousand.

Since the dimensions of high voltage equipment increase at least as fast as voltage V, then the volume of stressed dielectric increases as V³ or V⁴. The successful production of a HV component obviously requires good design, but perhaps more important, needs extremely good quality control both in material and processing in order that the variability be kept small. Unlike gases, liquids and vacuum, a puncture in solid insulation normally means fabricating another component. This alone is a strong argument against single large solid dielectric components at high voltage. The capacitor manufacturer solves the problem by climinating early failures after and during production; this may involve using up part of the useful life of the capacitor. The cable manufacturer tests each drum length of cable after production. Failures can then be removed by good jointing techniques.

6.3.4 Environment

The nature of the surrounding medium affects the breakdown voltage of solid insulation, but usually for the reasons discussed earlier, that

is, corona at the edges of the electrodes, surface tracking, or chemical attack. Moisture in particular should be excluded from solid insulation since it encourages electrochemical deterioration.

The ambient temperature is important since it determines the hot-spot temperature of the insulation. To prevent thermal breakdown, the working stress is usually reduced for increasing ambient temperature. Sustained operation at elevated temperature can lead to insulation degradation. This depends on the temperature and the type of insulation. A bibliography on thermal ageing of electrical insulation is given in reference (40).

The useful life, as well as some of the mechanical properties, of solid and liquid insulation is affected when subjected to relatively large doses of high energy ionizing radiation. Black (41) notes that the effects are similar to those of stress ageing and exposure to corona. The main effects of radiation in hydrocarbons and polymeric materials are:

- (1) Cross linking of molecules to form gels.
- (2) Evolution of hydrogen and low molecular weight fragments.
- (3) Molecular degradation by main chain scission.
- (4) Formation and annihilation of unsaturated groups.
- (5) When air is present, degradation due to exidation.

The ability of a material to withstand a given dose of radiation depends in a complex way on the chemical structure. Materials which cross link include natural and synthetic rubber, polyester, polystyrene, nylon, polyethylene, PVC and polypropylene. Materials which suffer chain seission include mylar, lucite, PTFE, cellulose products, urea and melamine formaldehydes and unfilled phenolic resins, as well as some of those which cross link. Table 6.8 shows shows dose levels at which the insulation shows measurable degradation of properties. Lifetime dose may be 100 times these values.

Further details on the effects of radiation and environment can be found in Clark .

Table 6.8 Dose of high energy radiation to produce measurable changes in properties.

Material	Dose in Megarads
PTFE	0.02
Polyester	0.3
Polymethylmethacrylate (lucite)	0.8
Cellulose Acetate	3.0
Polycarbonate	3.0
Urea Formaldehyde	8.0
PVC	9.0
Polyethylene	20.0
Polyethylene Terephthalate (mylar)	20.0
Silicone	100.0
Polyimide	500
Polystyrene	800
Epoxy (aromatic type)	2000

6.3.5 Waveform

The intrinsic strength should be independent of waveform except for very fast pulses (several nanoseconds). In practice, the voltage waveform is important not only to the local breakdown strength, but also to the electric field distribution and intensity in all but the simplest insulation systems. For example, field distribution in general will be determined either by conductivity, or permittivity, depending upon the frequency of the applied voltage. Above a particular frequency the field is determined largely by permittivity; and below by conductivity. This critical frequency is given in Table 6.9 for a number of commonly used solid dielectrics and transformer oil. The critical frequency is very low, and obviously many detests on insulation, for example with voltage raised on a ramp or in steps every few seconds or even minutes, are in fact "ac" tests as far as the dielectric time constant is concerned.

As an example, consider two dielectrics in series, say lucite (f == 5.5×10^{-4} , i.e., 140 seconds per cycle) and oil(f_c = 7.2×10^{-3} , i.e., 800 seconds per cycle). At frequencies higher than 7.2 x 10^{-3} the field distribution is largely determined by permittivity rather than conductivity. At frequencies lower than 5.5×10^{-4} , the field distribution is largely determined by the conductivities. At intermediate frequencies there is a phase difference between the electric fields in the two media; the magnitude being determined by the respective conductivity and permittivity. Consider the common situation where a gap of gas or vacuum dielectric is in series with a solid. The dielectric constant is essentially unity and the conductivity extremely low for the gas or vacuum until ionization occurs, which often triggers breakdown. Assuming zero conductivity in the gas or vacuum, the minimum field which can occur in the gap is at frequencies higher than that characteristic of the solid, and is given by $\epsilon_{s}E_{s}$ where ϵ_{s} and E_{s} are respectively the dielectric constant and electric field in the solid. The value of conductivity to use for vacuum or gas becomes difficult to determine at the higher fields because it is no longer zero and conduction may be strongly localized (e.g., field emission

Table 6.9 Frequency "Constant" (Hz).

Material	ę r	^p (ohm-em)	fc	Hz .
High Voltage Porcelain	6. 1	1013	2.9 x	10-2
Alumina	10.0	5 x 10 ¹⁴	3.6 ×	10-4
Pyrex	4, 5	1014	4.0 x	10-3
PTFE	2.2	1017	8.2 ×	10-6
Lucite	3. 3	1015	5.5 x	10-4
Epoxy - unfilled	3. 5	1015	5.1 x	10-4
- alumina	5, 5	1014	3.3 x	10-3
Phenolic-Mica-Filled	5, 0	1013	3.6 x	10-2
Polyethylene	2,2	1015	8.2 x	10-4
Nylon	4.0	1014	4.5 x	10-3
Rubber(hard)	3.0	1017	6.0 x	10-6
Silicone Rubber	3.0	1014	6.0 x	10-3
Polystyrene	2,55	1018	7.0 x	10-7
PVC	3.3	1013	5.5 x	10-2
Transformer Oil (mineral)	2, 5	1014	7.2 x	10-3

Note: ac values for ρ can vary by one or two orders of magnitude.

Where a range was given, the mid-point is used.

Data is normally for low voltage and 20°C.

 $\varepsilon_{\rm r}$ is a low-frequency value (60 to 1000 ${\rm H_{Z}}$).

The value $f_{\mathbf{c}}$ is the frequency where conduction and displacement currents are equal.

$$f_c = \frac{1.8 \times 10^{12}}{\rho \epsilon_r}$$
 (\rho in ohm-cm)

from microscopic points). In the dc case such conduction can establish a charge distribution which is self-relieving, with regard to stress, and stabilizing.

6.3.5.1 Direct Voltage

For most materials, the working dc stress for a given life is greater than the peak ac stress by about a factor two, due mainly to the reduction in the number of partial discharges and a certain amount of local stress relieving (electrical conductivity is a function of temperature and electric field). Discharges occur more readily when the voltage level changes, but also occur at steady voltage depending on the relaxation time of the void. The most common failure with mixed dielectrics on dc is electrochemical deterioration. Tracking is also a problem.

6.3.5.2 Power Frequency

At high voltage, thermal breakdown can occur, especially if the ambient temperature is high, as for example on cables carrying peak or overload currents. Failure by partial discharges, however, is probably the main reason for failure at high stress. For insulation operated above the corona inception voltage, discharges occur each half cycle; the number depending on the voltage excess over the inception level. Thus the life reduces rapidly with increasing stress above the CIV. Liquid impregnated insulation can show a reduction in CIV after sustained operation at normal stress. This is probably because many commonly used impregnants evolve gas under electric stress. Certain gas absorbing additives can reduce the effect. Temperature cycling can result in a similar effect.

6.3,5,3 Pulse

Thermal breakdown is unlikely for low repetition rate short pulses. Breakdown after a small number of pulses is probably due to intrinsic breakdown, whereas partial discharges account for breakdown after many pulses.

Theoretical and experimental studies indicate that for most solid dielectrics, the pulse strength is independent of risetime down to about ten nanoseconds. Exceptions include liquid impregnated insulation and glass. The former shows a variation in strength with impulse waveform due to the impulse strength depending on the pulse strength of the impregnant. (43) Glass (44) shows an increasing strength for pulses shorter than a few microseconds. In this respect it is more like a liquid and of course has a similar structure being a super cooled liquid, i.e., having a lack of long range order.

For most materials, the breakdown process is very rapid, with formative times of the order of a few nanoseconds. Figure 6.13 shows some data for several materials under ramp voltage applications. (45) The formative time decreases with increasing overvoltage but increases with the thickness of the dielectric. Since gases, liquids and vacuum show increased breakdown stresses for pulses shorter than a few microseconds, this presents a problem with insulation coordination for fast rising voltages. Thus highly stressed solids have no inherent protection against fast overvolting pulses.

The effect of partial discharges on the pulse life characteristic of solid insulation depends on many factors. Alston (20,46) has reviewed some of these and concludes that for polythene in particular,

- (1) Void size and location are important (worst next to cathode).
- (2) Peak to peak, peak, and rate of voltage application or removal affect life.
- (3) Time at stress and voltage reversal affect life.
- (4) Increasing the time interval between unidirectional pulses can reduce the life (depends on relaxation time of the material).
- (5) At a given stress, life is independent of sample thickness.
- (6) Life is reduced by reversing polarity between pulses.
- (7) Discharges per pulse is reduced for pulses less than a few microseconds in duration.

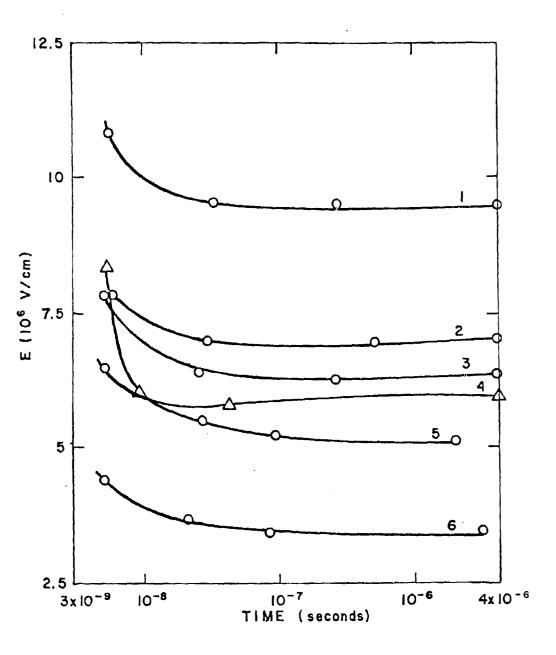


Figure 6.13 Variation of the dielectric strength of styroflex (1), teflon (2), mica (3), lucite (4), polystyrene (5), and bulk teflon (6), with the voltage rise time; uniform field (Ref. Mel'nikov 45).

Martin, ⁽³⁴⁾ using thin sheets of mylar, found a life/stress relationship similar to that in Section 6.3.1, for pulse application. He found the value of "n" to be 7.5. By using thinner layers of insulation, the breakdown stress was increased even when the total sample thickness was the same. Hayworth reported a similar effect which is made use of in capacitor manufacture (Figure 6.14). Derating curves for voltage reversal are also given.

6.3.6 Nonuniform Field

For very nonuniform fields, a polarity effect exists for many materials. The breakdown voltage of a positive point to plane geometry appears to be about 70% of the negative point value. The calculated electric field at the tip of a negative point is in excess of the intrinsic value. Mason accounted for this by assuming that the conductivity increases with increasing field and acts as a stress relieving mechanism. Continuous application of stress can lead to breakdown by treeing (48) (branching discharge paths).

6.4 Conclusions

It is clear from the previous sections that the design of solid insulation in systems is not a straightforward matter. The starting point is normally the technical requirements and constraints. These include some of the following: working voltage and waveshapes, dimensions, life, weight, temperature, environment and cost. Many materials will be ruled out at this point by difficulties either in mechanical support or lack of availability in the required geometry. In this respect, cast insulation has a great advantage over, say, plastic film. The next step is perhaps to examine which materials can operate at the necessary stress to give the required life. This is difficult since seldom will appropriate data be available. The manufacturers' test figures, usually obtained according to ASTM on 1/8 inch thick samples, are of little use. Examination of Table 6.10 illustrates this point. Thus one must search the literature for test data obtained under conditions near to

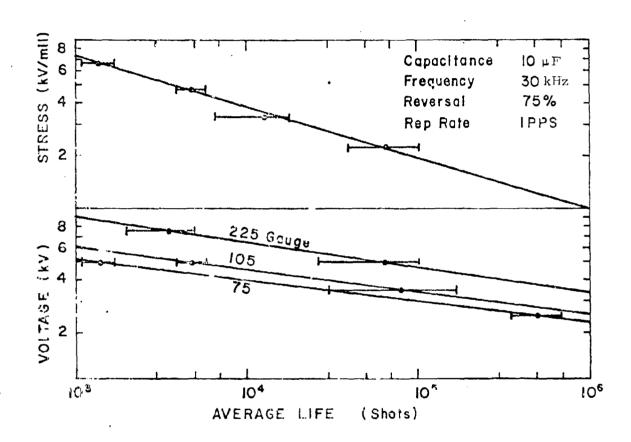


Figure 6.14 Average life in shots versus stress in kV/mil and voltage in kV for polyester film. (Hayworth, Ref. 47).

those of the problem and then make intelligent adjustments based on some of the information in earlier sections. There is, however, no substitute for good sample testing if cost and time permit. There is a marked absence of high-voltage solid dielectric information in the literature; gases and liquids have been much better investigated and reported. Apart from one or two references related to high energy density capacitors, (47) the most useful data to the pulse power designer is that contained in the unpublished work of J.C. Martin et al., at the U.K. Atomic Weapons Research Establishment, Aldermaston, England. His memoranda contain much information on several plastics (mylar, polyethylene, lucite, polypropylene) at high voltages and stresses for volumes up to tens of liters. Information on epoxy resins at high voltage is very limited. Recent reports (36,50) give some data at voltages in excess of a hundred kilovolts for dc, pulse, uniform and nonuniform fields. Reference (36) also gives some data on methylmethacrylate and styrene and also includes some data on flashover strength in compressed gases.

As mentioned earlier, the interfaces between the solid and metal electrodes and other medium (gas, liquid or vacuum) usually present problems. With good design, the interface flashover strength can be made to approach the breakdown strength of the medium. Vacuum under slow pulse and do is an exception. Good design involves taking care with the triple joint (where metal, solid and medium meet), and the electric field distribution. In addition, care is needed during manufacture and assembly to reduce contamination, particularly moisture. Surface finish is usually quite important.

Finally, Table 6.10 lists some of the properties of commonly used insulating materials. These should only be used as a guide. The use of more detailed sources of data is recommended for final design. Some useful references are given. (51-55) The Electronic Properties Information Center, Air Force Materials Laboratory reports in particular provide a survey of most materials, covering properties and processing. The large number of books available on prastics, epoxy resins, etc. has discouraged the author from single properties and preference.

Table 6.10 Properties of some solid dielectrics in common use. (Continued Overleaf)

	Tensily Stenath	Compressive Strength ps(x 10 ⁻³	Electic Modulus Est x 1075	Elongation	Specific Heat (cels, OC/co)	Court, of Linear Expansion (per OC x 10 ⁵)	Heat Distortion Temp, ^O C	Thermal Conductivity (cals/sec/cm ² / oC/cm x 10 ⁴)
Polyenijna (LD)	:-3		0,15-0,39	909-991	0.55	1.4-13	35-50	9:-+
Folly enhydene (RD)	2-5		0.9-1.7	40-300	0.55	14-18	40-50	4-16
\$0.14 Out \$1.14 or						14-18		
Polyaminerak	5.5-10.5	13-14	2-6	'r' -	0.32-0.35	7-5	50-75	1.9-2.0
1 : 1 : 1 : 1 :	1.8-2.C	t- ;;	6, 58	100-400		3-10	130-135	9-6
PVC (mg/d)	2-10	6-11	0.2-2.6	1-5		5-18.5	60-80	3-4
PVC (plastered)	(O - *)		0.1-0.7	200-400	0.3-0.5	7-25		3-1
Polymerial Methologiate								
Acrons	ص د-	12-14	2.5-5	1-15		6-8	65-90	2.4-6.0
Nyton	Ø1	5.5-14	0.4-4	60-300	9.4	8-15	05-150	5-6
Polyce of the	6-10.5	F	1.7	60-109		7	:35-145	·\$ - +
o the total	ភា ។ ហ	15-35	9-10	0.5-1.0	0.3-0.4	3-7	115-150	4-:3
Polyester Resin (M-117 ked)	5-5	7-21	0.5-0.6	5-300	0.25	3.5	61-200	6-10
11 11 1 1 1 1 1 1 1 1 1 1 1 1 1 1 1 1	27.5	9-27	3-:8			2-6	90-230	9-+
. We will a Constant and	11.23		3.3.6	55-150		1.8-2	236-240	3.63
E. Co. T. Canada Garage Co. Co.			:3					
Polytrienouse (linear)								
C 1 4 C 4 L 1	ڻ- ا -	0.275				11-37	>300	
			105		. 176			28
(1) (1) (1) (1) (1) (1) (1) (1) (1) (1)			60-110		. 186	.32		26
3 1:	8-50	30-425	1.5-5.2					70-500
E Vultage Pontulain	a) -,	35-80 00-80	0.7-1.4					29-50
1 a		40-120	1-1.5			0.5-0.8		60-120
Nuscovite (potassium micz)	01-0	27-32	200-300			0.32		
Fall (magnesium mica)								

Table 6.10 (Continued) Properties of some solid dielectrics in common use.

Max. Operating Temr. In Air 9C	Dielo Cors	Dieluctrie Constart 1 MHz	Por Factor	Power Faster x 10 ³ Hz 1 MHz	Resistivity L-cm	1/8" Dielectric Strength (ASTAI)	Dielectric Strongth (few min.s)
83 E3	2.28-2.32	2,28-2,32	6.1-6.5	0.1-0.5	1017-1019	400-500	2500-4700
105	2.75-2.32	2.25-2.38	0.1-0.5	0,1-0,5	1017-1019	4CG-500	2500-4700
		2.0			;		2000
0	2,4-2,7	2.4-2.7	0.1-0.3	0.1-0.4	1017-101	500-700	
000	2-3.3	2-2.3	0.2-6.3	0.2-0.5	1015-1017	499-509	3900-4000
ic,	بر بن	2.5	0.9	15-30	1312-1016	456-1300	425-1360
	i)	in :†:	50-150	70-170	1011-1014	230-800	250-1600
	 	2.76	59	7.	5 × 10 16	500	
10	3.6-3.5	5.1-3.3			1014-1017	+50-550	
in 100	3.9-7.6	က ()	85		1913-1914	336-430	1500-1760
	3,1	2.6	01-0		1018	496-500	1500-2400
	5-6	4.5-6.4	24-25	12.15	1012-1013	400-200	
	3.8-4	2.8-4.9	10-20	16-100	1013-1014	500-600	
165	3,3-5,5	3.1-4.7	8-30	19-30	1015-1015	400-600	
155	3.2	3.2	(7)		1012-1019		7000-10,000
	4.	÷.÷	38	24	10 t	27.5	
	5.6-4.7	3.3-3.9	14-55	30-40	101 ² -101		
200-280	3.5-5	3.6-3.8		4.1-4.2	101-1013	150-400	
	3.78	3,78		0.2	> 10 ¹⁹		
	5.3	"; 3		٠ .	;		
	8-9.5	8-6.5	0.5-1.5	0.7-2	1014-1016		
	5-3	5.4-7.5	8-25	6-10	10,2-10,4		
		15 x 10 t		0.2-50	1013_1015		
	<i>t</i> -9	2-9	0.1-0.3	1-5	1015_1016	1000-3000	
	5-6				1013-1014	1300-3000	

SECTION 6

REFERENCES

- (1) Whitehead, S., "Dielectric Breakdown of Solids," Oxford Press, p. 115.
- (2) Griemsmann, J.W., "Plastics for Electrical Insulation," Interscience, 1968.
- (3) Von Hippel, As. fur Physik 1931, 67, p. 707, 1932, 68, p. 309, 1939, 75, p. 145.
- (4) Frohlich, Physical Society; Reports on Progress in Physics, 1939, p. 411.
- (5) O'Dwyer, J.J., J. Phys. Chem. Solids, Vol. 28, 1967, pp. 1137-1144.
- (6) Cooper, R., Brit. J. App. Phys., 1966, Vol. 17, p. 149.
- (7) Cooper, R., Elect. Review, February 19, 1965.
- (8) McKeown, J.J., Proc. IEE, Vol. 112, No. 4, 1965, pp. 824-828.
- (9) Artbauer, J., Griac, J., IEE Trans. Elect. Ins. EI-5, No. 4, pp. 104-112.
- (10) Mason, J.H., Progress in Dielectrics, Vol. I, Wiley, 1959.
- (11) Fava, R.A., Proc. IEE, Vol. 112, No. 4, 1965, pp. 819-823.
- (12) Billings, M.J. and Smith, A., IEEE Trans. Elect. Insulation, Vol. EI2, No. 3, December 1967, p. 131.
- (13) Starr, W.T., Insulation, October 1967, p. 128.
- (14) Mason, J.H., Proc. IEE, 98, Part 1, 1951.
- (15) Mason, J. H., Progress in Dielectrics, Vol. I, Wiley.
- (16) Garton, C.G., Gas Discharges and the Electrical Supply Industry, CEGB Conf., England 1962 (Butterworth), pp. 481-488.
- (17) Whitehead, S., Dielectric Breakdown of Solids, Oxford Press, p. 128, 1951.
- (18) Martin, J.C., AWRE (Aldermaston, England) Reports, 1965, 1966.
- (19) Hayworth, B.R., IEEE Trans. Elect. Ins., Vol. EI-3, No. 2, May 1968, p. 47.
- (20) Alston, L.L., Proc. IEE, Vol. 112, No. 4, Ap. 1965, p. 814.
- (21) Ware, P.H., 7th Insulation Conference (1967), p. 255.
- (22) Artbauer, J., Griac, J., IEEE Trans. Elect. Ins., Vol. EI-5, No. 4, pp. 104-112.

- (23) Currence, P., IEEE Paper 68 C6, Elect. Ins. 53, p. 28.
- (24) McGuiness, E.W., Insulation, April 1969, p. 14.
- (25) Bobo, S., Research/Development, March 1968, p. 48.
- (26) McMahon, E.J., IEEE Trans. Elect. Ins. EI-3, No. 1, 1968, pp. 3-10.
- (27) Fujisawa, Y. et al, IEEE Trans., Vol. PAS-87, No. 11, 1968, pp. 1899-1905.
- (28) Yasui, T. and Hayami, T., Sumitomo Electric Tech. Rev., No. 12, March 1968, p. 27.
- (29) Schulein, E., ETZ, Part B, Vol. 20, No. 13, June 1968.
- (30) Gumbel, E.J., National Bureau of Standards, App. Mathematics Series 33, 1954.
- (31) Weber, K.H. and Endicott, H.S., AIEE Trans., Vol. 75, III, p. 371, 1956.
- (32) Epstein, B. and Brooks, H., J. Appl. Phys. 19, pp. 554-550, 1948.
- (33) Creedon, J., Physics International Internal Report, PHR-20-70, June 1970.
- (34) Martin, J. C., "Volume Effect of the Pulse Breakdown Voltage of Plastics," AFWL Dielectric Strength Notes #3, (1965).
- (35) Eustance, J. W., Insulation/Circuits, May 1970, pp. 43-46.
- (36) Ion Physics Corporation, "Low Impedance Simulator Studies," Contract DASA 01-69-C-0091.
- (37) Morton, V.M. and Stannett, A.W., Proc. IEE, <u>115</u>, No. 2, December 1968.
- (38) Milton, O. and Wentz, J. L., Insulation, May 1966, pp. 71-76.
- (39) Milton, O., Insulation, November 1967, pp. 59-65.
- (40) Goba, F.A., IEEE Trans. Elect. Ins. EI-4, No. 2, pp. 31-58, 1969.
- (41) Black, R.M. and Reynolds, E.H., IEE Conf. Dielectric and Insulating Materials, London, April 1964.
- (42) Clark, F.M., Insulation Materials for Design and Engineering Practice, Wiley and Sons, New York.
- (43) McMath, J.P.C., Grzybowski, S. and White, T.J., Proc. Elect. Insulation Conf., September 1971, pp. 150-153.
- (44) Azam, M.N., Brit. J.A.P., Vol. 12, August 1961, pp. 419-420.

- (45) Melnikov, M.A., Elektrichestvo 2, 64, 1959 (Russian).
- (46) Alston, L.L., Proc. International Conf. on Gas Discharges and the Electrical Supply Industry (Butterworths, England), 1962).
- (47) Hayworth, B.R., IEEE Trans. Elect. Insulation, Vol. EI-3, No. 2, May 1968, pp. 47-49.
- (48) Olyphant, M., Gas Discharges and the Electricity Supply Industry, Butterworths, London, 1962, pp. 447-460.
- (49) Goulsbra, D. et al., IEE Conf. Dielectric Materials (England), July 1970, pp. 276-280.
- (50) Schiweck, L., Dr. Ing. Thesis, Technical University Braunschweig, Germany, 1969.
- (51) Insulation/Circuits--Directory/Encyclopedia. Published annually by Lake Publishing Corporation, Texas.
- (52) "Materials Engineering" (Materials Selector Issue--annually).
- (53) Von Hippel, A., "Dielectric Materials and Applications," Wiley.
- (54) Clark, F., "Insulating Materials for Design and Engineering Practice," Wiley.
- (55) Air Force Materials Laboratory, EPIC Reports (Electronic Properties Information Center).

SECTION 7 VACUUM DIELECTRIC

7.1 General Discussion

As the pressure of a gas is reduced below atmospheric the dielectric strength falls to a minimum value and then begins to rise again. Section 4 discussed this in terms of Paschen's law (Figure 4.1) which states that the breakdown voltage of a gas is a function of the product of pressure and gap. The shape of the Paschen law curve at pressures below that for minimum sparking voltage indicates that larger gaps will break down at lower voltage than smaller gaps, and this is found to be true in practice. Attempts to make a small gap break down can lead to a discharge around either a longer path of length corresponding to that determined by the pressure and the Paschen minimum or the longest path available in the volume. Designing for this region of gaseous breakdown is discussed at length in reference (1). As pressure is reduced towards a value corresponding to that where the mean free path approaches the length of any possible discharge path the Paschen law no longer holds, as would be expected from its theoretical justification based on gas ionization. Dielectric strength then becomes relatively high. The transition region between the Paschen discharge range and that where the mean free path is large has largely been ignored by experimentalists, probably because of experimental difficulties. It is of little practical interest, except insofar as it marks the upper end of the true vacuum regime which is a desirable operating region for some vacuum devices (later). In the following discussion of vacuum insulation it can be assumed that the mean free path is large compared to the dimensions of the system, and as a consequence a charged particle drawn from one electrode to another is unlikely to collide with a residual gas molecule. This vacuum range usually exists in systems below about 10⁻³ torr.

In general, vacuum is used as a dielectric not for its insulating properties but for other reasons. Typical reasons are -- a need for long mean free paths, for example as in electron tubes and velocity separators; where it is desired to minimize drag, for example in the electrostatic gyro; and where it is the natural environment, i.e., in space.

There are several good sources of information on electrical breakdown in vacuum, or to put it more positively, vacuum insulation. Hawley and Maitland published a comprehensive bibliography in 1967⁽²⁾ citing 556 articles. These were classified by subject matter and cross indexed. Slivkov has written a book on the subject, ⁽³⁾ and a Handbook of Vacuum Insulation was prepared by Mulcahy and Bolin for the U.S. Army Electronics Command. ⁽⁴⁾ An International Symposium on the subject was initiated in 1964 (MIT) and repeated in 1966 (MIT), 1968 (Paris) and 1970 (Canada) and is scheduled for September 1972 (Poznan, Poland). The Proceedings of these Symposia, which are referred to extensively later, essentially present the state of the art in the field. Much of the earlier work is confused by poor technique, and the interested reader, with some exceptions, is advised to concentrate on the period since 1930. There is more than enough literature in that recent period, particularly in the Symposia proceedings to give a detailed education in the subject.

The mechanisms which limit voltage performance in vacuum can be broadly classified as field emission, field emission initiated breakdown, clump initiated breakdown, and microdischarges. These are associated with action at electrode surfaces, which leads to the generation of vapor locally when a specific voltage is exceeded and then vacuum arcing in the vapor. The ultimate requirement for electrical breakdown is a local temperature sufficiently high to produce the vaporization necessary for the arc.

Field emission, which is discussed briefly in Section 3, can not only limit voltage performance by current drain, but also can lead to complete collapse of insulating strength (vacuum arcing) through its contribution

to one of several possible breakdown mechanisms. In 1928, Fowler and Nordheim, (5) using the newly developed quantum mechanics theory, developed an expression for electron field emission current (I) which can be simplified to

$$I = AE^2 e^{-B/E}$$
 (1)

where

E = electric field strength

A = constant, depending on the emitter area

B = constant, depending on the work function of the cathode surface

The exponential term in expression (1) is dominant, and with pure field emission a plot of log I versus 1/V for an electrode system is usually linear. Even when numerous emitting points exist on a surface a linear plot is obtained, as has been explained by Tomaschke et al. (6)

From expression (1), using the appropriate constants, appreciable currents would be expected at fields of the order 3×10^7 V/cm; whereas, normal emission is experienced at <u>macroscopic</u> fields of the order 10^5 V/cm because of microscopic stress intensification on the cathode surface. This intensification is usually associated with microprojections, or whiskers, on the surface, and it is usual to apply a enhancement factor (β) to the macroscopic field to account for emission. A value β = 500 is a good design assumption.

At small gaps, for example less than 1 mm, and short applied pulse durations (later), it can reasonably be assumed that vacuum breakdown is initiated by field emission (although another process may produce the field emission site). However, at larger gaps and with continuous voltage or long duration pulses there is ample evidence that other mechanisms exist. Recent papers by Chatterton, (7) Rohrbach, (8) Mesyats (9) and Davies give a pood insight into the data and concepts which will be treated more briefly here.

To begin with it will be assumed that ultra high vacuum conditions exist (10⁻⁸ torr range or below) and that there is an absence of "significant" organic contamination. "Significant" refers to the presence or absence of imperfect electrode surface conditions which allow microdischarges to exist (later).

Cathode initiated breakdown: In this case breakdown is initiated by the vaporization of a microprojection or whisker on the cathode due to intense field emission from the projection. The vaporization temperature is achieved by the combination of Joule heating and the Nottingham effect (in some cases at higher temperatures the Nottingham effect may exert a cooling influence).

Anode initiated breakdown: Here breakdown is produced by melting at a spot on the anode due to bombardment by the electron beam associated with an emitting point on the cathode.

Utsumi and Dalton (11) have studied the factors which determine whether cathode initiated or anode initiated breakdown occurs. They were able to develop ranges within which a particular type of initiation occurred, these ranges being a function of the field intensification (β) and the gap spacing (Figure 7.1).

Microparticle initiated breakdown: This mechanism of breakdown is based on the "clump" hypothesis first expounded by Cranberg. (12) This assumes the existence of "loosely bound" microparticles on an electrode surface, which become detached under the action of the electric field and accelerate across the gap. Slivkov (13) has postulated that the clump must have sufficient energy to vaporize itself when it strikes the opposite electrode, and the resultant vapor must be sufficient to start a gas discharge. These considerations lead to a relationship V = Kd^{0.625} where V is the breakdown voltage, d is the gap spacing and K is a constant. Olendzkaya (14) has suggested, for larger diameter particles, that breakdown may be triggered by a small discharge between the particle and the electrode it is approaching. There is various evidence (7) confirming that "clumps" exist in vacuum gaps in one form, or another, and that they move between electrodes.

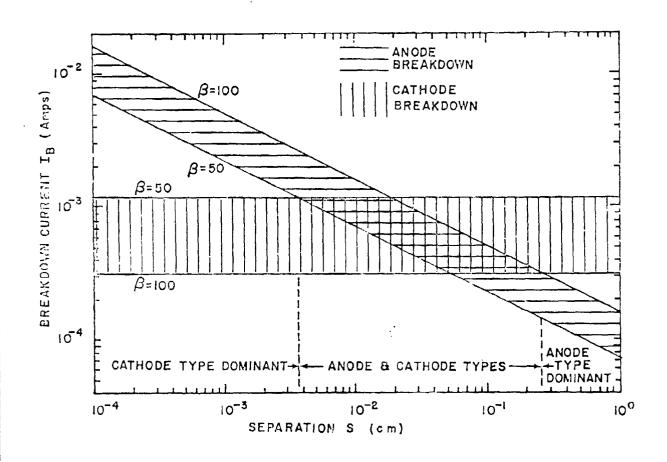


Figure 7.1 Theoretical anode and cathode dominated regions of field emission initiated breakdown.

Combinations of the above mechanisms can exist and lead to breakdown. For example, Little and Smith (15) and Biradar and Chatterton (16) have found craters on cathodes caused by microparticle bombardment. Protrusions at those craters can cause field emission and breakdown. On the other hand Davies and Biondi (10) postulate with considerable theoretical and experimental justification, that breakdown can be caused by the avalanche amplification of current in the vapor produced by the evaporation of an anode microparticle during its transit to the cathode. The particle is heated by the electron beam which initially caused its detachment from the anode.

It has been shown by Rohrbach⁽⁸⁾ and others that different time lags exist for the various breakdown processes. For example, because of the small thermal inertia of a microprojection the delay in cathode initiated breakdown is less than 1 us, whereas as much as 1 millisecond is required for anode initiated breakdown. Time lags in the range 1-100 us would be expected for the microparticle initiation process.⁽⁸⁾

Turning now to the "contaminated" situation, which is a common characteristic of most vacuum systems, it is essential to consider the effect of absorbed foreign material on the electrode surfaces. (17) Contamination on the cathode will product confusing and varying emission data - for example, in parallel experiments, Kelsey and Tedford examined the prebreakdown emission current in two systems, one oil diffusion pumped with a liquid nitrogen trap at about 5×10^{-7} torr and the other baked and ion pumped at about 10^{-10} torr. The former gave variable Fowler Nordheim plots indicating a "3" as high as 700, whereas the latter gave good plots with a 8 about 100.

More important than this, perhaps, is the propensity for microdischarge generation when contamination, usually organic, is present. A microdischarge is a small self-quenching pulse of current occurring at a specific threshold voltage related to the electrode condition and having a total charge $> 10^{-7}$ coulombs lasting 50 usec to several milliseconds. It most

commonly occurs at gaps above about 1 mm. A typical pulse is shown in Figure 7.2. A transient increase in pressure is generally observed when microdischarge occurs. If voltage is raised carefully so that the pressure does not become excessive a steady increase in the threshold voltage can usually be achieved to a point where sparking occurs.

The bulk of the evidence indicates that microdischarges are initiated by ion exchange, although most of the current is electronic, presumably because of the high secondary emission coefficient of electrons by ions. A cumulative mechanism according to

$$AB \ge 1 \tag{2}$$

is indicated where

A = number of negative ions produced/positive ion

B = number of positive ions produced/negative ion

The ions involved appear to be predominantly of hydrogen, and experiments using magnetic fields to deflect the electron current have shown that initiation is related to the ions, not the electrons. (19) Goldman et al (20) have monitored the transient development of microdischarges at voltages below 50 kV and found that initially the charge carriers are predominantly electrons, but as the process develops there is a change to ions predominating, which seems to conflict with the above mechanism. Also, some data (21) indicates that particles much heavier than hydrogen ions are involved in the microdischarge, so that at the present time the mechanism which initiates the microdischarge is in question. Measurements have been made by Smith (22) on the coefficients A and B under applied voltage pulses at higher levels (>>100 kV), and a product AB just above 1 obtained.

In large systems which have to support very high voltages in vacuum, for example velocity separators, it is uneconomic to have ultra

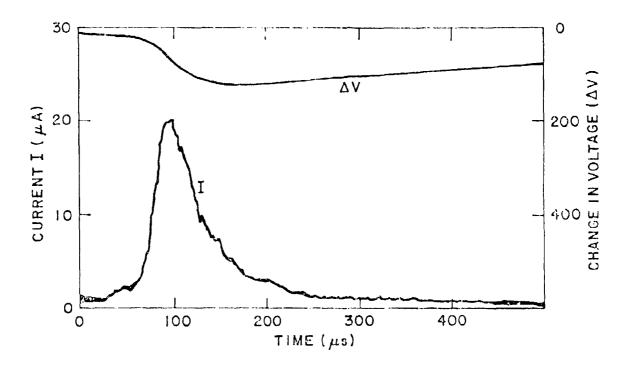


Figure 7.2 Microdischarge - voltage and current for steel electrodes, 1 mm gap, 22 kV (after Boersch et al, Z. angew., Phys. 13, 450 (1961).

high vacuum, and surface conditions exist which produce microdischarges associated with various areas in the system - the integrated effect of the pulses appearing as a relatively steady loading on the supply when the threshold voltage is reached. As noted earlier, this threshold voltage can be raised by controlled conditioning. Also, operation at a specific gas pressure just below the gas discharge region (e.g. 10^{-3} torr) makes a very significant increase in the threshold voltage. Presumably the residual gas atoms interfere with the multiple ion transits required to initiate the microdischarges. Tinguely et al (23) describe the technique they use in achieving a working gradient of 700 kV across 7 cm in a 2 meter separator at CERN (pressure 7.10⁻⁴ torr of helium-neon mixture). Operation at higher gas pressure can also be used to reduce field emitting microprojections on the cathode, or local contamination levels, by ion sputtering (Figure 7.3). The ions are produced in the gas close to the emitting point by the electrons from the point. This has been treated by several investigators.

From the above discussion it is obvious that electrode material and its surface condition are of critical importance in vacuum insulation. To minimize surface contamination it is desirable to use "clean" pumps, such as turbomolecular or ion, rather than oil diffusion pumps, and sources of organic contamination in the system should be eliminated or minimized. (23,27) The exception to this is where voltage is applied in very fast pulses, less than 1 μs in duration perhaps, in which case contamination is of less concern.

Mulcahy and his colleagues have conducted extensive experiments at voltages up to 300 kV at 10^{-8} torm in a bakeable vacuum system to provide design information for high power tubes. (28) These experiments were statistically designed and controlled to determine the important factors in vacuum breakdown and their interaction. Table 7.1 shows these factors with recommendations for tube (and other) designers.

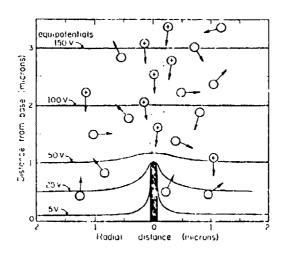


Figure 7.3 Schematic representation of selective ion bombardment of a one micron (10^{-4} cm) projection. Calculated equipotentials are shown for an average electric field of 5 x 10^5 V/cm.

Table 7.1 Factors and effects in vacuum insulation.

FACTOR	EFFECT ON BREAK- DOWN VOLTAGE	INTERACTS WITH:	RECOMMENDATIONS
ANODE MATERIAL	Refractory metals have higher E.D.V.'s than non-refractory metals.	Conditioning. Discharge Energy, Gas Content	Use retractory metals; especially when high energy discharges are to be endured.
CATHODE MATERIAL	Cu better than Al. No significant difference between Ni, Ti, SS.	Gas Content, Anode Material - with many moderate or high energy discharges the cathode becomes covered with a layer of anode material.	Some improvement can be obtained with high strength cathode materials.
CONDITIONING	Increases B.D.V. by more than a factor of 2 in most cases.	Discharge Energy, Anode Material	Conditioning technique is very important. If high energy discharges are possible, conditioning should use high energy, discharges and a good anode material.
GAP	B. D. V. is proportional to: Cap below .75 cm;, to . Gap above .75 cm;	Gas Content, Geometry	When appropriate break a large gap into a series of small gaps.
GEOMETRY OF ELECTRODES	Spherical or curved surface better than ilat surfaces. Small areas better than large areas.	Gas Content, Polarity	Use geometries which minimize highly stressed area, even if this increases the maximum electric field.

Table 7.1 (Continued).

FACTOR	EFFECT ON BREAK- DOWN VOLTAGE	INTERACTS WITH:	RECOMMENDATIONS
SURFACE. FINISH	Not significant if surface is reasonably smooth and clean.	Contamination,	Do not expend effort be- yond that which produces a clean and reasonably smooth surface.
GAS	Fure gases have a neglible effect, but gases exposure seldom reduces with dust and ouganic con-18.D.V. to below unconditamination reduce the tioned level. B.D.V.	Degree of Conditioning; exposure seldom reduces B.D.V. to below uncondi- tioned level.	Avoid exposure to contaminated gases.
BARIUM	Temporary reduction in B.D.V. that can be conditioned away.	Cathode (lowered B.D.V. only when on Cathode), Conditioning, High Energy Discharge.	Proper conditioning tech- niques can minimize de- grading effects.
MAGNETIC FIELD	Lowers B.D.V. for gaps <.75 cm - raises B.D.V. for gaps > .75 cm.	Сар	Avoid magnetic field in highly stressed regions.
PROCESSING BAKEOUT (GAS CONTENT)	Bakeout increases B.D.V.	Electrode Material and Geometry	Hydrogen or vacuum firing of electrodes can be beneficial. Complete system bakeout is useful.
TIME	The longer the period of application of stress the more likely a low breakdown woltage.	Conditioning, Contamina- tion	Minimize time at highest stress but do not leave without stress or deconditioning may occur.

Table 7.1 (Continued).

FACTOR	EFFECT ON BREAK- DOWN VOLTAGE	INTERACTS WITH:	RECOMMENDATIONS
PREBREAKDOWN CURRENT	High prebreakdown currents can heat anode and lead to breakdown.	Gap, Magnetic Field, Conditioning, Electrode Material	When possible, condition to produce low prebreak-down currents.
DIELECTRIC	Cathode coatings can raise B. D. V. significantly.	Polarity - Anode coating usually detrimental; con- ditioning	Apply a thin dielectric film to the cathode when possible.
PRESSURE	As the glow discharge pressure range is approached the B.D.V. goes through a maximum.	Geometry; Conditioning	When possible, use "high" pressure operation or con- citioning.
ELECTRODE TEMPERATURE	Heated cathodes may raise E.D.V.; heated anodes lower B.D.V.; cryogenic cooling may raise B.D.V.	Polarity; Contamination	More investigation of this factor is required.

In the following sections the general features of vacuum insulation will be treated under Section 7.2, Continuous Stressing, largely because most of the studies have been made with dc. Where exceptions or differences exist for alternating or pulsed voltage conditions they will be discussed in the appropriate sections.

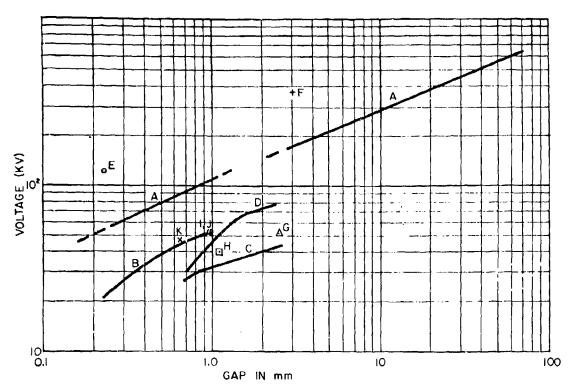
7.2 Continuous Stressing

7.2.1 Breakdown Across Unbridged Gaps With Continuous Voltage

In considering the relationship of breakdown voltage to gap spacing it can be stated to a very rough approximation that the voltage varies linearly with gap below about 1 mm and with the square root of the gap above that value. Figure 7.4 shows a compilation of experimental data $^{(29)}$. With good technique stresses of 1 MV/cm can be insulated across 1 mm over small areas ($\sim 20~{\rm cm}^2$) and 0.13 MV/cm across 6 cm with slightly larger area ($\sim 600~{\rm cm}^2$).

Data such as those shown on Figure 7.4 have to be used with care, since in many instances the experimental conditions are not explicitly known and, as has already been indicated, they can strongly influence performance. Also, in many cases, the data represent the maximum voltage which could be achieved - often after long periods of conditioning, and the values do not represent a useful operational level.

McCoy et al⁽³⁰⁾, in a program to develop vacuum insulated electrostatic generators where operating gaps have to be small (< 1 mm), have reported on the effect of metallurgy in vacuum insulation. The data they report is the maximum voltage which can be supported for 5 minutes. Vacuum conditions were reasonably free of organics (mercury diffusion pumps with liquid nitrogen traps and pressures 5×10^{-7} torr to 1×10^{-6} torr). Figure 7.5 shows the insulation strength obtained for commonly available stainless steels. Curve 1 shows performance with electrodes which were not given a final wipe



Α. Ref. 13, steel electrodes, area $\approx 1~\text{cm}^3$, breakdown voltage. ₿. Ref. 4, steel electrodes, area = 1 cm², insulation strength. Present experiments, steel, area $\approx 20~\mathrm{cm}^2$ (traces of dust),

C.

D,

Ε.

- insulation strength. Present experiments, steel, area ≈20 cm² (nondusty),
 - insulation strength.
 - Rsf. 14, molybdenum, outgassed at 1400 C, area $< 1~\mathrm{cm^2}$, bdv.
- F. Ref. 15, molybdenum, outgassed to bright red heat, area <1 cm², bdv. Model-generator gap,
- G, and H.
- Present experiments, Inconel, area =20 cm²) insulation
- strength. Present experiments, nickel, area≈20 cm3 insulation J.
- Present experiments, AM-355 Alloy, area≈20 cm²) Insulation strength.

Figure 7.4 Vacuum-breakdown voltages and insulation strength.

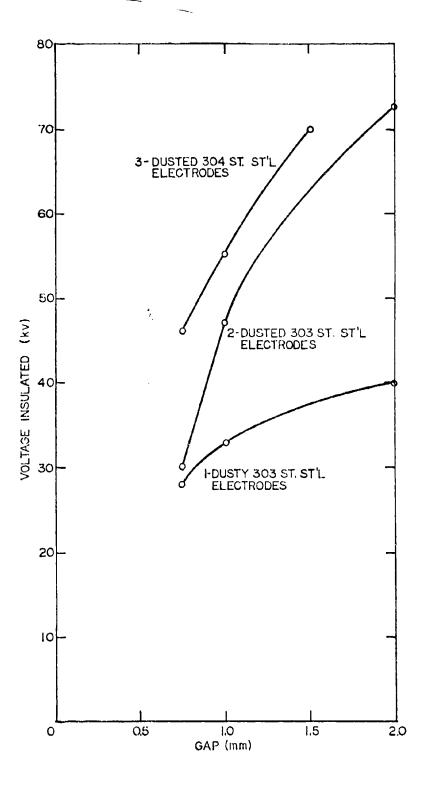


Figure 7.5 Voltage insulated vs gap for 303 & 304 stainless steel electrodes.

with lens paper before pumpdown. Tables 7.2 and 7.3 show the strengths for various high strength alloys indicating the importance of composition. Surface finish also is important (Figure 7.6). It is worth roting that because this work was aimed at the development of a high speed generator, the interest was concentrated on materials with a high strength to weight ratio, which led to the examination of titanium alloys. The favorable indications (Figure 7.6) were noted by other investigators, and titanium alloy electrodes are now a critical feature of high gradient accelerator tubes. McCoy and his coworkers concluded that where high field supporting surfaces had to be formed from high strength materials the following should be observed:

- (1) Materials should have a minimum of non-conducting particles dispersed throughout the metal matrix. This can be accomplished by choosing allotropic transformation type alloys to reduce precipitates, and by specifying vacuum melted materials to reduce impurities.
- (2) Electrodes should be given a very fine polish using metallographic techniques to produce surface finishes less than 2μ in rms.
- (3) Anode material should be chosen with as much care as cathode material. A high temperature material is preferred.
- (4) The material should be as hard as heat treatment and/or cold working will allow.

This paper also describes good finishing and cleaning technique.

In the course of a study of breakdown mechanisms at higher voltages, Rohrbach⁽³¹⁾ has determined the threshold voltage for microdischarges and other discharges for stainless steel in ultra high vacuum conditions (Figure 7.7). Results before and after the tests (10⁵ discharges) are shown and are in reasonable agreement. Huguenin and his colleagues⁽³²⁾ have examined

Table 7.2 Insulation strengths obtained using buff polished high strength alloy electrodes.

gap = 1 mm

Electrode Material	Insulation Strength (kV)
304 Stainless Steel	60
Udimet A	55
Inconel-718	50
303 Stainless Steel	43
Inconel	43
Incone1-X	40
Haynes-25	24
Udimet-41	23
Hastalloy B	15
Multimet	10
ΛM-355	60

Table 7.3 Insulation strengths obtained using metallographically polished allotropic transformation type alloys.

gap = 1 mm

Electrode Material	Insulation Strength (kV)
AM-355	75
Ti-7Al-4Mo	110

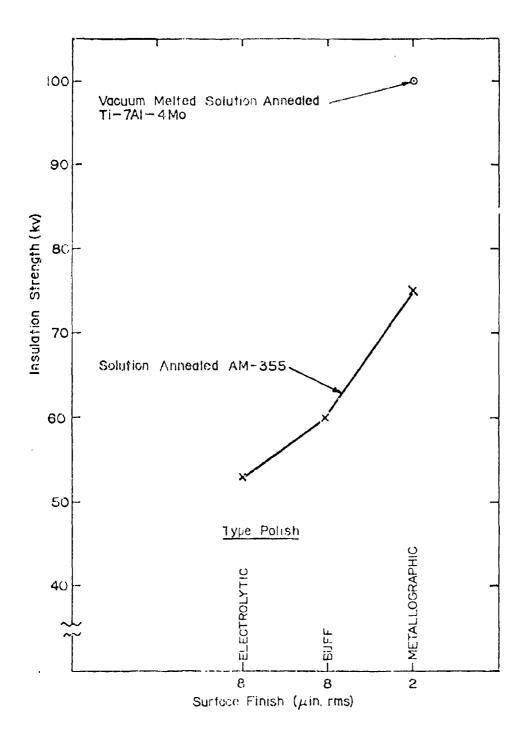


Figure 7.6 Insulation strength as a function of electrode surface finish

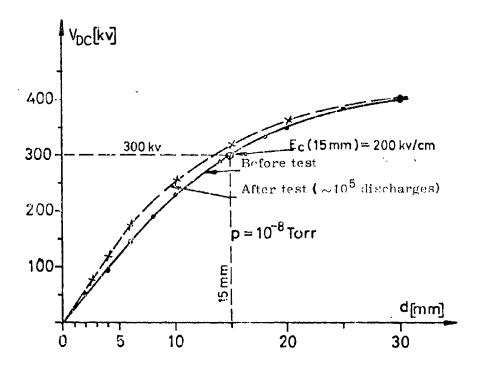


Figure 7.7 Insulation of continuous voltage and threshold for microdischarges and breakdown.

the insulation strength between titanium electrodes up to 850 kV with the results shown in Figure 7.8. In this case the voltage plotted is that giving a current less than 10^{-7} A. The best results are 20 MV/m at 1 cm, 16 MV/m at 3 cm and 13 MV/m at 6 cm. The electrode area was about 600 cm² and the pressure 10^{-7} torr.

There are several techniques which can be used to improve the performance of vacuum gaps. In one of these, already discussed, the pressure is raised either to raise the microdischarge threshold (at higher voltages) or to sputer down emitting protrusions (at lower voltages). As might be expected, the increase in the microdischarge threshold is an instantaneous effect, and the sputter reduction takes time. An improvement similar to that obtained on the microdischarge threshold by pressure increase can be obtained by protecting one electrode surface by a grid, biased to suppress secondaries from the surface it is protecting. Arnold has discussed this effect briefly with regard to tests on a positive bushing in vacuum. The grid used was about 85% open and spaced about 2 cm from the surface it was protecting. Application of a suppressing bias, i.e. more negative than the surface it protects, or vice versa, gives an immediate large increase in the loading threshold voltage (Table 7.4). A bias voltage of less than 1 kV is sufficient. Arnold attributed the improvement to an effective reduction in area of the stressed surfaces (below). More recently, Smith (34) has experimented with electrodes made with wires with encouraging success, perhaps for similar reasons.

The reduction in insulation strength with increasing area is as evident in vacuum as in other highly stressed dielectrics. Denholm has reported information on this effect for 304 stainless steel and titanium alloy at 1 mm gaps (Figure 7.9), and Simon and Michelier for larger gaps and correspondingly higher voltages. Their data, shown on Figures 7.10 and 7.11 is for cathode and anode of stainless steel (Figure 7.10) and cathode of anodized aluminum and anode of stainless steel (Figure 7.11). Performance

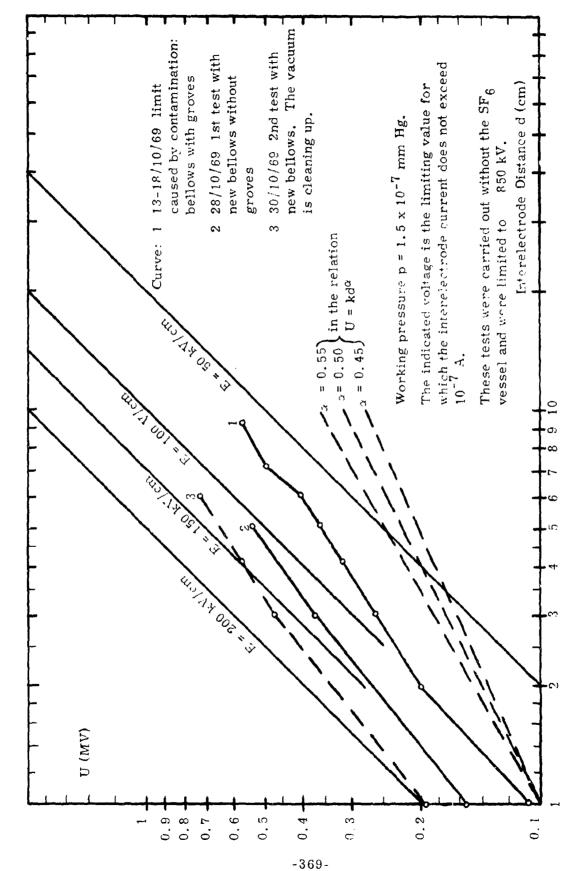


Figure 7.8 Voltage in vacuum between titanium electrodes as a function of the gap.

Table 7.4 Vacuum breakflown voltage V in kV for a bushing at ambient pressure p torr, utilizing voltage biased grids.

•	Measured values	values	Calculat from Vox	Calculated values from Voca-0.21
	_6 10 torr	_6 torr 10 torr	_6 10 torr	-4 10 torr
With no biased grids	+280	+820	+280	+820
With chamber grid only	+340	+ 1040	+350	+1030
With bushing grid only	+360	no data	+290	no data
With both grids activated	+410	no data	+410	no data
		•		

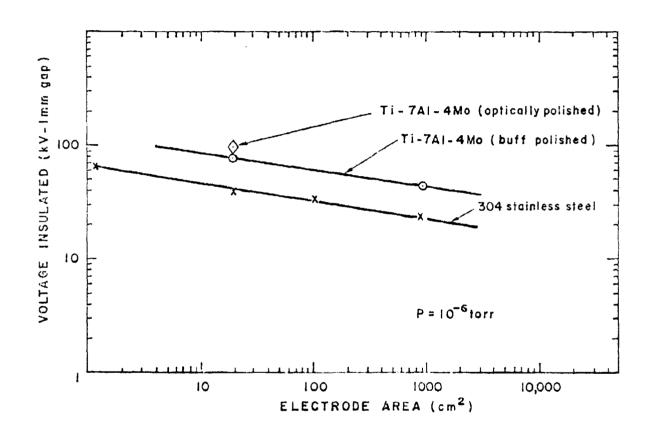


Figure 7.9 Electrode area effect (after Denholm et al (35)).

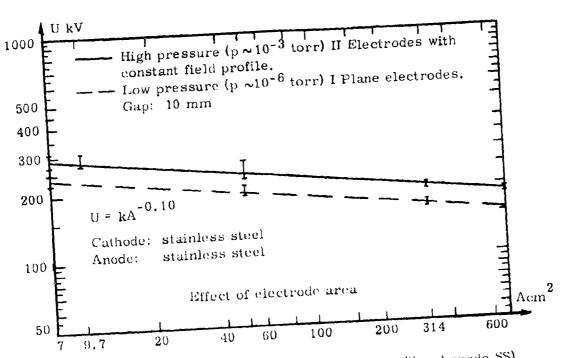


Figure 7.10 Effect of electrode areas (cathode, SS and anode SS).

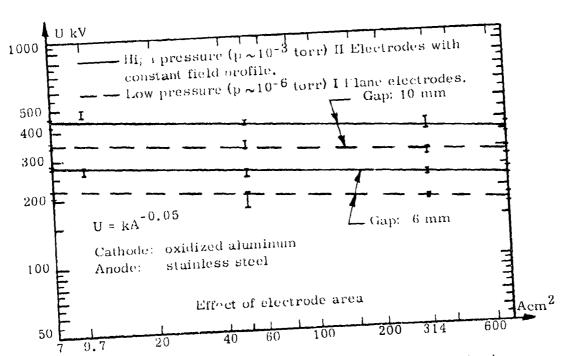


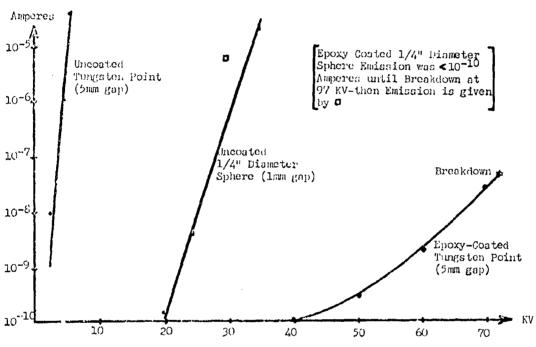
Figure 7.11 Effect of electrode areas (cathode oxidized aluminum, and anode SS).

for both the high vacuum (10⁻⁶ torr) and optimized pressure (10⁻³ torr) condition is shown. Comparing Figures 7.9, 7.10 and 7.11 it can be seen that the area effect is more severe at the smaller gaps (higher stresses), and least severe with the anodized cathode.

Dielectric coated cathodes were pioneered at MIT, particularly by Jedynak (37) who showed that breakdown voltage could be increased by as much as 70%, and prebreakdown current reduced by 2-4 orders of magnitude, by the application of a dielectric film to the cathode surface. Jedynak's article discusses the theory which supports the breakdown voltage improvement, based on the suppression of field emission by the dielectric film. Analyzing his results, and theory, he provided the following specifications for the cathode film:

- (1) Resistivity of at least 10¹¹ ohm-cm.
- (2) Dielectric constant as high as obtainable consistent with the other requirements.
- (3) Dielectric strength of at least 10⁶ volts/cm.
- (4) Film thickness between 10-25 microns.
- (5) Mechanically hard and smooth with high abrasion resistance and high adhesion strength.
- (6) No gas bubbles within the film. However, experiment shows that bubbles much smaller than the film thickness can be tolerated.
- (7) Low vapor pressure and low moisture absorption.
- (8) Chemically resistant to attack by water and solvents.

Further, the cathode substrate should be brought to a mirror finish before application of the film. Belin and Trump (38) have examined the effect of dielectric coatings in strongly nonuniform cathode fields and at 1 mm uniform field gaps. The dramatic effect of coating a negative point is shown on Figure 7.12, and Table 7.5 shows the performance of coated uniform field gaps. It can be



Note: Anode in all cases was of type 304 Stainless Steel, Pressure 1 x 10^{-5} torr

Figure 7.12 Typical bare and coated cathode performance in nonuniform field.

Table 7.5 Typical bare and coated cathode performance in uniform field at 1 mm gap.

	Distant.	Maximum	771	Emissio	n Current i	n Amperes
CATHODE COATING	First Spark KV	Steady Voltage KV	Final Breakdown Voltage KV	Prior to First Spark	At Maximum Voltage	At Finel Voltage
None Stainless Steel	28	55	50	3 x 10 ⁻¹⁰	10 ⁻⁵	10 ⁻⁵
None Aluminum	36	46	44	1 x 10 ⁻¹⁰	10-5	10-5
SiO ₂ Stainless Steel	50	40	30	< 10 ⁻¹⁰	10-7	10 ⁻⁵
Alumina Aluminum	64,	45	20	6 x 10 ⁻⁹	10-6	10 ⁻⁵
Epoxy Stainless Steel	56	40	30	10-9	10-6	10 ⁻⁵

Note: Anode in all cases was type 304 Stainless Steel, Pressure 1 x 10^{-5} torr

seen that the performance of alumina on aluminum is relatively impressive, particularly with regard to the first spark.

The group at CERN have utilized anodized aluminum cathodes extensively to give high performance in their separators. (23,39) Reference 39 describes the process used to provide the alumina layer. Figure 7.13 shows the performance of 20-cm diameter electrodes with and without cathode coatings both at high vacuum and at the optimum pressure. It can be seen that there is a gain with dielectric coatings both at high vacuum and when operated at higher pressure $(10^{-4}-10^{-3} \text{ torr})$. The plot also again shows the superiority of titanium alloy over stainless steel (304).

Another form of dielectric cathode surface is obtained by using glass cathodes. (40) These are successfully employed in the velocity separators at Lawrence Radiation Laboratory, and are run hot (105° C) so that the glass resistivity is reduced to about 4×10^8 ohm cm. These separators (15 feet long, electrodes 12 inches wide) operate at 625 kV across 2-4 inch gaps.

The effect of contamination of the organic kind has already been discussed. It can be removed at some expense by using a completely organic free, bakeable system (metal O'rings, ion or turbo molecular pumps etc.) and operating at ultra high vacuum. However, another form of contamination, which in many cases is essentially present, is that due to evaporation from oxide cathodes. Staprans (42) notes that typical cathode areas are about 100 square centimeters, and that the critical gap is usually between the focus electrode and the anode, at several centimeters from the low work function emission cathode. The emitter is usually a tungsten barium dispenser type or of barium oxide coated nickel. Staprans (42) has provided a valuable collation of stress data from operating tubes, according to whether the gap experiences do, long pulse ($\sim 100~\mu sec$), or short pulse ($< 10~\mu sec$). The data, shown on Figure 7.14, show that on the average the short pulse operation is significantly better than do operation, by a factor of 2 perhaps. The relative performance for long pulse operation is not so obvious, but Stapran makes

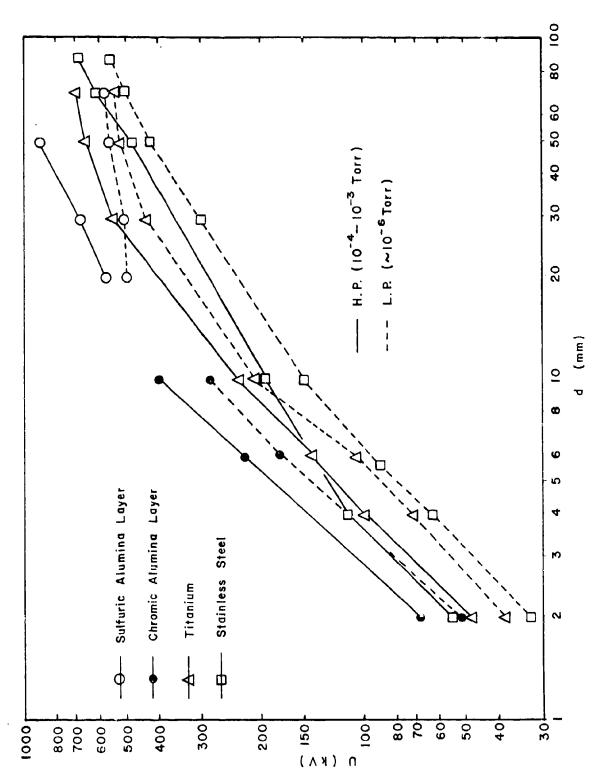


Figure 7.13 Log U - log d plot.

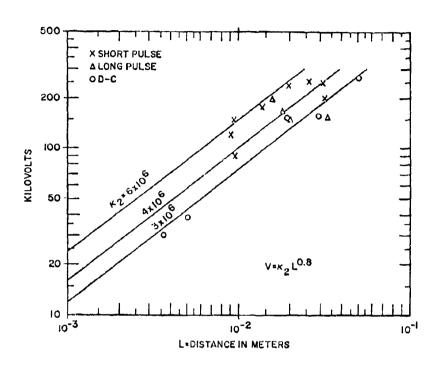


Figure 7.14 Voltage holdoff properties of some tubes.

certain assumptions in pursuing tube design optimization. Mulcahy and Bolin (44) have examined the effect of barium contamination, noting a significant fall in breakdown voltage when a barium cathode was operated. Voltage deterioration was particularly severe when high energy discharges occurred between the electrodes in the presence of barium contamination.

Another factor which can be important to performance is the presence of magnetic field, and its interaction with charged particle movement in vacuum can be rather complex, particularly where dielectric stand offs are involved. Germain et al have examined the case of a quadropole electric field, noting that electron streams are concentrated along field lines thereby enhancing the power density at the anode. In this case reduction of voltage performance because of the magnetic field was not a major problem, if care was taken. With crossed field separators operating at 200-300 gauss it is found necessary to first establish the electric field before applying the magnetic field. (45) In reference (28) it is noted that applying a magnetic field (to 500 gauss) transverse to the electric field slightly raised the breakdown voltage for gaps less than 1 cm and slightly lowered it for gaps more than 1 cm. Experiments with a magnetic field parallel to the electric field could not be conducted because the magnetic field produced flashover of the insulating bushing at a very low voltage level.

7.2.2 Flashover Across Dielectrics with Continuous Voltage

As with gas and liquid dielectrics, the bridging of a gap in vacuum with a solid insulator lowers the insulation strength. Hawley has published a comprehensive review of solid insulators in vacuum as of 1968. The negative end of the insulator is by far the more important, as has been shown, for example, by Kofoid and Coenraads et al. To achieve good flashover performance it has been found essential to have intimate contact between the negative end of the insulator and the metal electrode, or to shield the junction to reduce the stress. In fact, both conditions are desirable.

Figure 7.15 shows a plot of voltage performance versus length across alumina ceramic cylinders where care was taken to have intimate contact by silvering the insulator ends and the terminal stress was reduced by an internal shield. (47)

An electron beam deflection technique has been used by de Tourreil and Srivastava $^{(48)}$ to show that the insulator surface acquires a stable and relatively uniform positive charge in a time much less than a minute - the charge remaining for days after the voltage is removed unless the pressure is raised to 5 x 10^{-3} torr. They suggest, as have others, that this charge exists because of the secondary emission of electrons from the dielectric surface.

The choice of insulator materials for use in vacuum tends to be limited to the inorganics, for example electrical porcelain, alumina or glass (usually pyrex), more because they are not a source of contamination to the rest of the system, rather than because of their superior flashover performance. There are obvious advantages if organics such as lucite or epoxy can be used as a vacuum insulator, and under fast pulse conditions (later), where contamination does not detract significantly from vacuum gap performance they are frequently used. For dc conditions where optimum overall system performance is required the knowledgeable designer chooses inorganic insulation. Srivastava et al (49,50) have studied the flashover of unglazed porcelain, alumina and pyrex at voltage up to 400 kV, and all performed similarly. However, in the long term, porcelain gave more trouble, probably because of porosity. With the insulators recessed into the electrodes 400 kV could be supported across 11.5 cm. Germain et al (39) has determined that with proper fabrication techniques 250 kV-300 kV can be supported across 4 cm of porcelain, alumina or steatite. He noted that it is important that the insulators be unglazed.

Shannon et al have examined many shapes of pyrex (borosilicate) glass to determine the best form of accelerator tube ring. Results for 25 mm long samples carefully borded to stainless steel electrodes with polyvinyl

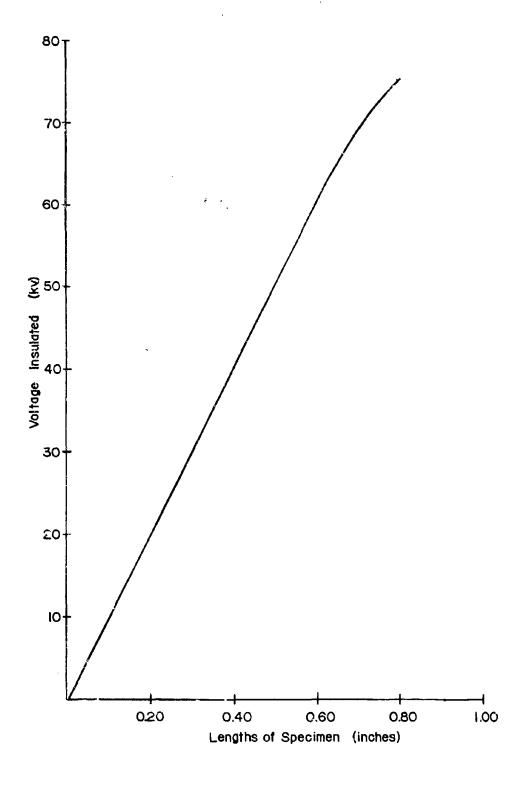


Figure 7.15 Insulation strengths over ${\rm Al}_2{\rm O}_3$ surfaces in vacuum.

acetate are shown on Figure 7.16. Experiments were also conducted to determine resistance to spark damage.

The use of shields to reduce the stress at the negative termination has been widely employed. Finke (52) has experimentally studied the optimum position and clearances for a negative end shield using a spherical shape. An example of the improvement in performance which can be achieved is shown on Figure 7.17.

For the highest voltage applications it is advisable to break the insulator surface into sections, controlling the voltage experienced by each section. This, of course, is standard practice in accelerator tubes. Britton et al (53) have used this technique to design a vacuum bushing which supported 1 MV across a 30 cm length.

7.3 Alternating Stressing

Comparatively little work has been reported on the strength of vacuum gaps under alternating voltage conditions. At power frequencies, bearing in mind the relatively short time constants of the various breakdown mechanisms which have been proposed, it would be expected that the peak breakdown voltage would correspond to, or be slightly larger than, the debreakdown voltage. It is worth considering the fact that polarity reversal occurs in the accase, and that conditioning by sparking or microdischarge loading is a common technique. For example, an anode damage region becomes a cathode region in the next half cycle, and vice versa. In comparing de and ac data it should also be remembered that circuit impedance characteristics can be quite different (discharge energy). Denholm has examined the de, ac and impulse strength of typical engineering metals at small gaps in an oil diffusion pumped vacuum system ($\sim 10^{-6}$ torr) with the results shown on Figure 7.18. More recently, Erven et al (55) have reported 60 Hz studies, again conducted in a dynamically pumped system but at larger gaps. Their breakdown voltages are given in Table 7.6.

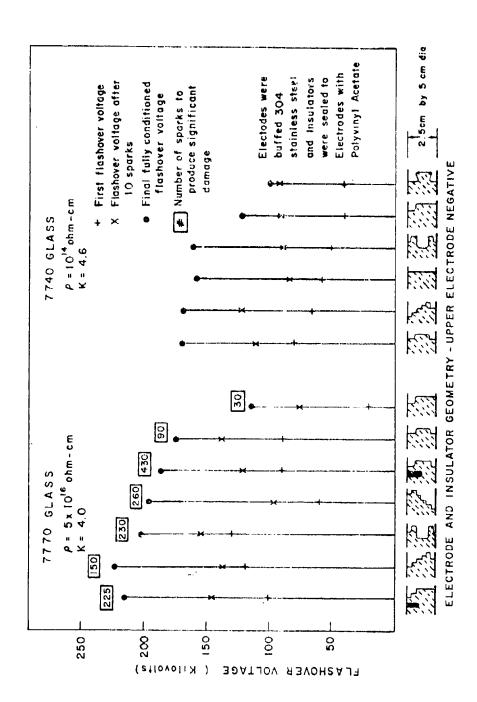


Figure 7.16 dc flashover of glass insulators of various shapes.

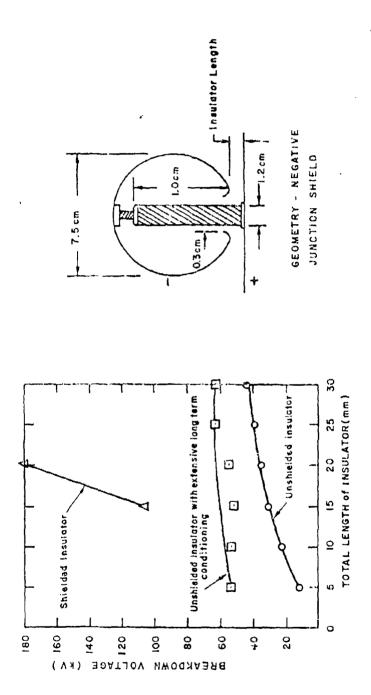


Figure 7.17 Effect of shielding negative junction with re-entrant sphere flashover voltage of standoif insulation.

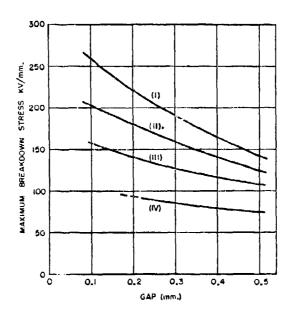


Figure 7.18 Maximum breakdown stresses and insulation strength, steel: (i) impulse voltage, 12/50 waveform; (ii) alternating voltage, 50 cps; (iii) direct voltage, rate of rise 6 kV/second; (iv) insulation strength (maximum dc voltage for zero breakdown in 1 hour).

Table 7.6 60 Hz breakdown voltages.

	<u>0.5 cm</u>	1.0 cm	
Titanium	140 kV rms		
Stainless Steel	110	150	
Aluminum	100	150	
Chromium Copper	95	130	
Copper (OFHC)	85	125	

The ranking of metals, as in Denholm's studies, is essentially the same as the dc case.

The 60 Hz and 21.5 MHz breakdown between tungsten electrodes has been studied experimentally and theoretically by Kustom. (56) His data at 60 Hz (for tungsten) are somewhat higher than for that given by Ervin (Table 7.6), even for titanium, perhaps because of the small size of his electrodes (1.4 cm diameter). A comparison of Kustom's 60 Hz and 21.5 MHz data is given in Figure 7.19. Hill (57) has conducted rf studies at 30 MHz between carefully prepared aluminum alloy electrodes at 10⁻⁷ torr in a turbomolecular pumped system. The gap range studied was 1-4 mm and he concluded that the breakdown voltage was given by

$$V = 31 d^{0.7}$$
 (3)

where d is the gap in millimeters and V is the voltage in kV peak. Lefebvre (58) has reported on the conditioning of a proton linear accelerator operating at 200 MHz.

Consider now the problem of alternating voltage flashover of solid dielectrics in vacuum. Little has been done at power frequency. Kuffel et al, (59) in a comparison of flashover under dc, ac and impulse voltage conditions found, using samples of plexiglass, that the 60 Hz breakdown voltage was about 50% below the dc value. This suggests that a charging process on the dielectric, which takes longer to stabilize than a power frequency half cycle, effectively improves the field distribution in the dc case.

At higher microwave frequencies, the flashover of dielectrics in waveguides at high power is a well known problem. This has been discussed by Hayes and Walker (60) for titanium dioxide in particular. They note that improving edge contact, as discussed earlier, by silvering, and glazing the titania has a highly beneficial effect on voltage performance. This is demonstrated on Table 7.7, which shows performance at 3,000 MHz.

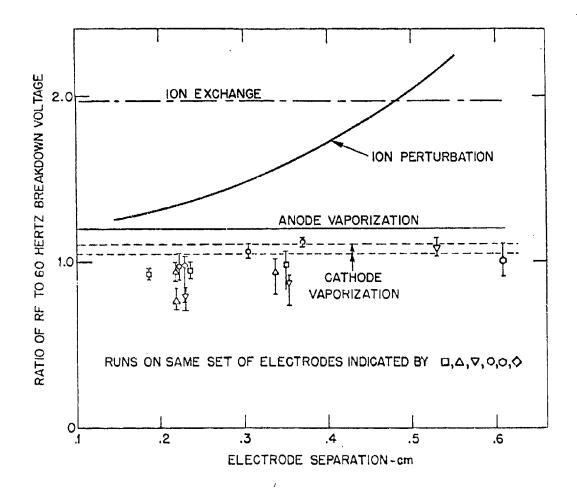


Figure 7.19 Ratio of vacuum breakdown voltage at 21.5 MHz to 60 Hz.

Lines show ratio expected from the following theories:

Ion Exchange - Breakdown due to secondary ion emission and the cumulative interchange of negative and positive ions.

Ion Perturbation - Breakdown due to electron emission enhanced by the

field produced by positive ions.

Cathode Vaporization - Breakdown due to thermal instability at an electron

emitting projection on the cathode.

Anode Vaporization - Breakdown due to thermal instability produced at the

anode by electron bombardment.

Table 7.7 Vacuum breakdown in a titania-loaded cavity.

Electric Intensity at the Disc Surface Maximum Maximum Peak Power Radial Intensity At Breakdown Axial Intensity kV/cm kV/cm kWPlain-titania disc 11.3 700 214 1 202 10.7 620 Glazed disc with silvered edges 17 322 1 1550 17 322 2 1550 Plain disc with silvered edges 11.8 224 750 1 9.9 187 2 650

7.4 Pulsed Stressing

7.4.1 Pulsed Breakdown of Unbridged Gaps

Studies have been made on the strength of vacuum under pulse conditions both to clarify the mechanism of breakdown and because of certain important devices that either have to operate pulsed or may experience transients during service. The largest application of pulsed voltage in vacuum is probably in high power tubes such as klystrons, as discussed by Staprans. In that case the duration can be as short as a few microseconds. Another application, at much shorter time regime, (tens of nanoseconds) is in flash X-ray devices, and of course vacuum devices utilized by the power industry, such as switches, have to withstand the standard and switching impulse tests.

A vacuum gap, in general, can withstand significantly higher stresses under pulsed conditions than under continuous or alternating voltage conditions. As will be seen later in this section the reverse can be true for the vacuum insulator, depending on the duration of the pulse. For the gap case the performance under pulsed stressing improves as the duration of the pulse is reduced, and the following discussion starts with consideration of the longer pulses and proceeds to the shortest examined to date (subnanosecond).

Denholm had indicated the relative performance of small gaps under direct, alternating and pulsed voltage conditions under "engineering" vacuum conditions, i.e. with oil diffusion pumping and with pressure in the 10^{-6} torr range. Unquestionably in this type of vacuum electrodes are subject to significant organic contamination. From Figure 7.18 it can be seen that the impulse (12/50 wave) breakdown voltage is about double the continuous voltage insulation strength (maximum voltage for no breakdown in one hour). Staprans, at larger gaps subject to contamination by low work function materials, but not to organics, has demonstrated on the average a doubling

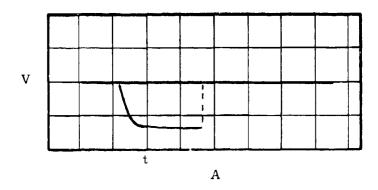
of operating stress between the continuous and "shorter" pulse voltage condition. This shorter pulse duration is not greater than 10 μ sec and probably not much less than 5 μ sec. The relationship he derived from operating tubes in the range 25-300 kV subject to this form of pulse was

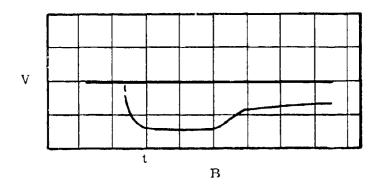
$$V_{\text{max}} = 6x10^6 L^{0.8}$$
 (4)

where V is in volts and L in meters. The areas subject to this stress would be in the range 10-100 cm 2 , and the adjacent oxide cathode about 100 cm 2 in area.

In a program to clarify vacuum breakdown mechanisms, Smith and Mason (63) have examined the impulse breakdown of a 2 cm gap between relatively large area stainless steel electrodes (~2,000 cm²). The vacuum conditions were typical of many large systems. Pumping was with a 20° C baffled oil diffusion pump augmented by a liquid nitrogen cooled cylinder. The pressure was 2x10⁻⁶ torr. The waveform applied had a risetime of 4 microseconds and a discharge time constant of about 5 milliseconds. After some dc conditioning at a 5 cm gap the impulse tests were conducted at 2 cm. Breakdown was at 290 kV which compared with an extrapolated continuous voltage value of 185 kV. It was noted from the oscillograms that there were three types of breakdown (Figure 7.20); namely

- (1) A sharp (complete) breakdown with the voltage collapse taking less than 1 μsec and with a time lag averaging about 24 microseconds (Figure 7.20 A). A few time lags were less than 4 μsec .
- (2) An incomplete breakdown characterized by a smooth drop of about 100 kV over a period of 10 µsec. The slope of the voltage fall corresponded to about 20 amperes drawn from the impulse generator followed by a flow of 3 amperes at





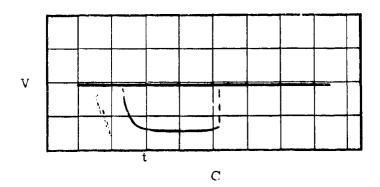


Figure 7.20 Oscillograms showing three types of breakdown. (Time base $\sim 1~\mu$ s/cm)

the lowered voltage (Figure 7.20 B). This was accompanied by a liberation of gas ($\sim 1.5 \times 10^{-3}$ torr), presumably from the electrode surfaces.

(3) The third type of breakdown appears to be a combination of1) and 2), starting as 2) and breaking in to 1) (Figure 7.20 C).

The breakdown described in (1) is seen as a bright localized spark whereas that in (2) is a diffuse, glow-like discharge. In later papers (64,22) the authors describe a series of convincing experiments on effect b) which indicate that it is due to an ion exchange mechanism, as discussed earlier, with a product AB just greater than one.

Rohrbach (8) has studied the impulse breakdown of vacuum gaps (titanium electrodes of area ~80 cm²) over the same general range as Smith and coworkers but in an ultra high vacuum bakeable system((~10⁻⁹ torr). again with the objective of elucidating breakdown mechanisms. The technique used was to apply a 300 kV continuous voltage across the gap then to superimpose an impulse voltage having a risetime of 100 ns and a decay time constant of 132 ms. In this way a total voltage up to 700 kV was obtainable. Some 50,000 pulsed measurements were taken and analyzed by computer to give breakdown probability and time lag at different gaps and total applied voltage. For example, at 8.5 mm the 50% probability of breakdown occurred at 550 kV and zero probability at 500 kV (Figure 7.21). At a gap of 9-10 mm there was a transition zone and at larger gaps the breakdown field fell significantly. Analysis of the time lag distributions suggested the existence of three mechanisms. Very short time lags (0.1-1.0 µsec), independent of voltage and gap, are characteristic of an initiation mechanism based on cathode projection vaporization. Very long time lags (milliseconds), linearly dependent on the gap spacing, are characteristic of anode vaporization. Intermediate times are characteristic of discharge initiation by microparticles. The transition gap region was defined as where the three mechanisms, cathode, anode and microparticle vaporization are more likely to exist simultaneously at voltages close to the static breakdown potential (~300 kV at 10 mm).

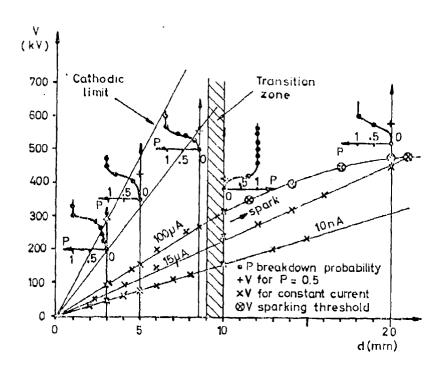
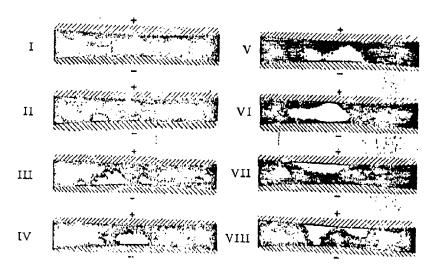


Figure 7.21 Discharge probability P.

(Lines show voltage levels for 10 nA, 15 $_{\rm u}$ A and 100 $_{\rm \mu}$ A currents, and sparking level. Probability of breakdowns at the specific gaps for specific voltages are shown by the small probability curves.)

Most of the studies at very short pulse durations, less than 10⁻⁷ seconds, have been conducted in the USSR, particularly by Mesyats and his colleagues. A great deal of information on breakdown in this time regime was supplied by them at the III and IV International Symposium on Discharges and Electrical Insulation in Vacuum, and is reported in the Proceedings. More recently. Mesyats has summarized the status of fast vacuum breakdown processes at the 10th International Conference on Phenomena in Ionized Gases. (65) In this time regime (<1 µsec say) breakdown is associated with the explosion of microscopic projections on the cathode surface and the progress of the resultant plasma flare across the gap. Mesyats has been able to show this process occurring together with the corresponding current growth (Figure 7.22) associated with electron emission from the plasma flare. The term "explosive emission" has been coined for this current from the flare, and it is of particular technical interest because it occurs with very high current density and with high voltage still existing across the gap, thus making possible flash X-ray and intense electron beam devices. (61,66) Mesyats discusses the emittance characteristics of such diodes in reference (65), and notes that for 5 ns duration pulses a current density of 4×10^9 A/cm² has been achieved without emitter destruction. He also states that emitter destruction occurs over a large range at a constant product of the square of the current density and the pulse duration, namely 4×10^9 amp 2 sec/cm 4 .

The speed with which the vacuum gap breaks down when subject to pulsed overvoltages (and also in many continuous voltage cases—is determined by the velocity of the cathode flare as it moves towards the anode. This has been measured $^{(65)}$ for several cathode materials, lies in the range 1.5-3.0 x 10 cm/sec, and is relatively constant with time and only weakly dependent on the applied voltage. Mesyats notes that 2.0 x 10 cm/sec is typical. Ravary and Goldman have examined the switching (closing) time of negative point to positive plane gaps with a 15 nanosecond risetime pulse generator, and concluded that for gap less than 25 mm the closing time



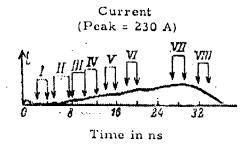


Figure 7.22 Development of gap luminosity in nanosecond breakdown of vacuum gaps.

was proportional to the gap $(\sim 10^{-6} \text{ sec/cm} \text{ at 26.2 kV})$ and independent of the electrode materials. With gaps less than 1 mm their results agreed with those of Mesyats.

Finally, at very short duration (down to 10⁻¹⁰ sec) Juttner et al⁽⁶⁸⁾ have examined the production and destruction of emitters on extended metal surfaces at 10⁻⁹ torr. Their experiments support Jedynak's ⁽⁶⁹⁾ observations that whiskers are produced by discharge vapors. Below a critical pulse length (<2 ns) the production of new emitting sites is strongly reduced, and conditioning with such short pulses can reduce the breakdown probability to zero.

7.4.2 Pulsed Flashover Across Dielectrics

The flashover of dielectries in vacuum depends not only on the pulse duration but on the shape (i.e. risetime) as well. Kuffel (59) has examined the effect of waveshape and compared impulse, alternating, and continuous voltage performance (Figure 7.23). He used plexiglass cylinders of 25 mm diameter and lengths between 5 and 20 mm. The ends were ground and polished then plated with a layer of silver to give intimate contact with the terminating electrode system. The vacuum system was pumped with a liquid nitrogen trapped oil diffusion pump and the ultimate pressure was about 10⁻⁷ torr. To get reasonably consistent pulse breakdown voltages it was necessary to first condition with continuous voltage and allow about 30 minutes between successive breakdown. Figure 7.23 shows the mean performance of 5 samples. Results after conditioning were reproducible to within +5%. The standard impulse voltage (fastest wavefront used) gave the highest flashover voltage, but less than the continuous voltage case, as shown in Figure 7.23. As the wavefront duration was increased to 80 µsec the strength fell, as illustrated on Figure 7.24, then started to rise again. This effect is attributed to space, or surface charges on the insulator.

There have been several investigations on the flashover of dielectrics under shorter duration pulses, mostly in support of flash X-ray tube

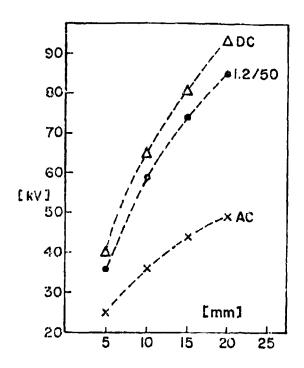


Figure 7.23 Comparison of dc, ac and 1.2/50 μ sec. FO characteristics (p = 1 x 10⁻⁵ torr).

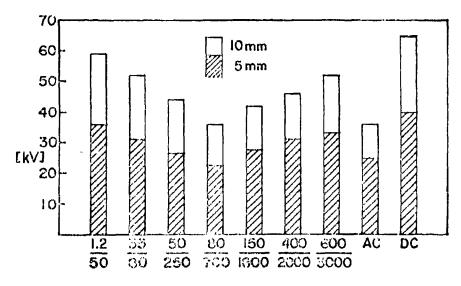
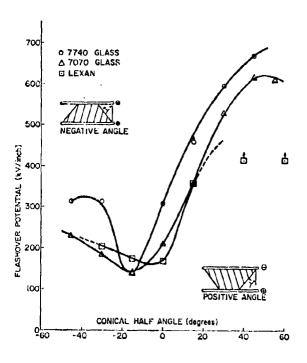


Figure 7.24 Effect of surge front duration on FO voltages. (Pressure 1 x 10^{-5} torr sample thickness 5 mm and 10 mm).

design. (70,71,72) Smith (70) appears to be the first to publish in this time regime and note the beneficial effect of insulator shaping in the form of a conical frustum, the broad end being negative. Similar studies were later conducted by Watson and Shannon (71) in cooperation with J.C. Martin at AWRE. Figure 7. 25 shows some of their data obtained with an effective pulse duration in the range 75-100 ns. In a later publication (73) Watson propounded a breakdown theory based on charging of the insulator surface by the emission of thermionic electrons generated within the dielectric by the electric field, and electron secondary emission down the surface. More recently, Milton has confirmed and significantly expanded the earlier studies by Smith. Watson and Shannon. In the fast pulse regime breakdown is insensitive to pressure, experiments can be conducted under relatively crude vacuum conditions, and organic insulators are practical materials for many applications. Milton used test samples 1.27 cm long in the shape of a conical frustum having a base diameter of 5 cm. Specimens were sandwiched between 10 cm diameter aluminum electrodes finished with 600 grit aluminum oxide. Gleichauf (74) reported that there is no appreciable difference in dielectric flashover performance with different electrode materials.

Two waveforms were used in Milton's experiments, the slower had a duration of 10 μsec and a risetime of 5 μsec . The test voltage was set so that breakdown occurred on the rising portion of the wave, i.e. within 5 μsec . The faster wavefront had a duration of 100 ns and a risetime of 50 ns, chosen to resemble the waveform applied to large electron beam accelerator tubes.

With the longer pulse, test voltage was limited to 300 kV by vacuum flashover of the test chamber. It was also noted that improving the electrode surface finish (e.g. $1/4-\mu$ diamond polish) could raise the performance of some samples, such as lucite, beyond the test limit. A survey of the strength of many common dielectrics was made using a frustum with a base angle of 450. The results are shown in Figure 7.26. The cast nylon performance



41 1

Figure 7.25 The flashover strength of glass and lexan as a function of geometry.

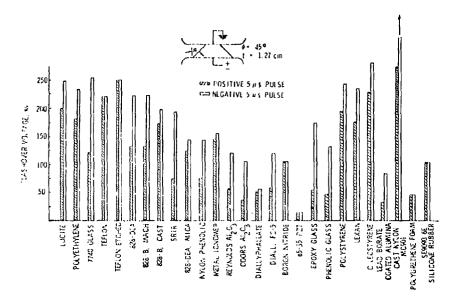


Figure 7.26 Flashover voltage for some dielectrics.

is remarkably good, the high dielectric constant PZT remarkably bad, and Teflon could withstand only one breakdown before deterioration. Figure 7.27 shows the performance of lucite plotted against the square root of the gap distance, and Figures 7.28 and 7.29 the performance of various materials as a function of cone angle.

Less information was obtained with the faster 100 ns pulse than with the 5 µs risetime. Figure 7.30 shows data for lucite. The minimum performance angle noticeably shifts from 0°, with the longer pulse, to -20° with the shorter, in general agreement with Watson's data, and the fast pulse flashover strength is significantly greater than the slow. It was noted that the conditioning effect (typically over 10-15 pulses) that could be obtained with the slower pulse was relatively small, about 10% of 50% for the fast pulse.

7.5 Design Considerations

As noted at the beginning of this section vacuum dielectric is used as an insulant more by necessity than choice, usually where the unrestricted passage of charged, or uncharged, particles is required. Apart from the hazard of radiation, which should always be considered when high voltage is associated with an evacuated volume, vacuum can be an expensive dielectric to "achieve", particularly if the ultra high vacuum regime is required. It is important to understand where very low pressures are essential, and where they are not. At one extreme, with pressures of 10⁻⁸ torr or less, systems are completely inorganic, usually bakeable and metal gasketted, and expensive. At the other, pressures as high as 10⁻³ torr can be used with evacuation by cheap untrapped oil diffusion pumps, or even good rotary pumps. Many organic materials are satisfactory for use in this pressure regime. However, the only area where high electrical fields can be achieved in such a grossly contaminated situation is in fast single pulse applications where the duration of the pulse is short compared to ion movement times, e.g. in

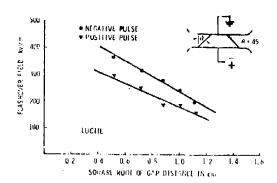


Figure 7.27 Flashover strength versus gap distance for lucite. Pulse risetime about 5 μs .

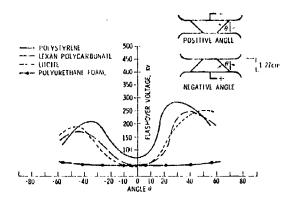


Figure 7.28 Flashover voltage versus angle $\,\theta$ for some insulators. Pulse risetime about 5 μs .

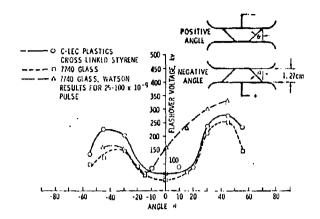


Figure 7.29 Flashover voltage versus angle θ for 7740 glass and crosslinked styrene. Pulse risetime about 5 $\mu s.$

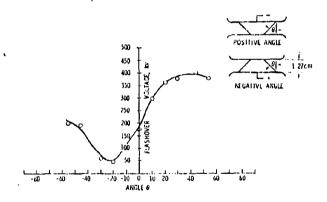


Figure 7.30 Flashover voltage versus angle θ for lucite. Pulse risetime about 50 ns.

low impedance flash X-ray units based on explosive emitter technology. Apart from this time regime, the best advice for reliable performance is to utilize organic-free systems and careful high vacuum technique. Often other factors besides dielectric performance, such as sensitive cathodes, dictate superior vacuum requirements.

The lengths which should be taken in achieving clean vacuum depends on the application. For example, in an experimental situation where long conditioning periods and occasional breakdowns may be tolerable, a system with a well trapped diffusion pump and organic gasketting may suffice, whereas on an industrial production line, or where the system has to be used with expensive equipment, such as a high energy accelerator, reliability is more critical and cleaner vacuum techniques are in order.

Several good texts on vacuum technique exist, (75, 76, 77) starting with the classic by Dushman, but the subject is worth a brief discussion, particularly in relation to vacuum insulation. There has been some controversy about the best vacuum pumping methods to use where reliable vacuum insulation is required, for example in nuclear physics equipment. For many applications mercury rather than oil diffusion pumps are used to reduce organic contaminants, but in recent years ion and turbomolecular pumps have been increasingly utilized. Several recent advances in vacuum insulation technology are in systems evacuated by turbomolecular pumps.

In considering the design of a "clean" system it should be noted that a monomolecular layer can form on a surface in one second at 10⁻⁶ torr, and in particular where electron beams are involved a steady build up of contaminants can occur. Ennos⁽⁷⁹⁾ has used this fact to assess the relative contamination caused by various sources in a vacuum system (Table 7.8). The choice of the best O'ring material is also important where elastomer sealing is used (Table 7.9).

Obviously the cleaning of surfaces which experience high electric fields in vacuum is important. Even surfaces which are not exposed should

Table 7.8

Relative Contamination Caused by Vacuum Materials
(t = 100 min, I = 0.01 A/cm², V = 2 kV)

Material .	Treatment	Thickness of Contamination Deposit(Å)
Diffusion pump oil (Apiezon B)	As supplied	1700
Silicone diffusion pump oil (Dow-Corning 703)	As supplied	500
Vacuum grease (Apiezon M)	As supplied	1500
Apiezon W Wax (cold)	As supplied	< 50
Black neoprene (heavily loaded to give oil resistance)	Boiled in aqueous and alcoholic potash	< 50
O-ring rubber gasket material (W. Edwards and Co., Ltd., London)	Boiled in aqueous and alcoholic potash	600
Brass strip*	Well handled and not subsequently cleaned	700
Brass strip	Cleaned in acid	< 50
Aluminum strip*	Well handled and not subsequently cleaned	700
Aluminum strip	Cleaned in aqueous potash	< 50

^{*} Area of metal equal to internal surface area of electron gun.

Table 7.9
Outgassing Rate for Various Polymers (77)

Polymer	q (to	Outgassing Rate, orr liter/cm ² sec)	x 10 ⁷
	1 hr.	4 hrs.	10 hrs.
Buna S. Butyl Rubber	20	6	
Epoxy (Araldite)	20	10	
Lucite	19	10	
Neoprene (B)	26	8	3.8
Buna N. After 100° C Bake (4 hrs.)	80 10	20 0.6	10 0.4
Nylon	26	12	
Polyethylene	2.3	1.15	
Kel-F	0.4	0.17	
Teflon	2	0.75	
PVC	5	2.8	
Silicone Rubber	70	20	
Viton Unprocessed After 150 ⁰ C Bake in Air (4 hrs.)	4 0.01	1.8 0.003	0.002

be cleaned as effectively as possible, since they provide a source of contamination for the other critical areas (Table 7.8). Various methods of cleaning have been used for electrode surfaces. For example, at CERN the following cleaning procedure is commonly used for metal surfaces exposed to high gradient in vacuum: (80)

- (1) Hot perchlorethylene, vapor and liquid.
- (2) Ultrasonic dip with detergent and hot distilled water rinse.
- (3) Cold acetone dip.
- (4) Cold ethyl-alcohol dip.
- (5) Vacuum degassing at 10⁻⁴ torr and 80° C for twelve hours followed by dry nitrogen filling to prevent reabsorption of water vapor when the tank is opened.

In addition, before this cleaning procedure, great care is taken in polishing to insure that no organic materials are inserted into the material. For example, the common method of buffing with a polishing compound is prohibited, and silicon carbide and alumina powders are used instead to produce a fine finish. Where the application justifies the expense, as discussed earlier, the complete vacuum vessel should be baked, typically to 400° C for 6-8 hours. One measure of the effectiveness of technique, at least for gaps above 1 mm, is the initial threshold voltage for microdischarge generation, usually evidenced as a current loading in the system. In the limit it would be expected that no microdischarges should occur, only discrete vacuum sparks at high voltage.

Table 7.1 provides guidance on the best metals to use for vacuum insulation. This is general agreement with reference (30) which gives more specific guidance. Area effect has to be borne in mind where stressed areas are large, as discussed earlier (Figure 7.9, 7.10 and 7.11).

Several special techniques can be applied to improve performance over that obtainable with the better metal surfaces. The dielectric coating of cathode surfaces is attractive, particularly where anodized aluminum can be

used, as discussed earlier. Operations in a higher pressure range can be most effective where not inadmissable for other reasons (e.g. cathode poisoning). This is particularly true at larger gaps and higher voltages which usually are associated with big systems which cannot be baked for economic reasons, and as a consequence where current loading (microdischarges) is prevalent.

Figure 7.31 shows data obtained by Cooke (26) on the effect of pressure on the current loading threshold voltage. He was able to conduct his experiments into the Paschen discharge region (curve 4) because in his equipment the test gap was the largest available for discharge. In larger systems the Paschen region is entered at a lower pressure because of the greater length of the maximum path available to the gas ionization discharge process. As already discussed, operation at a relatively high pressure can also be used to reduce field emission by the "self-sputtering" effect.

Biased grids (33,81) and open surfaces in general (34) are also effective in raising the threshold level of the microdischarge effect. This is probably because grids reduce the effective area, but there may also be a benefit from the curvature of the field lines around wires. The curvature may tend to inhibit the development of the ion chain mechanism which is generally thought to initiate microdischarges. Grids are effective in a "contaminated" situation, but have to be used with care on a negative surface because of electron emission resulting from the field intensification they produce. Special techniques can be adopted in accelerator tubes to inhibit current loading problems associated with ion mechanisms. One of these involves the use of a biased grid. (81) Another utilizes inclined field electrodes, carefully configured so that the particle which is being accelerated "undulates" through the tube, whereas unwanted ions can experience only minimal acceleration before being trapped in the electrode system.

Finally, it should be noted that the operation of ion gauges and pumps is based on the production of ions, and consequently they should be

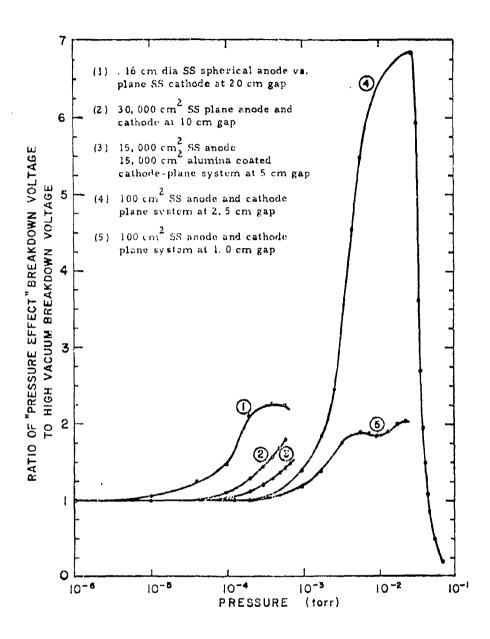


Figure 7.31 Pressure effect for various electrode systems.

shielded from regions which are subjected to high stresses. For example, in some situations it has been noted that an operating ion gauge in the wall of a vacuum vessel has prevented the achievement of the required voltage level - switching off the gauge immediately improves voltage performance. Also, a gauge improperly placed can bombard a bushing or stand-off surface with positive ions, since those surfaces tend to charge negatively, as discussed earlier. The reverse considerations are also true, i.e., electrical discharges in vacuum can react with unshielded ion gauges to blow fuses, or worse, in the gauge circuitry.

SECTION 7

REFERENCES

- (1) Schonhuber, M.J., "Breakdown of Gases Below Paschen Minimum: Basic Design Data of High Voltage Equipment," IEEE Trans. PAS-88, 2, 101 (1969).
- (2) Hawley R. and Maitland A., "Vacuum as an Insulator An Indexed Bibliography," Chapman and Hall, London (1967).
- (3) Slivkov, I. N., "Electrical Insulation and Discharge in Vacuum," Atomizdat, Moscow (1966), FTD-MT-24-123-71.
- (4) Mulcahy, M. and Bolin, P.C., "Handbook of Vacuum Insulation," TR-ECOM-00394-13 (1971).
- (5) Fowler, R. M. and Nordheim, L. W., "Electron Emission in Intense Electric Fields," Proc. Roy. Soc. A119, 173 (1928) and A121, 626 (1928).
- (6) Tomaschke, H. E. et al, "The Role of Electrode Projections in Electrical Breakdown" bc. Symposium I (1964), p. 13.
- (7) Chatterton, P. esent Status of Vacuum Breakdown Research,"
 Proc. Symposius IV 370) Addenda.
- (8) Rohrbach, "Re onship Between Spark Time-Lag Spectra and the Mechanisms Leading to Breakdown between Plane Titanium Electrodes in Ultra-high Vacuum!" Proc. Symposium IV (1970), p. 68.
- (9) Mesyats, A.G., "The Role of Fast Processes in Vacuum Breakdown,".
 Tenth International Conference, Phenomena in Ionized Gases, Oxford,
 England, (1971).
- (10) Davies, D. K. and Biondi, M. A., "Mechanism of D. C. Electrical Breakdown between Extended Electrodes in Vacuum," J. A. P. 42, 8, 3089 (1971).
- (11) Utsumi, T. and Dalton, A.C., "Cathode and Anode Induced Breakdown and Their Criterion," Proc. Symposium II (1966), p. 151.
- (12) Cranberg, L., "The Initiation of Electrical Breakdown in Vacuum," J. A. P. 23, 518 (1952).
- (13) Slivkov, I. N., "Mechanism for Electrical Discharge in Vacuum," Sov. Phys. Tech. Phys. 2, 1928 (1957)
- (14) Olendzkaya, N.S., "Flashover of a Vacuum Gap when Coordinating Particles Pass between the Electrodes," Radio Eng. Electron Phys. 8, 423 (1963).

- (15) Little, R. P. and Smith, S. T., "Investigations into the Source of Sharp Protrusions which Appear on the Flat Cathode Surfaces as a Result of the Application of High Electric Fields," Proc. Symposium II (1966), p. 41.
- (16) Biradar, P. I. and Chatterton, P., "Cathode Surface Structure and Prebreakdown Currents," Proc. Symposium III (1968), p. 35.
- Van Oostrom, A., "Surface Effects in Vacuum Breakdown," Proc. Symposium IV (1970), p. 1.
- (18) Kelsey, J. and Tedford, D.J., "Emission in Vacuum," Proc. Symposium IV (1970), p. 107.
- (19) Boersch, H. et al, "The Contribution of Negative Ions to the Mechanism of Microdischarges," Proc. Symposium II (1966), p. 317.
- (20) Goldman, M. et al, "Study of the Initiation of Microdischarges," Proc. Symposium IV (1970), p. 266.
- (21) Arnal, R. et al, "Transit Times in Microdischarges and Observation before the Spark," Proc. Symposium IV (1970), p. 56.
- (22) Smith, W. A. et al, "Impulse Breakdown of Large Gaps in Vacuum," ibid, p. 96.
- (23) Tinguely, R. et al, "The New Short Separators at CERN" (in French), Proc. Symposium III (1968), p. 254.
- (24) Lyman E. M. et al, "The Effect of Gas Pressure on Electrical Break-down and Field Emission," Proc. Symposium II (1966), p. 33.
- (25) Chatterton, P.A., "The Effect of Gas Species and Concentration on Prebreakdown and Breakdown Phenomena," ibid, p. 195.
- (26) Cooke, C. M., "Residual Pressure and Its Effect on Vacuum Insulation," ibid, p. 181.
- (27) Kovarik, V.J. and Sluyters, T.J.M., "Development of Three 80. KV High Gradient Accelerating Tubes," Proc Symposium IV (1970), p. 172.
- (28) Ion Physics Corporation, "High Voltage Breakdown Study, Final Report," TR-ECOM-00394, (1970).
- (29) Denholm, A.S. et al, "Electrostatic Generators for Spacecraft," Astronautics, p. 46, June (1962).
- (30) McCoy, F. et al, "Some Effects of Electrode Metallurgy and Field Emission on High Voltage Insulation in Vacuum," Proc. Symposium I (1964) Addenda.

- (31) Rohrbach, F., "Measurements of Delay Time of Very High Voltage Breakdown in Ultra High Vacuum" (in French), Proc. Symposium III (1968), p. 396.
- (32) Huguenin, J. et al, "The Insulation up to 1-4 MV between Titanium Electrodes as a Function of the Distance to Date, 850 KV" (in French), Proc. Symposium IV (1970), p. 166.
- (33) Arnold, K., "Vacuum Breakdown Phenomena at 1 Million Volts: A Postscript," Proc. Symposium II (1966), p. 73.
- (34) Smith, W. A., "Wire Electrodes in Electrostatic Separators," Proc. Symposium IV (1970), p. 185.
- (35) Denholm, A. S. et al, "The Variable Capacitance Vacuum Insulated Generator a Progress Report,". Proc. of Symposium on Electrostatic Energy Conversion, (1963), PIC-ELE 209/1.
- (36) Simon, D. J. and Michelier, R., "Experiments on an Electrostatic Separator with Multiple Plates" (in French), Proc. Symposium III (1968), p. 263.
- (37) Jedynak, L., "Dielectric Coatings in Vacuum Gaps," Proc. Symposium I (1964), p. 147.
- (38) Bolin, P.C. and Trump, J.G., "Insulating Vacuum Gaps with Dielectric Cathode Surfaces," Proc. Symposium III (1968), p. 50.
- (39) Germain, C. et al, "Technological Developments of the CERN Electrostatic Separator Program," Proc. Symposium II (1966), p. 279.
- (40) Edwards, G. W., "Velocity Spectrometers used in Bevatron Deflected Beam Research," Proc. Symposium III (1968), p. 296.
- (41) Brodie, I., "The Effect of the Presence of an Oxide Coated Cathode on the Voltage Insulation of Nickel Electrodes in Vacuum," Proc. Symposium I (1964), p. 237.
- (42) Staprans, A., "Voltage Breakdown Limitations of Electron Guns for High Power Microwave Tubes," Proc. Symposium II (1966), p. 293.
- (43) Germain, C. et al, "Influence of a Strong Magnetic Field on High Voltage Insulation in Vacuum: a Study of the Particular Case of a Quadrupolar Electric Field," Proc. Symposium IV (1970), p. 152.
- (44) Sanford, J., Brookhaven National Laboratory, Private Communication (June 1964).
- (45) Hawley, R., "Solid Insulation in Vacuum: A Review," Vacuum, 18, 383 (1968).

- (46) Kofoid, M.J., "Effect of Metal-Dielectric Junctions on Breakdown," Elect. Eng. 80, 182, (1961).
- (47) Coenraads, C. et al, "Electrostatic Power Generators for Space" American Rocket Society Reprint 2555-62 (1962).
- de Tourreil, C. and Srivastava, K.D., "Surface Charges and High Voltage Breakdown Across Insulators in Vacuum," Proc. Symposium IV (1970), p. 251.
- (49) Srivastava, K.D., "Electrical Discharges on Insulating Surfaces in Vacuum-Recent Observations," Proc. Symposium II (1966), p. 229.
- (50) Srivastava, K.D. and de Tourreil, C., "Electrical Breakdown Across Ceramic Insulators in High Vacuum under D.C. and Pulse Voltages," Proc. Symposium III (1968), p. 243.
- (51) Shannon, J. P. et al, "Insulation of High Voltage Across Solid Insulators in Vacuum," J. Vac. Science & Tech. 2, 5, 234 (1965).
- (52) Finke, R.C., "A Study of Parameters Affecting the Maximum Voltage Capability of Shielded Negative Dielectric Junction Vacuum Insulators," Proc. Symposium II (1966), p. 217.
- (53) Britton, R. B. et al, "Ability of a Voltage-Graded Surface to Support a High Voltage in Vacuum and in a Pressurized Gas," Rev. Sci. Inst. 34, 185 (1963).
- (54) Denholm, A.S., "The Electrical Breakdown of Small Gaps in Vacuum," Can. J. Phys. 36, 476 (1958)
- (55) Ervin, C. C. et al, "60 HZ Vacuum Breakdown Studies in a Dynamically Pumped System," Proc. Symposium IV (1970), p. 219.
- (56) Kustom, R.L., "The Behavior of High Voltage Vacuum Gaps Under the Influence of Radio Frequency Fields," Argonne National Laboratory, RLK-3 (1969).
- (57) Hill, C. E., "30 MHz Radio Frequency Voltage Breakdown of Electrode Gaps Between 1 and 4 mm in a Clean High Vacuum," Proc. Symposium IV (1970), p. 137.
- (58) Lefebvre, J. M., "Report on the Conditioning of a Proton Linear Accelerator (20 MeV) and on an Electrostatic Inflector," Proc. Symposium III (1968), p. 286.
- (59) Kuffel, E. et al, "Breakdown Across Insulation Surfaces in Vacuum under Direct, Alternating and Surge Voltages of Various Wave Shape," Proc. Symposium IV (1970), p. 227.
- (60) Hayes, R. and Walker, A.B., "Vacuum Breakdown at a Glazed Ceramic Surface," Proc. IEE 111, 3, 600 (1964).

- (61) Denholm, A.S., "High Voltage Technology," IEEE Trans. Nuclear Science, NS 12, 3, 780 (1965).
- (62) Lee, T. H., "Industrial Applications of Vacuum Insulation," Proc. Symposium IV (1970), p. 195.
- (63) Smith, W. A. and Mason, T. R., "Preliminary Measurements of Time Lags to Breakdown of Large Gaps," Proc. Symposium II (1966), p. 97
- (64) Smith, W. A. et al, "Impulse Breakdown and the Pressure Effect," Proc. Symposium III (1968), p. 203.
- (65) Mesyats, G. A., "The Role of Fast Processes in Vacuum Breakdown," Proc. 10th Int. Con. Phenomena on Ionized Gases (1971), p. 333.
- (66) Uglum, J. R. et al, "Pulsed Field Emittance Cathode Emittance Measurements," Rev. Sci Inst., 40, 11, 1413 (1969).
- (67) Ravary, P. and Goldman, M., "Study of the Initiation of Breakdown in Vacuum by the Analysis of Closing Times," Proc. Symposium IV (1970), p. 272.
- Juttner, B. et al, "Production and Destruction of Field Emitters on Extended Metal Surfaces by Nanosecond Pulse Discharges," Proc. Symposium IV (1970), p. 102.
- (69) Jedynak, L., "Whisker Growth in High Voltage Vacuum Gaps," J. A. P. 36, 2587 (1965).
- (70) Smith, I.D., "Pulse Breakdown of Insulator Surfaces in a Poor Vacuum," Proc. Symposium I (1964), p. 261.
- (71) Watson, A. and Shannon, J., "Pulsed Flashover in Vacuum," Proc. Symposium II (1966), p. 245.
- (72) Milton, O., "Pulsed Flashover of Insulators in Vacuum," IEEE Trans. Electrical Insulation, EI-7, No. 1, p. 9, (1972).
- (73) Watson, A., "Pulsed Flashover in Vacuum," J. Appl. Phys., 38, 2019 (1967).
- (74) Gleichauf, P., "Electrical Breakdown over Insulators in Vacuum," J. Appl. Phys. 22, 766 (1951).
- (75) Roseberry, F., "Handbook of Electron Tube and Vacuum Techniques," Addison-Wesley, Reading (1965).

- (76) Kohl, W. H., "Handbook of Materials and Techniques for Vacuum Devices," Rheinhold, C. M., New York (1967).
- (77) Holkeboer, D. H. et al, "Vacuum Engineering," Boston Technical Publishers, Cambridge (1967).
- (78) Dushman, S., "Scientific Foundations of Vacuum Technique," Wiley, New York (1962).
- (79) Ennos, A., "The Sources of Electron-Induced Contamination in Kinetic Vacuum Systems," Brit. J. Appl. Phys. <u>5</u>, 27 (1954).
- (80) Huguenin, J. et al, "The New 500 keV Single-Gap Pre-Injector Tube for the CERN Proton Synchrotron Linac," Proc. Symposium II (1966), p. 259.
- (81) McKibben, J. L., "Experience with Back-Biased Accelerating Tubes," Proc. Symposium I (1964), p. 337.
- (82) Purser, K. M. et al., "Properties of Inclined-Field Acceleration Tubes,", ibid. p. 317.

Symposium I - 1964 "Insulation of High Voltages in Vacuum" and Addenda.

Symposium II - 1966 "Second International Symposium on Insulation of High Voltages in Vacuum."

Symposium III - 1968 "Discharges and Electrical Insulation in Vacuum."

Symposium IV - 1970 "Discharges and Electrical Insulation in Vacuum" and Addenda.

SECTION 8 SWITCHES IN GENERAL

Earlier sections of this report have discussed the properties and applications of dielectric media wherein the designer of high voltage equipment, particularly the pulsed power variety, may accumulate and store electrical energy prior to its delivery to a load. The remaining sections of the report deal with switching devices whereby the stored energy is transferred from storage, through pulse shaping elements, if any, and finally to the intended load. The load itself may be an energy-transforming device such as a laser or microwave tube; or, it can be an energy-dissipating element such as a resistor in a protective fault circuit.

The nature of the load and its requirements or capabilities in terms of risetime, falltime, synchronization and pulse repeatability together with the output configuration of the energy store and pulse-forming-network (PFN) will in large measure determine the choice of switch. Although most switches will be required to close a circuit with some specified precision, some switches must be able to open a circuit rapidly when, for example, energy is stored in the magnetic field of an inductor rather than in the electric field of a capacitor.

A range of commercially available devices including both hard and soft vacuum tubes, mechanical interrupters and solid state components can accomplish many of the required switching functions. Where off-the-shelf switching devices are inadequate, usually at the higher discharge energies and voltages or faster risetimes, it is necessary to employ a custom-designed spark discharge device. Where the operating ranges of the commercial and custom devices overlap, financial considerations as well as a certain amount of personal preference will influence the choice. However, the prudent designer will weight heavily the advantages of purchasing a proven package of guaranteed performance.

This section first describes certain commercially available switching devices considered useful in high voltage equipment design. The latter part of this section reviews the more common types of custom-designed switches, their characteristics and limitations. Subsequent sections of this report give detailed accounts of the many special switches which can be designed and built by utilizing the dielectric media already described.

8.1 Commercial Switch Tubes

Switch tubes include both "hard" vacuum and low-pressure-gas or "soft" devices. The hard vacuum types depend upon the timely injection of an electron beam or plasmoid between cathode and anode to close the switch. Multi-element power tubes such as high frequency tetrodes are operated as fast switches for modulator service.

Tetrodes and linear beam tubes are high impedance (100's of ohms) devices with capabilities up to 1 kA at 60 kV for tetrodes and 30 A at 250 kV for the beam tubes. Experimental linear beam devices to switch 200 A at 225 kV are under development. (1)

The plasmoid-injected triggered vacuum gap $^{(2)}$ (TVG) can pass up to 100 kA while holding off up to 150 kV. These are notable for their wide operating range (2-150 kV) and rapid recovery of dielectric strength (10 kV per μ sec). However, lifetimes tend to be limited to the order of a thousand shots and damage is likely to occur whenever ratings are exceeded.

"Soft" tubes of interest here are the ignitron and thyratron. The ignitron is a mercury-pool-cathode diode which has a third electrode to initiate an are discharge through the mercury vapor between cathode and anode. Ignitrons, widely used in CTR work, (3) have high current and charge passing capability but require long (several seconds) recovery between discharges at high ratings. Their current-handling capability is enhanced by their suitability for parallel operation in banks containing hundreds of tubes. Developmental models such as the General Electric Z-5234 have been designed for

100 kA, 80 kV operation passing up to 30 coulombs per pulse. As long as mounting position or environment can be kept compatible with the mercury pool, system designers can use series parallel arrangements of more standard tubes to good advantage. At the expense of a shortened tube life, ignitron ratings can be substantially exceeded without sudden, catastrophic failure.

High power thyratrons contain an anode, one or more control grids and a thermionic cathode in a ceramic envelope with a filling of hydrogen or deuterium. The greater mass of the deuterium ion results in less mobility and a corresponding increase in recovery time by $\sqrt{2}$ over a hydrogen-filled tube of the same geometry. Lower ion mobility also results in reduced surface recombination effects and a lower arc drop (~ 100 V). Deuterium is mainly used in high power tubes, where recovery time may be of less importance than hold-off voltage and dissipation.

Tetrode thyratrons are suitable for parallel operation. Although no theoretical limit to parallel connections exists, a convenient practical limit is six tubes. (4) Series operation can be accomplished with individual tubes. However, the complexity of the arrangement (multiple voltage level heater transformers) favors a series array of several gaps within a single envelope. The development of such thyratrons has been extended to 3 and 4 gap devices holding off 40 kV per gap which can be triggered by a single driving pulse of a few hundred volts. (4)

The advantages of thyratrons as switching elements in high voltage pulse generators include wide unadjusted operating range, high pulse repetition rate (prf) operation with low jitter (1-5 ns), long life and relatively low trigger requirements. Disadvantages (compared with spark gaps) include large inductance, longer switching time, current and voltage limitations, and heater maintenance power. Ratings of thyratrons are usually referred to the high prf of modulator operation. For crowbar and other low-duty requirements a considerable increase in current passing may be achieved without harm. However, some reduction in peak forward voltage rating is advisable under the dc holdoff conditions experienced in crowbar-type applications.

Parameters of interest to non-modulator users of thyratrons are not always readily available from the manufacturers. An indication of these parameters is given in the test results on the CX1168 in which the anode di/dt of 5 kA/ μ sec was exceeded by more than an order of magnitude in single shot duty. Operation at 4 pps with di/dt = 18 kA/ μ sec was performed over 10 times with no pulse form deterioration and a jitter < +2 ns. (5)

Soviet interest and utilization of thyratrons in short-pulse high-voltage generators is indicated by the catalog of relevant parameters of their thyratrons in Table 8.1. Mesyats (6) gives a detailed description of a circuit designed to overcome the large self-inductance of heavy duty thyratrons thus enabling their use for generating high-voltage nanosecond pulses. The method, in which a thyratron is used as the switch on a two-stage coaxial line pulse generator, reduces the switching time by including a shunt capacitance and series non-linear inductance in the anode circuit of the thyratron. For nanosecond pulse generation a ferrite-cored coil is suggested as the non-linear inductance.

A listing of representative switch tubes commercially available in the US and UK is given in Table 8.2. Suppliers include English Electric Valve, EG&G, General Electric, Machlett, RCA, ITT and Westinghouse.

8.2 Solid State Switches

Arrays of transistors or thyristors have been used to provide the intermediate triggering stages of some fast, high voltage systems. For example, several GA200 thyristors, each of which will switch a 100 A pulse in 10 ns at 100 volts hold-off under repetitive operation have been used to provide 10 kV trigger signals to high voltage nanosecond pulse generators. (7) Thyristor-switched modulators operating at peak powers of 60 kW (single-thyristor) and 2 MW (series stack of thyristors) are described by Robinson. (8)

Table 8.1 Characteristics of Soviet thyratrons.

			Thyra	atron t	уре		_
Parameter and	max 1	mar :	mar 1	mar 1	Metall	ic-cer	amic
Parameters	325/16		TGI-1 700/25		TGI-1 1000/25	TGI-1 3000/50	TGI-1) 500/16
Requirements on stability, %: for power source for ignition for heating of hydrogen generator	5 10 0.4	5 10 0.4	8 10 0.4	1.5 10 0.8	8 10 0.4	-	-
for heating of cathode . for amplitude of firing voltage	1	1	1	1 2	1	-	-
Delay of discharge in nominal mode, nsec Front in nominal mode with	<u>+</u> 1	<u>+</u> 1	<u>+</u> 1	+4	<u>+</u> 1	_	
heating voltage of 6.3 V, nsec Minimum front at Uheat	15	20	25	35	20	25	15
V (nsec)	10	12	15	24	15	15	10
microhenrys Pulse anode current in	0.15	0.15	0.35	0.7	0.2	0.3	0.12
nominal mode, A Pulse anode current at	325	400	700	2500	1000	3000	500
t = 100 (nsec) (exper- sp imental data), A Average anode current, A. Repetition frequency, Hz Maximum anode voltage, kV. Heating current, A Maximum amplitude of feed-	10 ³ 0.2 103 16 8.5	10 ³ 0.5 450 16 11	2·10 ³ 1 500 25 20	7·10 ³ 2·5 250 35 55	3·10 ³ 1 700 25 20	10· 10 ⁻³ 4 50 87	10 ² 0.5 10 ³ 16 15
back voltage, kV	16	5	5	5	5		3.2
kilowatts	-	4	25	43	25	250	3

TABLE 8.2 SOME COMMERCIAL SWITCHING DEVICES

Manufacture: Designation	Device Class.	Peak Forward Peak Forward Anode Voltage Anode Current	Peak Forward Anode Current	Peak Fower	Average Current	Total Charge	PRF (225)	Deforized	Delay	Jitter	Jitter Risetime	Typical Pulse Duration
Machlett 7500	Troce	150 kV	20 <i>A</i> .	3 MW			30,	o~	0~		<100 ns	25 25
General Electric GL-6228	Ignitzea	30 kV	30 kA				0.03	500 at				
English Electric Valve BK194	Lenitron	25 kV	130 k.a				0.2	sm 01	& 		200 A/ns	150 ms
ITT 8479/KU-275C	Hydroger. Thyratron	50 kV	• 5 kA	125 MW	<t €</t 		~1090	s:001~ 0001~	300 ns	ខ្លួ	10 A/ns	~10 ~
EG&G HY-5	Hydro _s en Thyratron	up to 45 kV	5 k.ż.	100 MW	8 A		~1000	s: 001~				s: 01~
English Electric Valve CX1162	Deutenum Thyration (double gap)	80 kV 80 kV 70 kV	2.5 kA 4 kA 40 kA	100 XW	2.5 A	2 As	700 60 C. 1	≥1001~	<200 ns	<5 ns	5 A/::s	"s 01 ~
english Electric Valve CX1192	Deutenium Tri natnon (triple gap)	120 kV 120 kV 105 kV	6 kA 10 kA 60 kA	350 MW	6 A	2 As	60 60 0.1	≥i ns	100-250 ns 1-5 ns 10 A/ns	2 - 5 8 n S	10 A/ns	~10 ∴s
*General Electric 2R-7518	Trigger Vacuum Gap	150 kV	100 kA			3. A.S		10 kV/ LS	500 ns	100 as		
EG&G GP-32B	Trigatron	48 kv	163 KA		_	ક્ષ્યા		~100 s	30-100 ns	~10 ns	~10 ns <100 ns	10 us
Luton L-3322	Linear Buem	150 kV	30 A	750 kW	_	2-01						20

*Not readily avainble from manufacturer.

Note: The numbers on this table are not necessarily those of the manufacturers · some are derived estimates. Peak voltage and current may not alw attained simultaneously.

ä

8.3 Vacuum Interruption Devices

These switches which open and close by means of mechanical movement of electrodes in a vacuum insulating medium are described in Selzer's review article. (9) They are of interest here only because of the very high average power capability demonstrated by the series connection of two separate interrupters to achieve a 34.5 kV, 1500 MVA rating. (10)

8.4 Switches for Inductive Storage Systems

In applications (11) which require the storage of enormous amounts of energy, say 10⁸ joules or more, energy density considerations show that only inductive storage systems are practicable. Inductive stores transfer energy from a prime power source to the load in a manner which can be considered as a dual of the technique used with capacitive stores. That is, the inductive store requires that a switch be opened while passing maximum current, whereas the capacitive store requires a switch to be closed while holding off maximum voltage.

The switching of an inductive store is shown in the circuit and waveforms of Figure 8.1. After the energy store L_1 has been filled from the power supply, the switch S_1 is opened at the time t_1 with a reverse voltage u_s appearing across the switch. At t_2 the load (L_2 and R_2) is connected by means of S_c . The steepness of the current rise in the load is determined by the voltage u_3 and the load inductance L_2 . At the time t_3 the load current hegins to drop exponentially from its maximum value. The switch S_c could be a triggered spark gap, if low jitter is desired.

Much ingenuity has been expended in the development of opening switches for inductive stores. (12) Relatively fast-opening switches in high current circuits naturally entail high voltages due to the di/dt within the inductive store itself. The switches must be capable of withstanding the resultant high voltage and large amounts of energy dissipation. Interrupting

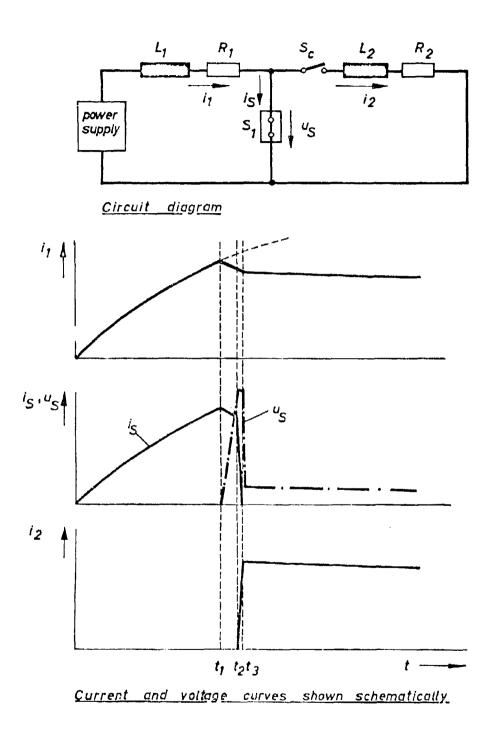


Figure 8.1 Single-stage inductive storage system.

switches suitable for the multimegajoule, megampere range involve fuses which are exploded by more or less sophisticated circuitry. (11, 12, 13, 14)

Experiments (15) with non-exploding switches have attained circuitbreaker voltages of 50 kV at currents of approximately 10 kA while enduring a linear rise of voltage across the switch of 1.7 kV/ μ s. It is suggested that such devices may attain voltages of 100 kV with rates of rise of a few kV/ μ s at currents of the order of 10 Å. Circuits which utilize non-exploding switches by taking up a portion of the energy in a capacitor are found in references (11) and (15).

8.5 Discharge Gap Switching

By far, the bulk of custom-designed switches are closing devices whose basic characteristics are voltage hold-off, rate of current rise, current capacity, delay, jitter, dielectric recovery and operating life. The relative importance of these characteristics depends entirely on the intended application of a particular device. In the high voltage equipment to which this report is directed, switches are closed by means of an electrical discharge through a gaseous, liquid, solid or vacuum dielectric medium.

The methods of initiating this process are several - by overvolting, field distortion and by introduction of charged particles by means of a laser, electron beam or auxiliary discharge. These methods will be discussed in detail in later sections as they pertain to switching in the various dielectric media.

8.5.1 Delay and Jitter

In general, the designer intends that a switch close upon receipt of a logic command from some point in the system or when certain predetermined conditions of electric stress are applied to the switch either intentionally or in a fault condition. Precision of closure can and usually must be

greater in the former mode of operation. Synchronization of switch closure depends on how long it takes the switch to close after the signal or stress is applied (delay), and how accurately the delay is repeated from closure to closure. This accuracy in repeating delay is termed "jitter" but may be quantitatively defined in somewhat diverse ways by various investigators. When sufficient data are available, an rms jitter value can be defined as the standard deviation from the arithmetic mean delay, assuming the delay data form a normal distribution. (16)

Delay in switch closure can be conveniently understood as having two components: a statistical part and a formative part. The statistical delay is that time between the initiation command and the appearance of the first free electron. Although this electron can be obtained by chance, such as from cosmic ray showers, it is usually advantageous to reduce or eliminate the statistical lag by providing a source of free electrons either in the initiation signal, as by an auxiliary discharge, or on a standby basis as by continuous ultraviolet illumination of the switch gap. The formative time is the delay between the arrival of the first electron and the completion of a conducting path through the dielectric sufficient to essentially eliminate the potential difference between the switch electrodes.

Usually, but not always (see Section 9.3) the jitter will be a nominal (\sim 10%) percentage of the delay.

8.5.2 Risetime Consideratio

For very fast risetimes the performance of the switch is critical, especially in low-impedance systems. The geometry of the switch, associated circuitry and the discharge growth are each significant. Choice of coaxial, spherical, or linear configurations may be determined largely by the form of the system components to be connected by the switch.

Circuitry utilized to shorten risetime includes the peaking gap and peaking capacitor techniques. The operating principle of a peaking gap

is based on the fact that the slow-rise portion of an incoming wave (on a transmission line) is reflected back to the source, and the forward propagating wave assumes a risetime corresponding to the characteristics (length, dielectric medium) of the last gap. Thus a short gap in the center conductor of a transmission line can be greatly overvolted by a high voltage pulse traveling along the line toward the gap. The rapid closure of this gap results in a steepening of the pulse as it passes beyond the gap. This method of pulse sharpening is most suitable for steepening an already fast-rising pulse.

A peaking capacitor is used to offset the effect of primary energy store inductance on the risetime of an output pulse from a pulsed power device. Simply stated, the inductor is filled with energy and the desired load current established prior to switching into the load. This scheme, similar in concept and aim to that mentioned in reference (6) for use with thyratrons, is described in EMP systems reports such as reference (17).

There are two phases of current growth through a switch, known as the resistive and inductive phases. The resistive phase occurs with the heating and expansion of the developing spark channel. Its duration depends directly on the density of the dielectric and inversely on the electric field and driving impedance. A theoretical analysis of the resistive phase is given by O'Rourke. (18) Although the inductance changes with time during channel formation, it is usually considered constant for estimating purposes and amounts to about 15 nH per cm for a 1 mm diameter channel. Empirical determinations of these phases of current growth obtained by Martin (19) for various dielectrics are listed later in appropriate sections.

Risetime may be improved by increasing the electric field, thus reducing the resistive phase, and by decreasing the channel inductance. Under certain carefully controlled conditions multiple, current-sharing channels can be developed across the gap. Since the channel inductances are effectively in parallel, a substantial reduction in risetime may be obtained. One must bear in mind the mutual inductance of the channels when predicting the advantages of the multichannel technique.

8.5.3 Lifetime, Erosion and Deionization

The optimum fast closing switch is one using a solid dielectric because of the high electric field possible and dielectric density. Lifetime. however, is limited to one shot. Switching in liquid may be specified, particularly as an output switch in pulsed power systems in which the same liquid is used for energy storage. Electrode erosion rates in liquid are extremely high, however, even in the optimum case where the acoustic impedance of electrode material and the liquid are reasonably well matched. Massive shock waves and mechanical forces are encountered when switching very large energies in liquids. Decomposition of liquid dielectrics requires special purification equipment and processing if repetitive operation is desired. Gas switches encounter much less electrode damage and have selfhealing dielectric properties. Decomposition of high dielectric strength gases such as ${\rm SF}_{\rm g}$ and some Freons in enclosed switches results in conducting deposits which ultimately limit device lifetime by degrading its dielectric envelope. Erosion of electrodes in gas switches can be reduced substantially, especially in high repetition rate applications, by careful choice of materials. A sintered composite which combines the high thermal conductivity of copper with the refractory properties of tungsten has been found useful in resisting erosion in gas switches.

When a switch must return to a non-conducting state in a fraction of a second, the deionization time of the device must be considered. Since dielectric recovery is not a linear function of time, compensation for the switch deionization time can sometimes be made in the charging circuit, for example, with inductive charging instead of simple resistive charging.

Repetitive switching with any device requires that the system designer account for the thermal load on the switch and its environs determined by the operating duty cycle.

SECTION 8

REFERENCES

- (1) Welker, F., RADC, Private Communication (October 1971).
- (2) Lafferty, J.M., "Triggered Vacuum Gaps," Proc. IEEE <u>54</u>, 23-32 (January 1966).
- (3) Smart, D.C., "Some Switching Problems in Controlled Thermonuclear Research," Proc. IEE 106, Part A, #2, IEE Convention on Thermonuclear Processes, 107 (April 1959).
- (4) English Electric Valve Co., Ltd., "Hydrogen Thyratrons Preamble," available from Calvert Electronics International, New York (November 1970).
- (5) O'Hanlon, H. and Zanasco, J.P., "A High Voltage Thyratron Switch for the Fast Inflector of the ISR," Proc. of the 10th Modulator Symposium, pp. 337-350, sponsored by AGED, New York City (May 1968).
- (6) Mesyats, G. A., Nasibor, A.S. and Kremnev, V.V., Formation of Nanosecond Pulses of High Voltage, Translation No. FTD-HC-23-385-71 pp. 116-127 (1970).
- (7) Moriarty, J.J., Milde, H.I. and Hipple, J.E., "Multimegavolt Modulator Study," RADC-TR-70-107, Section 2.2 (August 1970).
- (8) Robinson, T.H., "Circuit Configuration and Thyristor Rating for Solid State Modulators," Proc. of the 10th Modulator Symposium, pp. 83-107, sponsored by AGED, New York City (May 1968).
- (9) Selzer, A., "Switching in Vacuum: a Review," Spectrum 8, 26-37 (June 1971).
- (10) Lee, T.H., "Industrial Applications of Vacuum Insulation," Proc. of the IVth Int. Symp. on Discharges and Electrical Insulation in Vacuum, pp. 195-201, Waterloo (September 1970).
- (11) Knoepfel, H., Pulsed High Magnetic Fields, North Holland Publishing Co. (1970).
- (12) Early, H.C., "Switching Inductive-Energy-Storage Apparatus," Proc. of the IDA Pulse-Power Conference, Vol. I, pp. 186-193, AD434802 (March 1963).
- (13) Maisonnier, C., Linhart, J.G. and Gourlan, C., "Rapid Transfer of Magnetic Energy by Means of Exploding Foils," Rev. Sci. Instr. 37, 1380-1384 (October 1966).

- (14) Lebedev, S.V., "Explosion of a Metal by an Electric Current," Sov. Phys. JETP 5, 243-252 (February 1957).
- (15) Salge, J. and Brilka, R., "Investigations on Switching Schemes for Inductive Storage Systems," Fifth Symposium on Fusion Technology, Oxford (July 1968).
- (16) Mack, C., Essentials of Statistics, (Plenum Press, New York), pp. 35 and 70 (1967).
- (17) Ion Physics Corporation, SIEGE II, Phase II, Vol. I, Section 3, Report No. AFWL-TR-69-81 (1969).
- (18) O'Rourke, R.C., "Note on Cylindrical and Plane-Parallel Spark Channel," in Report No. AFWL-TR-69-80, p. 230 (July 1970).
- (19) Martin, J.C., "Duration of the Resistive Phase and Inductance of Spark Channels," AFWL Switching Notes, Note 9 (December 1965).

SECTION 9 GAS SWITCHES

Spark gaps which utilize gas at pressures about one atmosphere or greater are widely used for their relative simplicity of design and controlability. Gas switches can pass high currents and withstand voltages in the multimegavolt region with increased pressure and use of electronegative gases such as those described in Section 4.

Uniform field geometries provide that maximum and mean gradients do not vary widely. Spherical or hemispherical electrodes are often used; however, electrodes having Rogowski or Bruce profiles (Section 2.2.7) result in more uniform fields. Nonuniform fields are often used to advantage, especially in fast-operating switches (cf Section 9.1.2).

Gases commonly used include N_2 , CO_2 , air, SF_6 . Freons and mixtures of these. Despite similar electric strength, N_2 is preferable to air for its inertness.

9.1 Overvolted Switch

The simplest type of switch is the overvolted switch in which the gap voltage is increased until dielectric breakdown occurs. Variations on this theme include reduction of gas pressure or changing its properties--as by heating--until breakdown occurs.

Taken by itself, such a gap has rather poor synchronization properties. However, when closed by a fast-rising pulse with a voltage greatly in excess of the self-breakdown voltage (SBV) of the gap, an overvolted switch can close quite rapidly and with low jitter, as, for example, when it forms part of a three-electrode switch described below.

9.1.1 The Rope Switch

A clever circumvention of the characteristically large jitter of the overvolted type of switch is the "rope switch". This switch (1) takes advantage of the statistical distribution of switch breakdown times to realize a high-voltage, low-jitter spark gap from a series connection of identical low-voltage gaps. Assuming a normal distribution of firing delays, a series array of N gaps will have n gaps breaking down early, that is, at one or two standard deviations below the mean voltage. However, the remaining N-n elements will keep the switch open. Around the mean voltage most of the remaining switches will fire. Those switches which would ordinarily fire late (at one or two standard deviations above the mean voltages) will have almost the entire series voltage impressed across them, whereupon they close rapidly. The upper and lower ends of the normal distribution of the individual switch are essentially removed as factors in the performance of the N-stage switch, thus sharpening the delay distribution and jitter of the array.

Experimental results with a 10-stage rope switch closing a 200 kV "gap" gave a maximum jitter of 11 ns and standard deviation of 3 ns, a factor of 3 lower than single gap performance. Dual channel breakdown of rope switches yielded a risetime of 26 ns compared with 33 ns for single channel.

9.1.2 Nonuniform Geometry

Tests of high power overvolted gaps for the RES LC generator output switch $^{(2)}$ showed best results with a point-to-plane geometry consisting of a stainless steel cylindrical anode with a knife-edge at its surface which faced a large-diameter, brass disk cathode. This device switched 500 kV across a 3 cm gap in SF₆ at 15 psig.

A thin cone gap operating up to 350 kV in SF $_6$ and Freon-12 is described in (1). Risetimes of 2-3 ns are reported⁽²⁾ for Freon-12 and 3-5 ns for SF $_6$ as shown in Figure 9.1.

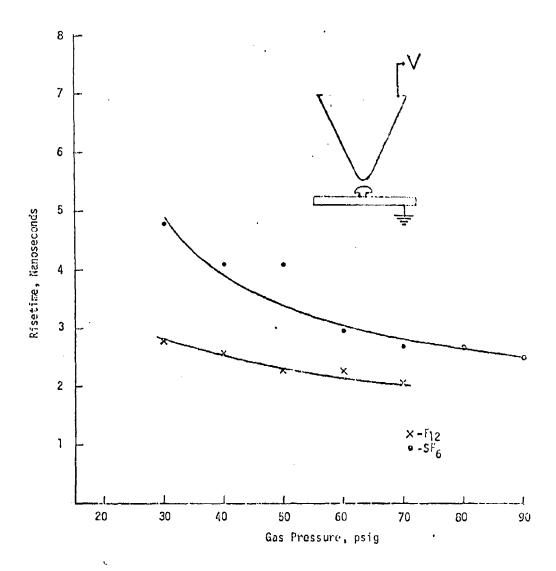


Figure 9.1 Risetime of thin-cone gap.

Another overvolted switch of interest is Martin's $^{(3)}$ 3-meter-long edge gap which is really a point-to-plane stretched out over 3 meters. This switch closed a line of 0.45 ohm impedance at 105 kV in 5-8 ns by means of 140 channels which closed within a span of 0.6 ns. The risetime of a single channel across the same impedance was estimated at 110 ns, thus indicating a factor of 20 improvement with the multichannel gap. The jitter of such a switch, expressed as a fraction of the mean breakdown voltage, has been measured as approximately 1/2% when the charging time is about 100 ns, rising to 2% for charging times of 2 μ s. Breakdown data for edge-plane gaps at pressures >30 psig in SF₆, Freon-12, N₂ and air are given in (1) for breakdown voltages of 200-350 kV. Jitter as low as 7 ns is observed for N₂, with air and SF₆ yielding about 10 ns.

The above examples illustrate the adaptation of the simplest of gas switches to quite sophisticated operation.

Operation of a 150 psig SF₆ switch at 3.5 MV is described in detail in reference 5. Gap spacing between hemispherical steel electrodes was set at 4.5 cm for a design goal of 2.5 MV. The standard deviation of switch closure for 1 µs charging time was pressure dependent: 6.3% at 150 psig and 4.2% at 100 psig. Reference (5) discusses switch performance in the context of an EMP system risetime.

9.1.3 Repetitive Operation and Fast Restriking

The limit to repetitive operation and other occasions of rapid reapplication of voltage to a switch is often set by the dielectric recovery time of the switch. When lifetime requirements are high and minimum maintenance is available, electrode erosion may become a limiting factor.

Both dielectric recovery and electrode erosion are applicable to most switch designs; however, their experimental determination usually involves simple geometry such as the overvolted or simply-triggered switch. Hence, these subjects are treated in this subsection.

9.1.3.1 Dielectric Recovery of the Spark Gap

To restore the dielectric strength of a switch after discharge, the charge carriers produced during the discharge must disperse and the electrodes must lose heat. Dielectric recovery is established when the dielectric strength exceeds the reapplied stress.

A survey of the literature concerning arc recovery reveals the subject to be an extremely complex one involving several or all of the following parameters; electrode material and geometry, gas composition and pressure, arc length, and current.

Most of the work on arc recovery can be found in the periodical literature (cf references (6) through (12)) and a comprehensive review of experimental data by Milde. (13) Although generalizations must be interpreted with considerable care, it is worthy of note that gaps using Elkonite (14) electrodes have demonstrated better voltage recovery than those with copper or tungsten. (9) As might be expected, recovery is favored by increasing gas pressure. In order of increasing recovery times several common gases are listed: (13) H_2 , SF_6 , CO_2 , O_2 , He, Air, N_2 and Ar.

Perhaps the most significant dielectric recovery information for the designer is shown in Figure 9.2. Note the nearly flat recovery of voltage with time during the first 100 μs after switching. This behavior should be borne in mind when specifying the charging waveform for a high repetition rate system.

Methods of enhancing the recovery time include the placement of a series of discs within the gap to aid cooling as in Früngel's (15) hydrogen quenching spark gap, or the flowing of air through the gap to cool it and remove discharge debris. The former method has been demonstrated to be reliable in the range of 6-12 kV with peak currents of 0.5-500 kA at up to 300 kHz. Extension to 300 kV has been reported with the use of many discs. The switch described in (16) has demonstrated a 100-hour life at 50 Hz while passing 2.5 kA in 2.7-μs pulses in the 20-to 60-kV range.

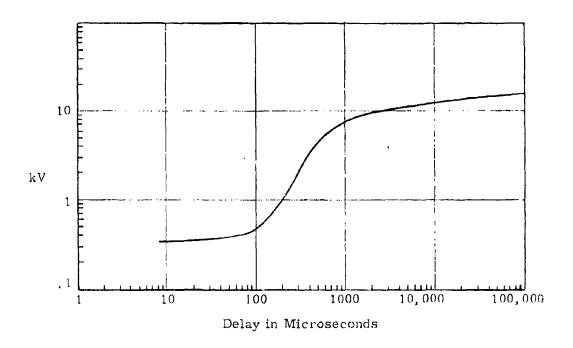


Figure 9.2 Are recovery strength in N_2 at 1 atmosphere. (1/4 inch gap, 3/4 inch cylindrical electrodes (CU), 400 ampere arc)

(From G. A. Farrall and J. D. Cobine, IEEE Trans. on Power Apparatus and Systems PAS-86, 927, 1967)

9.1.3.2 Electrode Erosion

The operating characteristics of spark gap switches depend on the geometry of electrodes which may become distorted by erosion. Furthermore the products of erosion, sometimes in combination with gas decomposition products, can become deposited on insulating surfaces of the switch thereby shortening its life.

Erosion of electrode material is due to heating which occurs mainly from bombardment by charged particles. Hence it is sensitive to current density and gas composition. As a result of brief powerful thermal thuxes and limited heat conduction of electrode material, such surfaces can be heated to melting and vaporizing temperatures. Two regions of erosion can be distinguished experimentally. At currents up to tens of kA, erosion results primarily from vaporization. For much larger currents the erosion increases abruptly, corresponding to loss of material by the ejection of motion metal.

This subject is treated in some detail in the Soviet literature which is comprehensively reviewed in reference (17). It is interesting to note that the most durable Soviet material is reported to be AVM-30, a copper-tungsten composite apparently similar to Elkonite (Table 9.1). Other materials recommended in (17) are molybdenum and tungsten. Results with heat-resistant steels, brass and copper are reported to be less favorable.

A study of fast, overvolted gaps in repetitive operation was made by Proud and Huber (18) in the voltage range of 40 to 70 kV. Risetimes as law as 50 ps were measured in single shot operation. Cathode erosion experiments at 400 pps showed remarkable erosion resistance for Elkonite when compared to copper electrodes in air at atmospheric pressures. No further improvement was found when pure tungsten was substituted for type 30W3 Elitonite.

Table 9.1
Properties of Copper-Tungsten Composites

Material	Elkonite 10W3	Elkonite 30W3
Composition (by volume)	57% W, 43% Cu	66% W, 34% Cu
Density (gm/cm ³)	14.7	15.8
Electrical Conductivity (% IACS)	46	~40
Thermal Conductivity (egs units)	0.61	0.57
Ultimate Tensile Strength (psi)	90,000	~90,000

Other tests on Elkonite at higher energies at 1-10 pps are described in (19). For the lower rates erosion in SF $_6$ was found proportional to the charge passed, \int idt. The observed rate of $\sim 10~\mu g$ per coulomb is similar to Belkin's result for copper cathodes at one atmosphere of helium in discharges of less than 40 kA. The results of (19) implied the following statements useful in spark gap design with Elkonite:

- (1) Erosion is a strong function of pressure, increasing superlinearly with pressure up to 45 psia and at least linearly to 60 psia.
- (2) Erosion in an atmosphere of SF₆ is increased with increasing PRF in the range 0.2 to 10 pps.
- (3) Erosion is reduced by the addition of 50% Ar to a 3 to 1 mixture of Freon-116 and N₂O₂.
- (4) Erosion in SF_{R} is not strongly affected by electrode polarity.
- (5) Erosion in the Freon-N₂O-Ar mixture (see above) is polarity-sensitive, being greater for an anode.

9.2 Three-Electrode Switch

The addition of an additional electrode to the simple two-electrode gap described above provides a vehicle for initiating closure on command. Two basic forms of the three-electrode switch are the field distortion switch and the trigatron.

9.2.1 The Field-Distortion Switch

A typical field-distortion switch is shown in Figure 9.3. Prior to switching, the sharp-edged mid-plane electrode is held by means of capacitive and/or resistive grading at the potential corresponding to the equipotential established at its physical location in the field between the main electrodes. Closure in the swinging cascade mode is illustrated in Figure 9.4. In this

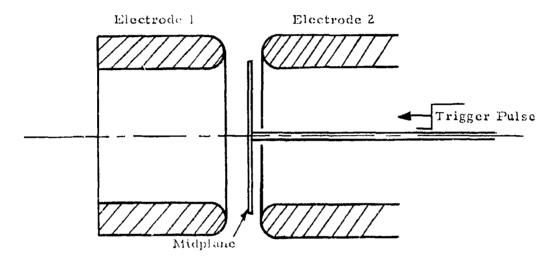


Figure 9.3 Field distortion switch.

Vwx = WORKING VOLTAGE OF GAP x

Vwy = WORKING VOLTAGE OF GAP y

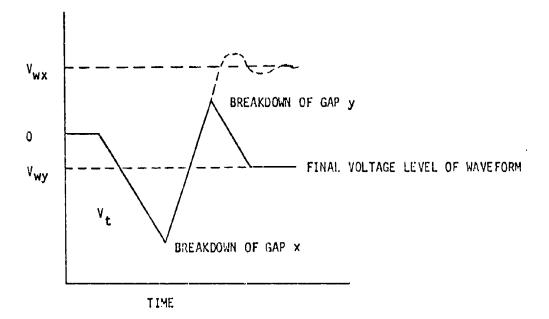


Figure 9.4 Swinging cascade breakdown mode for 3-electrode switch.

mode a trigger pulse V_t is applied to the mid-plane electrode thus creating field intensification, ionization and breakdown of the larger gap x. When gap x breaks down the voltage on the mid-plane electrode swings to the opposite direction, greatly overvolting the smaller gap y. A simultaneously overvolted (SOV) mode is also possible in which both gaps are overvolted to breakdown by the trigger voltage alone. Operation in the SOV mode is said to minimize risetime and produce a clean wavefront. This mode requires a fast-rising ($\sim 10 \text{ kV/ns}$) trigger voltage to be applied to the center electrode.

The proportion of spacings between the mid-plane and main electrodes should be 60/40 to 70/30. Barnes et al have demonstrated the inadequacy of the 50/50 spacing for wide range triggering. In the same reference are described 60 kV, field-distortion spark gaps with an inductance of 15-18 mH which operate at a peak current of 450 kA, passing 7 coulombs per pulse. No deterioration was noted after 2000 shots. A trigger requirement of at least 4 kV/ns was pointed out in (23). Further analysis (24) of the same type of switch indicates ±2 ns jitter with an 18 ns risetime with 60/40 gap ratio. Earlier development and design criteria for these switches are given in (25).

A 15 kV, 1.5 ns risetime, air spark gap using a "heater" capacitance to create a high-conductivity spark is described by Vorob'ev and Korshunov. (26)

An important aspect of risetime is the resistance time of the spark channel. As mentioned in Section 8, an empirical expression has been published by Martin (27) for the resistance time of a gas spark channel in nanoseconds:

$$t_{r} = \frac{88}{10^{8/3}} \left[\frac{\rho}{\rho_{O}} \right]^{1/2} \left[\frac{1}{E^{4}Z} \right]^{1/3}$$
 (1)

where E is the field along the channel in MV/cm

Z is the generator driving impedance in ohms

 $_{\rho}\,/_{\rho}$ is the ratio of the gas density to that of air at NTP

Judged by the $_{\rho}$ / $_{\rho}$ term hydrogen would be an attractive candidate for fast risetime switching. Experimental comparison of H_2 and air in a three-electrode gap is presented in (28) in which a factor of two improvement in risetime is observed for H_2 over air. However, jitter is noticeably greater, which fact is attributed to a shift to the swinging cascade mode rather than SOV operation. Means of maintaining SOV mode are discussed.

In considering the mid-plane gap for very high voltage switching, it should be noted that trigger voltage requirements are inherently high, being nearly equal to the holdoff voltage of an entire switch.

9.2.2 The Trigatron

The trigatron form of switch initiates closure by both ionization and field distortion. A third electrode, usually a pin, small relative to the main electrodes, is mounted coaxially within and insulated from one of the main electrodes. A discharge is initiated between the trigger pin and its host electrode by means of a pulse of, say, a few tens or hundreds of kilovolts thereby providing the necessary charge carriers plus local field intensification which rapidly cause the main gap to conduct. See Figure 9.5.

The mechanism of trigatron closure has been studied in some detail. (29-33) At least two stages of discharge development may be distinguished: a threading of the gap with filamentary discharges on application of the trigger pulse and the development of a main stroke propagating at 10^8 - 10^9 cm/sec which can be explained by the streamer mechanism (Section 4.1).

Of more immediate concern to switch design is Shkuropat's summary of trigatron operation according to electrode polarity shown in Table 9.2. This summary pertains to gaps operating in excess of 40% VSB

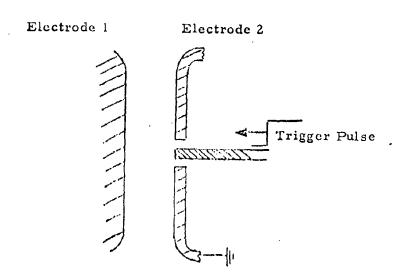


Figure 9.5 Trigatron.

Table 9.2
Electrode Polarity and Trigatron Characteristics

Range	Jitter	Trigger Electrode	Opposite Electrode	Host Elect ro de
1	1	+	-	+
wider	rter	-	-	+
- w.j	sho	-	+	-
		+	+	· -

where field distortion is the primary triggering mechanism. For lower operating voltages stable operation requires high-current (~60 kA) triggering.

A limited range of trigatrons is available commercially (Table 8.1). Many special designs have been developed using a high pressure gas dielectric such as N₂, CO₂, SF₆ at pressures from 100-400 psi. Operational voltages have been as high as 10 MV. Such switches have significant dimensional departures from the ~50 kV devices studied by Shkuropat, but are comparable in size to the MV switches examined by Broadbent and Shlash, (30) having main electrodes of meter dimensions and gap lengths of tens of centimeters.

Low voltage (20-100 kV) trigatrons have trigger requirements similar to the swinging cascade devices already described; i.e., trigger voltage must be a substantial portion of the main gap voltage. Megavolt trigatrons have the distinct advantage of requiring relatively low trigger voltages to initiate fast switch closure, with an amplitude ~200 kV being adequate (34) even for switches with main gap potentials >10 MV.

The precise control and low jitter operation achievable with multi-megavolt trigatrons has made possible the operation of such switches with a multiplicity of simultaneously-triggered, current-sharing channels. Extensive data on the operating range of double-channel multimegavolt switches are presented in (19). One of the most notable trigatrons is the six-channel, 4.5 MV output switch in the ARES (35) EMP generator which has consistently exhibited risetimes well below 10 ns.

Other state-of-the-art examples of large trigatrons are the 3-MV, 250 kA Gamble I switch and the array of four 2 MV switches passing 400-800 kA through 4-10 atmospheres of SF_6 in the Blackjack (36) facility.

9.3 Photon Initiated Switch

The energy required to produce the initial electrons or to preionize the discharge path during a switch closure can be supplied by means of photons ranging from ultraviolet to infrared. Non-coherent sources of ultraviolet radiation have long (37) been used as a means of providing the initial electron in both switches and voltage breakdown measurements to eliminate the statistical delay time. For direct photoionization of O₂ and N₂ molecules, photons with wavelengths 990 Å and 790 Å, respectively, are required. When photons are used to overcome the work function of the electrode surface, it is found that photoelectron emission grows rapidly with decreasing photon wavelength, the threshold wavelengths for Cu, Fe, and Al being in the range 2600-3000 Å. Because of the absorption of such shortwave radiation in air, it is necessary to keep the source of quanta as near as practicable to the target. Use of 1100 Å - radiation will minimize the absorptive effect of intervening air.

Typical applications of this technique utilize fast-rising spark gaps or mercury-vapor lamps as sources of UV radiation. Sometimes, as in the case of a multiple-switch device (e.g. Marx generator), spark gaps may be arranged so that the gaps which fire earlier irradiate the later-firing gaps.

The application of UV radiation for preionizing the discharge path has been reported by Bradley (38,39) who found an order of magnitude increase in streamer velocity in an irradiated, pulse-charged, 1-cm gap in the range of 1-12 atmospheres of N_2 . His sources of UV include a fast-rising spark gap and a super-radiant N_2 laser operating at 3371 Å.

Although the electromagnetic radiations from a spark gap and from a laser are of identical nature, the processes whereby gas breakdown occurs in the presence of one or the other type of radiation are substantially different. Principally, laser radiation is coherent and capable of being focused to very intense power densities. The resulting gas breakdown and electrode interactions provide the basis for the very precise method of switch closure known variously as the laser-triggered switch (LTS) and the laser-triggered spark gap (LTSG). Before discussing these devices, let us consider some of the basic phenomena which influence their behavior.

Laser induced breakdown of gases has been the subject of considerable research. A review of this work by DeMichelis $^{(40)}$ contains a thorough

synopsis of the breakdown mechanisms together with a bibliography of 161 papers published in the open scientific literature through May 1968. Included in the review are discussions of the effects of gas pressure and laser wavelength on breakdown power threshold. Some more recent literature is very briefly described in (41).

For the gases of interest to switch designers, the power required for breakdown decreases with increasing pressure to at least 1000 psig. (40) After reaching a peak around 6000 Å, the wavelength dependence of breakdown appears to decrease monotonically with increasing wavelength. Some recent measurements in Ar show a power requirement of 10^{11} to 10^{10} W/cm² in the range 7300 Å to 8400 Å, (42) which is reduced to ~10⁸ W/cm² at the 10.6 μ m (106,000 Å) wavelength of the CO₂ laser. (43)

In most switching work the laser beam is focused on or very near the surface of an electrode, thus complicating the understanding of spark formation still further. Gases liberated by reason of evaporation of part of the electrode surface will interact with the laser beam in the production of the initiating discharge. A source of initiating electrons exists also in the thermionic emission of electrons from local hot spots on the target electrode as suggested in (37), (44) and (45). Khan has calculated the factors which maximize the Richardson heating of an electrode and suggested electrode materials in order of decreasing preference: Ta, W, brass, Al and Cu. A number of papers dealing with electrode-laser interactions are included in reference (46).

The nature of the path between the initiating discharge and the opposite electrode has an important bearing on the delay and jitter encountered in switch breakdown. In the event that the spark gap axis and laser path are co-linear, the studies of streamer propagation over long paths (47) and the onset of self-focusing are pertinent. Self-focusing deals with the establishment of a dielectric waveguide in a medium whose dielectric constant increases with electric field intensity, but which is homogeneous in the absence of an

electromagnetic wave. $^{(48)}$ This effect has been studied to a large extent in the USSR $^{(49)}$ and Canada. $^{(50,51)}$ Two important characteristics of self-focusing are the existence of breakdown regions less than 5 μm in diameter and the threshold estimates of 1-80 MW in air over the pressure range 100-1 atmosphere.

Laser-triggered switching has been reviewed by Guenther and Bettis. (52,53) Although Pendleton's (54) early work dealt with irradiation orthogonal to the axis of the dielectric gap or electrode, most of the subsequent work has utilized a coaxial geometry similar to that in Figure 9.6 in which the laser beam is focused on or slightly below the electrode surface. The mechanism of breakdown in the LTS is generally understood as a two-step process in which the initial electron density grows in avalanche fashion while partially traversing the gap until a critical number of electrons exists such that the avalanche evolves into a streamer which very rapidly closes the remaining gap. (52,53) The streamer theory, initially proposed in connection with Q-switched laser pulses (~10 µs duration) has recently been found in agreement with experimental behavior (55) of a nitrogen gap triggered by means of a 7-ps pulse. The avalanche-streamer breakdown model is summarized in equation (2) for the switching delay in closing a gap of width d:

$$t = \frac{\ln n_{c} - \ln N_{o}}{c' V} + \frac{d - X_{c}}{s}$$
 (2)

where

n = critical number of electrons at avalanche-streamer transition

X = distance from target electrode to point of avalanchestreamer transition

 N_0 = initial ionization

 α = first Townsend coefficient of the gas

v = electron drift (~avalanche) velocity

s = streamer velocity

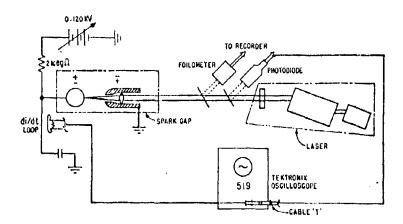


Figure 9.6 Schematic diagram of the laser-triggered switching apparatus.

Two regions of delay can be identified (52) in terms of their associated jitter. First, when the total delay is less than the duration of the laser pulse, the value of N_o continues to increase, thus reducing switch jitter to a minimum. Second, when delay is significantly greater than pulse duration, the growth of the avalanche includes statistical fluctuations which result in a jitter of about 10% of the delay. Under certain conditions in which laser power density at the target electrode is kept constant, the delay may be increased while maintaining low jitter by decreasing the power density along the discharge path. (56)

In assessing the effect of laser power on LTS operation it is necessary to consider the beam divergence θ of the laser and the focal length f of the lens, since the minimum spot size upon which the laser power can be directed has a diameter $a = f \theta$. The pulse duration must also be taken into account as evidenced in Figures 9.7 and 9.8 which show a distinct turning point in jitter when the delay has dropped below the total laser pulse duration. As can be understood from the variation of gas breakdown threshold with wavelength, this factor must also be considered.

For the cost-conscious designer of an LTS system for a single gap or for one who must close several switches by means of the same laser beam, an estimate of the minimum power to do the job is necessary. Assuming a jitter of very few nanoseconds to be allowable, Table 9.3 has been compiled to show representative operating parameters and laser specifications which relate to power available for switching. The information in the table, although not intended to be comprehensive, does show the potential advantage of the longer neodymium wavelength. For high repetition rates, of a few tens of pps, only the Nd:YAG is feasible. As shown in reference (57), subnanosecond jitter at up to 50 pps can be achieved with very low power from a Nd: YAG laser.

As is clear from the parameters in equation (2), the gas composition is of considerable importance. Generally ore should try to couple

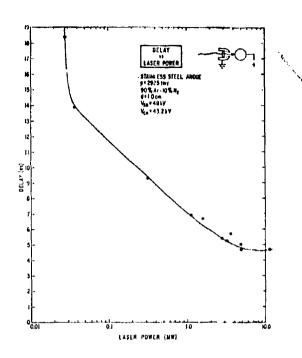


Figure 9.7 Delay versus laser power from 0.028 to 11 MW.
Total laser duration 14-15 ns.
The pulsewidth (FWHM) 5.5-6.5 ns.

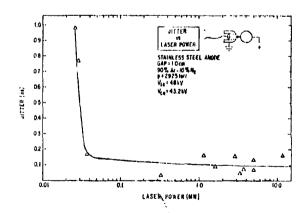


Figure 9.8 Jitter versus laser power.

Table 9.3 LTS operation and power related laser parameters.

d	Voltage	Gap	ن م	7 ressilt	Focal Length	Beam Divergence (mrad)	Power	Wavelength (A)	Laser Crystal
relerence	(NA)		8	o trocont					
Dewhurst et al	20	4.85	N 2	1240 torr	20		100 kW	10,600	Nd:glass
Alcock et al	20	0.5	' Z°	11 atm	20	0.6	2 kW	6,943	Ruby
(45) Khan	20	48	Air	3 atm	100	လ	28 MW	6,943	Ruby
Bettis and Guenther	20	10	90% Ar, 10% N,	2925 torr	54	8 .	28 kW	10, 600	Nd:YAG
Deutsch	100	ఱ	85% Ar, 15% N,	8 atm	40	က	1 MW	6,943	Ruby
(60) Guenthe and Bettis	1000	30	×6	350 psi	50	2	170 MW	6,943	Ruby
Moriarty et al	2000	20	, % _e ,	150 psi	165	1.5	85 MW	6, 943	Ruby
Moriarty et al	3000	110	50% Ar, 40% N ₂ ,	300 psi	165	1.5	160 MW	6,943	Ruby
			$10\% \mathrm{SF}_{6}$						

reasonable dielectric hold off capability with a high $_{\alpha}$ v product. Fortunately the power threshold for laser-induced breakdown goes inversely with pressure, just the opposite of dielectric strength. Thus the addition of a gas with larger photo-absorption cross-section, such as Ar can be offset to some extent by increasing the gas pressure. The effects of gas composition and pressure have been shown in several references. (45, 56, 57, 58) In general, delay and jitter go down as the percentage of Ar is increased. Dielectric holdoff considerations usually eliminate the use of 100% Ar in switching applications. A mixture of 50% Ar, 40% N₂ and 10% SF₆ was used in a 3-MV switch which was triggered in 10 ±0.7 ns by means of a 160 MW pulse from a high-brightness, Q-switched ruby laser. Delay data for this switch is shown as a frequency of occurrence diagram in Figure 9.9.

The effect of switch polarity is quite small and more of academic than practical interest. (53) Guenther and Bettis (60) have observed that a charged anode target is preferred. Other investigators (56,58) have not observed a polarity effect in their range of operation.

The precision with which a spark gap can be closed using LTS recommends this technique for multiple-switch operation in which the laser beam is split one or more times either to initiate a number of synchronous gaps or to produce two or more distinct, current-sharing channels across a single spark gap. The operation of four 50 kV gaps at 50 pps with a synchronization of ~0.1 ns is reported in reference (61). A diagnostic system for indicating synchronization is also described. In this case, splitting of the laser beam is achieved by means of glass plates inserted in the beam at a predetermined angle. A similar technique is reported by Khan (45) for a five-gap system at 30 kV. The application of multigap LTS to Marx generator operation is described in (56). Double-channel LTS has been reported in the megavolt range in references (53) and (56). Both papers report a reduction in risetime by nearly a factor of two when current-sharing exists between the two channels. Beam splitting must be quite precise to observe

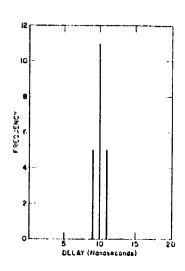


Figure 9.9 Frequency of delay occurrence.

Gas: 300 psig, 50% Ar, 40% N_2 , 10% SF_6

Gap: 11 cm; Potential: + 3.05 MV, 94% SBV

E/p: 17.4 V/cm torr; Laser Power: 160 MW @ 6943 A

full current-sharing. Because of spatial non-uniformities in the laser beam cross section, it is important to use a beam splitter which divides the entire beam rather than a segmenting type of divider which spatially cuts up the beam (i.e., like a pie, for instance).

9.4 Electron Beam Initiated Switch

The ionization required to close a gas-insulated switch can also be achieved by means of a beam of high-energy electrons. In early Soviet work (61) performed at Leningrad Polytechnical Institute in 1939, electron beams were accelerated by pulsed discharge devices of 2000 and 700 kV. The firing voltage of an air-insulated spark gap was found to decrease by 50% below its static value when the electron beam was directed along the electric field between the electrodes. No decrease was noted for opposite polarity. A reduction of electron beam intensity by two orders of magnitude did not change the effect of the beam on switch closure. Furthermore, gamma-radiation occurring simultaneously with the electrons was shown to be ineffective in reducing the firing voltage.

More recent work $^{(62)}$ reviewed in (61) studied the triggering action of 3-4 MeV electrons with a pulsed current of 0.2 A on a uniform field spark gap insulated with N_2 and H_2 at pressures from 12.5-500 torr. When triggered, the closing voltage of the spark gap dropped to 20% of the static discharge voltage, which fell between 1.2-13 kV depending on gap length (0.6-10 mm) and pressure. Breakdown was said to be caused by field distortion introduced into the gap by the space charge created by the electron beam. Delay time, which was not studied, was estimated as 100 μ s or less as the maximum voltage was approached.

A discussion of the current-voltage characteristics of an electron-beam initiated discharge in high pressure gas is given in (63). A titanium window foil was used to pass the 20 cm 2 electron beam into a gap having widths of 2-20 mm at pressures of 1-16 atmosphere of N_2 . Gap voltage

was in the range 5-250 kV pulsed and 5-50 kV static. The electron beam had a maximum energy of 180 keV and an average energy of 80 keV. The discharge growth time was determined to vary from 240 to about 10 ns as the gap voltage was increased from 100 to 210 kV at pd = 5320 torr cm.

Most recently, electron-beam switching in high pressure gas has been reported by Abramyan et al, (64) who used a Tesla transformer to charge the spark gap to 0.2-1 MV. An electron beam of 150-400 keV and a current of ~10 A was injected through a 5 µm Al foil in 5 ns along the axis of the gap and directed at a positive, pulse-charged electrode. It was found that an increase in the operating voltage from 55% to 85% VSB decreased the delay from the range 100 to 150 ±30 ns (for various beam energies) to the range 20 to 40±1 ns. Operation below 50% VSB did not result in a discharge. Above 85% VSB self-maintaining breakdowns would occur infrequently. The time delay was found to decrease as the energy of the injected electrons was decreased from 430 to 150 keV, a result in accord with the increased stopping power of gas for lower energy electrons.

In eight atmospheres of N_2 the gap was closed at 360 kV, 86% VSB, by means of a 150 keV, 3 A electron beam in a time of 20 ± 1 ns. In eight atmospheres of natural gas, switching could be carried out at voltages near 1 MV.

The rate of discharge development $\sim 2 \times 10^8$ cm/sec does not contradict the results of streamer breakdown theory.

9.5 Design Considerations

When system requirements of high current, high voltage, low inductance, short delays and wide range of voltage control exist that cannot be met by commercially available switching devices (Section 8), the gas-insulated spark gap should be given serious consideration in the custom design of a switch. Gas insulated switches are self-healing, capable of repetitive operation with minimum maintenance, and when suitably enclosed, relatively quiet in operation.

The previous sections have described various forms of gas switches, categorized primarily according to their method (or lack thereof) of triggering. The order of the discussion is indicative of the level of complexity of the triggering scheme. Economy of design will be served by choosing the least complicated method of switching that will satisfy the operating requirements. The three-electrode gap in one of its forms is usually satisfactory. Experimenters who already have high-powered lasers and who wish to synchronize an event with the output pulse of the laser have found the laser-triggered-switch quite useful. The LTS is a most convenient technique for operating an electro-optic cell to gate out a single mode-locked pulse from a train of such pulses.

Except for those operating in atmospheric air, switches must be integrated with the rest of the high voltage system. It is fortunate, indeed, if a high pressure switch is to be operated in the same dielectric environment as the energy store being switched as, for example, in the multimegavolt, gas-insulated flash X-ray machines used in nuclear weapons effect simulation. Usually the gas-insulated switch must be isolated from a liquid, gaseous or vacuum environment by means of a solid dielectric cell such as lucite, or fiberglass. Electrode plates are held in place by means of dielectric bolts or threaded rods which are usually located outside the switch cell in the host dielectric. Design of the switch cell and fastening rods requires consideration of the voltage flashover data discussed in appropriate earlier sections of this report.

At all times when handling compressed gases, due attention must be paid to the significant amount of mechanical energy stored in a volume of compressed gas. Standard ASME codes should be adhered to in the design and utilization of pressurized gas enclosures. Chemical hazards, such as the toxic decomposition products of SF_6 and Freon, must also be guarded against.

Hazards which may seem unusual to the average high voltage worker are present in the use of lasers for spark gap triggering. Personnel

should be protected by means of eye-goggles which reject the laser output wavelength. The danger is more subtle at wavelengths beyond the visible region. In can be said, however, that personnel danger is likely to be greater from the high voltage supplies used to operate lasers than from the lasers themselves.

Optical components should be properly coated and constructed of bubble-free material to avoid damage from high powered laser beams. A cost tradeoff can be made in this case, however, especially in developmental programs. For example, one can purchase 100 or more simple lenses from Edmonds Scientific for the price of a single anti-reflection-coated, fused silicalens of similar focal properties.

SECTION 9

REFERENCES

- (1) Maxwell Laboratories, Inc., "Investigating Means of Reducing the Weight of Large RES Generators," Report No. MLR-90, AFWL EMP-HAS 3-3, pp. 51 and 79 (April 1970).
- (2) Maxwell Laboratories, Inc., "Res. II, Phase II Program," Report No. MLR-61, AFWL EMP-HAS 3-2, Section 3 (Oct. 1969).
- (3) Martin, J.C., "Multichannel Gaps," AFWL Switching Note No. 10 (March 1970).
- (4) Smith, I., "Ground-Based Pulser Design Study," PIFR-265, AFWL EMP-HAS 3-7, p. 4 (July 1970).
- (5) Aslin, H., "Electromagnetic Pulse System," Vol. II, Report No. AFWL-TR-69-15, pp. 66-80 (Sept. 1969).
- (6) Churchill, R.J., Parker, A.B., and Craggs, J.D., "Measurement of Reignition Voltage Characteristics for High Current Spark Gaps in Air," J. Electronics and Control 11, 17-33 (1961).
- (7) Edels, H., "Properties and Theory of the Electric Are," IEE Paper No. 3498 (Feb. 1961).
- (8) Vanyukov, M. P., Isaenko, V. I. and Travleev, G. N., "Dielectric Strength Recovery of a Spark Gap in a Repeating Discharge Regime," Soviet Phys. -Tech. Phys. 7, 544-548 (Dec. 1962).
- (9) Parker, A.B., Poole, D.E., and Perkins, J.F., "The Measurement of Electrode Surface Temperature and its Role in the Recovery of High-Current Spark Gaps," Brit. J. Appl. Phys. 16, 851-855 (1965).
- (10) Curzon, F. L. and Gautam, M.S., "The Influence of Electrode Heat Transport in Spark Recovery," Brit. J. Appl. Phys. <u>18</u>, 79-87 (1967).
- (11) Farrall, G. A. and Cobine, J. D., "Recovery Strength Measurements in Arcs from Atmospheric Pressure to Vacuum," IEEE Trans. on Pow. App. & Syst. PAS-86, 927-932 (Aug. 1967).
- (12) Becher, W. and Massonne, J., "Decomposition of SF₆ in Electrical Arcs and Sparks," Electrotechnisch Z (ETZ) A, 91, 605-610 (Nov. 1970) in German.
- (13) Milde, H. I., "Dielectric Strength Recovery of a Spark Gap," Appendix D of Multimegavolt Modulator Feasibility Study (U), Report No. RADC-TR-68-241, AD-392426, pp. 143-158 (July 1968).

- (14) Mallory Metallurgical Co. Trademark for sintered copper-tungsten composite material.
- (15) Frungel, F. B. A., <u>High Speed Pulse Technology</u>, Vol. I, Section B, "Switching Means," Academic Press, N. Y. (1965).
- (16) Smirnov, S. A., Makhenko, L. A. and Shendrovich, A. M., "A Trigatron for Large Currents in High-Voltage Apparatus," Instr. and Exp. Techniques, Translation pp.503-506 (May-June 1961).
- (17) Komel kov, V. S., <u>Technology of Large Impulse Currents and Magnetic Fields</u>, Translation FTD-MT-24-992-71,pp. 208, ff (1970)
- (18) Proud, J. M. and Huber, H. J., "Picosecond Risetime Switch Study," Report No. RADC-TR-67-400, AD820141 (1967).
- (19) Moriarty, J. J., Milde, H. I. and Hipple, J. E., "Multimegavolt Modulator Study," Report No. RADC-TR-70-107, Section 4 (Aug. 1970).
- (20) Belkin, G.S., "Vaporization of Metal Electrodes by Pulsed Currents," Sov. Phys. Tech. Phys. 13, 1256 (1969).
- (21) Markins, D., "Characteristics of a Pressurized Three-Electrode Spark-Gap Switch," in Report No. AFWL-TR-69-80, p. 248 (July 1970).
- (22) Maxwell Laboratories, Inc., High Altitude Simulation Stady Program, MLR-95, AFWL EMP-HAS 3-7 (July 1970).
- (23) Barnes, P. M., Gruber, J. E. and James, T. E., "The Parallel Operation of Low-Inductance High-Current Spark Gaps without Transit Time Isolation," J. Sci. Instr. 44, 599 (1967).
- (24) Gruber, J. E. and James, T. E., "Fast Pulse Breakdown of Non-Uniform Field Pressurized Air Spark Gaps," Proc. IEE, 115, 1530-1534 (Oct. 1968).
- (25) Bishop, A. E. and Edmonds, G. D., "Low Inductance 100 kV Switch (Spark Gap) for Starting, Diverting and Clamping Capacitor Discharges," Proc. IEE 113, 1549-1556 (Sept. 1966).
- (26) Vorob'ev, G. A. and Korsbunov, G. S., "Switching Characteristics of a Three -Electrode Spark Gap," Sov. Phys-Tech. Phys. 12, 1251-1254 (1968).
- (27) See Section 8, Reference 19.
- (28) Reference 1, p. 112.
- (29) Broadbent, T. E., "Spark Initiation; Experimental Techniques and Measurement of the Rate of Discharge Formation," Electrical Review (G. B.), pp. 620-624 (23 Oct. 1964).

- (30) Broadbent, T. E. and Shlash, A. H. A., "Characteristics and Breakdown Initiation of Triggered Spark Gaps with Uniform Applied Field at Very High Voltages," Proc. IEE 112, 2152-2158 (Nov. 1965).
- (31) Shkuropat, P. I., "Electrical Characteristics of Controlled High-Current Triggered Air Spark Gaps," Sov. Phys. -Tech. Phys. 11, 779-783 (Dec. 1966).
- (32) Shkuropat, P. I., "Investigation of Preignition Process in Trigatron Operating in Air," Sov. Phys. -Tech. Phys. 14, 943-948 (Jan. 1970). Note: The original submission of this work was in 1966, so it follows quite closely on the previous reference despite publishing 'ime lag.
- (33) Mesyats, G. A., Bychkov, Yu, I., and Iskol'dskii, A. I., "Nanosecond Formation Time of Discharges in Short Air Gaps," Sov. Phys. -Tech. Phys. 13, 1051-1055 (Feb. 1969).
- (34) Ion Physics Corporation, "SIEGE II, Phase II Final Report," Vol. I, Section 2 (May 1969).
- (35) Ion Physics Corporation, "Electromagnetic Pulse System," Report No. AFWL-TR-69-15, Vol. 1 (1969).
- (36) Maxwell Laboratories, Inc., "High-Current Low-Impedance Accelerators," DNA 2746F, MLI-111 (Dec. 1971).
- (37) Komel'kov, op-cit, pp. 167, ff.
- (38) Bradley, L. P., "Avalanche-Streamer Breakdown of Highly Overvolted Pressurized Gases," Bull. Am. Phys. Soc. 15, 1639 (1970).
- (19) Bradley, L. P., "Highly Overvolted Gas Spark Gaps for Electron Beam Generators," IEEE Trans. on Nucl. Sci. NS-18, 477-478 (June 1971)
- (40) DeMichelis, C., "Laser Induced Gas Breakdown: A Bibliographical Review," IEEE J. Quantum Elec. QE-5, 188-202 (April 1969)
- (41) <u>Digest of Literature on Dielectrics</u>, Vol. 34, for the year 1970, National Academy of Sciences, Washington, D. C. (1972).
- (42) Alcock, A.J., DeMichelis, C. and Richardson, M.C., "Wavelength Dependence of Laser-Induced Gas Breakdown Using Dye Lasers," Appl. Phys. Lett. 15, 72-73 (15 July 1969).
- (43) Generalov, N.A., Zimakov, V.P., Kozlov, G.I., Masyukov, V.A. and Raizer, Yu. P., "Gas Breakdown under the Influence of Long-Wave Infrared Radiation of a CO₂ Laser," JETP Lett. 11, 228-231 (5 April 1970).
- (44) Steinmetz, L. I., "Laser-Triggered Spark Gap," Rev. Sci. Instr. <u>39</u>, 904-909 (1968).

- (45) Khan, S. H., "The Laser Triggered Spark Gap," Ph. D. Thesis, Univ. of Oxford (July 1969).
- (46) Swarz, H. J. and Hora, H.eds., <u>Laser Interaction and Related Plasma</u> Phenomena, Plenum Press (1971).
- (47) Vaill, J. R., Tidman, D. A., Wilkerson, T. D. and Koopman, D. W., "Propagation of High-Voltage Streamers Along Laser-Induced Ionization Trails," Appl. Phys. Lett. 17, 20-22 (1 July 1970).
- (48) Chiao, R. Y., Garmire, E. and Townes, C. H., "Self-Trapping of Optical Beams," Phys. Rev. Lett. 13, 479-482 (12 Oct. 1964).
- (49) Askar'yan, G. A., "Waveguide Properties of a Tubular Light Beam," Sov. Phys. JETP 28, 732-733 (April 1969).
- (50) Korobkin, V. V. and Alcock, A. J., "Self-Focusing Effects Associated with Laser-Induced Air Breakdown," Phys. Rev. Lett. 21, 1433-1436 (11 Nov. 1968).
- (51) Alcock, A.J., DeMichelis, C., Korobkin, V. V. and Richardson, M. C., "Preliminary Evidence for Self-Focusing in Gas Breakdown Produced by Picosecond Laser Pulses," Appl. Phys. Lett. 14, 145-146 (1 March 1969).
- (52) Guenther, A. H. and Bettis, J. R., "A Review of Laser-Triggered Switching," Proc. IEEE 59, 689-697 (April 1971).
- (53) Guenther, A. H. and Bettis, J. R., "Laser-Triggered Switching," pp. 131-172 of Reference 46.
- (54) Pendleton, W. K. and Guenther, A. H., "Investigation of a Laser-Triggered Spark Gap," Rev. Sci. Instr. 36, 1546-1550 (Nov. 1965).
- (55) Dewhurst, R.J., Pert, G.J., and Ramsden, S.A., "Picosecond Triggering of a Laser-Triggered Spark Gap," J. Phys. D., Appl. Phys. 5, 97-103 (Jan. 1972).
- (56) Moriarty, J. J., Milde, H. I., Bettis, J. R. and Guenther, A. H., "Precise Laser Initiated Closure of Multimegavolt Spark Gaps," Rev. Sci. Instr. 42, 1767-1776 (Dec. 1971).
- (57) Bettis, J. R. and Guenther, A. H., "Subnanosecond-Jitter Laser-Triggered Switching at Moderate Repetition Rates," IEEE J. Quantum Elect. QE-6, 483-491 (Aug. 1970).
- (58) Deutsch, G., "Triggering of a Pressurized Spark Gap by a Laser Beam," Brit. J. Appl. Phys. (J. Phys. D) 1, 1711-1719, Scries 2 (1968).

- (59) Alcock, A.J., Richardson, M.C. and Leopold, K., "A Simple Laser-Triggered Spark Gap with Subnanosecond Risetime," Rev. Sci. Instr. 41, 1028-1029 (July 1970).
- (60) Guenther, A. H. and Bettis, J. R., "Laser-Triggered Megavolt Switching," IEEE J. Quantum Elect. QE-3, 581-588 (Nov. 1967).
- (61) Komel'kov, op. cit. pp. 177-178.
- (62) Clarke, J. D. and Hutton, P. J., Proc. of Sixth Int. Conf. on Ionization Phenom. in Gases, Vol. 2, p. 347, Paris (1964).
- (63) Kovalchuk, B. M., Kremnev, V. V., Mesyats, G. A. and Potalitsyn, Yu. F., "Discharge in High Pressure Gas Initiated by Fast Electron Beam," 12th Int. Conf. on Phenom. in Ionized Gases, p. 175, London (1971).
- (64) Abramyan, E.A., Borob'ev, V.V., Egorov, A.A., Elkin, V.A. and Ponamarenko, A.G., "Initiation of a Discharge in a Megavolt Gas Spark Gap by an Electron Beam," Instrumentation and Experimental Techniques, Translation pp. 130-131 (Jan.-Feb. 1971).

SECTION 10 LIQUID SWITCHES

Liquids possess self-healing properties similar to gases, and generally have relatively higher dielectric strengths. Thus, lesser gap spacing can be used for comparable voltages with a resultant lowering of switch inductance and risetime. Moreover, the inclusion of a liquid switch, liquid energy store and liquid-filled PFN in a single container offers obvious advantages over a system in which the switch contains a different dielectric medium than the connected elements.

Since the do self-breakdown voltage of a liquid dielectric switch is quite erratic due to entrained bubbles, impurities, and density gradients, this type of switch should be considered only for pulse-charged operation. Closure of liquid-filled switches can be accomplished by many of the same techniques already described for gas switches.

10.1 Overvolted Switch

Overvolted gaps insulated with oil or water have been widely used to provide fast-rising pulses in a simple manner. Jitter of 3 or 4% of the delay time and closure gradients of 400 kV/cm in oil and 300 kV/cm in water have been obtained for microsecond pulse-charge times. (1) A 3 MV oil gap overvolted switch in a 30 ohm Blumlein pulse has exhibited a closure time of about 40 ns for a 5 cm gap setting. This switch is said to be reusable for more than 100 pulses. (2)

Risetime of the pulse due to the duration of the resistive phase can be calculated in ns from

$$t_{\rm R} \sim \frac{5 \,\rho}{Z_{\rm o}} \frac{1/2}{1/3 \,E_{\rm B}}$$
 (1)

where

- ρ is the density in gm/cc
- Z is the driving impedance
- $\mathbf{E}_{\mathbf{B}}^{}$ is the mean breakdown field strength in MV/cm

This relation was used in reference (3) to make a design choice of pressurized SF_6 over oil as the insulant in a proposed 5 MV output switch for a RES II system.

Some preliminary tests on a 250 kV, three-channel water switch are described in reference (4), which showed both streak and time-integrated photographs of the closings. Jitter time between channels was less than 200 ns and current sharing was unequal.

Multichannel switching at 400 kV in an edge-to-plane geometry 34 cm long has been reported by Martin. (5) The edge required periodical sharpening during liquid breakdown tests. In view of the severe personnel hazards, not to mention the carbon by-products, the use of C Cl₄ for the dielectric fluid reported in (5), should be discouraged.

A 200 kV self-breaking multichannel water switch was examined for the Super COGEN⁽⁶⁾ program. An average of the data showed risetime decreasing from 25 ns to 10 ns as the number of channels firing increased from 2 to 6, while operating into a 1.6 ohm load.

10.2 Three Electrode Switch

The field-distortion or mid-plane switch has been used with some success in pulse-charged, liquid-filled gaps. Water gaps have been used up to 3 MV in both single and multichannel modes. Oil gaps have been operated at levels up to 5 MV. (1) A mid-plane, double-channel water gap for operation up to 300 kV is discussed in (6).

Tests of a 45 kV trigatron insulated with technical water is reported by Aksenov et al. (7) The geometry is essentially that of the gas trigatrons described earlier, except that the trigger electrode is a disk having a diameter almost half that of its host electrode. The auxiliary discharge takes

place across an annular gap 0.15 cm wide, and the main gap spacing is 1 cm. A trigger voltage pulse of 22 kV was used while the main gap was operated at 20-35 kV. A maximum delay time of 60-80 μ s was noted for main gap breakdown when the trigger pulse and main gap pulse arrived simultaneously. Main gap delays of less than 10 μ s were observed when the main pulse arrived \sim 80 μ s after breakdown of the trigger gap. This latter mode of operation also resulted in maximum current output (\sim 25 kA).

Another reference to liquid-filled switches, concerning transformer oil, indicates their use has not been popular in the USSR because of their instability and short life. (8)

Two instances of repetitive operation of three-electrode liquid switches have not resulted in very useful devices. Proud and Huber (9) investigated the possibility of dispersing the impurity growth due to electrophoresis and flocculation in transformer oil by means of agitation, but found that the maintenance of high purity in a repetitive gap was not practical. They compared non-earbonizing liquid nitrogen with oil in the same gap and found hold-off improved fourfold. Their motivation for recommending further effort with liquid was the observation that the spread of breakdown lag data was only 20% as wide for liquid as for gas.

A mechanically triggered three-electrode switch in fluorocarbon FC-77 fluid is described by Wilson. (10) A pair of stainless steel electrodes with one-inch separation were triggered by means of a rod electrode rotating between them at 60 or 120 pps, depending on drive motor rpm. Running times of 2 to 6 hours at 50 kV were achieved by means of filtering the fluid about once per minute. Jitter times were about $\pm 10~\mu s$ - quite reasonable for a mechanical switch.

10.3 Laser Initiated Switch

Liquid-insulated LTS has been discussed in the review articles of Guenther and Bettis. (11,12) Since streamer velocities in liquids are considerably

slower than those of gases, shorter gaps and more powerful (brighter) lasers are advisable for fast switching.

In a dc charged switch insulated with transformer oil, Marolda used a 500 MW ruby laser to close a 0.365 cm gap. Delay times varied from the microsecond region for orthogonal irradiation to less than 30 ns in the coaxial geometry (Section 9.3).

LTS has been reported in pulse-charged water ⁽¹⁴⁾ gaps at 430 kV and oil gaps at up to 700 kV. ⁽¹⁵⁾ The work with oil is described in some detail by Zigler ⁽¹⁵⁾ who attempts to relate liquid and gaseous breakdown theories in the absence of any well formulated theory of liquid breakdown. The nonlinear self-focusing ^(16, 17) phenomenon mentioned in connection with gases probably plays a part in preparing the breakdown channel. An interesting observation in this connection can be made concerning LTS in a 20 mm oil-filled gap charged to a few percent of SBV. In this case it was observed that the laser pulse crossed the gap as much as 150 ns before the application of any voltage across the gap, thus indicating that the preionized gap retains its low impedance for hundreds of nanoseconds after the passage of the laser beam. Zigler also demonstrated experimentally that a focus position 2 mm below the electrode surface gave best results. Delay times as low as 10 ns with jitter of +1 ns were recorded.

10.4 Design Considerations

As stated earlier, the liquid dielectric switch is self-healing and can be convenient to use in a low impedance system which employs similar liquid in its energy store and PFN. Though messy at times, liquids such as oil and water are far safer than compressed gas, as implied by the fact that pressure vessels are hydrostatically tested before requiring them to withstand gas at similar pressures.

Liquid dielectric switches should be restricted to pulse-charged operation, and to systems where the convenience of impedance matching

outweighs their relative imprecision. Applications for LTS in liquid should be examined with due consideration of the cost of the high-powered lasers required and the damage to lenses and laser crystals likely to be experienced due to shock propagation in the liquid and stimulated Brillouin scattering (18) which can direct the laser beam back on its source.

Erosion of electrodes in liquids is enhanced by the concentration of the spark into a narrow channel, a fact which is used to advantage in spark-machining. (19) Investigators in the machining field using a kerosene dielectric have found anode erosion to be much smaller than that on the cathode because of the adhesion of carbonized particles of kerosene on the anode surface. (20) In their tests, copper or silver anodes underwent ~1% of the erosion (by weight) of carbon steel cathodes. Similar favoring of the anode in MA/cm² discharges in kerosene is reported in reference (21). Experimental results are given for electrodes constructed of Cu, Ni, Fe, Al, W, Mo, Pb and Sn.

For breakdown strengths of switching liquids consult Section 5 of this report and reference (22).

SECTION 10

REFERENCES

- (1) Martin, J. C., "Nanosecond Pulse Techniques," Circuit and Electromagnetic System Design Note No. 4, p. 25, AFWL (April 1970).
- (2) Smith, I., Rice, G. and Aslin, H., "Advanced Flash X-ray System," Vol. I, p. 74, AFWL-TR-68-113 (April 1970).
- (3) Physics International Co., "RES II Study Program," Report No. PIFR 150, AFWL EMP-HAS 3-4, Appendix D (March 1969).
- (4) Vitkovitsky, I. H., "Multichannel Switching for High Power Discharges," NRL Memorandum Report 1831 (preliminary report) (Oct. 1967).
- (5) Martin, J.C., "Multichannel Gaps," Switching Note No. 10, p. 25, AFWL (Mar. 1970).
- (6) Kraemer, J. H., Moore, R. G., Murphy, C. J. and Riepe, K. B., "Phase I Super COGEN Program," Interim Report DASA2158, No. B-3867, pp. 5-18 (1968).
- (7) Aksenov, I. I., Bocharov, V. K., Smirnov, S. A., "Controlled Discharge in a Liquid," Sov. Phys. -Tech. Phys. 13, 1389-1392 (April 1969).
- (8) Mesyats, G. A., Nasibov, A. S. and Kremnev, V. V., Formation of Nanosecond Pulses of High Voltage, Translation FTD-HC-23-385-71, p. 125 (Moscow, 1970).
- (9) Proud, J. M. and Huber, H. J., "Picosecond Risetime Switch Study" RADC-TR-67-400, AD820141 p. 12 (1967).
- (10) Wilson, A. R., "Repetitively Operated High Voltage Pulse Generator Feasibility Study and Test Evaluation," EG&G Technical Report SRO-26 (Nov. 1968).
- (11) Guenther, A. H. and Bettis, J. R., "Laser Triggered Switching," in Laser Interaction and Related Plasma Phenomena, H. J. Swarz and H. Hora, eds., Plenum Press, pp. 131-172 (1971).
- (12) Guenther, A. H. and Bettis, J. R., "A Review of Laser-Triggered Switching," Proc. IEEE 59, 695 (April 1971).
- (13) Marolda, A. J., "Laser Triggered Switching in a Liquid Dielectric," IEEE J. Quantum Elect. (Corresp.) QE-4, 503-505 (Aug. 1968).

- (14) Lupton, W. and Burton, J. . "High Voltage Pulses and Electron Beam Accelerator Development," NRL Memorandum Report 2169 (1 July 1970).
- (15) Zigler, G. L., "Laser Initiated Conduction of an Overvolted Liquid Dielectric," M. S. Thesis, Air Force Inst. of Tech., WPAFB, Ohio AD857-481 (June 1969).
- (16) Chiao, R. Y., Garmire, E. and Townes, C. H., "Self-Trapping of Optical Beams," Phys. Rev. Lett. 13, 479-482 (12 Oct. 1964).
- (17) Engelhardt, W., "Self-Focusing and Plasma Formation in Transparent Media," Appl. Phys. Lett. 15, 216-217 (1 Oct. 1969).
- (18) Wiggins, T.A., Wick, R.V., Rank, D.H. and Guenther, A.H.,
 "Stimulated Brillouin Scattering in Liquids," Applied Optics (Lett.)
 4, 1203-1205 (Sept. 1965).
- (19) Bucklow, I. A. and Cole, M., "Spark Machining," Metallurgical Review, Review No. 135, pp. 103-118, The Metals and Metallurgy Trust, Great Britain (1969).
- (20) Motoki, M., Lee, C. and Tanimura, T., "Electrode Erosion Due to Transient Arc Discharge in Dielectric Liquids," Electr. Eng. Japan 87, 75-83 (1967).
- (21) Il'in, V. E. and Lebedev, S. V., "Destruction of Electrodes by Electric Discharges of High Current Density," Sov. Phys. -Tech. Phys. 7, 717-721 (Feb. 1963).
- (22) <u>Digest of Literature on Dielectrics</u>, Vol. 34, 1970, National Academy of Sciences, Washington, D. C. (1972).

SECTION 11 SOLID SWITCHES

Solid dielectric switches offer the advantage of very low impedance and high current capability. These switches are commonly used at dc voltages up to 100 kV, and operation has been reported at levels as high as 500 kV, pulse-charged. (1) A significant and obvious disadvantage to solid dielectric switches is their lack of self-healing and the necessity of replacing the dielectric after each event. Triggering of such switches is accomplished either by electromechanical puncturing for microsecond jitter or by means of an exploding foil or wire situated between and insulated from the main electrodes to achieve modest jitter of tens of nanoseconds. In the latter case, not only the dielectric, but also the trigger assembly must be replaced after each shot.

11.1 Overvolted Switch

The simplest form of solid dielectric switch is one in which a sheet of polyethylene or mylar is pressed between a pair of electrodes and then overvolted. Rather erratic behavior can be expected from such a simple arrangement because the discharge path will usually be a flashover path - which defeats the whole purpose of the very narrow gaps and consequent low inductance inherent to the solid dielectric switch. Although one could increase the flashover path sufficiently in principle to eliminate the flashover mode, it is more practical to overcome this behavior by purposely weakening the dielectric in one or more spots by stabbing it before insertion between the electrodes.

Reference (2) describes a method of attaining precise and reproducible stabbing of polyethylene. Sheets of stabbed polyethylene were inserted between electrodes and pulsed by a capacitor discharge. The self-breakdown voltages of 30-, 60- and 80-mil polyethylene sheets were determined as a function of the stab depth. These data are reproduced in Figure 11.1

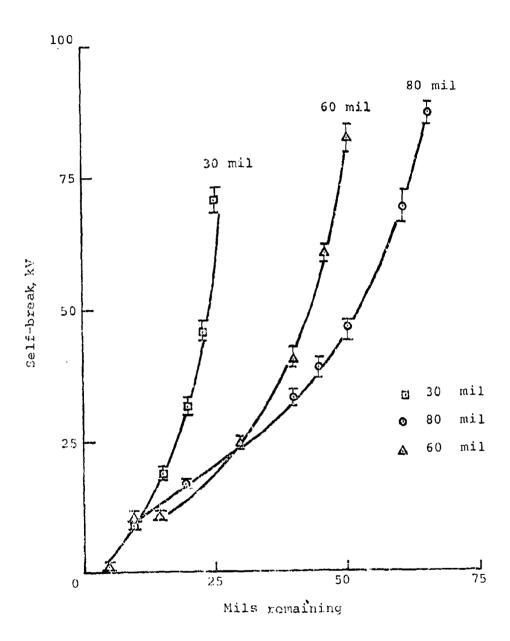


Figure 11.1 Self-break curve for polyethylene switches.

which shows self-breakdown voltage versus the thickness of material remaining beneath the stab. It is interesting to note that care was taken in these tests to cover the stab depressions tightly with an electrode so that water from the surrounding pulse-line would be kept out of the depressions. The depressions, always near the positive electrode, were thus filled with air which broke down on application of the high voltage pulse, thereupon distorting the field in the polyethylene to breakdown. The air breaks down readily since its lower dielectric constant causes most of the initial stress to appear in the air-pockets.

Stabbing can also be accomplished, though less precisely, in situ in dc charged switches. A deformation is caused by a remotely operated hammer or weight driving some sort of punch or tack into a thin copper or aluminum sheet electrode, eventually causing intrinsic breakdown in a very small volume. (1)

11.2 Multi-Electrode Switches

A solid dielectric switch belonging to this class may be a simple extension of the hammer-and-tack switch described above, in which the deformation takes place between one electrode and a midplane trigger foil or it may utilize one or more electrically or explosively triggered intermediate electrodes.

The simplest form of a three-electrode solid switch is shown in Figure 11.2. An advantage of the mid-plane foil is the growth of numerous channels from the highly stressed edges of the grounded trigger foil. An experimental determination of the number of channels formed as a function of the main gap ratio implied satisfactory operation for 0.3 < q < 0.6 where

$$q = y/(x + y)$$

y = dielectric thickness between trigger and ground

x = dielectric thickness between trigger and -V

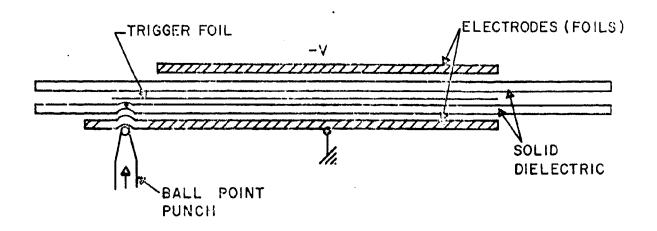


Figure 11.2 Mechanical triggering method.

These tests were made at a constant 5 kV/mil for 4 mil and 6 mil mylar inserts. As the stress was increased in the range 3 to 6 kV/mil, the number of switch channels was observed to increase.

The same switch, triggered by a capacitively coupled 35 kV trigger signal rising in 20 ns, operated with a delay of 19.7 ns and jitter $<\pm10$ ns when used to switch a 20 μ sec, 1 ohm stripline charged to 50 kV.

A detailed account of solid dielectric switches reported between 1956 and 1966 is given by Komel'kov. (4) Of the eight references cited, which describe triggering schemes such as exploding wires, explosive detonators, electrodynamic hammers and lasers, only one, attributed to Komel'kov and Aretov in 1956 was of Soviet origin. Their switch utilized a ring of six explosive detonators to switch 1.4 MA at 40 kV through polyethylene insulation.

A high power switch has been described $^{(5)}$ in which the mid-plane foil (0.025 mm thick copper) is separated from one main electrode by the principal dielectric, 0.5 mm thick polyethylene, and from the other main electrode by a thin, pre-punctured sheet of 0.075 mm thick polystyrene. The puncture is a hole of 5×10^{-4} mm area. Since breakdown of the switch is mainly attributed to explosive pressure generated in the vaporization of the trigger foil, a small puncture in the polystyrene car be considered more effective in concentrating the discharge on a small portion of the foil, thus facilitating vaporization. It is noted that the explosive pressure so generated is sufficient to puncture the polyethylene even when no voltage is impressed across the main insulation.

This switch was designed to satisfy inductance requirements $\sim 10^{-8}$ H and has closed successfully on pulses of up to 430 kA, passing 170 coulombs at 40 kV. Delay times in the microsecond range with jitters (standard deviation) of a few hundred nanoseconds were observed. Erosion of the main electrodes was distributed over the electrode faces by changing the position of the prepuncture in the trigger insulation. The triggering signal was directly coupled between the foil and main electrode from a capacitor discharge producing a 300 kHz signal of 100 kA peak at 10 to 20 kV.

11.3 Laser Initiated Switches

Solid dielectric switches can also be triggered by means of a focused high-brightness laser directed in a coaxial configuration as has been described for liquid and solid switches. This method has been demonstrated by Strickland who applied de voltages of 30 to 85 kV across gaps insulated with Lexan and Teflon 0.010 inch to 0.020 inch thick. Currents carried were 0.6 to 1.7 kA.

The particular breakdown phenomena which control the solid LTS are not established. The self-focusing of the laser beam due to non-linearities in the dielectric as well as further energy deposition in the resultant plasma probably has some effect. A discussion of solid dielectric breakdown is found in Section 6 and reference (8).

Strickland reported delay times as low as 2 ns with jitter of ±2 ns. A transition point in delay was observed when the applied voltage was 45 kV across 10 mil Lexan. At this point delay jumped discontinuously from ~10 ns to the microsecond range. Multichannel switching was initiated by sandwiching a thin foil between two dielectric sheets. Laser-induced breakdown of the first gap caused an overvolting of the remaining gap which discinged in numerous channels around the edges of the foil, similar to the conventionally triggered three-electrode gap described in Section 11.2. Another advantage of the grading provided by the sandwiched array is an increase in voltage hold-off for a given switch thickness.

11.4 Design Considerations

Relatively few materials have been widely used in solid dielectric switches. Of these, Mylar has the greatest dielectric strength and will therefore allow the shortest breakdown gap. For example, 10 mils of Mylar or 60 mils of polyethylene would be appropriate for a 150 kV switch. However, if low inductance is of prime importance, it should be noted that stabbed polyethylene can be made to break down in enough current-sharing channels to

compensate for its increased thickness. (2) In the event an automatic feed system (4,5) is desired for rapid replacement of spent dielectric, a flexible material such as polyethylene or Teflon is indicated. For applications requiring precise, machined thicknesses, clearly a rigid material such as Lexan or polystyrene is required.

Solid dielectric switches can be used wherever fast-rising, high currents at moderate voltages are required and sufficient time is available between pulses to replenish the dielectric and trigger foil (if used). The short gap spacings minimize inductance and have associated high field intensities which reduce the resistive phase to a few nanoseconds. The resistive phase, $t_{\rm R}$ is given (9) for solids of unit density (e.g. polyethylene) by

$$t_{R} = \frac{5}{2^{1/3} E^{4/3}} \quad \text{nanoseconds} \tag{1}$$

where Z is the driving impedance in ohms

E is the applied field in MV/cm

If precise synchronization with other prior events must be accomplished an electrical or LTS triggering technique may be required. Synchronization with later events may be adequately achieved by means of a probe such as a Rogowski coil sampling the current rising in the switch. In the latter case, or when synchronization is unimportant, the simplicity of the overvolted stab switch or mechanically initiated switch can result in relatively substantial cost reduction.

SECTION 11

REFERENCES

- (1) Martin, J. C., "Nanosecond Pulse Techniques," Circuit and Electromagnetic System Design Note No. 4, AFWL, p. 26 (April 1970).
- (2) Shope, S., Smith, I., Yonas, G., Spence, P., Ward, R., and Ecker, B., "Development and Applications of Mylar Striplines," Report No. DASA-2482 (Jan. 1970).
- (3) Maxwell Laboratories, Inc., "Development of Fast, High-Voltage, High Energy Pulse Generators and Generator Components," Report No. DASA 2260 (30 Jan. 1969).
- (4) Komel 'kov, V.S., <u>Technology of Large Impulse Currents and Magnetic Fields</u>, Translation FTD-MT-24-992-71, pp. 241-251, Moscow (1970).
- (5) Alston, L. L., Whittle, H. R., Mosson, G. A. and Baines, G. C., "Some Experiments on a High-Power Closing Switch with Polythene as the Main Dielectric," Proc. IEE 112, 1424-1430 (July 1965).
- (6) Strickland, D. M., "A Laser-Triggered Switch Employing Solid Dielectrics," M. Sc. Thesis, Air Force Inst. of Tech., WPAFB, Ohio, AD 855-852 (June 1969).
- (7) Engelhardt. W., "Self-Focusing and Plasma Formation in Transparent Media," Appl. Phys. Lett. 15, 216-217 (1 Oct. 1969).
- (8) <u>Digest of Literature on Dielectrics</u>, Vol. 34, 1970, National Acad. of Sciences, Washington, D. C. (1972).
- (9) Martin, J. C., "Duration of the Resistive Phase and Inductance of Spark Channels," Switching Note No. 9, p. 4, AFWL (Dec. 1965).
- (10) Huddlestone and Leonard, <u>Plasma Diagnostic Techniques</u>, p. 8, Academic Press (1965).

SECTION 12 VACUUM SWITCHES

The additional complexity of using high vacuum (10⁻⁵ to 10⁻⁷ torr) processing techniques in constructing and maintaining vacuum switches can be compensated by their advantages:

- (1) High dielectric strength.
- (2) Rapid deionization time.
- (3) Wide voltage range.
- (4) High current capability.
- (5) Low inductance.
- (6) Quiet operation.

Vacuum's ability to recover its dielectric strength is compared with that of N_2 , H_2 and SF_6 in Figure 12.1. The ultimate breakdown voltage of a vacuum gap depends primarily on the condition of the electrode surfaces. Since the surface condition varies considerably from shot to shot, as much as 108% in Lafferty's measurement, (1) it is not practical to attempt to control breakdown voltage of a vacuum switch accurately by adjustment of the electrode spacing. Furthermore, one must consider the effect of electrode roughening on voltage holdoff when using data from vacuum breakdown measurements (Section 7 and reference (2)) to design vacuum switch gaps.

Although most of the commercial switching devices described in Section 8 operate at pressures low enough to be properly called vacuum switches, this section is concerned only with prototype and other custom-designed vacuum switches. The particular characteristics of vacuum interruption devices (i.e., mechanically-opened, normally-closed electrodes in vacuum) are treated in Selzer's review.

Insulating materials integral to the switch include synthetics such as Lucite, Teflon and polyethylene as well as porcelain, ceramic and glass.

The exterior of the gap is protected from flashover in many cases by immersion

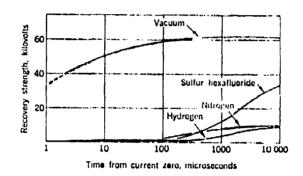


Figure 12.1 Recovery strength for vacuum and gas; 1600 amperes, 6.35 mm gap, gas pressure 1 atmosphere.

in oil or high pressure electronegative gas. In general, an internal spontaneous firing of the switch is not damaging, whereas external flashover is usually catastrophic for sufficiently large currents.

The spark gap can be made up of a single pair of electrodes or can be partitioned into several smaller gaps by means of conducting discs, especially for higher voltage operation. Figure 12.2 shows that the dependence of spontaneous breakdown voltage upon pressure becomes more sensitive as the spacing between electrodes is increased. Therefore, high energy switching requires adequate continuous pumping of out-gassed material, and, at higher voltages, the partitioning of the anode-cathode region into segments 5 to 7 mm wide. Sectioned gaps, though more stable, are more difficult to control. A sectioned gap is illustrated in Figure 12.3.

To initiate closure of a vacuum gap one must supply some charge carriers. These may be injected in the form of a plasma jet, localized spark, or even a neutral gas which becomes readily ionized; or the carriers can be obtained from within the gap by irradiating its electrodes, discs or walls with a high-power laser. The method chosen, as well as the details of its implementation will have much to do with the delay and jitter in switch closure. Since the injection of neutral gas does not result in a short delay, it is not considered further except in connection with one of the other methods, each of which is discussed in the following three subsections.

12.1 Spark-Initiated Vacuum Gap

This type of switch is similar (and in some cases identical) in form to the trigatron described in previous sections. However, its operating characteristics are substantially different. Although few studies exist, it is established (5) that delay substantially depends on gas pressure, polarity of the triggered electrode, spark gap voltage and igniting spark parameters.

Hancox⁽⁶⁾ has measured triggering delay in spark gaps operating in the range 10^{-3} to 3 x 10^{-2} torr, a region in which residual gas (nitrogen)

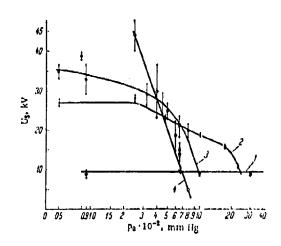


Figure 12.2 Dependence of the spontaneous breakdown voltage (U_s) of a partitionless spark gap on the initial pressure (p_0) for various interelectrode spacings. 1) 5; 2) 15; 3) 25; 4) 35 mm.

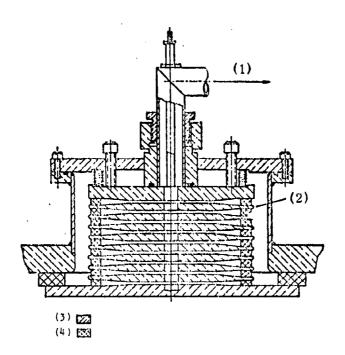


Figure 12.3 Design of sectioned spark gap.

- (1) To vacuum system
- (2) SF₆ under high pressure(3) Brass
- (4) Teflon

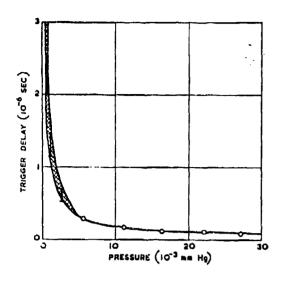
molecules can supply charge carriers once they are ionized. The dependence found for firing delay time versus pressure and gap voltage is shown in Figure 12.4. The trigger device was a 1 mm diameter tungsten wire in an insulating sleeve 1-mm-thick set flush with the surface of the negative electrode. Delay was independent of the polarity of the 15-kV, 100-ns pulse from a 330-ohm cable.

More detailed measurements on vacuum disc switches are reported by Aretov et al. for a 40-kV, 370-kA switch in the 10⁻¹ to 10⁻³ torr range. The effects of trigger voltage and the polarity of the triggered electrode are shown in Figure 12.5. Clearly the triggered cathode is the preferred mode for low delay and jitter. The shorter delays encountered when the cathode is triggered may be understood from the fact that the majority of the injected electrons are accelerated toward the anode thus developing the avalanche ionization; when the anode is triggered, on the other hand, a two-step process takes place in which the cathode is bombarded by positive ions, whereupon secondary electrons are emitted to develop the avalanche and the small plasmoid injected by the triggering device ultimately closes the gap.

Cormack and Barnard⁽⁸⁾ have described a low-inductance switch of the "trigatron" form which has been used as a crowbar switch with one-nH inductance over the range 0.5 to 25-kV and up to 500-kA. With argon filling in the range 18 to 60 microns, a jitter of 10 ns was observed for a positive trigger in the cathode, and the delay was as low as 40 ns.

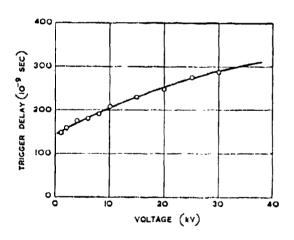
Higher current switches triggered by auxiliary spark gaps have been described by Hagerman and Williams whose 75-kV sectioned device passed 10^6 A. Maximum chamber pressure was 5×10^{-4} torr. Lifetime of the trigger pin was 50 to 100 firings, and that of the main spark gap was several hundred shots.

A non-sectioned gap developed at Leningrad Polytechnic Institute was aged (conditioned) to hold off 200 kV. This switch is controllable over



(a)

Results with nitrogen in the high-voltage gap at 4 kV.



(b)

Results with nitrogen at a pressure of 10-2 mm Hg in the high-voltage gap.

Figure 12.4 The effect of pressure and voltage on triggering delay.

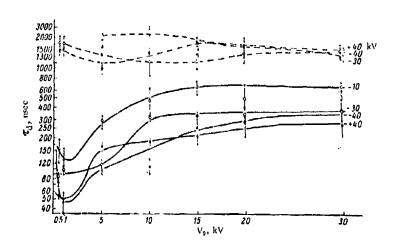


Figure 12.5 The delay ($t_d = f(V)$) in the firing of an unpartitioned spark gap (d = 35 mm) as a function of V_0 , the initial voltage applied to it, with triggering from the cathode (continuous curves) and from the anode (dashed curves); the trigger pulse amplitudes were -10, -30, and ± 40 kV. The base pressure p_0 in the chamber is 5×10^{-3} mm Hg.

the range 20 to 150 kV, passing 2 MA at 150 kV when continuously pumped to 10^{-5} tour. Ignition is accomplished by means of a 20 to 25 kV spark discharge which passes several kA across the polyethylene insulation between the core of the trigger cable and its host electrode. The delay and jitter depend on the operating voltage of the switch; at 150 kV, the delay is no greater than 200 μ s. Repeated operation at the 2 MA level requires additional voltage conditioning to operate at 150 kV. Below the 100 to 120 kV level, repeated aging is not required so long as the repetition rate does not exceed one shot per 5 or 10 minutes. (5)

12.2 Plasma Injection

This type initiation is usually required in lower pressure (<10⁻⁴ torr) switches which are unable to supply sufficient charge carriers in response to the stimulation of an auxiliary spark. Characteristics of switching by means of plasma streams depend on the stream velocity, charged particle density distribution, and the polarity and voltage of the electrodes. Sometimes a longitudinal magnetic field is used to reduce the effects of the chamber walls. In all cases, optimum operation is achieved when the high voltage electrode is negative and the plasma stream originates at the grounded electrode. (5)

The data of Azizov and Komel'kov ⁽¹⁰⁾ in Figure 12.6 for 30 kV, 400 kA gaps closed by plasma jets from coaxial injectors shows a voltage dependence of time lag of the same character as found in gas filled switches, namely, the delay is reduced as the operating voltage is increased. Delay times are measured from the entrance of the plasma stream into the gap to closure. Depending on the mass of plasma accelerated, the total delay time from injector turn-on is 200 to 400 μ s. For voltages below 2 kV particle densities of at least 10 ¹⁵ per cm ³ are required; whereas, at higher operating voltages 10 ¹³ particles per cm ³ would suffice. In the case of positive polarity high frequency current oscillations are observed which are not

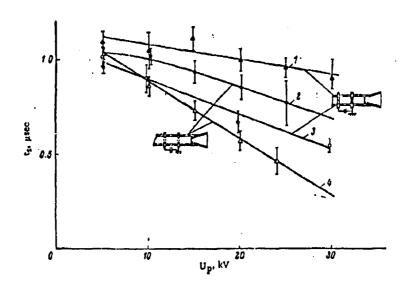


Figure 12. 6 Variation of the time lag of the discharge with the voltage for negative (4) and positive (2) polarities of the high voltage electrode. Ring electrodes. (3, 1) The same for cases where electrode II is represented by a solid disk and electrode I is a disk with a hole of diameter 6 cm.

present with negative polarity on the main electrodes. A 3 kOe longitudinal magnetic field does not mitigate the polarity effect.

A type of plasmoid-triggered gap which has already been developed into a sealed-off, high vacuum (10⁻⁷ torr) commercial device is the triggered vacuum gap (TVG) first described by Lafferty. (1) A hydrogen plasmoid is injected into the gap such that commutation is accomplished by the production of a glow discharge which rapidly becomes a metal vapor arc. Titanium hydride provides the hydrogen host material. This ceramic insulated device will close a 30 kV main gap in 100 ns with 30 ns jitter by means of a 10 A trigger signal. For dc applications it is best to set the positively-pulsed trigger in a recess in the negative main electrode (as for spark-triggered vacuum switches). Less trigger energy is required in this mode than if the trigger is isolated or connected to the positive electrode.

Like other vacuum gaps, the TVG has a wide voltage range: 300 to 3000 volts for a 0.086 inch gap, 2 to 150 kV for the ZR-7518 (obtainable on special order from General Electric Company). These switches will carry 10's of kA and have been constructed for operation at up to 100 kA.

12.3 Laser-Triggered Switch

The irradiation of electrodes, discs or walls with a high powered laser causes the explosive emission of clusters of ionized and neutral particles. Komel'kov⁽⁵⁾ suggests that the characteristics of vacuum switches initiated in this manner would have much in common with injected plasma devices and that the expected delay would not be much less than that obtained with spark ignition. Vaporization of discs and insulating walls is said to be more promising than irradiation of an electrode but would require one or more discharge tracks rather than a point burst. The necessity for very high power lasers and rather special optics is pointed out. ⁽⁵⁾

Experiments have been performed by Gilmour et al (11,12) which were directed toward a 300 kV, 1 kA vacuum switch having a duty cycle of

0.001 at 20 to 300 pps and a 1000 hour life. A ruby laser (6942 Å) and a pulsed nitrogen laser (3371 Å) were used for the testing of a 20 kV, 10 MW prototype. The risetime of the output current was polarity dependent: $\sim 1~\mu s$ for a negative target and $\sim 100~\mu s$ for the positive electrode target. The thrust of this research has been diverted from the laser-triggering aspects and concentrated more on a magnetically quenched, fast opening switch. (12, 13)

12.4 Design Considerations

A designer chooses a vacuum gap when he needs its fast recovery time and the compactness resulting from its high dielectric strength but has requirements on current, voltage or timing which cannot readily be met by commercial devices.

To achieve low inductance the current distribution can be improved by encouraging the current to flow near the outer boundaries of the switch rather than allowing it to become compressed in a small channel near the switch axis. This enhanced current distribution can be attained by inserting a dielectric obstruction in the center of the cavity which forces the discharge path to have a larger cross-section as it travels closer to the outer walls of the switch cavity. As with the walls the choice of dielectric obstruction material must take into account the capability of the pumping system to handle vaporized material as well as the degree of metallization (see below) which can be tolerated on the dielectric. A larger current distribution is also encouraged by an increase in the mass of gas released near the walls as, for example, when a narrow slot (5) is used as the discharge cavity rather than a cylinder.

Choice of materials, both conducting and insulating, influences not only the characteristic operation (as for slot gaps) but also the life of the switch and maintenance intervals. Electrodes are damaged mainly by non-uniform current distribution which can be reduced somewhat by discouraging high density single channel discharges. Long life requires the initiation of multiple channels when the switch is used to discharge more than 40 to 50 kJ.

It is interesting to note that the decrease of dielectric strength in spark gaps with synthetic insulators is not due to the precipitation of metal vapors on the walls. In fact, these materials themselves vaporize to the point that a gas cushion forms on the surfaces so as to shield them from metal vapor deposition. This is not so for porcelain and glass which may become metallized at large currents, except when relative thermal conductivities leave such insulators hotter than the conducting surfaces, thus encouraging the precipitation of metal vapor back on the electrodes. It has also been found that Teflon is less ablative than Lucite when heated in a discharge. The presence of organic matter such as pump oil leads to the deposit of conducting carbon films on insulators after switching. Therefore, the use of cold traps or oil-less pumps, turbopumps for example, is required. Lifetimes of the switches described in reference (5) are in the range of 10 to 10 t

Outside the Soviet Union, sectioned vacuum gaps (Figure 12.3) are widely used. Approximately 5 to 8 kV per section is allowed. Partitioning discs have apertures covering 30% of their area, not always aligned on the same axis, so as to avoid total breakdown if a single section fires spontaneously. Brass and stainless steel are typical electrode and disc materials. (5)

Finally, although vacuum gaps do not present the explosion hazard of high pressure gas gaps, the rapid acceleration of charged particles in the vacuum environment results in radiation from which personnel and sensitive equipment must be shielded.

; ·

SECTION 12

REFERENCES

- (1) Lafferty, J.M., "Triggered Vacuum Gaps," Proc. IEEE <u>54</u>, 23-32 (Jan. 1966).
- (2) Digest of Literature on Dielectrics, Vol. 34, 1970, National Academy of Sciences, Washington, D. C. (1972).
- (3) Selzer, A., "Switching in Vacuum: a Review," IEEE Spectrum, pp. 26-37 (June 1971).
- (4) Aretov, G.N., Vasil'ev, V.I., Pergament, M.I., and Tserevitinov, S.S., "Electrical Strength of Vacuum Disc Switches," Sov. Phys. Tech. Phys. 11, 1548-1555 (May 1967).
- (5) Komel'kov, V.S., Technology of Large Impulse Currents and Magnetic Fields, Translation FTD-MT-24-992-71, pp. 95-163, Moscow (1970).
- (6) Hancox, R., "Triggering Mechanism of Low-Pressure Spark Gaps," Rev. Sci. Instr. 33, 1239-1244 (Nov. 1962).
- (7) Aretov, G.N., Vasil'ev, V.I., Pergament, M.I., and Tserevitinov, S.S., "Delay Characteristics of Vacuum Disc Switches," Sov. Phys. Tech. Phys. 12, 90-96 (July 1967).
- (8) Cormack, G.D. and Barnard, A.J., "Low Inductance Low Pressure Spark Gap Switch," Rev. Sci. Instr. 33, 606-610 (June 1962).
- (9) Hagerman, D.C. and Williams, A.H., "High-lower Vacuum Spark Gap," Rev. Sci. Instr. 30, 182-183 (March 1959).
- (10) Azizov, E. A. and Komel'kov, V.S., "Switching of Discharge Gaps by Flasma Jets," Sov. Phys. Tech. Phys. 13, 468-475 (Oct. 1968).
- (11) Gilmour, A.S. and Clark, R.J., "Laser-Triggered Switch Study," Report No. RADC-TR-67-45, AD 810505 (Feb. 1967).
- (12) Clark, R.J., "Laser-Triggered Switch Study," Report No. RADC-TR-68-355, AD 846056 (Dec. 1968).
- (13) Gilmour, A.S., Jr., and Lockwood, D.L., "A New Vacuum Controlled Switch for High-Power-Pulse Generation and Crowbar Service," Proc. of the 10th Modulator Symposium, pp. 262-273, AGED, New York City (May 1968).

SECTION 13

GENERAL DESIGN CONSIDERATIONS

An attempt has been made to discuss and summarize all factors relevant to dielectric and switch design, but the size of the subject makes some omissions likely. With a few exceptions, the dielectric data presented cannot be used directly for design, even allowing for the temporal, area or volume effects which are treated at some length in the text. A factor of safety should be applied. The size of this factor depends on the application, including such considerations as the significance of breakdown, duration of operation and so on. Where available, typical operating stresses have been provided to give a guide to factors of safety. Examples of this are given in Tables 4.19, 4.14 (gas), 6.1 (solid), and Figure 7.14 (vacuum). Even with this data care has to be taken that the processing, or quality control that permitted these values is not overlooked. For example, in Section 5, it is noted that one power supply manufacturer designs for oil stressed at 100 kV/in positive and 150 kV/in negative. This value is for degassed (e.g. vacuum treated) oil, and not all supply manufacturers have the appropriate facilities to so degas their oil, nor do they design their supply tanks braced so that they can be evacuated. The data presented is largely a compendium from many sources. It has been obtained with different degrees of experimental care and should be treated with discretion. The designer of very expensive equipment should assess the value of conducting dielectric tests directly related to critical aspects of his design.

We have noted that, in general, the maximum electric field strength determines breakdown voltage, and the usual design philosophy is to minimize intensification beyond the uniform field value V/d, where d is the distance between the parts to be insulated. This question of electric field design was discussed at some length in Section 2, and obviously configuration is important. However, it is worth noting that from practical considerations

orientation of the electric field system can also be significant. As an example, we have noted earlier that the presence of particles can have an adverse effect on voltage performance in a high pressure gas. It would be expected then, that for low frequency operations where particles have sufficient time to move in the field, a geometry such as a coaxial line would perform better with its axis vertical rather than horizontal, i.e. so that particles are removed by gravity from the inter-electrode area, and there is evidence of this effect in practice. The use of perforated screens to trap particles in a horizontal coaxial situation is one approach to this problem. Another example where field orientation can be important is with liquid dielectrics where bubbles can lead to a low breakdown values. Geometries should preferably be arranged so that bubbles, if any, are trapped in low field regions, and certainly not in high field regions.

In several applications of high voltage technology there are relatively standard approaches. For example, broadly similar transformer concepts are used to generate power frequency, although for the higher levels, particularly for test units, a choice can be made between a single unit or more than one cascaded units. Similarly for dc power supplies, although again there are choices with regard to the number of stages to be used, and particularly at the higher voltages, differing approaches to generation. The route chosen by a designer is intimately related to dielectric technology, biased by his experience and the resources at his disposal. The same biases obviously exist when a new, unconventional, design problem is posed. Generally more than one approach can be identified as being practical, and determination is usually made based on such factors as cost, size, relative simplicity and sometimes development time - depending on the application. For example, an airborne system imposes restraints not existing for ground based equipment.

The design process usually starts with the load - the input to the system is often quite flexible. In a pulsed power situation the system can usually be represented in general by the blocks shown on Figure 13.1. The

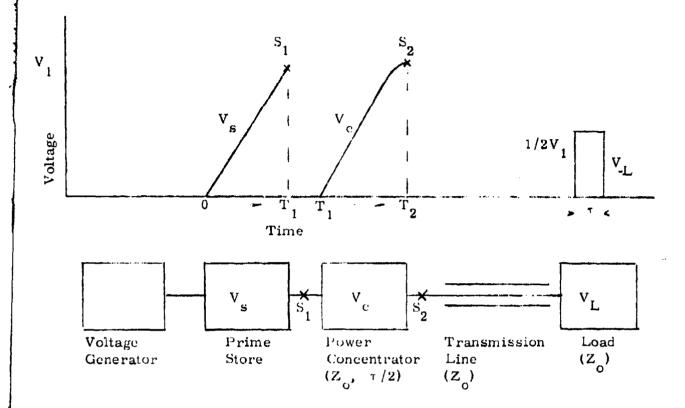


Figure 13.1 Generalized concept - pulse power system.

- Note 1. Time $0 \rightarrow T_1$ usually of the order of seconds for single pulse systems.
 - 2. Time $T_1 \rightarrow T_2$ usually about 1 usec.
 - 3. τ typically is 50 nsec.
 - 4. Case shown is for power concentrator matched to the load.

first block, representing high voltage generation, and the second block, representing primary energy storage, can be combined as in a Marx generator, or reversed as in a pulse transformer with primary circuit storage. The prime storage is usually a system of energy storage capacitors. In the case of a Marx generator these are arranged in stages which are charged in parallel then erected in series by interstage switches which are effectively switch 1. The power concentrator is typically a liquid dielectric capacitor which provides high energy density because of the high, short time, dielectric strength of liquids. The need for high energy density storage when fast pulses are required was discussed earlier in Section 1. A peaking capacitor is used in some applications to provide fast wavefront energy - in effect the peaking capacitor is "tuned" with the inductance of the prime store to provide the required risetime in the output transmission line or load. The close synchronization of switch 1 and switch 2 is of particular importance where peaking capacitors are used. The load is often connected directly to the output of the power concentrator. Where a transmission line is used it should be borne in mind that, as discussed in Section 1, the relative figures of merit for energy flow is not quite the same as for energy density because the velocity of propagation in the medium varies inversely with the square root of the dielectric constant. The third block, representing a power concentrator, or device to provide wavefront energy such as a peaking capacitor, may not be necessary, depending on the speed with which energy has to be supplied to the load.

A variety of sophisticated techniques have been developed to generate high pulsed power, and their utilization is intimately related to the performance of various dielectrics. Useful information on the techniques is contained in articles by Fitch and Howell, (1) Martin, (2) and Moriarty and Simcox, (3) and in books by Frungel (4) and Mesyats. (5) A good treatment of the subject of high voltage technology encompassing the many techniques and incorporating the dielectrics and switching information provided here would

involve more effort than is available, and that will be left for later authors. If wever, as a guide to determining suitable concepts it is useful to compare the energy densities possible with the various dielectrics. Table 13.1 provides information on maximum energy densities based on the breakdown strength of small samples. Operating stresses, in capacitors for example, are typically an order of magnitude lower (two orders of magnitude in energy density). Table 13.2 gives information on some of the more interesting materials taking account of area effects. In this case the active volume to store 100 kJ is given. Compressed gas would normally be used in a coaxial capacitor which could be charged to megavolts either with a pulsed or continuous voltage and switched at one end, usually in the same gas, into the load. Oil or water would typically be used in a coaxial geometry either as a simple coaxial line or in a Blumlein configuration, (1,2,3) and Mylar has been used in strip line geometries connected to give megavolt potentials by cascade switching (Marx or multiple Blumlein). (1,2,3)

Whereas gas or liquid insulated capacitors could be operated close to the stresses in Table 13.2 because breakdown is not normally destructive, this is not so for solid dielectric which must usually survive a reasonable number of shots. Table 13.3, due to J.C. Martin, takes account of this by stipulating 1000 shots life on the solid. The charging time duration of about 1 usec is a common value for liquid power concentrators charged by a Marx generator.

In designing for fast pulse generation and transmission it should be realized that the dielectric constant ε can be frequency (and field) dependent, although this is not usually a significant factor. Reference 6 summarizes measurements on the complex permittivity and permeability of more than 600 dielectrics for a frequency range of 10^2 to 2.5×10^{10} cycles per second, and for temperatures up to 500° C.

Finally, some comments on switches for pulsed power and their integration in systems. The previous sections have described a range of

Table 13.1 Energy densities in dielectrics.

Dielectric	e r	E (V/M)	W (joule/cm ³)*
Freon at 9.5 kg/cm ² pressure	<u>~</u> 1	5 x 10 ⁷	0.011
SF ₆ at 14 kg/cm ² pressure	_ <u>~</u> 1	6 x 10 ⁷	0.016
N ₂ and CO ₂ at 84 kg/cm ² pressure	\simeq 1	5.5 x 10 ⁷	0.013
Hexafluorine-nitrogen at 84 kg/cm ²	\simeq 1	6.7×10^{7}	0.02
Helium at 84 kg/cm ² pressure	\simeq 1	1.7×10^{7}	0.0013
Transformer oil	2.2	0.9×10^7	1.78×10^{-4}
Silicones	2.8	1.3×10^{7}	4.75×10^{-4}
Hydrocarbons	2	11×10^7	0.1
Distilled water	80	3.0×10^{7}	0.4
Ba-Sr Titanates	1800	107	0.79
Impregnated paper	2.23	1,2 x 10 ⁸	0.14
Polystrene	2.56	3.1 x 10 ⁸	1.08
Mica	3	1.6×10^{8}	0.34
Lucite	3	4×10^8	2.19

^{*}Based on measured breakdown strength of small samples. Actual gradients and energy densities obtainable in capacitors using these dielectrics are considerably lower.

Table 13.2 Active volume of dielectrics for 100 kJ.

Dielectric	<u>er</u>	<u>E (V/M)</u>	Active Volume M ³
SF ₆ (100-300 psi) ¹	1	25 x 10 ⁶	36
Mylar (0,006 mm) ²	3.2	5 x 10 ⁴	0.03
Mylar $(0.25 \text{ mm})^2$	3.2	3 x 10 ⁴	0.08
Oil ³	2.2	$\sim 4.0 \times 10^{7}$	~7.0
H ₂ O (atmos. press.)	80	\sim 1.5 x 10 ⁷	~1.0
H_2^{O} (atmos. press.) H_2^{O} (100 atmos.) ⁴	80	\sim 5.0 x 10 ⁷	~0.1

- 1. It is likely that the stress of 25 MV/M over the surface area required for 100 kJ at megavolt potentials could be achieved with relatively slow pulse charging at pressures in the middle of this range.
- 2. This is an average breakdown stress. Useful stress for reasonable life would be much less (see Table 13.3).
- 3. Effective charge time 1 us.
- 4. Based on latest experimental work as reported in the supplement of this report.

Table 13.3 Active volume of dielectric for 100 kJ (after J. C. Martin).

Plastics	Polythene	42 M ³
(1000 shot life)	Mylar	1.7
	Lucite	11
	Tedlar	12
Liquids	Oil	~1 0
(1 us charge)	Water	1.5 (uniform field)
	Water	0.4 (high negative field)

devices for the commutation of high voltage in a variety of environments with a wide choice of operating parameters. The tradeoffs and options available in an individual design exercise may be quite numerous.

Commercial devices such as the hard and soft switch tubes have been in service for many years in radar systems, particle accelerators and similar applications requiring a high degree of reliability and long operating life. Vacuum interrupters are in service in ac power distribution systems where very high reliability takes precedence over operating precision.

Extremely high voltages, in the multimegavolt range, are switched with maximum precision, speed and reasonable reliability by means of high-pressure gas switches. Most of the operating EMP systems and an experimental high-resolution radar use gas-insulated switches quite satisfactorily. Although it is often advantageous to switch in the same dielectric medium as the energy store, the precision with which gas switches can be controlled can result in an operating efficiency which justifies the engineering of a gas switch within a liquid energy store, as, for example, the Neptune facility at Ion Physics Corporation and the Gamble installation at the Naval Research Laboratory.

Liquid dielectric switches are often preferable in low-impedance systems which can be pulse-charged and utilize overvolted operation. Operating lifetimes are decidedly minimal because of erosion of electrodes and general wear due to shock-wave generation. Very fast risetimes can be attained in low-impedance PFN's by means of the peaking gap technique. Frequent repetition of switch closure is usually not practical.

For very high current transmission on a single shot basis, especially in a stripline configuration, the solid dielectric switch has been used with success. These are restricted to applications which allow ready accessibility between shots for obvious reasons. It would be hard to imagine a less expensive switch capable of such low-inductance, high current commutation. They have found use in weapons simulation equipment as well as more commercially oriented magnetic forming equipment.

Perhaps the most complicated of the non-commercial devices are the vacuum-insulated switches. However, they possess high current capability and remarkably wide operating voltage ranges. Their rapid deionization time is of value for repetitive operation well above the range of gasinsulated switches and for applications requiring quick opening - as needed with inductive energy stores. These switches have been used in a number of CTR applications.

In conclusion, we have found the quantity of information available, on the subject of dielectrics in particular, almost overwhelming. The condensation, collation and assessment given in these volumes provide a foundation for a succeeding effort on high voltage and pulse power technology, which may be deemed desirable. But that, fortunately, is another story.

SECTION 13

REFERENCES

- (1) Fitch, R. A. and Howell, V. T. S., "Novel Principles of Transient High Voltage Generation," Proc. IEE 111, 849 (1964).
- (2) Martin, J.C., "Nanosecond Pulse Technique," AWRE Report SSWA/ JCM/704/49 (1970).
- (3) Moriarty, J.J. and Simcox, G.K., "Megavolt Modulators for Nanosecond Radar," Proc. 10th Modulator Symposium, 274 (1968).
- (4) Frungel, F., "High Speed Pulse Technology," (2 vols.) Academic Press, N.Y. (1965).
- (5) Mesyatz, G. A., et al, "Formation of Nanosecond Pulses of High Voltage," Energia, Moscow (1970). FTD-HC-23-385-71.
- (6) Von Hippel, A., "Dielectric Materials and Applications," The Technology Press, MIT, John Wiley & Sons, New York (1954).

UNCLASSIF Security Classificati	IED				
		ROL DATA - R & D			
(Security classification	of title, body of abstract and indexing				
1. ORIGINATING ACTIVITY (Corporate author)		• • • • • • • • • • • • • • • • • • •	20. REPORT SECURITY CLASSIFICATION UNCLASSIFIED		
	Energy Sciences, Inc.		26. GROUP		
Burlington, Massa	chusetts 01803				
3. REPORT TITLE					
REVIEW OF DIELECT	RICS AND SWITCHING				
4. DESCRIPTIVE NOTES (Type of					
February 1971-Dec	ember 1972				
5. AUTHOR(S) (First name, middl	• • • • • • • • • • • • • • • • • • • •				
A. S. Denholm; J.	J. Moriarty; W. R. Bei	il; J. R. Uglum; G. k	C. Simcox;		
J. Hipple, S. V.	Nabio				
. REPORT DATE		76. TOTAL NO. OF PAGES	75. NO. OF REFS		
February 1973		534	431		
SE. CONTRACT OR GRANT NO.	F29601-71-C-0034	98. ORIGINATOR'S REPORT N	UMBER(S)		
å. PROJECT NO.	8809	AFWL- (R-72-88			
	8803	AFWL-1K-/2-88			
" Subtask No.	006	95. OTHER REPORT NO(5) (An this report)	y other numbers that may be essigned		
ď.	4				
10. DISTRIBUTION STATEMENT					
Distribution limi	ted to US Government as	gencies only because	test and evaluation		
information is di	scussed in the report or erred to AFWL (DYX), Kin	(Feb 73). Other requ	lests for this docu-		
11. SUPPLEMENTARY NOTES	irred to AFWL (DIX), KII	TERMIC AFD, NIII, 0/11/			
THE STATE OF THE S					
		AFWL (DYX) Kirtland AFB, NM 87117			
		Kirtiand Are	5, NP 6/11/		
13. ABSTRACT	(Distribution Limita	ation Statement B)			
Systems to genera	te high-power levels f		high voltage, and		
their design requ	ires special knowledge	of dielectric and sw	vitching technology.		
The treatment of	these technologies in :	this report starts w [.]	ith a discussion of		
alactoic field an	alveic than covere in	culation and cwitchir	ed in the four		

Systems to generate high-power levels frequently operate at high voltage, and their design requires special knowledge of dielectric and switching technology. The treatment of these technologies in this report starts with a discussion of electric field analysis, then covers insulation and switching in the four dielectric media; namely, gas, liquid, solid and vacuum. An extensive search of the literature produced a listing of relevant books, reports and papers and the establishment of a punched card classification and retrieval system specially designed for the subject area.

DD FORM .. 1473

UNCLASSIFIED
Security Classification

UNCLASSIFIED

Security Classification	LINE	C A	LIN	LINK B		LINK C	
KEY WORDS	ROLE	WΥ	ROLE	WT	ROLE	WΥ	
		l	}				
Die'ectrics			j		l		
Switching	l i	Į	ļ	1	ļ		
Energy storage Transients		ľ			İ		
Overvolt							
Triggered gap	i '			1	Ì		
Triggered gap Electrical breakdown							
	1						
				•			
	ļ					ı	
	1	,					
	}		1				
		!		:			
	i						
				}			
				İ	ŀ	}	
	į.			ļ	ļ :	1	
		1			<u> </u>	}	
				1			
	1					}	
•	Í		1			1	
			ļ	1	ļ	Į.	
				j			
		}					
	1			Ì	1	Ì	
	ĺ				1		
	Ì	1	l	1	1	1	
	ļ	1	ł				
		1	1		1	1	
		Ì	1]		1	
		1					
		1			1		
		1				1	
	1	1			1		
	ı	1	1	1	1	1	

UNCL	<u>assif</u>	IED		
Securit	v Clas	sifica	tion	